An Investigation into Pressure Delivery by Sport Compression Garments and Their Physiological Comfort Properties

A thesis submitted in fulfillment of the requirements for the degree of

Master of Technology

Elnaz Ashayeri

B. App. Sci. (Textile Technology)

School of Fashion and Textiles
College of Design and Social Context
RMIT University
March 2012

Declaration

I certify that except where due acknowledgement has been made, the work is that of the author alone; the work has not been submitted previously, in whole or in part, to qualify for any other academic award; the content of the thesis is the result of work which has been carried out since the official commencement date of the approved research program; any editorial work, paid or unpaid, carried out by a third party is acknowledged; and, ethics procedures and guidelines have been followed.

Elnaz Ashayeri

Acknowledgement

I would like to express my gratitude and deepest respect to all who contributed to this research; without whom this Master's thesis would not have been possible. I would like to show my deepest gratitude to my senior supervisor, Dr. Olga Troynikov, for her continuous guidance, advice, support and encouragement throughout my degree.

I am thankful to 2XU Pty. Lt., especially to Mr. Jamie Hunt, for providing material for this project.

I am extremely grateful to Mrs. Inna Konopov and Ms. Geraldine Van Lint for their support on both an academic and a personal level.

I would like to thank Ms. Trudie Orchard, Ms. Fiona Greygoose, Ms. Daniela Gentile, Ms. Nazia Nawaz, Ms. Leah Di Bartolomeo, Mr. Mac Fergusson, Dr. Lyndon Arnold, Mr. Farzad Mohades, Ms. Kate Kennedy, Ms. Sharon Koenig, Ms. Cherry Law and Ms. Fiona Gavens from school of Fashion and Textiles, RMIT University, for their constructive advice and assistance in practical and administrative aspect of this research.

I would also like to show my appreciation to Dr. Adrian Schembri and Dr. Anthony Bedford from school of Mathematics and Geospatial Sciences, RMIT University, for their valuable consultation and guidance on statistical analysis component of this research.

Above all, my utmost gratitude goes to my parents for their unconditional love and support.

Publications arising from the thesis

Journal paper:

Troynikov, O, Ashayeri, E & Fuss, FK 2011, 'Tribological evaluation of sportswear with negative fit worn next to skin', *Journal of Engineering Tribology, Proceedings of the Institution of Mechanical Engineers, Part J*.

Troynikov, O, Ashayeri, E, Burton, M, Subic, A, Alam, F & Marteau, S 2010, 'Factors influencing the effectiveness of compression garments used in sports', *Procedia Engineering*, vol. 2, no. 2, pp. 2823-9.

Troynikov, O & Ashayeri, E 2011, '3D body scanning method for close-fitting garments in sport and medical applications', *Ergonomics Australia - HFESA 2011 Conference Edition*, vol. 11, no. 16, pp. 1-6.

Table of contents

Table of figures

List of abbreviations

BMI	Body Mass Index
DOMS	Delayed Onset of Muscle Soreness
DVT	Deep Vein Thrombosis
Eq.	Equation
FE method	Finite-Element method
CG	Compression Garment
CS	Compression Stocking
CVI	Chronic Venous Insufficiency
MAD	Mean Absolute Difference
MCG	Medical Compression Garment
MEP File	Measurement Extraction Profile
MIU	Kinetic Coefficient of Friction
mmHg	Millimetres of Mercury
MMD	Mean Frictional Coefficient
MMT	Moisture Management Tester
MST	Medical Stocking Tester
MRI	Magnetic Resonance Imaging
OMMC	Overall Moisture Management Capability
OPM	Oxford Pressure Monitor
SCT	Sport Compression Tight
SMD	Surface Roughness Mean Deviation
STDEV	Standard Deviation
SCG	Sport Compression Garment

Abstract

Sport compression garments have gained popularity amongst fitness enthusiasts in recent years, whilst scientific knowledge on their performance in terms of pressure generation on the underlying limb and the physiological comfort of the wearer remains scarce. The aim of this research is to predict, measure and validate pressure generated by SCGs on the underlying tissue of human and to evaluate the physiological comfort performance of the garments.

Medical compression garments, their application, classification and the methods used in the prediction and validation of theoretical pressure inserted by them, were investigated through background research. This knowledge is used as a base, in order to predict and validate the theoretical pressure induced by sport compression garments. The theoretical pressure was predicted using the Law of Laplace, by testing the fabrics comprising sport compression garments for tensile properties according to a suitable method which was developed for the application under investigation. Validation of theoretical pressure was carried out through a linear regression model, whereby measured interface pressure generated by fabric sleeves over rigid cylinders was predicted with high accuracy, having the theoretical pressure as the predictor. Furthermore, the influence of composition of different fabrics within one garment on tensile properties and the resultant pressure was evaluated. It was observed that the amount and power of each fabric within the composition dictates the resultant pressure. The influence of the combination of weft and warp strain on interface pressure was also investigated and it was observed that the introduction of warp strain increases the resultant interface pressure.

The physiological comfort properties of fabrics comprising sport compression garments were examined with standard and developed methods of testing. The developed method consisted of the introduction of strain in the weft direction and/or moisture when testing the fabrics, with the aim of investigating the comfort properties of the fabrics in conditions close to the wear applications of these garments. The moisture management capacity of the fabrics investigated was rated as poor. The introduction of strain increased the thermal resistance and decreased water-vapour resistance, surface roughness and friction of fabrics, whereas the presence of moisture decreased the surface roughness and increased the friction.

Protocol was developed for taking lower-body measurements, relative to the application under investigation. A group of participants was scanned with a 3D body-scanner and the lower-body measurements were evaluated for participants who fitted the same size category of sport compression garments. Variations in circumferential measurements were observed, which ultimately affects the induced pressure from compression garments. Position of important lower-body points such as calf, knee, mid-thigh and maximum thigh were calculated in regards to crotch height along the leg for both genders, and by comparison to existing anthropometric knowledge, differences in the body proportions of different ethnic groups was revealed.

1. Introduction and outline of research

Sport compression garments (SCGs) have received much attention in recent years from athletes and fitness enthusiasts and there are numbers of claims common amongst manufacturers of these products, such as wearer's enhanced performance, reduced fatigue and faster recovery. The concept of SCGs is derived from compression garments (CG) used in medical applications which have been widely investigated, in terms of their application, classification, material, design, construction, and pressure profile. Whereas much research in recent years has focused on potential physiological benefits of wearing SCGs, little work has been done on evaluation of the material, construction, fit, physiological comfort and more importantly, pressure profile of SCGs.

In this research, existing knowledge relative to CGs for both medical and sport applications, was gathered and assessed, including the application, classification, material, design and construction, pressure profile and physiological benefits when such garments are worn. The study also investigated existing methods of prediction and validation of theoretical pressure, the pressure measurement devices and their calibration methods. Various physiological comfort attributes of fabrics investigated by researchers were evaluated. Lastly, various anthropometric data acquisition methods were summarised and related anthropometrical data, their variation amongst population and their relationship to other body parts, which are influential on the resultant pressure of CGs, were assessed.

Materials and methods engaged in this research were detailed: SCGs and fabrics comprising them were commercially sourced. Preliminary investigation was carried out on evaluation of tensile properties of the fabrics, and the construction and pressure profile of the SCGs. Calibration of the pressure-measuring device was attempted. Measured pressure was predicted from the theoretical pressure which was calculated from the tensile attributes of fabrics comprising the garments. Fabrics were evaluated in terms of their physiological comfort properties, namely thermal and water-vapour management, moisture management and tactile comfort. Finally, a protocol was developed to acquire lower-body measurements relative to SCGs and the body measurements derived from 3D body-scan of participants were processed. Body measurements and proportions between genders and within a size group were analysed.

2. Background research

In this chapter, literature relevant to CGs used in medical applications and their classification is explored. Existing knowledge in application of CGs in sport activities, their construction and material composing them as well as known physiological benefits of CGs for the wearer are reviewed.

2.1. Compression garments

CGs are used widely in medical applications and are cornerstone in care, treatment and rehabilitation of phlebological diseases such as venous deficiency, lymphoedema, and

oedema and in treatment of burn scars. CGs are tight fitting, worn as a second skin and are intended to exert pressure on the underlying limb of the wearer. In recent years, CGs have found their way from medical applications into sport activities.

In this section, the medical applications of CGs, their classifications and standards are described. Sport applications and classifications as well as fibres, fabrics and finishes used in SCG are explored. Finally, physiological outcomes reported from use of such garments in sport activities are presented.

2.1.1. Medical application

Compression therapy is a major treatment and/or support for treatments in phlebological diseases such as chronic venous insufficiency (CVI), varicose veins and venous leg ulcers (Baranoski et al. 2008; van Geest, Franken & Neumann 2003). Compression therapy has been practiced for many centuries with use of elastic and inelastic compression bandages, external intermittent compression therapy and MCGs, and it can be used as short/long term or as maintenance therapy.

Since early 1970s, CGs were found effective in prevention and rehabilitation of hypertrophic scars and in treatment of contractures and joint deformations (Macintyre & Baird 2005; Ng-Yip 1993; Wienert 2003; Williams, Knapp & Wallen 1998); compression has showed positive effect on wound healing since 1924 (Blair 1924; Wienert 2003). Suits, masks, gloves and hosiery were used for treatment of burn patients.

2.1.1.1. Venous deficiency, lymphoedema, oedema, and burn scars

In CVI, the return of venous blood to the heart is impaired usually due to reflux in venous system and is known as venous hypertension (Sieggreen, Kline & Geyer 2008). With compression therapy, pressure is induced on the leg, which narrows the varicose veins, reduces the blood volume, and in turn would increase the efficiency of calf muscle pump. Compression hosiery is used for maintenance of pressure in second step of treatment of CVI. According to severity of the venous insufficiency, a range of compression classes are prescribed and used for the treatment.

Lymphoedema, caused by damaged or abnormal lymphatic system, is an impaired localised fluid drainage; it causes change in size and shape of the affected area, such as swelling (Partsch & Jünger 2006). Compression therapy via compression bandages or compression hosiery have proven effective in reduction of localised swelling and treatment of lymphoedema, by reversing the fluid filtration from blood capillaries into tissue and decreasing the lymphatic load (Partsch & Jünger 2006).

Oedema is ‘accumulation of fluid in extra-vascular tissue’ (Partsch 2003). It is caused by increase in capillary permeability or capillary pressure between the blood vessel and the surrounding tissue and its imbalance with lymph drainage (Sieggreen, Kline & Geyer 2008). By application of pressure on local tissue, the loss of capillary fluid is reversed and the fluid is re-absorbed back into the vein and lymph vessels. Compression therapy is one

of the means in reduction of lymphatic fluid in the tissue, reducing the oedema (Partsch 2003; Sieggreen, Kline & Geyer 2008); it also enhances the tissue oxygenation and microcirculation (van Geest, Franken & Neumann 2003).

Hypertrophic scars occur as a results of thermal, electrical and chemical burns (Ng, SF, Parkinson & Schofield 1999; Wienert 2003). After treatment of second and third degree burns for three to four weeks, hypertrophic scars occur. If the burn is in joint area, it may cause deformation of joint as well. These scars are generally treated with compression therapy; CGs prevent protruding scars to form, resulting in flatter smoother scars. The pressure would reduce the blood flow and increase the local hypoxemia, preventing the excessive collagen formation. It also reduces the capillaries, making the scar paler; this prevents the vortex formation, and enables regular arrangement of orthologically parallel collagen fibres (Wienert 2003). The patients would wear the CGs to up to fifteen months for rehabilitation, and would renew their garments after two to three months due to loss in elasticity of the garment.

2.1.1.2. Classification and standards of MCGs

There are many available standards regarding MCGs: European standards for medical compression hosiery such as British standard for graduated compression hosiery BS 6612:1985 (BSI 1985), British standard for compression, stiffness and labelling of anti-embolism hosiery BS 7672:1993 (BSI 1993), British standard for non-prescriptive graduated support hosiery BS 7563:1999 (BSI 1999), French standard ASQUL (ASQUL 1999) and German standard RAL-GZ for medical compression hosiery 387:1 (RAL 2008). These standards do not necessarily comply with each other. There were attempts to produce a European standard for medical compression hosiery EVS-ENV 12718-2002 (EESTI 2001), which was unsuccessful (Clark & Krimmel 2006).

Each manufacturer of MCGs must comply with the specifications mentioned in one of the standards in garment design, materials, production, classification, labelling, packaging, testing and durability. MCGs could be of knee length, thigh length or pantyhose (toe or toe-less). In ready-made MCGs, a compression profile is generally defined. A compression value range and a proportion of the compression at various positions - such as calf to ankle and thigh to ankle - are defined for each of the graduated compression hosiery. Size of the garment is also defined through range of body measurements such as range of ankle, calf and thigh circumferences.

For instance, in German standard for medical compression hosiery (RAL 2008), four types of hosiery are defined as below-knee, mid-thigh, thigh and panty hosiery; the hosiery are manufactured either customised to body measurements of each individual or in standard sizes according to circumferential and length measurements defined in Figure 2.1. Important measuring points are A (toes), Y (heel), B (ankle), B1, C, D, E (knee), F, G and T (waist).

Compressive behaviour of the compression hosiery is also defined through extensibility of the fabric and the ‘practical elongation’ achieved through the hosiery over the leg. The German standard defines the following properties for quality assurance of medical

compression hosiery (RAL 2008): extensibility is change in size of hosiery in weft or warp direction as a percentage ratio of stretched to non-stretched hosiery; 'Practical elongation' is the percentage ratio of hosiery circumference over a leg to non-stretched hosiery circumference at respective measuring points; compression hosiery must have the minimum extensibility of 30% in warp and 120% in weft direction under 50 N stress and practical elongation of 15% to 120% when worn; ready-made hosiery can have maximum practical elongation of 50% in weft direction when worn; while customised hosiery must have the minimum extensibility of 80% in weft direction under same stress (50 N) and maximum practical elongation of 70% at measuring points F and G and at other measuring points, maximum 50% of the weft direction extensibility.

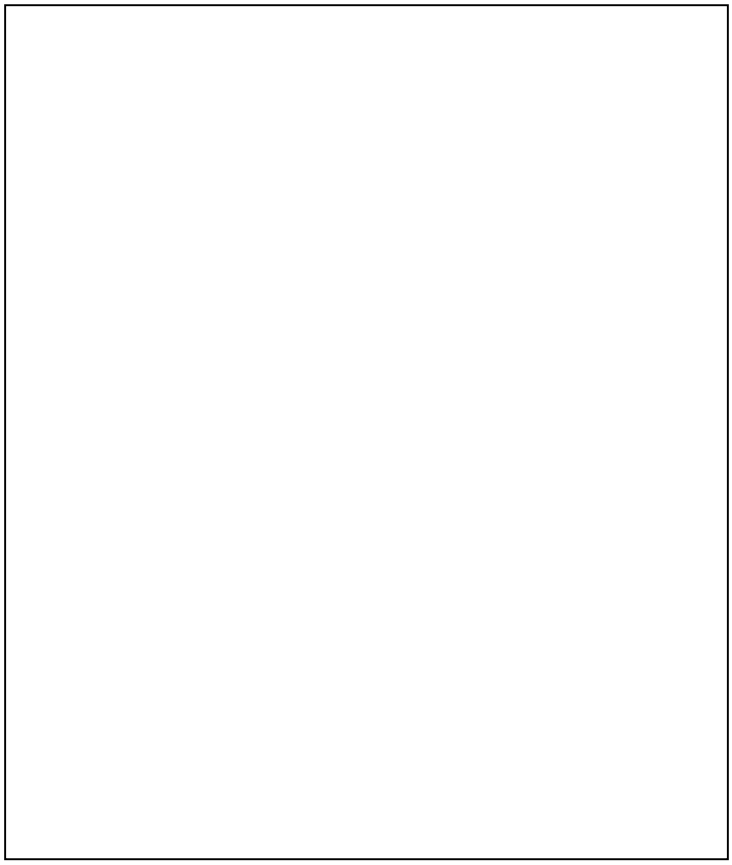

Figure 2.1 Measuring points - lengths and circumferences - Figure 1 in (RAL 2008)

Table 2.1 Compression classes and residual pressure ratio (RAL 2008)

Compression class	Compression intensity	Compression	Residual pressure ratio		
			At measuring point B1	At measuring point C	At measuring point F or G
		mmHg	%		
I	Low	18 to 21	70 to 100	50 to 80	20 to 60
II	Moderate	23 to 32	70 to 100	50 to 80	20 to 50
III	High	34 to 46	70 to 100	50 to 70	20 to 40
IV	Very high	49 and higher	70 to 100	50 to 70	20 to 40

Furthermore, German standard (RAL 2008) classifies compression hosiery into four compression classes with predefined pressure ratios (Table 2.1). Compression classes are determined by the pressure at measuring point B, which is tested using Hohenstein system (HOSY) compression test device. Residual pressure is defined as 'pressure exerted by hosiery at a point of the leg above the ankle, expressed in as a percentage based on the pressure at the ankle' (RAL 2008). These compression profiles are different to the compression profiles defined in British standards mentioned earlier.

2.1.2. Sports application and classification

In recent years, CGs have found new applications: prevention of deep vein thrombosis (DVT) on long-distant flights by wearing compression hosiery (Simmons 2011, Compression hosiery section); applications in sport including possible higher force and power production as well as improved proprioception, recovery and reduction of fatigue in all three types of strength, endurance and power (Voyce, Dafniotis & Towlson 2005); and injury prevention and rehabilitation (Bernhardt & Anderson 2005).

Performance sportswear must meet the needs of the body as well as the sport. The function of SCGs is to provide advantage for the athlete over their competitors and also to enhance the recovery of the wearer. Although the potential positive influence of wearing CGs on physiology and performance is widely accepted amongst athletes and weekend warriors, hard scientific evidence supporting these findings are indistinct (MacRae, Cotter & Laing 2011). While the negative influence of wearing CGs on performance and recovery are rarely reported, the existing research either points out the positive outcomes or the fact that CGs have no significant influence on the physiology and performance of the wearer (MacRae, Cotter & Laing 2011).

CGs have a negative fit over the body, which means that the garment is smaller than the limb measurement on which it is being fitted. The technical aspect of CGs functions through this negative fit; that is the generation of pressure on the underlying limb. With the strain in the fabrics comprising CGs, the garment keeps the limbs in correct anatomical position and reduces the muscle oscillation; with proper fit and skin contact, CGs improve the proprioception (kinaesthetic sense), 'the feeling in nerves in muscles and joints, and garments response to movement' (Das & Alagirusamy 2010).

Fatigue can be measured as loss of strength or muscular disruption and one of its major causes is muscle vibration. CGs support the muscles against 'shock waves and vibrations caused upon landing impact', reducing muscle vibration and thus fatigue (Voyce, Dafniotis & Towlson 2005). Wearing CGs enhances blood flow and venous return, increases the oxygenation of active muscles during exercise and impedes the lactic acid and waste build-up in muscle, resulting in faster recovery (Liu & Little 2009).

Generally, manufacturers of SCGs do not provide the details on the amount of pressure generated by their garments, but light or mild pressure is expected from a one layer SCG (Liu & Little 2009). Few researchers have measured and determined the pressure exerted by SCGs. Dascombe et al. (2006), for example, investigated the pressure inserted by

Sport SKINS Classic full-leg tight, custom-fitted according to height and weight of the subject, and reported to be approximately '9.1, 14.8, 17.6 and 19.3 mmHg along the posterior gluteus, medial vastus lateralis, medial gastrocnemius to medial ankle'. Sear et al. (2010) measured the pressure induced by SKINS unisex full-length bottoms and long-sleeved tops on their subject, wearing the CG at relative size according to height and weight (see Figure 2.2).

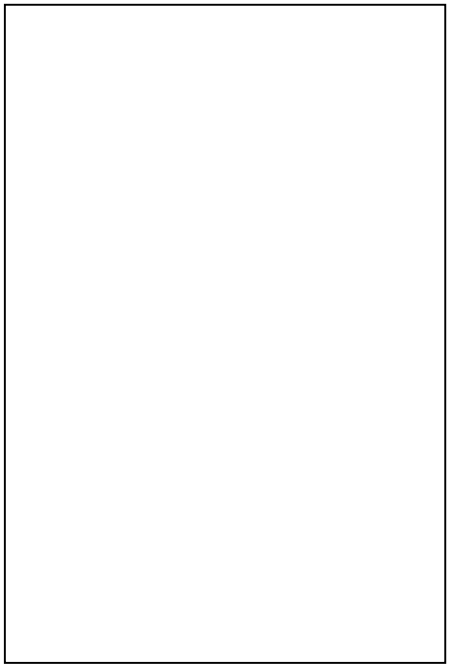

Figure 2.2 Pressure from SKINS unisex full-length bottoms and long-sleeved tops - Figure 1 in (Sear et al. 2010)

Paula Radcliffe, 'British record-breaking distance runner', was the first athlete known to wear over-the-calf compression stocking in competitions over a decade ago (Performance Apparel Markets first quarter 2010, p.4). Since then, a wide range of SCGs in the form of upper and lower and whole-body garments, sleeves and socks have become commercially available for wear during and after the exercise. SCGs are worn in sports such as football, basketball, netball, baseball, rugby, cycling, running, cross-country skiing, swimming and other sport activities.

In 2010, SCGs were more popular in US and Australia in comparison to Europe (Nusser & Senner). At the moment, 2XU and SKINS are two major Australian-based producers of SCGs. Other brands manufacturing SCGs were Adidas, Under Armour®, Nike, Champion, BodyScience, CW-X®, Speedo (Fastskin FS-Pro), Canterbury, Slazenger, and many more. Product range and technologies incorporated in SCGs by various manufacturers are many and varied; meanwhile, manufacturers of such products provide little or no clear data except for marketing jargon on the technologies used in their products, and no scientific evidence exists supporting their claims. For instance:

- Adidas promoted range of CGs with incorporating 'TECHFIT™ Padded Compression', 'TECHFIT™ Preparation' and 'TECHFIT™ PowerWEB™' technology for men's and women's training. 'TECHFIT™' technology was claimed to 'generate maximum

explosive power, acceleration and long-term endurance' and 'PowerWEB™' was claimed to 'actively support muscles, boosting power output and energy efficiency' (Adidas website 2011). 'PowerWEB™' is strategically placed thermopolyurethane (TPU) power bands which supposedly support and enhance the posture of the wearer (Performance Apparel Markets first quarter 2010, p.9). These product ranges include shorts, tights, tops, and elbow, calf and knee sleeves, providing high or medium compression (Adidas website 2011).

- CW-X® developed a range of compression products including tights, shorts, tops, support briefs, arm and calf sleeves and socks for men and women, for activities such as running, snow sports, hiking, yoga, triathlon/cycling and recovery, worn as an inner or outer layer. The products were claimed to provide targeted support through patented 'Support Web™' technology mimicking kinesiology-taping techniques, improving biomechanics during motion (CW-X Website 2012).

- SKINS 'dynamic' gradient CGs were designed for cycling, triathlon, golf, snow, active for all sports and recovery in form of sleeveless, short and long-sleeved tops, shorts, half and long tights, calf tights with and without a stirrup and sleeves (SKINS website 2012). Gradient compression claimed to increase circulation, improve oxygenation and lactate shuttle for enhanced performance and less pain. 'A400' garments were based on '400 points' from 3D body-scans of athletes. 'A200' and 'RY400' range were promoted for active people and recovery, respectively (SKINS website 2012). SKINS were recommended and endorsed by the Australian Physiotherapy Association (MediaNet Press Release Wire 23 April 2010).

- 2XU introduced a range of CGs in the form of tights, shorts, short and long-sleeved tops, stockings and socks, guards and sleeves for men and women for sport activities such as running/gym, swimming, cycling and triathlon (2XU website 2011, Compression section). Specific garments were recommended for injuries such as hamstring strain, shin splints, hip and back pain, delayed onset of muscle soreness (DOMS) and cramping muscles during the exercise for support and/or after the exercise to reduce muscle soreness post exercise. 2XU has been official compression partner of the Australian Institute of Sport (AIS) for its athletes and associated research and development program since 2009 (2XU website 2011).

- BODYSCIENCE (BSc) produced shorts, tights, triathlon-suits, cycle wear, arm warmers and socks for men's and women's running, soccer, tennis, rugby, training, combat sports, cycling, golf and multi-sport (BScCompression website 2012). The garments were claimed to provide 'Targeted® compression' to major muscle groups and were tested for body mapping gradient compression (BScCompression website 2012). Similar to other SCG manufacturers, their garments were supposed to enhance the performance of the wearer, reduce injuries and hasten recovery.

- Under Armour® stocked SCGs for both genders in the form of tights and leggings; shorts in various lengths; short, three-quarter and long-sleeved tops with various necklines; and socks. 'ArmourGrip™' technology was used with 'tackified compound' to grab and hold the gear locked into place for 'less slippage' (Under Armour website 2012). The 'locked-in feel' of the CGs was claimed to support the muscles, improve balance and performance, enhance circulation and speed up the recovery (Under Armour website

2012). The ‘Revolutionary X design’ in some of the garments mimicked ‘the functional anatomy of the body’s core area to boost muscle performance’ (Under Armour website 2012). The SCGs were designed to be worn for cross-training, running, football, hockey, hunting, basketball, track and field, and as a base layer.

All the above-mentioned brands promote CGs in various forms including tops, shirts, shorts and tights. Some brands recommend a specific range for a special type of activity or recovery from specific injury, while they do not provide any scientific detail on how the products function. Meanwhile, all the products are claimed to provide enhanced performance and faster recovery for the wearer. Some brands claim to take into account the human anatomy, through ‘body mapping’ or 3D body scanning; while others claim to use kinesiology-taping techniques or provide targeted support to specific muscles; which again are not scientifically supported. It seems likely that the various technologies claimed to be implemented in design and production of commercial SCGs are only to attract consumers with marketing jargon without any support backing up manufacturer’s claims.

2.1.3. Fibres, fabrics and finishes used in SCGs

Sportswear is greatly influenced by advances in textiles from a technical perspective, and by athletic achievement (Bramel 2005). Various fibres, yarns, fabrics and finishing technologies are used by different SCG manufacturers, to achieve the required function of SCGs in terms of performance and comfort.

Commercially available SCGs are made up of fibre blends which achieve the required negative fit and comfort, such as elastomeric fibres blended with other fibres such as nylon, polyester and cotton (Liu & Little 2009) and eco-friendly fibres such as bamboo ('Sustainability in performance apparel: meeting the demands of an eco-conscious marketplace' fourth quarter 2009). For instance, Under Armour® generally used blends of elastane with nylon, polyester or nylon/polyester (Under Armour website 2012), such as ‘Under Armour® Recharge™ whole-body compression suit’ which was made up of 75% nylon and 25% elastane (Kraemer et al. 2010). Compression shirts and ‘TECHFIT™ preparation 3-stripes short tights’ by Adidas composed of 75% nylon and 25% elastane and 79% polyester, 12% nylon and 9% elastane, respectively (Adidas website 2011). CW-X® manufactured their ‘Ventilator tights’ from 80% polyester (Coolmax®) and 20% elastane (CW-X website 2012) and Canterbury used 74.5% polyester (Coolmax®) and 25.5% elastane in the ‘Mercury compression range’ (Canterbury Website 2012, base layer section). The ‘Double dry’ compression shirt by Champion® was made up of 88% polyester and 12% elastane and Nike blended 96% nylon and 4% elastane in the ‘Dri-fit compression shorts’ (Liu & Little 2009). Unisex full-length bottoms and long-sleeved tops by SKINS reportedly had fibre composition of 76% nylon microfiber and 24% elastane (Sear et al. 2010).

High elastane content is required to achieve compression in swimwear ('New developments in performance swimwear' third quarter 2009), while fabric construction also influences the stretch and recovery of the fabric and thus the pressure delivery by SCGs. SCGs are made from warp and weft knitted fabrics, with each manufacturer claiming

longer durability and more power generation through the fabrics they use. 2XU is known to use weft knitted fabrics while Adidas, SKINS and BSc used warp knitted fabrics.

Inner brushed fabrics for colder climates by SKINS or technologies such as 'ColdGear® and HeatGear®' by Under Armour®, 'WarmStretch™' by CW-X® and 'Thermo-Control' by BSc were put in practice in SCGs for enhanced comfort of the wearer; 'CLIMALITE® and CLIMACOOL®' by Adidas, 'Coolmax®' by CW-X® and 'Perma-Dry' by BSc were also employed in order to enhance the moisture management of SCGs; UV protection was provided in SCGs: UPF50+ by SKINS, BSc, CW-X® and 2XU and UPF30+ by Under Armour®; Anti-odour finishes were applied to SCGs by 2XU and 'UA Capture™' by Under Armour® and 'Body-Fresh' (through silver weave) by BSc.

Various fibres, fabric constructions and finishing technologies mentioned above are common in SCGs; yet their claimed functionalities require clarification, as none is provided by the manufacturers.

2.1.4. SCG design and construction

'The technology associated with the design, cutting and manufacture of performance clothing is highly complex' (McCann 2005). And in highly technical garments such as SCGs, the design and construction of the garment with the selection of the material enable the claimed functions of the garments. The requirement of the sport activity dictates the 'cut and detail and fabrication' of the sport garments (McCann 2005). Furthermore, sizing becomes more important in technical garments (MacRae, Cotter & Laing 2011).

Material, pattern, design and sizing of the SCGs directly influence the amount of pressure generated by the garment. Some manufacturers claim to provide gradient compression generated by their SCGs. This amplifies the importance of the sizing and fit of the garments for the wearer. Mostly, SCG manufacturers employ Body Mass Index (BMI) for their sizing mechanism, which uses height and weight as a basis of the sizing system; while SKINS not only uses BMI but also had two additional body shape categories for women: 'small waist relation to the hip and thigh' and 'little variation in shape from waist to the hip and thigh' (SKINS website 2011).

The functionality of the SCGs is claimed to be improved through various design factors, once again with absence of scientific information on how these design factors and technologies function and the claimed outcomes are achieved: for instance, the SCGs by BSc provide 'Targeted® Compression', achieved through muscle specific panels and 'Body Mapping Technology'. 'TECHFIT™ PowerWEB™' in long tights by Adidas supposedly supports gluteus muscle (Liu & Little 2009). A combination of fabrics was used by 2XU, with placement of more powerful fabric at the back of the tights, provides extra support for the calf and hamstring. 'Conditioning WEB™, Support WEB™ and EXO-Lite Seamless Support Web™' in various SCGs by CW-X® mimics kinesiology techniques, providing targeted support to lower back, ABS/core, hip flexors, quads, hamstring, IT band, knee and calf/Achilles. Last but not least, SKINS 'biomechanically placed Memory MX fabric' inserts constant and controlled compression on the body.

Strategically placed panels are incorporated in various SCGs to improve the performance and/or comfort of the wearer. ‘Carbon-infused panels’ at thigh area in SKINS ‘Triathlon TRI400’ suits and shorts are claimed to reduce chafing (40% less friction) and ‘ultra smooth Toray fabric’ made of Cationic polyester and elastane to remove drag within the same garment. Mesh panels are used for enhanced breathability such as strategically placed mesh-ventilated panels by Under Armour® and breathable mesh panels at various targeted areas by BSc, Canterbury and CW-X®.

Seams are an important aspect of SCGs; they influence the comfort of the wearer, as they can cause chafing or skin irritation. Seams also affect the extensibility of the fabric comprising the garment. Most SCG manufacturers including but not limited to 2XU, Adidas, CW-X®, Canterbury and Under Armour® used flat-lock seams. Gradient compression could be achieved by seamless technology with inlaid elastomeric yarns ('Seamless knitting and stitch-free seaming technologies in performance apparel' first quarter 2006). 2XU and Adidas also employ seamless technology in some of their products.

Features such as elastic waist used in ‘TECHFIT™ preparation 3-stripes’ short tight and gathering at bust for support and lift in ‘TECHFIT™ seamless hug all-in-one’ by Adidas, ‘Silicone Leg Double Sided Gripper’ for securing the garment in place on the body by BSc, ‘unique hook-and-loop sock lock closures’ to keep the socks secure by Under Armour® are design features of SCGs for improved functionality and enhanced comfort of the wearer.

Furthermore, additional technologies were incorporated into SCGs through garment engineering; for instance, incorporation of a GPS device and heart rate monitor into CGs carried out by SKINS in affiliation with Australian Rugby Union, enabled both the performance enhancement of wearing SCG as well as gathering of accurate data from players while active (Sun Herald 06 June 2010, p.68).

2.1.5. Physiological benefits of using SCGs

SCG manufacturers claim that wearing CGs improves various aspects of performance of the wearer, reduces muscle damage and fatigue as well as aids the recovery after the exercise. Some of these claims are supported with evidence and some as reported by MacRae, Cotter & Laing (2011) are ‘taken out of context’. There is a growing trend in examination of physiological effects of SCGs; oxygen uptake, heart rate and blood lactate level as well as performance and recovery time after the exercise and in some cases comfort was measured and investigated with compression and control garments. According to Doan et al. (2003), first study of this kind was carried out in 1987 by Berry and McMurray, demonstrating improved blood lactate removal after maximal exercise. Some of the research outcomes on this topic are documented below, which mostly addresses positive and likely positive or no significant effect from wearing CGs. In very rare occasions, negative outcome of wearing CGs are reported by researchers.

Doan et al. (2003) studied the effect of wearing compression shorts on performance of track athletes specializing in sprint or jump. Reduced hip range of motion in 60 m sprint,

increased jump height and decreased muscle oscillation in countermovement jump, and increased skin temperature in 5 minutes cycling was observed.

Bernhardt & Anderson (2005) examined the effect of wearing compression shorts on active range of motion, balance, agility, proprioception, endurance and power of healthy active subjects focusing on the hip area. No significant performance enhancement from wearing sport compression shorts was reported by the researchers, but they suggested that wearing SCGs 'may be useful for injury prevention and during recovery from injury' (Bernhardt & Anderson 2005).

Ali, Caine & Snow (2007) compared the influence of wearing knee length graduated compression stockings (CS) (18 to 22 mmHg pressure at ankle) to control stockings, during and after intermittent and continuous running on performance and recovery of recreationally active subjects. They observed no benefits in wearing CS on intermittent shuttle running. In continuous 10 km run, DOMS was reduced 24 hours after the exercise and only few participants complained of muscle soreness having worn CSs.

Ali, Creasy & Edge (2010) investigated the influence of wearing graduated CS at various grades of low (12 to 15 mmHg) and high (23 to 32 mmHg) on performance and recovery of competitive runners on fast paced running. No physiological benefits such as difference in heart rate, oxygen intake and blood lactate during exercise and no significant effect on muscle function and soreness between trials was noted from wearing CSs. Between low and high range CSs, low range was described to be more comfortable for running.

Kemmler et al. (2009) studied the effect of below knee CSs with constant compression at the calf muscle (18 to 20 mmHg) on running performance of moderately trained runners. Significantly enhanced running performance and maximum speed was recorded, yet other physiological parameters were not affected by CSs.

Sear et al. (2010) concluded 'likely' moderate strength enhancement in total distance covered and low-intensity activity distance during a prolonged high-intensity intermittent exercise while wearing whole-body CGs, as well as 'likely' increase in tissue oxygenation index. The whole-body CG used in the investigation provided pressure range of 17.8 ±2.2 mmHg at the ankle, decreasing to 9.2 ±1.6 mmHg at the hip, 5.9 ±0.8 mmHg at the waist, 5.3 ±0.5 mmHg at the chest, 7.3 ±2.5 mmHg at upper-arm and 5.8 ±1.0 mmHg at forearm area.

Duffield, Cannon & King (2010) evaluated the performance of voluntarily and evoked muscle performance on rugby players wearing lower-body CGs as well as recovery 24 hours after intermittent sprint and stretch shortening cycle activity. While no significant effect was mentioned, they advised that wearing CGs 'may' have minimal effect on above mentioned parameters.

Effect of lower-body CGs on post exercise recovery was investigated by Davies, Thompson & Cooper (2009) after 5x20 plyometric drop jumps on trained netball and basketball team players. They suggested that creatine kinase (sign of muscle damage) and perceived muscle soreness 'may' be reduced by wearing CGs after exercise, but the performance was not affected.

Jakeman, Byrne & Eston (2010) examined the effect of full leg CSs on performance and recovery of physically active subjects after plyometric exercise inducing muscle damage. They observed decreased muscle soreness and decrement in muscle performance, enhanced recovery after jump performance, and no significant effect on creatine kinase.

Kraemer et al. (2010) reported enhanced recovery by wearing whole-body CGs after an intense heavy resistance workout on resistance-trained subjects. Reduced muscle soreness and fatigue rating, and higher vitality rating was noted while wearing CGs after the exercise.

In contrast to the researches usually carried out, Goh et al. (2011) monitored the influence of lower-body CGs on time to exhaustion, skin and rectal temperature, VO_2, heart rate and rating of perceived exertion at cold and hot conditions of 10° and 32°C, during sub-maximal and maximal running and compared the results to not wearing CGs on recreational runners. The only difference observed from wearing CGs was higher skin temperature at 10°C, and lower rating of perceived exertion during sub-maximal running at 32°C.

Enhanced muscle oxygenation and its associated metabolic benefits are deemed to be reasons for physiological benefits of wearing CGs (Sear et al. 2010), due to improved blood delivery and enhanced microcirculation (Millet, Perrey & Foissac 2006; Perrey 2008). Lawrence & Kakkar (1980) claimed optimum pressure gradient for lower limb to be 18 mmHg at ankle, decreasing to 8 mmHg towards the upper thigh, generating fastest venous flow (14, 8 and 10 mmHg at the calf, knee and lower thigh, respectively). Yet contradictory results are observed by researchers examining the physiological benefits of wearing CGs. The differences in reported results are most likely due to differences in study set-up, nature, duration and intensity of exercise, the condition, number and sex of subjects, the CG and the amount of pressure induced on the underlying limb and the moment CG is worn (during, after or during and after exercise) as well as the parameters measured.

On the other hand, the placebo effect of wearing CGs could lead to perceptual advantage and encourage positive outcomes (Ali, Creasy & Edge 2010; Duffield, Cannon & King 2010; Kemmler et al. 2009; MacRae, Cotter & Laing 2011). In most studies, a control garment was used along with CG; yet the fact that CGs compress the underlying limb impedes offsetting the placebo effect. Which is why in the study carried out by Duffield, Cannon & King (2010), even though no physiological benefits were recorded from wearing CGs for recovery after exercise, the placebo effect brought about comments of self-reported perception of recovery from subjects.

In conclusion, few researchers claimed significant performance enhancement, whereas most reports consisted of no significant performance or physiological benefits observed from wearing CGs. Nonetheless, decreased muscle soreness and fatigue ratings were more commonly recognised amongst the investigations. Inconsistent observations from different studies, however, suggests requirement for further investigation on this topic.

2.1.6. Summary

The concept of SCGs came from MCGs used for many years in treatment and/or support for treatments in phlebological diseases such as CVI, varicose veins, venous leg ulcers as well as burn scars. MCGs have been extensively studied for their material, construction, pressure delivery and physiological benefits, while the amount of research carried out on SCGs is little, but growing. Unlike MCGs, there are no standards in existence for production and quality assurance of SCGs, and there are some substantiated and some unsubstantiated claims for physiological benefits of wearing SCGs during and/or after the exercise.

SCGs are claimed to improve the performance and reduce the chance of injury of the wearer by supporting and keeping the muscles and ligaments aligned and by increasing proprioception. Enhanced muscle oxygenation and removal of lactic acid build-up and waste is supposed to reduce the fatigue and speed up the recovery of the athlete. Various researchers examined possible physiological benefits of using SCGs during and after exercise. There are more reports on insignificant performance enhancements or physiological benefits of wearing CGs in sport activities than on confirmed positive outcomes. Decreased muscle soreness and fatigue ratings, however, seems to be more likely amongst other claims. Inconsistent results from different studies suggest requirement for further investigation on this topic.

Similar to any technical garment, SCGs benefit from advances in textile technology, in terms of fibres, fabrics, finishes and garment engineering. Elastomeric fabrics comprising SCGs not only provide good fit and ease of movement, they also insert pressure on the underlying limbs. SCG manufacturers claim to engage garment engineering, using body measurements, fibre and construction, to enhance functionality and comfort of the garment. However, there is no scientific information available on technologies engaged by manufacturers in production of SCGs, and the amount of pressure intended to be generated by the garments on the underlying limb. Their claims are rarely scientifically supported and seem be self-marketing to gain competitive advantage over other manufacturers.

2.2. Compression prediction, measurement and validation

The degree of interface pressure generated by CGs over the underlying limb of human is crucial in wellbeing and comfort of the wearer. Excessive or insufficient pressure delivery or incorrect pressure gradient could have adverse physiological effects; it could cause tissue damage or compromise the circulation in the limb (Thomas & Fram 2003).

Prediction, validation and measurement of pressure generated by compression bandages, hosiery and garments are challenging; which is why numerous investigations have been carried out on this topic by researchers and experts within the medical and sport industry. Different theoretical methods were considered in prediction of interface pressure. Wide range of different pressure-measuring devices, developed or available commercially, were used to measure the interface pressure and validate the theoretical

pressure ‘in vitro’, over rigid cylinders or mannequin legs as well as ‘in vivo’, over human body in static or dynamic state.

2.2.1. Methods of theoretical prediction of pressure generated by CGs

Some of the methods of theoretical prediction of pressure generated by CGs used by researchers are mathematical/numerical modelling using Finite-Element method (FE method) and approximation of Law of Laplace.

Okss & Lyashenko (1999) studied the distributed forces within the elastomeric fabric, engaging various mathematical and physics theories and laws, and the ‘geometrical meaning’ of the limb (curvature of the surface of the limb). They concluded that the pressure induced over the body from the elastomeric textiles/garments depended on ‘mechanical parameters’ of the fabric (fabric tension) and on the geometry of the limb. Eliminating the mechanical characteristics of the fabric, an equation was reached from lengthy analysis of the above, where the pressure was directly proportional to the distributed tension and inversely proportional to the curvature radius. Triangular FE method was applied in modelling the textile material considering various hypotheses; from this model, a technique was derived predicting the pressure induced from CGs over a limb. FE method was also used by Dai et al. (2007), where the pressure was simulated below the knee by modelling both the CS and the ‘three-dimensional biomechanical lower limb’ having bone and soft tissue; the model revealed that the pressure was not evenly distributed over the limb, and that the pressure at lower radius was higher than at the higher radius regions.

Cross-section of the lower leg was investigated by Liu et al. (2007), at ankle, calf and thigh, and by Avril et al. (2010) at calf. Magnetic Resonance Imaging (MRI) scans were used for extracting a cross-section of the limb at respective points, providing internal morphology of fat, muscle and bones and FE method was applied for pressure modelling of CS/CGs. Liu et al. (2007) simulated the pressure engaging a numerical model and reported highest pressure at anterior side of ankle to knee section, similar pressure magnitudes in medial and lateral sides of the calf and widest pressure differences at various positions along the knee perimeter. Tissue deformation was also studied, where it caused inner tissue stress changes. Liu et al. (2007) concluded that anatomical structure of the leg, CS design and its physical properties influenced the pressure induced over the limb at various locations over the same region. Avril et al. (2010) observed that internal morphology of the leg greatly impacted the transmission of pressure on internal tissue of the leg.

Modelling of soft tissue using FE method is not sufficiently addressed within research and it is difficult to identify accurate elastic properties of soft tissue in human body (Avril et al. 2010). In spite of the mentioned drawbacks, Avril et al. (2010) noted variation in pressure along the leg, which confirmed reports by Dai et al. (2007) and Liu et al. (2007). Additionally, Avril et al. (2010) reported variations of up to 35% in pressure inside the leg. Taking into account relative precision of 15% in their approach, they suggested that the fat

was less compressible than muscle under interface pressure and that the difference in elastic properties of fat and muscle affected the pressure transmission inside the leg.

It is useful to analyse the limb morphology, in prediction of the induced pressure generated by CGs over the limb, yet it is impractical to MRI every leg. Apart from that, the FE method shortcoming, in inaccuracy of soft tissue elastic characteristics, limits the practicality and efficiency of this approach at this stage. Besides, not all the models developed by the researchers were validated with measured pressure over human limb, which brings up the question of the accuracy of predicted and simulated pressure.

Alternative approach in theoretical prediction of pressure generated by CGs is approximation of Law of Laplace. Law of Laplace (Figure 2.3) defines 'the relationship between the pressure across a closed elastic membrane or liquid film and the tension in the membrane or film' (Thomas 2002).

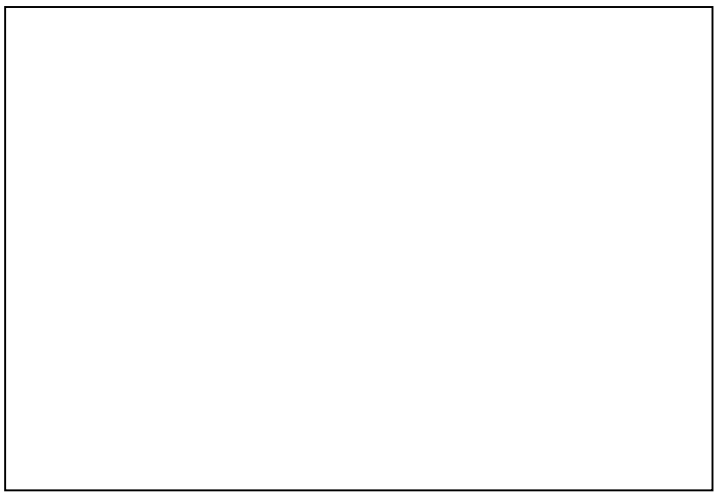

Figure 2.3 Law of Laplace (Hyperphysics website 2011)

Law of Laplace, Eq. (1), is used for prediction of pressure delivery to a cylinder covered with fabric sleeve; where fabric tension and radius of the cylinder are known (Macintyre, Baird & Weedall 2004; Ng, SF, Parkinson & Schofield 1999; Thomas 2002).

$$T = PR \tag{1}$$

where T is the tension (N), P is the pressure (Pa) and R is the radius of the cylinder (m).

Pressure in CGs is usually expressed in millimetres of mercury (mmHg), fabric tension is measured per unit length and limb circumference is measured instead of limb radius; hence, units in Eq. (1) are usually converted to units common within the industry. Eq. (2) is a result of unit conversions:

$$P = \frac{KT}{C} \tag{2}$$

where P is the pressure (mmHg), K = 470 is the conversion constant, T is the fabric tension (N/cm), and C is the cylinder circumference (cm).

In addition, it is necessary to take into account number of layers of fabric applied (Thomas 2002). Thomas & Fram (2003) offered modified equation for cases where more than one layer of fabric is used, Eq. (3):

$$P = \frac{KnT}{C} \tag{3}$$

where P is the pressure (mmHg), K = 470 is the conversion constant, n is the number of layers, T is the fabric tension (N/cm), and C is the cylinder circumference (cm).

The fabric is extended in both warp and weft directions over the limb. But the fabric tension required for theoretical pressure prediction is achieved from the strain-stress curve of the fabric tested in the circumferential direction within the CG across the leg (weft direction). Tension derived from strain in warp direction is generally not used in theoretical pressure predictions and circumferential direction (weft direction) is the direction assumed that generates pressure on the underlying tissue. The fabric tension (stress) depends on the practical elongation of the garment over the body.

Strain-stress curve is derived from various methods of testing for determination of tensile properties of fabrics. In order to achieve strain-stress curve for a fabric, 'an increasing force is applied gradually to a textile material' (Saville 1999). Standard methods such as BS4952:1992 (Macintyre, Baird & Weedall 2004) and BS2907:1992 (Yildiz 2007) were used for testing fabrics for strain-stress curves. Instruments such as dead weight system (Ghosh, S et al. 2008) or constant rate of extension tensile testing machines such as Instron tensile testing machine (Ng, SF, Parkinson & Schofield 1999; Saville 1999; Thomas & Fram 2003; van der Wegen-Franken et al. 2006), Nene M5 (Macintyre, Baird & Weedall 2004), Zwick dynamometer (Partsch, Partsch & Braun 2006), and biaxial tensile tester (Lin et al. 2010) were chosen by various researchers for determination of tensile properties of fabrics.

S. Ghosh et al. (2008) used dead weight system of loading to analyse the effect of four stress values of 80, 120, 160 and 200 gf/cm on strain of fabrics. The specimen held a constant length to width ratio of 1:2 during the test, with one stationary and one movable wooden clamp. The method engaged by these researchers is over-simplistic and not very accurate. Furthermore, a full strain-stress curve is not achievable with this method, since only four stress loads were applied. Constant rate of extension tensile testing machines are readily available in textile testing laboratories and are more suitable and commonly used to draw strain-stress curve for fabrics.

Thomas & Fram (2003) tested compression bandages for strain-stress curve. They cycled the specimen for four times to 100% strain. They observed that the stress at relative strains decreased as the specimen was cycled from first to fourth cycle. Macintyre, Baird & Weedall (2004) followed standard method BS4952:1992 for determination of tension of fabrics when strained to 25%. The theoretical pressure predicted from fabrics strained to 25%, using Law of Laplace equation, provided a predicted pressure range of less than half to twice the recommended pressure of CGs. Van der Wegen-Franken et al. (2006) strained the specimen in bands, cut out of the CS, six times to its 'maximum circumference' and recorded the maximum stress at the last cycle. Partsch, Partsch & Braun (2006) cut out slices of CSs in sizes Small to Large at

measuring point B1; they cycled the slices for five times to a ‘light overstretch’ according to RAL-GZ (RAL 2008) and on the sixth cycle to the half of the length of their circumference (13.25, 15, and 17 cm for sizes Small, Medium and Large, respectively) and recorded the strain-stress curve.

Various methods were used when testing for tensile properties of fabrics: standard and non-standard methods, testing to various strains and different number of cycles, and testing to ‘maximum circumference’ and ‘light overstretch’. This demonstrates lack of consensus amongst researchers on the suitable testing method for tensile properties of fabrics. The strain and number of cycling of fabrics is important for theoretical pressure prediction; number of cycling of samples influences the relative strain-stress at each cycle as reported by Thomas & Fram (2003). Logically, increasing number of cycles would decrease the amount of stress required to achieve a relative strain, as eventually the fabric becomes exhausted. Furthermore, sufficient information on a wide range of strain is required to enable prediction of pressure for variable leg circumferences.

Gaied, Drapier & Lun (2006) attempted to measure the uni-axial response of the fabric under strain. They cycled the fabric specimens five times to 80% strain. From the recorded stress, they predicted the theoretical pressure for the cylindrical circumference of the leg (average pressure around the leg perimeter - global) as well as considering variable radius of the limb curvature (124 points) along its circumference (pressure at various positions around the leg perimeter - local). The local pressure prediction showed variation in pressure due to curvature of the limb, which was not accounted for in the average (global) pressure prediction.

Despite being a valuable method, the theoretical prediction of local pressure is not practical for each measurement point along the leg and on each human limb, as the measurement of radius and prediction of local pressure even with constant fabric stress is very time-consuming.

From the Law of Laplace equation, the theoretical pressure is directly proportional to fabric tension and inversely proportional to limb radius/circumference. The validity and accuracy of Law of Laplace is widely investigated and addressed in detail in section 2.2.2.

2.2.2. Pressure measurement methods and devices

Researchers have attempted to validate the theoretical pressure generated by CGs using various methods. Validation methods included comparison of the theoretical pressure with measured pressure on rigid cylinders and mannequin legs (‘in vitro’) and on human limbs (‘in vivo’).

Rigid cylinders of variable circumferences usually represented various sizes of human limb, with or without a cover such as neoprene foam, simulating human skin.

S.F. Ng, Parkinson & Schofield (1999) validated the theoretical pressure predicted by Law of Laplace through its comparison to the measured interface pressure over rigid cylinders of various circumferences, representing thigh, forearm and hand. They reported that the measured pressure decreased with increase in cylinder circumference, though not

linearly, and that the measured pressure was inversely proportional to cylinder circumference. Interestingly, they observed that even when the fabric stress was zero, resulting in zero theoretical pressure, some interface pressure was recorded as a result of 'residual or contact pressure' between the CG and the cylinder; the measured contact pressure was dependent on cylinder circumference. So a regression model was produced to predict the measured interface pressure from fabric tension and cylinder circumference. They concluded that the theoretical pressure 'compared favourably' with the measured pressure over rigid cylinders.

Macintyre, Baird & Weedall (2004) employed the same validation method for the theoretical pressure predicted by Law of Laplace. They concluded that at 25% strain in weft direction, the Law of Laplace accurately predicted the pressure induced over 'large' cylinder models (circumference > 30 cm), while the pressure over 'small' cylinder models was overestimated in case of one fabric but estimated with 'variable accuracy' for other fabrics. They also reported that increase in fabric stress increased the pressure induced over same cylinder model and increase in cylinder circumference reduced the induced pressure when the fabric stress was constant, confirming the Law of Laplace.

Lin et al. (2010) attempted to validate the theoretical pressure over a rigid cylinder using fabrics for sports applications. They reported 'fairly good accordance' between the measured and predicted pressure using Law of Laplace at low interface pressures of 10 to 20 mmHg at relatively high range of fabric strains in weft direction (up to 80% strain in weft direction). This suggests that the fabrics investigated were not suitable for SCG applications.

Above findings complied with Law of Laplace, where the pressure was in direct relation to fabric stress and inverse relation to cylinder radius. Meanwhile, Melhuish et al. (2000) findings were not totally in agreement with Law of Laplace. They measured the interface pressure induced from compression bandages over rigid cylinders covered with foam. The interface pressure reduced with increase in cylinder radius, yet the scale of the effect of change in cylinder radius on pressure was not proportional to the change in radius; small changes in cylinder radius had greater influence on pressure than large changes in cylinder radius. They measured the interface pressure over cylinders covered with foam of variable hardness with constant bandage tension and cylinder radius, and concluded that the foam thickness had obvious effect on measured interface pressure; increase in foam hardness increased measured interface pressure. As expected and also observed by Melhuish et al. (2000), the surface properties underlying the CGs, foam simulating human tissue or an actual human tissue, impact the measured interface pressure. The reason for usage of cylinders with rigid surface is to eliminate wide range of variables affecting the measured interface pressure; but these variables must to be taken into account when the pressure is measured over human limb, also mentioned in section 2.2.1 in analysis of pressure at calf cross-section.

In addition to cylinders, mannequin legs were used to represent a human leg, generally with defined ankle and calf or modelled from an actual leg of a human. Mannequin legs had rigid surface to eliminate the complexities of the limb tissue and/or circular circumference to eliminate the complexities of the shape of the limb.

Gaied, Drapier & Lun (2006) measured the interface pressure at multiple locations around the leg perimeter (twelve locations around the calf, fourteen around the knee and seventeen around the mid-thigh) over a mannequin leg 'molded out of plastic' from a real leg. They reported variation in measured pressure around the perimeter of calf region, due to limb morphology; flat and concave areas recorded zero pressure and pressure peaks were recorded at areas where muscle protruded. Same applied to knee and thigh regions with the difference of higher variation of pressure around the knee perimeter due to more unevenness compared to thigh region. Variation in pressure seemed to be directly in relation with limb curvatures and concavity (limb morphology).

When Gaied, Drapier & Lun (2006) compared the mean measured pressure at each region to theoretical pressure predicted by Law of Laplace, they could not explain the difference in pressure values from changes in circumference. According to the researchers, the difference between measured and predicted pressure 'must be related to the geometry' of the region and also the fact that the conditions of tensile testing of fabrics prior to pressure prediction did not match the conditions where the pressure was measured. As reported by same researchers (Gaied, Drapier & Lun 2006), leg geometry influenced the measured pressure due to variations on the measuring site and its possible effect on measurement procedure. The concave area at each section was regarded in the circumferential measurement of the region (added to the circumference), having inverse effect on predicted pressure; while the concave areas recorded zero pressure, which was considered in the mean measured pressure in the region. The limb morphology has an obvious effect on validation of theoretical and measured pressure. For this reason and as mentioned earlier (section 2.2.1), researchers compared the local predicted pressure considering the radius of each location around the circumference with the local measured pressure where 'reasonable agreement' was found between the two.

Wooden model legs of various sizes of Small, Medium and Large, in accordance to medical stocking prescribed sizes, were also used in pressure validation; the pressure was measured at four measuring points of B to D along the model leg (Figure 2.1). Partsch, Partsch & Braun (2006) found comparable results between the theoretical pressure by Law of Laplace and measured pressure over wooden model legs. It must be noted that the wooden legs in Partsch, Partsch & Braun (2006) research had cylindrical circumference in contrast to mannequin leg molded from human leg used by Gaied, Drapier & Lun (2006); thus, the wooden legs with cylindrical circumference were more similar to rigid cylinders, due to elimination of concave and protruding areas around the leg perimeter, and for this reason stronger agreement was noted between the predicted and measured pressure.

The Law of Laplace was stated to be practical in prediction of pressure over rigid surfaces, yet the prediction of pressure over soft tissue was not as straight forward (Melhuish et al. 2000). Limb circumference is far from cylindrical shape; hence, using local radius in prediction of theoretical pressure and validation of measured pressure in comparison to global measured pressure (average pressure around the leg perimeter) is more valid. The definition of the limb morphology at each region, however, is improbable in reality.

Pressure measurement on human leg, ‘in vivo’, is different to ‘in vitro’ pressure measurements, due to complex geometrical shape of the leg as well as biomechanical interaction between the CG and the combination of tissues at various locations along the leg (Gaied, Drapier & Lun 2006; Liu et al. 2005).

Macintyre, Baird & Weedall (2004) attempted to validate the theoretical pressure predicted by Law of Laplace, not only on variable rigid cylinder in sizes Small and Large, but also with measured interface pressure over human forearm and thigh. They stated, as ‘in vitro’ method, that Law of Laplace overestimated the pressure over small limb circumference (forearm) by 10.9 mmHg, which is very significant. Yet the pressure at larger circumference (thigh) was accurately predicted by Law of Laplace.

Liu et al. (2005) measured the interface pressure induced by CSs on human leg at four locations including smallest ankle, widest calf, knee over mid-patella and mid-thigh, and at four positions around the perimeter of each location (anterior, medial, lateral and posterior). They found that the pressure level differed at the same height but around the perimeter of the leg (at four directions). The pressure reading at anterior was the highest while the pressure at medial and lateral positions were the lowest of all four around the leg. This shows that the pressure is not uniformly distributed along the lower leg perimeter. Meanwhile, a study of cross-section images of the four locations mentioned above demonstrated that the pretibial region and Achilles tendon zone caused very high pressure readings in comparison to the pressure readings at the same height but other directions (Liu et al. 2005). A gradient pressure, however, was observed in medial side of the leg from ankle to the thigh region, which is where one of the important superficial veins (long saphenous vein) exists. This agrees with what was discussed earlier about limb morphology ‘in vitro’ pressure measurements.

In most of the studies on ‘in vivo’ pressure measurements generated by CGs, the measured interface pressure was compared to theoretical pressure. Yet in the study by Giele et al. (1997), the measured interface pressure was compared to sub-dermal pressure generated by CGs. It was revealed that the interface pressure recorded over the soft tissue was higher and the interface pressure recorded over bony regions was lower than what was sub-dermally measured over same regions. The reason for difference in interface and sub-dermal pressure was inaccuracies of interface pressure measurement (garment distortion) or the fact that the pressure was not transmitted into the sub-dermis completely. Knowledge on the differences between the interface and sub-dermal pressures increases the efficiency of CG design for specific applications, especially in MCGs, but measurement of sub-dermal pressure is invasive and hardly repeatable.

Number of researchers measured the interface pressure on the legs in standing, supine and when leg was flexed and even when walking to compare the pressure at various postures (Mosti & Mattaliano 2007; Partsch, Partsch & Braun 2006; Stolk, Wegen van der-Franken & Neumann 2004; Wertheim et al. 1999; Wildin et al. 1998). Leg at rest has its minimal circumference; on active standing and walking, however, the limb circumference increases depending on the measuring point, due to muscle contraction and protrusion of muscle tendon. The increase in leg circumference influences the pressure generated by CG over the leg. Different lower leg circumferential measurements in standing and lying was reported in various studies, yet an arbitrary increase of 1 cm is assumed by

researchers (Partsch 2005). Measuring point B1 demonstrated the highest pressure difference between standing and supine (Partsch, Partsch & Braun 2006) and the highest change in circumference was caused by dorsiflexion (Stolk, Wegen van der-Franken & Neumann 2004).

Wildin et al. (1998) measured interface pressure on human models and analysed the effect of posture on interface pressure. For verification of repeatability, they calculated the mean intra- and inter-observer error, which was statistically low relative to accuracy of pressure-measuring device (error of 0.3 and 0.8 mmHg relative to ±4 mmHg device resolution). Different positions investigated were supine, standing, sitting with knee flexed to 45° and 90°. They concluded that the leg geometry influenced the pressure distribution along the limb circumference, similar to what was reported from 'in vitro' interface pressure measurement over rigid mannequin legs. And in regards to body posture, drastic increase in pressure was recorded when ankle or knee flexed. Increased circumferential measurement due to joint flexion led to increase in fabric stress and hence increase in interface pressure. This agrees with what is known about the relation between the fabric tension, limb circumference and the pressure.

Other researchers measured the variations in interface pressure during walking (Stolk, Wegen van der-Franken & Neumann 2004), where continuous pressure measurement was required. Some of the MCGs are required to be worn both when resting and active, thus it is important to know the variation in pressure due to postural change from resting to active. A comfortable low pressure at rest and higher pressures in active state is generally required from MCGs; as a result, analysis of the CG behaviour to postural change is necessary for accurate and efficient pressure delivery to the limb.

In summary, the interface pressure is measured over cylinders, mannequin legs, and human limbs. Depending on the method, some researchers were able to accurately validate the theoretical pressure and some have reported variations between the theoretical and measured pressure. The reason is the method of testing of tensile properties of fabrics, the method, device and the location where the interface pressure was measured as well as the resolution of the measuring device and many other variables causing variations in measured pressure. CGs would be worn over human limbs, which do not have cylindrical circumference nor are rigid by nature; the limb morphology and the combination of tissues at various locations along the leg introduce complexities in measuring the interface pressure. The researchers, however, tend to eliminate or reduce some of the factors influencing the interface pressure to be able to study other factors in more depth and find the relation between each variable and generated interface pressure.

The selected region where the pressure is measured along the human leg is of great importance. The variation in underlying bone, muscle, fat and subcutaneous tissue affects the interface pressure readings along the leg perimeter, as explained earlier. Bony regions of the leg and tendons are not ideal for interface pressure measurement as the measured pressure is under great influence of the hardness of these regions (Melhuish et al. 2000; Partsch et al. 2006), while on soft tissue, the sensor would 'sink into' the tissue under the pressure of CG and the pressure reading would become lower (Liu et al. 2005). The variation in leg geometry causes variation in limb curvature and radius, leading to change in pressure readings and the pressure at concave areas where the garment does not

touch the tissue is zero (Okss & Lyashenko 1999). Apart from that, another very important factor in interface pressure measurement is the measuring device itself.

The pressure sensors used for measurement of interface pressure ideally should have certain properties: they must be flexible to conform to body curvature and must be of a practical size to be able to measure the local pressure (Gaied, Drapier & Lun 2006); the sensor thickness as well as 'local ballooning', in case of some sensors which are inflated with air, must not influence the extensibility of the CG as it will affect the recorded pressure (Liu et al. 2005; Wildin et al. 1998); the sensitivity of the sensor to pressure must be in agreement with the pressure range expected from the CGs (lower end of pressure range, 20 to 60 hPa) (Ferguson-Pell, Hagisawa & Bain 2000; Gaied, Drapier & Lun 2006); the sensor must be accurate, durable, reliable, have high resolution, low cost and many more ideal characteristics (Partsch et al. 2006); furthermore, in case of dynamic pressure measurement (working pressure), the device must have the capability of continuous pressure recording in order to obtain the pressure profile.

Each interface pressure-measuring device and sensor has its advantages and limitations. Fluid-filled sensors and resistance sensors are both used for dynamic pressure measurements; the former is flexible but becomes thick when filled and the latter is thin but sensitive to curvature and stiff. Fluid-filled sensors are thin, flexible and easy to use for static pressure measurements, yet require additional equipment for working pressure measurements (Partsch et al. 2006).

Even though commercial pressure-measuring devices exist, their high costs encourage researchers in developing pressure monitors themselves. The research outcomes resulted from use of both commercial and developed devices could be reliable, as long as accuracy and reproducibility of data are thoroughly investigated. Some researchers calibrated the pressure-measuring devices according to instruction of the manufacturers and some analysed the accuracy and reproducibility of the pressure readings by various additional calibration methods and tests, and came up with recommendations regarding the device.

An interface pressure-measuring device was developed by Sawada (1993) using a rubber balloon, a catheter and a control-inflator (VBM). This device measured the pressure in a range of zero to 88 mmHg, which is a wide range of pressure considering the expected pressure induced by CGs. The device was calibrated using a simulated air chamber. The researcher placed the sensor in a closed rubber bag, where it was compressed and the pressure was measured with a manometer. The device accurately matched the pressure reading from the manometer within the pressure range mentioned above.

Hafner et al. (2000) also used rubber bag, filled with silicon oil, and a piezoresistive pressure transducer. They calibrated the pressure sensor in a range of zero to 120 mmHg by suspending the sensor vertically in air for zero pressure and measuring the pressure induced by a sphygmomanometer placed over the sensor at gaiter area. To verify the accuracy of the sensors, they also compared the pressure readings of the device induced by medical CSs to the compression classes of stockings provided by the manufacturer. They reported pressure accuracy of ±3 mmHg. The verification of accuracy of a pressure-measuring device over human limb is complicated due to complexities of human limb and

its effect on pressure readings, mentioned earlier. Furthermore, the compression classes of medical CSs is not an accurate measure for validity of a pressure-measuring device; the variable pressure measurement conditions and techniques could lead to discrepancies between the pressure readings by manufacturers and researchers.

A developed pressure-measuring device mounted on a plastic cylinder with its diameter measuring 10.2 cm was used by King & Doessler (2001). They mounted five resistance sensors, diameter of each measuring 1.3 cm, in a line across the length of the cylinder at 2.5 cm intervals. A digital voltmeter was attached to each sensor point, converting the applied pressure into voltage. According to the manufacturer of the resistance sensors, the sensors required calibration after every fifty measurements or every three months; yet due to variability and lack of reliability of the sensor resistors, researchers exerted pressure using a sphygmomanometer at each sensor point and then converted the voltage to pressure in Millimetres of Mercury after each set of measurements. This method ensured correct conversion of voltage to pressure.

Another developed device was used by S. Ghosh et al. (2008), for measurement of interface pressure over mannequin leg. The device consisted of 'three resistance foil strain gauges' inserted into the mannequin leg with protruding pins which detected the pressure induced by CG. Researchers calibrated the device using dead weight system.

Temperature-compensated Fontanometer sensor, based on 'strain gauge principle', was used for interface pressure measurement by Wertheim et al. (1999). The rectangular sensor was situated on one side of a rigid disc with 3 mm thickness and 12.6 mm diameter. Not being pneumatic or fluid-filled, this sensor could be used for both static and dynamic interface pressure measurements (±3 mmHg accuracy). The sensor was calibrated using a water column and an air chamber. Despite being capable of recording dynamic interface pressure, this sensor was rigid and relatively thick, which inhibits its conformation to body curvature and causes excessive strain in CGs.

Textilepress was a pressure-measuring matrix based on Law of Laplace (Maklewska et al. 2007). It consisted of 70x50 mm measuring field and two types of measuring tensometric sensors, one sensor measuring the radius of curvature and the other the fabric tension. This device had a high resolution of ±1 mmHg but narrow measuring pressure range of 0.70 mmHg ±10% and minimum bending radius of 20 mm.

Oxford Pressure Monitor MK II (OPM), an electro-pneumatic sensor, was used by various researchers for interface pressure measurement (Hui & Ng 2001; Ng, SFF & Hui 1999; Veraart, Pronk & Neumann 1997; Wildin et al. 1998). OPM had flexible cell sensor of 20 mm in diameter with a pressure range of zero to 300 mmHg and accuracy of ±4 mmHg. The device was calibrated prior to pressure measurement with the use of sphygmomanometer and a clamp provided by the manufacturer. The device was pneumatic, thus the pressure was measured with the sensor cell being pumped with air; yet the small dimensions of the cell (2 cm^3) did not cause significant ballooning, and therefore it did not affect the fabric strain and recorded pressure (Wildin et al. 1998).

Kikuhime pressure-measuring device was also used by many researchers (Mosti & Mattaliano 2007; Partsch 2005; Van den Kerckhove et al. 2007). It was a flexible pneumatic interface pressure sensor with an oval polyurethane balloon, 30x38 mm in

dimensions and 3 mm thick polyurethane foam sheet at zero pressure (Flaud, Bassez & Counord 2010). Before the pressure measurement was taken, the balloon was pumped with air using a syringe, in order to get a stabilized reading of zero pressure. The pressure was then transmitted directly from the balloon to the transducer. Partsch (2005) calibrated the sensor fifteen times at 20, 40, 60, 80 and 100 mmHg with the use of sphygmomanometer on human limb at measuring point B1 and compared the pressure readings from the sensor to the manometer reading. Partsch (2005) reported the percent deviation between the manometer and the device as a measure of accuracy, and coefficient of variation as a measure of precision of the device. Highest precision of the sensor was recorded for higher pressure ranges and highest accuracy was recorded at 80 mmHg, while least accuracy and precision at 20 mmHg with 3 mmHg deviation and 7.1% coefficient of variation. Later on, Mosti & Mattaliano (2007) relied on Partsch's (2005) analysis of accuracy and precision of the device and did not investigate it any further in their research.

The pressure range expected from CGs are not always as high as 80 mmHg, where Kikuhime device was most accurate and precise; and 3 mmHg deviation is not significant as most pressure-measuring devices have an accuracy pressure range of 3 to 4 mmHg as mentioned earlier. Yet, calibration of a pressure sensor over human limb adds more variability to the equation, which could be limited by calibration over rigid surfaces.

For measure of accuracy of the same device (Kikuhime pressure-measuring device), Van den Kerckhove et al. (2007) used a water column for its calibration; unlike Partsch (2005), they reported linear relationship between the water column pressure and measured pressure from the device, even at low pressure of 20 mmHg. Furthermore, the 3 mm thickness of the sensor increased the limb circumference by 3 mm, leading to 1 and 1.25 mmHg increase in pressure recording of various fabrics, depending on tensile behaviour of fabrics. Flaud, Bassez & Counord (2010) confirmed the linearity of the measured pressure of the same device with the reference pressure, tested in a pressurised chamber. They also reported low systematic error (global error of 4.3% with a bias of -1.4 mmHg), repeatability and sensitivity to bending of 15%, which was not higher than the systematic error of the device.

Macintyre (2007) used I-scan 9801, a temperature sensitive sensor with six columns and sixteen sensing cells. The device had a wide pressure measurement range of zero to 260 mmHg, adjustable to narrower range with higher sensitivity according to the application. The sensor was equilibrated using a bladder tester at four different loads, according to recommendation of manufacturer (Macintyre 2011). A bladder tester inserted uniform pressure over the sensor cells. Macintyre (2007) used this device to measure the pressure inserted by CGs on cylinders and human limbs. She calibrated the sensors before and after each of every ten measurements. Regression equation derived from calibrating the sensor with a calibrated sphygmomanometer was applied to raw data. In this way, accurate and reliable measurements (±2.5 mmHg accuracy) were enabled in a pressure range of 3 to 50 mmHg.

In 2011, the researcher revisited the calibration method for I-scan 9801 (Macintyre). She studied the effect of different materials used in calibration process and in contact with the sensor cells. Polyurethane foam with 3 mm thickness and a highly polished steel

weight was found to provide consistent results when calibrating. A two-point power law calibration was done using the set-up mentioned above (foam and weights) on flat surface, providing 20 and 80% of maximum expected load. A two-point power law calibration is useful where wide range or load/pressure is required. Despite the findings of other researchers and after the equilibration of sensor cells, the variation between the pressure reading of cells were significant and Macintyre (2011) did not find the sensors reliable and accurate after this calibration method. She then calibrated the sensors using a calibrated sphygmomanometer over a foam covered glass cylinder at zero and six different pressures (7.4 to 44.4 mmHg). Forty accurate and reliable measurements could be made on a calibrated sensor from this method. She then used the same principles (cylinder and sphygmomanometer) and further improved the calibration method so that the pressure measurements were accurate and reproducible with maximum discrepancy of 2.1 mmHg between measured and applied pressure. She reported that this method was applicable to cylinders with +30 cm circumference. The reason for the cylinder circumference recommendation could be that cylinders with smaller circumferences would cause further bending of the sensors, discarding the calibration. Finally, the developed improved method led to acceptable calibration (Macintyre 2011).

The requirement for lengthy calibration after few measurements is time-consuming and not practical and the sourcing of the most suitable material is problematic, as also reported by the researcher. A pressure-measuring sensor with higher accuracy and less likely to have a drift after certain number of measurements, is more efficient, especially in commercial applications.

Talley pressure monitor consisted of a ‘disc-shaped polyvinyl chloride (PVC) sensor cell’ with 0.5 mm thickness and resolution of 0.1 mmHg (Flaud, Bassez & Counord 2010). The sensor was pumped with air, where the electrical contacts on both sides of the sensor cells lost contact. The air was then slowly released and when the electrical contacts on sensor cells made contact again, the pressure was recorded. There were two sensor cell sizes of 28 and 100 mm in diameter. V. Allen, Ryan & Murray (1993) calibrated the device using foam and weights and reported global error of 12% and repeatability with a range of 0.52 mmHg. Williams, Knapp & Wall (1998) found Talley Model SD500 to be unreliable in interface pressure measurement, due to wide range of pressure measurements for one set of MCG at one site of measurement. Chan & Fan (2002) calibrated the device using a sphygmomanometer and did not reveal the results. Yet, Flaud, Bassez & Counord (2010) listed linear response to reference pressure from a pressurised chamber, low systematic error of 3% with a bias of -0.3 mmHg (lower than the resolution of the device) and repeatability of the results. Yet the error of pressure measurement due to flexion of the sensor was relatively high (up to 36%). This was also reported for Talley pressure monitor by Bain (PhD thesis 1997) in (Ferguson-Pell, Hagisawa & Bain 2000).

Ferguson-Pell, Hagisawa & Bain (2000) used Flexiforce by Tekscan. The device had a thin flexible fluid-filled interface pressure sensor using a pressure-sensitive ink. The change in electrical resistance of the ink within the sensor changed inversely with change in applied pressure (Ferguson-Pell, Hagisawa & Bain 2000). Researchers tested the sensor for drift, linearity, repeatability, hysteresis using various weights and for response to flexion using cylinders and pressurised sleeve. They observed that the sensor had acceptable repeatability, linearity and hysteresis, while showing higher variability at lower

pressures. Similar to Talley pressure monitor, the flexion of the sensor significantly affected the pressure readings at small radii of curvature (< 32 mm). Liu et al. (2007; 2005) used the same sensor; they calibrated the pressure sensor, using different weight levels of 5 to 55 g and recorded the corresponding voltage signals induced from the weight covering the sensor area of 71.1 mm^2 (2005).Pressure-voltage corresponding relationship was found to be linear and it was used for sensor calibration. Lin et al. (2010) used the same calibration method and did not report the outcomes.

SIGaT® sensor, developed in 1997, was a pneumatic sensor. It had a pocket sensor in two sizes of 30x30 mm^2 or 60x50 mm^2. The device measured the interface pressure by inflation with air at constant flow (Gaied, Drapier & Lun 2006). The pressure was recorded when the air pressure in the plastic pocket sensor was equal to pressure induced by CG. Gaied, Drapier & Lun (2006) calibrated the SIGaT® sensor, by immersion under water of a known depth, and verified measured pressure validity through reproducibility of results with statistically low mean scatter of ten pressure readings (below 7%). Different sized sensors recorded various pressures mainly due to pressure-measuring site morphology; larger sensor was found to be more sensitive to sharp variations around the limb perimeter. Researchers concluded that the integration of pressure in three dimensions influenced the recorded measured pressure and that the longitudinal curvature as well as transverse curvature and the sensor size affected the pressure measurement. This suggests that the pressure measurement over mannequin legs or human legs with variable curvature in three dimensions is different to the measured pressure over cylinders with only transverse curvature in one direction.

Medical Stocking Tester (MST) employed the same pressure-measuring method as SIGaT® sensor; the only difference was that MST pumped in the air automatically when the test started, while SIGaT® sensor was inflated using manual pump. MST by Salzmann had thin plastic sleeves (0.5 mm in thickness), with four or six paired electrical contact probes (Finnie 2000; Flaud, Bassez & Counord 2010). The sensor probe was inflated until the contacts were broken and the pressure within the sensor sleeve at each point was slightly over the pressure inserted over the probe. Simultaneous pressure measurement at four to six points is possible using MST sensors in short and long length, respectively. Dale et al. (2004) and Partsch, Partsch & Braun (2006) did not investigate calibration for MST pressure monitor, due to report of consistency from previous researchers. Alternatively, Flaud, Bassez & Counord (2010) thoroughly investigated the linearity of the response, measurement accuracy, repeatability, and sensitivity of the probe to bending of MST MKIII device; they tested the sensor probe on a flat surface within a pressurised chamber at six different levels for the measure of linearity; measurement of repeatability was tested nine times at the pressure level of 25 mmHg, again at the flat surface within the pressurised chamber; the sensitivity to bending was measured by measuring the pressure over two cylinders of 5 and 10 cm in diameter at two pressure levels of 10 and 30 mmHg within the pressurised chamber and was compared to the pressure readings from the flat surface in the same conditions. Linearity was found between the reference and measured pressure; the global error (measure of accuracy) was 15.4% with bias of 3 mmHg and the standard deviation of the measurements (measure of repeatability) was smaller than the resolution of the device (1 mmHg); the device was found sensitive to bending, as the measured pressure on curved surface was lower than the flat (measurement error of < 15%), and higher bent caused further decrease in pressure; the

measurement error due to flexion was, however, similar to systematic error. The researchers explained that the measurement mechanism of the device required the two sides of the probe to detach, causing the relatively high systematic error. They also referred to reports from other researchers on the same device; the repeatability error was slightly higher yet smaller than the resolution of the device.

Table 2.2 provides a brief comparison between the various pressure measuring sensors used by researchers.

Table 2.2 Reported advantages and disadvantages of various pressure measuring sensors

Pressure measuring sensor	Advantages	Disadvantages
Fontanometer Sensor	▪ Measuring static and dynamic interface pressure measurement ▪ ±3 mmHg accuracy	▪ Rigid ▪ Thick
Textilepress	▪ ±1 mmHg accuracy ▪ Measuring the radius of curvature and the fabric tension	▪ 0.70 ±10% mmHg pressure range ▪ 20 mm minimum bending radius
Oxford Pressure Monitor MK II	▪ Flexible cell sensor ▪ 0-300 mmHg pressure range	▪ ±4 mmHg accuracy
Kikuhime Pressure-Measuring Device	▪ Flexible ▪ 3 mmHg deviation	▪ Variable reports on accuracy ▪ Thick (3mm)
I-scan 9801	▪ Adjustable pressure range (0-260 mmHg)	▪ Temperature sensitive ▪ Requiring repeated calibration
Talley Pressure Monitor	▪ Thin (0.5 mm) ▪ ±0.1 mmHg accuracy ▪ 2 size sensors	▪ Sensitive to bending ▪ Variable reports on accuracy
Flexiforce	▪ Thin ▪ Flexible	▪ High variability at low pressure range ▪ Sensitive to bending
SIGaT® sensor	▪ 2 size sensors	▪ Sensor size affecting the measured pressure
Medical Stocking Tester	▪ Thin (0.5 mm) ▪ Four or six paired electrical contact probes ▪ ±1 mmHg accuracy	▪ Sensitive to bending

Various pressure measurement devices, employing various techniques to measure the pressure, and various calibration methods were used by researchers to investigate the accuracy and reliability of the pressure-measuring device. Calibration methods included pressurised chamber, water column and various weights, over flat and curved surfaces. Low systematic error independent to pressure range, reproducible measurements, thin and flexible sensors with low sensitivity to flexion, ease of calibration and sensor

placement between the limb and the CG, and in some cases real time data recording and portability depending on the application were characteristics required from interface pressure-measuring devices. It is important that the sensors used for pressure measurement are thin, flexible and have low sensitivity to bending; as ultimately the pressure must be measured over human limb with various curvatures; for instance point B at ankle is an important and difficult measuring site: with extensive variations in curvature and thus wide variations in radii along its circumference due to bony prominences as well as the tendon projecting. In conclusion, MST pressure monitor (Salzmann) is found to be relatively suitable for interface pressure measurement; as reportedly it has more advantages for interface pressure measurements than shortcomings.

2.2.3. Summary

Researchers have attempted to predict the pressure generated by CGs with various methods: mathematical/numerical modelling using FE method and approximation of Law of Laplace. The shortcoming of FE method is inaccuracy in representation of soft tissue elastic characteristics, which limits its practicality for theoretical prediction of pressure. Furthermore, not all the models developed by the researchers were validated with measured pressure over human limbs. While Law of Laplace is used widely in theoretical prediction of pressure generated by CGs over a limb with known radius, and its validity and accuracy is widely investigated. From the Law of Laplace, the theoretical pressure is directly proportional to fabric tension and inversely proportional to limb radius/circumference. It seems that even though Law of Laplace does not incorporate soft tissue characteristics either, it is most practical and most suitable for theoretical pressure prediction.

Theoretical pressure is usually validated by its comparison to measured interface pressure. Interface pressure is influenced by many variables such as the interface pressure-measuring device (its mechanism and accuracy), measuring site and the surface properties underlying the CG, limb morphology, and human posture. For this reason, researchers tend to reduce/eliminate some of the variables affecting the induced interface pressure by CGs, to be able to study other factors in more depth. An actual human limb does not have cylindrical circumference and is not rigid by nature, and the surface geometry and limb morphology introduce complexities in measuring the interface pressure. Thus, the interface pressure is measured over rigid cylinders, mannequin legs, as well as on human limbs.

Some researchers were able to accurately validate the theoretical pressure and some reported variations. One researcher noted that Law of Laplace accurately predicted the pressure over cylinders with small circumferences, while overestimated the large ones; while another group of researchers observed that even when the fabric stress was zero resulting in zero theoretical pressure, some interface pressure was recorded. ‘Fairly good accordance’ between the measured and predicted pressure using Law of Laplace was reported by one group, while other results were not totally in agreement with Law of Laplace.

One cause of variations in reported outcomes is the interface pressure-measuring device. An ideal interface pressure-measuring sensor must be flexible to conform to body curvature and of a practical size to be able to measure the local pressure. It must not cause 'local ballooning' and must not influence the extensibility of the CG. The sensitivity of the sensor to pressure must be in agreement with the pressure range expected from the CGs and the sensor must be accurate, durable, and reliable, with high resolution, low cost and many more ideal characteristics. On the other hand, the accuracy and reliability of interface pressure-measuring devices were usually evaluated by researchers through various means: dead weight system, sphygmomanometer, water column and air chamber.

In summary, from various pressure measurement devices available commercially, MST pressure monitor (Salzmann) is found to be relatively suitable for interface pressure measurement for CGs: it is thin and flexible, enabling simultaneous pressure measurement over several anatomical sites along the limb, accurate, reliable with small sensitivity to bending and is used commercially in medical industry.

2.3. Compression garments and comfort

Clothing must fulfil the needs defined by their intended use. SCGs are intended to enhance performance and recovery of the wearer but they are also intended to provide comfort. Comfort could be defined as 'physiological function' of sportswear (Bartels 2005); comfort is defined by Slater (1986) as 'a pleasant state of physiological, psychological and physical harmony between human being and his environment'. He also stated that comfort is a 'subjective phenomenon'. Thus, objective and subjective techniques are used in evaluation of comfort.

Comfort has four aspects: thermo-physiological, ergonomic, tactile and psychological comfort (Bartels 2011). Thermo-physiological comfort deals with the interaction of the clothing and thermo-regulation of the body; ergonomic wear comfort deals with clothing fit and ease of movement; tactile comfort deals with the interaction of the clothing and the skin, and psychological comfort deals with subjective comfort sensation towards fashion, brand, colour, and pattern.

2.3.1. Thermo-physiological wear comfort

Thermal balance of human body is maintained when the heat produced from metabolism and gained from the environment equals the heat lost by conduction, convection, radiation and evaporation (Gavin 2003). Thermo-physiological comfort of human depends on climate, clothing, and physical activity (Das & Alagirusamy 2010).

Clothing is considered as a system which interacts with the body (Fourt & Hollies 1970) and must support thermoregulation of the body by maintaining its thermal balance (constant body core temperature of 37°C) and providing a comfortable microclimate next to the skin (Das & Alagirusamy 2010; Li & Wong 2006). The heat generated from the body in extreme activities is controlled by varying skin temperature as well as varying perspiration rates providing evaporative cooling (Fan 2009), and the clothing must assist

the human thermoregulation system in various conditions, including transmission of heat from the skin and moisture from perspiration and sweating to the outer environment. In sport activities, the heat must be dissipated through sportswear to prevent overheating (Bartels 2011); if the perspiration in both forms of vapour (insensible) and liquid (sensible) cannot escape the skin and the garment next to the skin, the build-up of moisture on the skin compromises the comfort of the wearer (Fan 2009); in addition, it will also compromise the thermal insulation of clothing and cause body heat loss and post-exercise chill (Bartels 2011; Das & Alagirusamy 2010). The thermo-physiological or thermal wear comfort of clothing is evaluated through its moisture management (moisture permeability and liquid-water transport), and thermal and vapour resistance/insulation (Fan 2009).

Thermal insulation of fabrics depends on their fibre content, density, thickness, amount of air and moisture within the fabric, fabric weight, number of layers, air gap between the skin and the fabric, and wind velocity (Fan 2009; Majumdar, Mukhopadhyay & Yadav 2010). Thermal insulation is measured for fabrics comprising the garments, and garments themselves separately; as the thermo-physiological properties of fabrics cannot be directly translated into thermo-physiological properties of garments, due to other parameters such as the amount and part of body covered by the garment (clothing area factor), weight, layers, fit, the resultant air gap between the body and garment, variable temperature on different body parts and body positioning and movement influencing the thermal insulation of garments (Fan 2009; Huang 2006a; McCullough 1993). The same applies to water-vapour resistance of fabrics and garments.

Since SCGs have a negative fit, there is no air gap affecting their thermal insulation and vapour resistance. Some SCGs, however, have various fabrics composing the garment which may function as garment opening: mesh fabric is inserted in areas such as behind the knee or under the arm; depending on the properties of the mesh fabric and the amount of the fabric used, the overall thermal insulation of the garment is affected.

In high activity levels and hot environments, water-vapour resistance of fabric/garment becomes more important in the characterisation of thermo-physiological comfort (Huang 2006a). Water-vapour is transmitted through fabrics by diffusion and penetration in spaces between fibres, absorption by fibres and transfer and desorption within fibres as explained by Mecheels (1971) in (Hatch et al. 1990). Vapour transmission of clothing depends on type and moisture content of the fabric, perspiration rate as well as atmospheric conditions including temperature, humidity and wind velocity and demonstrates how well the fabric could transfer the insensible perspiration from the skin to the outer environment (Das & Alagirusamy 2010).

Interaction of liquid and fabric depends on various factors: ‘wettability of fibres, their surface geometry, the capillary geometry of the material, the amount and nature of the liquid, and the external forces’ (Kissa 1996). Liquid-water is transferred by two mechanisms: transfer through capillary interstices in yarns, and migration of water on fibre surfaces as explained by Mecheels (1971) in (Hatch et al. 1990). Liquid-water transmission of fabrics depends on fibre type and cross-section, fabric construction, weight, thickness and surface contact area with water and surface treatment (Fan 2009).

Many researchers investigated the effects of variable parameters, such as fibre, yarn and fabric properties, on thermo-physiological comfort of fabrics. Most fabrics, especially

knitted fabrics, have air trapped within their structure; thus when analysing the thermo-physiological comfort of fabrics, both systems including the fabric parameters as well as air, must be taken into account. Air has lower thermal conductivity (by ten times) than most fibres (Salopek Čubrić et al. 2012) and is known to act as an insulator (Bhattacharjee & Kothari 2009); hence, the presence of air within the fabric structure has potential effect on the thermo-physiological comfort of fabrics. Furthermore, air velocity over the fabric sample influences its thermal and water-vapour resistance (Huang 2006a), especially in fabrics with high air permeability, where increased air permeability decreased thermal and water-vapour resistance (Gibson 1993). At low air velocity, the resistance of boundary air layer above the fabric sample becomes more paramount than the resistance of the fabric itself, while higher air velocity improves the heat loss through convection and reduces the resistance of fabric to heat and evaporation (Hatch et al. 1990; Huang 2006a); especially when there is a gap between the fabric and skin which allows the air to pass though the fabric construction (Hatch et al. 1990). Furthermore, in transient conditions, the 'ventilating motion of air through the fabric' due to body motion increases the complexity of influence of air on thermal-physiological comfort (Rengasamy 2011).

Fabric thickness determines the distance that the heat and vapour must pass through from one side of the fabric to the other, and it has been reported as one of the paramount fabric parameters influencing thermal and water-vapour resistance of fabrics by many researchers (Bedek et al. 2011; McCullough 1993; Prahsarn, Barker & Gupta 2005; Salopek Čubrić et al. 2012). Bedek et al. (2011) observed a positive relationship between thickness and thermal and vapour resistance of fabrics.

Fabric porosity is the portion of air volume to the total volume of the fabric and was also found to be influential on both thermal and vapour resistance of fabrics (McCullough 1993) as well as the overall moisture management capability (OMMC) of fabrics measured on Moisture Management Tester (MMT) (Bedek et al. 2011). Porosity is calculated from mass per unit area of the fabric, fabric thickness and fibre density (Skinkle 1940), while it is also affected by stitch density (Dias & Delkumburewatte 2008). Dias & Delkumburewatte (2008) observed that a decrease in stitch density increased the fabric porosity and Hatch et al. (1990) reported that increased porosity led to lower thermal conductivity due to presence of more air within the fabric structure, where lower thermal conductivity led to higher thermal resistance. While in another study, decreased fabric thickness and mass per unit area was reported to increase porosity (more air within the structure), which in turn resulted in lower thermal resistance due to lower resistance to heat transfer (Salopek Čubrić et al. 2012). The degree to which each physical fabric parameter changes, influences the observed outcome, which in this case was the thermal resistance of fabric. As reported by Hatch et al. (1990), it was expected that an increase in porosity would result in higher thermal resistance, yet the decrease in thickness and mass per unit area must have had a greater influence on the observed thermal resistance of the fabric by Salopek Čubrić et al. (2012).

Furthermore, the distribution of pores within the fabric structure also influences the thermal resistance of fabrics and not just the amount of air within the fabric; therefore, in analysis of thermo-physiological comfort property of fabrics, sum of variable parameters and testing conditions must be taken into account, before coming up with a conclusion on the influence of one parameter on the observed outcome. As explained earlier, the testing

conditions such as air velocity, temperature and existence of air gap significantly influences the effect of presence of air within the fabric structure on the measured parameter, which could have contributed to the earlier contradictive reports.

Optical porosity is ‘expressed as transmittance (%) of visible light through fabric’ (Hatch et al. 1990). Black and white pixels from microscopic image of fabric represent fibres and open pores, respectively, and the percentage of white pixels to all the pixels (black and white pixels) in the area of the image is the optical porosity of the fabric.

From this method, pore size of the fabric structure can also be measured. Pore size within the fabric structure impacts absorption/wicking characteristics, thermal insulation, and the tactile properties of the fabric (Karaguzel 2004). Fabric pore size is influenced by stitch density, where an increase in stitch density reduced the pore size within the fabric structure, resulting in reduced air permeability (reduced air space) and led to lower moisture absorption rate (Karaguzel 2004). It is assumed that water-vapour is transferred from one side of the fabric to the other through fabric spaces by diffusion in air (Karaguzel 2004) and as mentioned earlier, reduction of air permeability increases the water-vapour resistance (Gibson 1993); therefore, a conclusion can be made that reduced pore size increases water-vapour resistance of fabrics.

Fabric stitch density and mass per unit area are strongly correlated; where an increase in stitch density, increased the mass per unit area of the fabric (Karaguzel 2004). Fabric thickness, mass per unit area and stitch density have inverse and fabric pore size has a direct relationship with fabric air permeability (Karaguzel 2004; Majumdar, Mukhopadhyay & Yadav 2010). High air permeability resulted in better thermal conductivity and heat transfer (Bedek et al. 2011; Huang 2006a); the reason being greater pore size, enabling heat to be transferred more readily. Additionally, optimum moisture vapour dissipation of fabrics was reported to be affected by low thickness and high air permeability (Prahsarn, Barker & Gupta 2005); yet even though, Hatch et al. (1990) observed higher water-vapour transmission through thinner and more porous fabrics, the difference in water-vapour transmission was not significant.

Wickability and liquid-water transfer of fabrics were observed to be influenced by hydrophilicity and surface energy of fibres (Hatch et al. 1990), as well as pore size and porosity of fabrics (Karaguzel 2004). The liquid could be transferred through the fabric pores ‘following a torturous path’ (Karaguzel 2004). Hydrophilicity of fibres increases the number of water absorbing groups, increasing the moisture regain of the fabric (Bedek et al. 2011) and higher surface energy of fibres results in higher wickability of fabrics (Hatch et al. 1990). Greater pore size resulted in higher moisture absorption rate (Karaguzel 2004), while fabric porosity was reported to have inverse relationship with OMMC of fabrics measured on MMT (Bedek et al. 2011). Lastly, hydrophilic finish on the inner side of fabric enhances the wicking rate of the fabric (Rengasamy 2011). Hydrophilic finishes are usually applied to nylon and polyester fabrics and especially in sportswear, in order to change the ‘interfacial tension’ and improve the wickability of the fabric in both horizontal and vertical direction (Hatch 1993); horizontal wicking defines the spreading of the liquid over the fabric surface, while vertical wicking demonstrates the movement of water through the fabric thickness.

The above mentioned correlations are applicable when thermo-physiological properties of fabrics are tested under steady state. Higher thermal conductivity of fibres was reported to result in reduced thermal resistance of fabrics with strong correlation by one group of researchers (Bedek et al. 2011), which itself (thermal conductivity of fibres) had positive relation with fibre moisture content (Hatch et al. 1990). Hatch et al. (1990) and McCullough (1993) found that fibre type had smaller and little effect on clothing insulation in steady state compared to fabric thickness, respectively; while the latter researcher, reported fibre type and finishes affected the heat and water-vapour resistance in transient conditions (McCullough 1993), possibly due to variable temperature and humidity. As the human body is not normally under steady state, the changes in physiological and environmental conditions would influence the thermo-physiological comfort properties of clothing (Huang 2006b); for instance, variations in air velocity, while in movement, affects the clothing insulation (both thermal and water-vapour insulation) (McCullough 1993); for this reason, the response of fabric/garment to transient conditions is also very important to be evaluated.

Prevention of heat stress could lead to competitive performance for the athlete and unnecessary heat and moisture next to the skin could have adverse effects on both performance and health. This is the reason why manufacturers use various technologies to provide enhanced thermo-physiological comfort for the wearer through their garments.

2.3.2. Ergonomic wear comfort and fit of the garment

A well-fitted garment must not interfere, impede or restrict the body movement relative to the end-use, activity and range of movement expected; this is the ergonomic wear comfort of clothing and it also extends to donning and doffing of the garment. When the garment impedes or restricts the body movement, it causes discomfort as well as increased metabolic cost (Ashdown 2011). Further, restricted cardio-vascular flow, skin abrasion, uncomfortable thermal or moisture condition and irritation can be derived from ill-fitting garments (Das & Alagirusamy 2010; Slater 1977).

Ergonomic wear comfort of garment depends on the garment construction and the elastomeric properties of the fabric(s) composing the garment (Bartels 2005).

Fabric properties affecting the body movement are weight, thickness, stiffness, stretch and recovery. SCGs are made of elastomeric knitted fabrics; knitted fabrics have inherent stretchability due to their construction, while introduction of elastomeric yarns would enhance their stretchability. Elastomeric fabrics provide controlled stretch and recovery, maintain shape and do not restrict body movement (Voyce, Dafniotis & Towlson 2005); they interact with the body and synchronize with movement, meaning they stretch when needed and recover when strain is removed. Range of extensibility as well as recovery from extension expected for various types of garments are reported (Ashdown 2011); yet in case of CGs, intended pressure dictates the required range of extensibility of the fabric, which depends on its elastomeric properties.

Pressure comfort of clothing is one of the aspects of ergonomic wear comfort and is related to the size, style and fit of the garment as well as fabrics properties (Das &

Alagirusamy 2010). SCGs support the wearer by generating pressure over underlying limb and holding the muscles and fat tissue in place (Ashdown 2011). The wearer is aware that pressure is a function of CG, so the tolerance and pressure range defined for ergonomic wear comfort of non-compressive garments are not applicable to CGs.

Garment construction influences its fit and the resultant wear comfort. Incremental or proportional approaches for pattern grading was used for many years, to provide range of sizes; but this method is problematic in gaining proper fit for a wide range of population with wide range of body shapes and proportions (Watkins 2011). Furthermore, body dimensions change in various activities and positions; human body expands and contracts in areas surrounding the joints in movements and so should the garment (Fan 2009): for instance, the elbows, the back, the seat and the knees are known as critical strain areas in the body (Li 2001).

Ergonomic wear comfort and functionality of sportswear is achievable by development of patterns where the static and dynamic sport needs are taken into account (Ashdown 2011): an example would be functional panel designs for cycling shorts, which follows body contour when the wearer is in cycling position (Liu & Little 2009). Acquisition of accurate body measurements in both static and active positions, however, is difficult. Yet rapid development of 3D body-scanners has the potential in surmounting this issue, which would result in garments with proper fit and ergonomic wear comfort. Meanwhile, subjective analysis (wear trials) is a method generally used for assessment of fit and wear comfort of clothing; in wear trials, a fit model who best describes the intended user of the garment would wear and trial the garment in the intended end-use conditions.

In the future, virtual simulation of garment fit with regards to fabric properties could replace the fit model, when the software will be more sophisticated in simulation of true fabric properties as well as human body parts and movements. The 3D body-scanning and garment virtual simulation could lead to production of made-to-measure garments instead of ready-made, providing perfect fit for each body size. This technology could also be used in analysis of body changes in active positions. The sizing system and 3D body-scanning application in acquisition of body measurements is discussed in more detail in section 2.4.

Testing standards such as method for ‘evaluating the comfort, fit and function of chemical protective suits’, ASTM STP 1154-1988 (Ashdown 2011), are a good strategy in analysis and quality control of garments. Development of testing standards for each type of garment concerning the comfort, fit and function according to activities and movements expected for the end-use could help manufacturers in evaluating and improving the ergonomic comfort of the garments. Taking into account the movements expected when wearing the garment from the first steps of the design, effective sizing systems and understanding body shape enable production of ergonomically comfortable and perfect fitting garments by manufacturers.

2.3.3. Tactile comfort

Tactile or neuro-physiological comfort of clothing is the 'mechanical sensations, which a textile causes at direct contact with the skin' (Bartels 2005). Garments and skin are in contact dynamically and continuously, causing touch sensation (Das & Alagirusamy 2011). Skin responds to physical stimuli (Kilinc-Balci 2011a), which is the static contact with the garment; while body movement, change in skin temperature and moisture content at skin surface generates new stimuli (Kilinc-Balci 2011b).

Tactile wear comfort depends on fabric tactile properties, skin properties, environmental conditions, activity level and garment fit (Kilinc-Balci 2011a). Tactile properties of fabrics are expressed as fabric prickliness, itchiness, stiffness, softness, dampness, clinginess, roughness, friction and the like (Barker 2002; Das & Alagirusamy 2011; Kilinc-Balci 2011b). It can be measured by evaluation of parameters such as number of surface fibres and contact points, wet cling to surface, absorptivity, bending stiffness, resistance to shear and tensile forces and coolness to touch which are mainly determined by fibre, yarn and fabric characteristics and fabric construction and finishes (Barker 2002).

Fabric-evoked itch and prickle, two of main reasons of discomfort, are mechanical stimuli activating superficial pain group of sensory receptors (Kilinc-Balci 2011a); they are caused by protruding fibres from the surface of the fabric and may cause skin inflammation (Das & Alagirusamy 2011). Fibre diameter, fabric thickness, surface roughness, cover factor and finishes as well as area of contact between fabric and skin, moisture content of the skin, gender and age influence the itch and prickle sensed from fabrics (Das & Alagirusamy 2011; Kilinc-Balci 2011a).

Roughness is sensed by touch group receptors, when fabric moves across and displaces the skin (Kilinc-Balci 2011a). Surface roughness is a measure of asperity height of the fabric surface and could lead to an unpleasant tactile feeling. Perceived roughness is dependent on fabric surface roughness, compression properties, fibre diameter, and fibre and fabric tensile properties (Das & Alagirusamy 2011; Kilinc-Balci 2011a). Roughness was defined by Behmann (1990) in (Das & Alagirusamy 2011) as 'irregularities in surface that can be described geometrically as the size of roughness elements or mechanically by the friction coefficients'.

Friction is the tangential force applied on the skin, when fabric slides over it (Das & Alagirusamy 2011). Friction is the frictional force working the opposite of the fabric movement. Dynamic coefficient of friction is defined by the ratio of frictional force to the applied load. Sliding velocity was also reported to influence the friction (Das & Alagirusamy 2011). Presence of moisture on skin surface is known to increase the friction on the skin (Das & Alagirusamy 2011; Kilinc-Balci 2011a), which is likely to occur in sportswear. Surface friction could cause problems such as blisters, irritations and abrasions (Baussan et al. 2010; Derler, Schrade & Gerhardt 2007).

Surface properties of fabric including surface roughness index correlates with prickliness sensed from fabric at initial phase of wear, when sweat is not present from activity (Barker 2002). As mentioned earlier, sweat-wetted skin increases the roughness and friction perceived from fabrics and causes wet cling, which is dependent on the fabric structure (Das & Alagirusamy 2011).

SCGs are in full contact with the skin due to their negative fit, producing stimuli, and these stimuli change with activity and occurrence of sweat on skin surface. Tactile wear comfort of clothing is one of the important aspects of comfort especially for garments worn next to the skin. Generally, tactile properties of fabrics are examined in their relaxed state, except in subjective evaluations (wear trials). Same as other comfort parameters such as ergonomic wear comfort, the end-use and conditions where garments are worn must be considered in comfort evaluations. Due to the negative fit of SCGs, the surface properties and topography of fabrics change due to strain. This may influence the sensory comfort property of fabric which should be investigated.

2.3.4. Comfort measurement and evaluation

Standard method for evaluation of comfort specifically for sportswear does not exist (Bartels 2011), yet some manufacturers are interested in assessing and evaluating comfort properties of functional sportswear, to gain competitive advantage over other manufacturers, and researchers are interested to find methods to improve these properties.

Field trials and wearer trials with human test subjects in climatic chambers (subjective) and laboratory tests (objective) for various aspects of comfort are used for assessment of comfort in sportswear (Bartels 2011).

Field trials, subjective evaluation of comfort, are carried out where a group of people, sometimes well-known sportsmen or journalists, wear the garment in normal activity. In this method, the garments are tested in real-life conditions and the subjects report their experience wearing the garment (Bartels 2011). While, wear trials, another method for subjective evaluation of comfort, are carried out in climatic chambers in controlled conditions, usually with set temperature, humidity and wind velocity, on a treadmill or bicycle ergometers. In the latter method, physiological data such as heart rate, skin temperature and humidity in microclimate between the garment and skin is measured (Bartels 2011). In wear trails, even though the climatic conditions are replicable, test subjects may not be in the exact same condition as the previous test.

Test methods using human subjects are time and cost-intensive and the reliance that can be put on human subjects is questionable. Furthermore, human subjects vary in ‘individual physiological and psychological response’ (Barker 2002); thus, objective evaluation of comfort is more reliable, less costly and time-consuming, and more importantly, reproducible.

Laboratory testing equipment is widely used for objective evaluation of various aspects of clothing comfort; for instance, thermal insulation of fabrics can be evaluated with sweated guarded hot plate. Sweated guarded hot plate measures the energy required to keep a heated surface covered with fabric at a set temperature. Yet as mentioned in section 2.3.1, separate analysis of thermal insulation of garments is required which could be carried out on a heated thermal manikin simulating the actual wear conditions of garments; heated thermal manikin measures the heat loss due to conduction, convection and radiation (Das & Alagirusamy 2010). Both sweated guarded hot plate and heated

thermal manikin are used for objective evaluation of vapour resistance of fabrics and garments, respectively, by measuring the evaporative heat loss (Fan 2009).

One method of objective analysis of liquid-water transmission is areal wicking 'spot' test (Fan 2009). Using a device such as MMT, drop(s) of liquid is dropped on the horizontally placed fabric at a set height; MMT measures liquid absorption, differences in water content, initial liquid absorption speed and spreading rates of liquid on both sides of the fabric, by measurement of changes in electrical resistance on upper and lower surface of the fabric.

Objective evaluation of tactile comfort of garments, generally carried out using the Kawabata system, relies heavily on subjective scaling (Kilinc-Balci 2011a). In subjective assessment, a subject is asked to rate the discomfort sensation on a defined scale or by psychophysical scaling, where absence or presence and intensity of a single sensation due to a physical stimuli is recorded using a psychological scaling (Fan 2009). The Kawabata system, however, uses a combination of subjective and objective evaluations to provide quantitative measure for fabric hand. Kawabata surface tester KES-FB4 is one of number of Kawabata testers used for measurement of fabric surface roughness and coefficient of friction using two contact sensors. One contact sensor measures the thickness variation by vertical deflection of the probe, while fabric is displaced in forward and backward motion, and the other measures the frictional force. The sensors move over the surface of the fabric under constant tension and speed.

Laboratory tests, however, cannot directly measure the comfort of garments. They usually measure some of parameters influencing the comfort, and the results need to be defined in regards to the comfort of the garment and their significance in relation to wearer perception of comfort (Bartels 2011).

2.3.5. Summary

Sportswear such as SCGs must fulfil their intended use, which comprises performance, support and recovery aid for the wearer as well as physiological function and overall comfort (Bartels 2011).

In sport activities, there is a dynamic interaction between the garment and the body: this includes thermo-physiological, tactile, ergonomic and psychological interaction. These are all dependent on various properties of the fabric and garment as well as environmental conditions and type and level of activity of the wearer.

There are many variables found to influence the thermo-physiological comfort of fabrics, which cannot be directly translated into thermo-physiological comfort of garments. Fabric thickness, porosity and presence of air within the fabric structure are found by many researchers as predominant parameters affecting thermo-physiological comfort of fabrics.

Ergonomic wear comfort requires the garment not to interfere, impede or restrict the body movement relative to the end-use, activity and range of movement expected from the garment and depends on the garment construction and the elastomeric properties of the fabric(s) composing the garment (Bartels 2005). While traditional methods in garment

production and sizing systems are problematic in gaining proper fit for a wide range of population, development of patterns taking into account the static and dynamic sport needs and engaging technologies such as 3D body-scanning and garment virtual simulation in the future could result in garments with proper fit and ergonomic wear comfort.

Tactile wear comfort of clothing is one of the important aspects of comfort, especially for garments worn next to the skin. SCGs are in full contact with the skin due to their negative fit, producing stimuli and causing touch sensation. Surface roughness and friction are two out of a number of measures of tactile comfort of garments. Surface roughness is a measure of asperity height of the fabric surface, and friction is the tangential force applied on the skin when fabric slides over it. Sliding velocity and presence of moisture on skin surface are known to influence the friction on the skin (Das & Alagirusamy 2011; Kilinc-Balci 2011a).

Comfort assessment of garments could be carried out subjectively using human subjects and/or objectively using laboratory testing equipment. Subjective analysis of comfort, however, is less reliable than objective analysis; as human subjects vary amongst each other, may not be in the exact same condition in different timelines and are less reliable than controlled testing equipment.

Standard method for evaluation of comfort specifically for sportswear does not exist (Bartels 2011), yet development of testing standards for each type of garment concerning the comfort, fit and function according to activities and movements expected for the end-use could help manufacturers in evaluating and improving the comfort of the garments.

2.4. Anthropometrics and non-contact body measurements

Anthropometric measurements of human body are used widely to assess health and shape of the body in medical applications, in assessment of nutritional status, health and growth of the body as well as in calculations for drugs, radiotherapy, chemotherapy dosage and prosthesis production (Croney 1971; Deason 1997; Treleaven & Wells 2007). Body shape, proportions and composition are used in ‘epidemiology, diagnosis, treatment and monitoring’ (Treleaven & Wells 2007). Anthropometric studies such as SizeUK and SizeUSA were two recent major epidemiological studies carried out, where the data was used in garment design and sizing systems (Allen, RM et al. 2005; Treleaven, Furnham & Swami 2006). Deformity detection, skin analysis, lung function and estimation of bleeding in haemophilia are examples for diagnosis usage of anthropometric data. Treatment applications included burn treatments, craniofacial surgery, treatment of eating disorder, and as mentioned earlier drug dosage prescription and production of orthotics and prosthetics. Monitoring of body length and shape, for example in managing obesity, is another use of anthropometric measurements (Allen, RM et al. 2005).

In apparel industry, anthropometric data affect the sizing systems, which subsequently influence the appropriate fit and comfort of the garments (Otieno 2008). Issues to consider

in collection and use of anthropometric data are how to measure the body, how to analyse the data and last by not least, how to interpret the data into sizing charts. Every anthropological study requires planning of the sampling of the population, position of landmarks which defines exactly where to take the measurements and the measuring method and the equipment. Age, race and body type are important in sampling of the population (Le Pechoux & Ghosh 2002; Yu 2004b). Additionally, vocational or professional occupation of individuals influences the body dimension variations (Le Pechoux & Ghosh 2002). The results from anthropometric studies are used in production of many national and international standards in body measurements and sizing systems (Otieno 2008); the standards, however, become outdated due to changes in body dimensions in every few years (Wang & Chao 2010) and subsequently become irrelevant to average human sizes (Istook 2008).

2.4.1. Body measurement acquisition methods

In previous attempts regarding collection of anthropometrical data, three anthropometrical points were chosen and used as key parameters in prediction of measurement of other parts of the body. Anthropometrical points such as height and difference between hip and bust circumference were common key parameters for the whole-body, and height, hip and waist circumferences were used as lower-body key parameters (Le Pechoux & Ghosh 2002).

Physical measurements are carried out using contact tools such as anthropometers, callipers, and measuring tapes. These methods are time-consuming, complex and limited. The position of the landmark and measuring instrument, the pressure inserted and also experience of the researcher is important in traditional contact measurement methods. Physical measurement with tape would possibly compress the fat and muscle tissue (Yu 2004a) and the accuracy of the measurements depends on the researcher. Even with landmarks, the traditional physical measurement could lead to invalid and inaccurate measurement, due to the difficulty in determination of the landmark position and the measurement method (Otieno 2008).

With rapid growth of 3D body-scanners, non-contact whole-body 3D scanning is replacing physical measurement tools (Le Pechoux & Ghosh 2002). 3D body-scanners enable collection of whole-body measurements as well as shape and contours of the body, which was not possible in physical methods.

3D body-scanners provide automated data collection, storage and analysis. This sophisticated technology is fast, efficient and claim higher accuracy and reproducibility of the measurement data in comparison to measurements taken using contact tools. The 3D body-scans can provide unlimited number of linear and non-linear body measurements. 3D body-scanner enables changes in description and positions where the body measurement is taken at any time. They can potentially be used in virtual production and simulation of garment fit (Istook 2008). This technology is widely used in medical, military, apparel and other industries (Mckinnon & Istook 2002).

Scanning systems use light based, laser based or sound wave systems to capture the image of the surface of the human body (Istook 2008). In some of the technologies the subject is rotated while the image is recorded and in the others the subject is still. The scanning process is usually very quick, so the effect of body movement of the subject is reduced. Despite being rapid in collection of unlimited number of linear and non-linear measurements (Yu 2004a) and being objective (Le Pechoux & Ghosh 2002), software is needed to interpret the collected 3D data and measurements. $[TC]^2$–NX16 system uses white light technology and has a scan time of 8 seconds. The 3D data points recorded form a cloud point which needs further processing in order to extract the body measurements. The 3D data point is filtered, smoothed out, filled and compressed before the measurements are extracted (Istook 2008).

Physical landmarks are used in traditional manual methods, defining the start and end of measurement in anatomical points usually from bony parts over the body (Otieno 2008); 3D body-scanners, however, have the built-in capability to identify the anatomical points. Yet as a standard for landmarks did not exist until 2008 (ISO 2008), landmarks in 3D body-scanners and anthropometrical definitions did not necessarily match; thus, landmark positions must be re-defined, if required, in order to comply with anthropometrical definitions.

In all methods of anthropometric data collections, age and demographic details of the participants are recorded and the participants are usually wearing minimal clothing to provide accurate body measurements. Ethical practice should be followed in all methods.

2.4.2. Measurement validation

3D body-scanning is used to overcome the inadequacy of manual measurements (Otieno 2008); however, its validity, reliability and integrity of data remains under investigation.

Some 3D body-scanners are known to record smaller than or larger measurements compared to traditional anthropometrical methods (Daanen & Hong 2008; Han, Nam & Choi 2010). Missing data from hard-to-scan areas such as top of the head, top of the shoulders, under the bust and chin, armpits, crotch and bottom of the feet are shortcomings of some 3D body-scanners. Subject movement (body sway during scan), surface texture (skin and hair) and landmarks (Istook 2008; Yu 2004a) may also cause issues, when generating a 3D body-scan.

Landmarking is found to be a major problem in measurements derived from 3D body-scans. Landmarking remains a problem in traditional body measurements as well and its accuracy depends on the skill of the operators (Kouchi & Mochimaru 2011). The definition of landmarks and measurement points from various 3D body-scanners do not comply with any standards, since a published standard for interpretation of measurements taken by 3D body-scanners did not exist until May 2010 (ISO 2010; Istook 2008; Simmons & Istook 2003). Even after publication of such standard, all 3D body-scanners are not capable of extraction of all the defined measuring points, especially as some of the defined measuring points requires the subject to be in a position such as seated position, which is not possible with some 3D body-scanners (ISO 2010). And according to the same

standard (ISO 2010), validation for accuracy of measurements extracted using 3D body-scanners is its comparison to corresponding traditional measurements; the measurements derived from 3D body-scans are deemed to be accurate when the mean difference to traditional measurements is equal or smaller than what is advised in the standard method. The acceptable mean difference of measurements from 3D body-scans to traditional measurement may be equal or smaller than 3D body-scanner resolution: for instance, the mean difference error allowance between extracted value and traditional measured value for the foot dimension is 2 mm, while the resolution of $[TC]^2$ 3D body-scanner is ≤ 3 mm in circumference ($[TC]^2$ n.d.). This means that there is a very high probability that the foot measurement derived from a 3D body-scan recorded with $[TC]^2$ 3D body-scanners is not acceptable in regards to the standard method. Kouchi & Mochimaru (2011) examined the body dimensions and landmarks positioning, and reported large inter-observer errors in traditional methods. According to the authors, landmark positioning has a major effect on inaccuracies of body measurements. Han, Nam & Choi (2010) also referred to manual measurement errors. This suggests that the traditional measurements have inherent errors themselves and are not a valid mean for verification of accuracy of measurements extracted from 3D body-scans.

Another major issue with 3D body-scans is the respiration and foot positioning of the subject, which affects the body measurements in upper- and lower-body, respectively (Mckinnon & Istook 2002). Studies were carried out to compare body measurements from traditional anthropometric methods with 3D body-scans (Brooke-Wavell, Jones & West 1994; Han, Nam & Choi 2010; Lu & Wang 2010; Mckinnon & Istook 2001; Mckinnon & Istook 2002; Simmons & Istook 2003); inherent error incorporated within physical measurement prevents the measurement data to match between the two methods.

There is no generally accepted evaluation on measurements derived from 3D body-scans (Kouchi & Mochimaru 2011); thus, the accuracy, reproducibility and comparability of the measurements derived from 3D body-scanners require further investigation.

2.4.3. Human body proportions

A table of proportionate body measurements existed in as early as 1820s, which tailors used for drafting patterns. Studies were carried out to relate the body proportions to health, growth and various diseases (Aldegheri & Agostini 1993; Bogin & Varela-Silva 2010; Sánchez-García et al. 2007; Strecker et al. 1997), and also for estimation of body composition or other body measurements (Baumgartner, Chumlea & Roche 1989; Duyar & Pelin 2003; Holliday & Ruff 2001; Mohanty, Suresh Babu & Sreekumaran Nair 2001). Ergonomists must deal with the fact that humans come in various shapes and sizes; thus, they use anthropometric data, body proportions and ratios usually collected for apparel industry (Lehto & Buck 2008). Even forensic scientists attempt to identify victims of disasters from their body size/height using human remains and skeletal collections such as hand, lower leg length, arm span and foot measurements (Özaslan et al. 2003).

Some studies compared anthropometric data change within one or between different populations. Different ethnic groups, genders and time cause variations in body measurements (Croney 1971; Lehto & Buck 2008): for instance, NASA recorded the effect

of time, where the human height increased worldwide over time since the mid 1800s. The variations in body measurements between ethnic groups and time were recorded: in early 20th century, Japanese tend to be shorter in height in comparison to Europeans, yet with time, this difference was changing. The effect of gender was demonstrated, where females tend to grow faster than males, yet males grow taller in total (Lehto & Buck 2008).

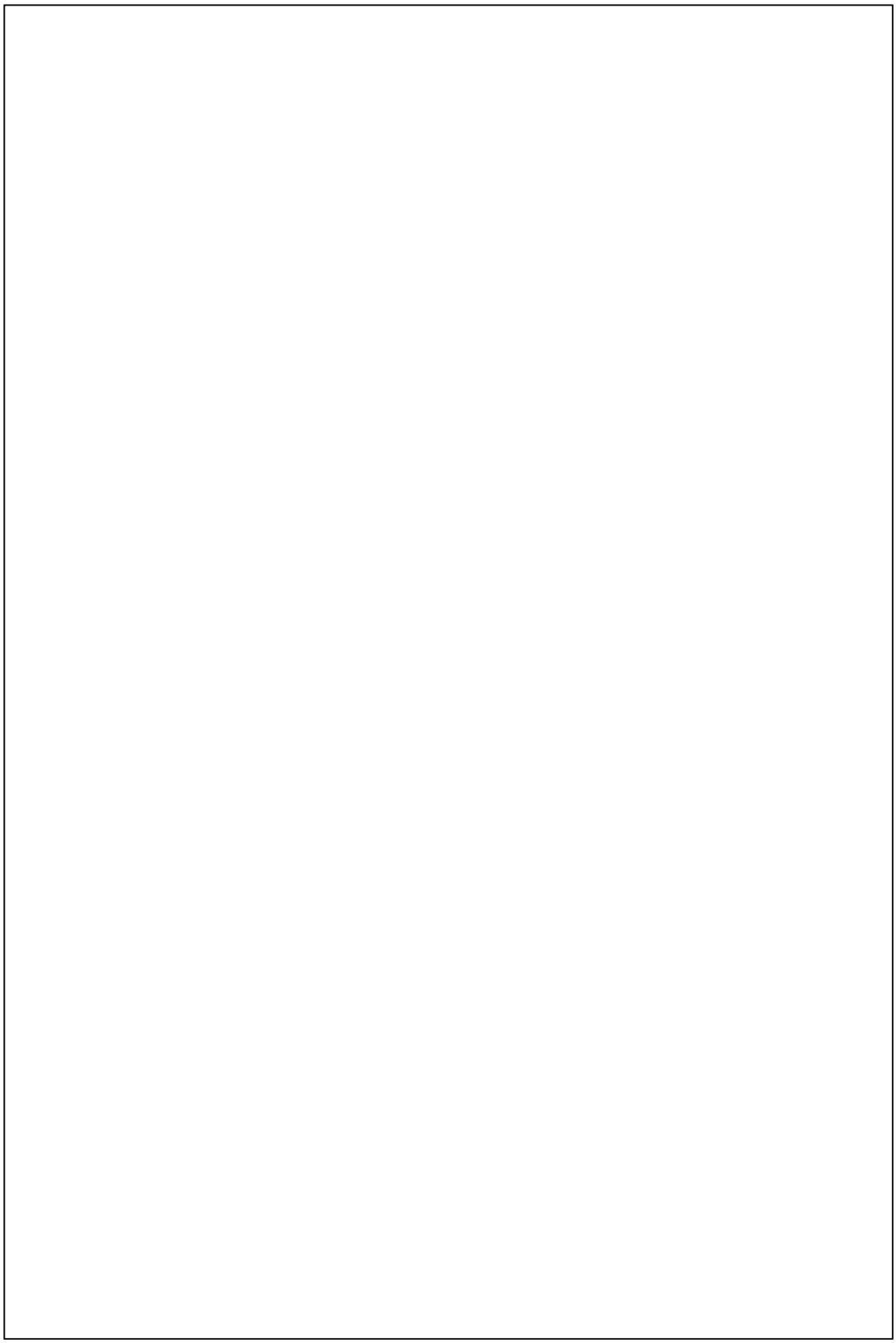

Figure 2.4 Body segment to height ratio in Swedish, Mediterranean and US males and females - Figure 2.8 in (Lehto & Buck 2008)

Generally, circumference measurements vary more widely than length measurements between humans (Keiser & Garner 2008); for this reason, extensive comparison was made between different body parts and body height: body parts are found to be strongly proportionate to body height (Lehto & Buck 2008) and usually the body dimensions are expressed as ratios to body height (Figure 2.4).

For instance, in Figure 2.4, the knee was positioned higher in Mediterranean than Swedish in both males and females, and knee was positioned higher in females from both ethnics, Mediterranean and Swedish, in comparison to males; this demonstrates the variations in body proportions in different ethnics and genders. It must be noted that even though body measurements are compared as a proportion to height measurement, the height of human changes with age. Some correlations were found between other parts of the body and body measurements other than height (Lehto & Buck 2008; Mohanty, Suresh Babu & Sreekumaran Nair 2001). An example is shown in Table 2.3, where above major diagonal (upper left to lower right highlighted in grey) were from NASA on females and below were from the US Air Force on males (Lehto & Buck 2008).

Table 2.3 Body measurement correlations – females highlighted in grey and males in white (Lehto & Buck 2008)

Characteristic	A	B	C	D	E	F	G
A – Age	-	0.22	0.05	-0.02	0.04	0.23	0.1
B – Weight	0.11	-	0.53	0.46	0.5	0.82	0.4
C – Stature	-0.03	0.52	-	0.93	0.91	0.28	0.33
D – Chest height	-0.03	0.48	0.98	-	0.9	0.22	0.28
E – Waist height	-0.03	0.42	0.92	0.93	-	0.24	0.31
F – Waist circumference	0.26	0.86	0.22	0.21	0.14	-	0.28
G – Head circumference	0.11	0.41	0.29	0.25	0.23	0.31	-

From correlations in Table 2.3, body measurements could be predicted from one another; furthermore, comparison could be made between genders: correlation between weight and height was +0.52 in adult males and +0.53 in adult females; this means that at the same height, females weighed more than males. At the same weight, adult male waist circumference was greater than females. In another study Özaslan et al. (2003) reported that body height could be more accurately predicted from lower-body measurements in comparison to the upper-body.

The correlation of body parts measurements such as chest and waist height or waist circumference as a proportion of height and also other correlations, as explained above, are useful in the estimation of body measurements from few available measurements. Meanwhile, it does not provide the whole-body dimensions. Depending on the population and application under investigation, specifically designed anthropometric studies would be beneficial in analysis of body dimensions and proportions for sizing chart development, pattern drafting and production of garments with perfect fit.

2.4.4. Summary

Anthropometric measurements of the human body are widely used in medical, military, apparel and other industries. Anthropometric data from any survey, however, would not necessarily apply to a specific populace under investigation; as the age, gender, ethnicity and occupation affect body size, shape and proportions of human. Furthermore, time causes variations in body measurements; therefore, the anthropometric data must be updated.

Acquisition of anthropometric data requires extensive planning and is very costly and time-consuming; thus, the prediction of body measurements from few available key parameters such as height and differences between hip and bust, or hip and waist circumferences were used in previous attempts in collection of anthropometrical data. Correlations between body height and other body measurements were found in the literature: it is reported that size of body parts are strongly proportionate to body height. The correlation of body parts measurements such as chest and waist height or waist circumference as a proportion of height and also other correlations are useful in estimation of body measurements from few available measurements. Meanwhile, it does not provide the whole-body dimensions.

3D body-scanning is a relatively new technology used in generation of anthropometric data, widely used in garment design and sizing systems. This technology has many advantages over traditional manual measurements such as speed and capability of production of unlimited number of linear and non-linear body measurements. Yet validity, reliability and integrity of data derived from 3D body-scans remain under investigation. Depending on the population and application under investigation, specifically designed anthropometric studies would be valuable in analysis of body dimensions and proportions for sizing chart development, pattern drafting and production of garments with perfect fit. On the other hand, in order to be able to use the anthropometric data derived from 3D body-scanners, they must comply with newly published standards regarding body measurement definitions and landmarking.

3. Research design

This chapter discusses the problem statement, the rational and hypothesis for present research aroused from background research. It also provides the methodology, methods and study limitations.

3.1. Problem statement and rationale for research

SCGs have become very popular in recent years amongst athletes and fitness enthusiasts. The rationale for wearing SCGs seems sensible, due to proved positive effect of CGs in medical applications and some research-supported and some unsubstantiated claims cited by the manufacturers of such garments. Despite an extensive amount of information available on medical compression therapy and MCGs, however, little knowledge is available on SCGs in terms of their material, fit, construction, mechanical

effects on the underlying human body and physiological comfort properties. More importantly, a gap in knowledge exists on the amount and distribution of pressure induced by SCGs on the underlying limb of the human.

The aim of this research was to predict, measure and validate pressure generated by SCGs on the underlying tissue of human and to evaluate the physiological comfort performance of the garments.

3.2. Research hypotheses

Fabric tensile properties affect the degree of pressure induced by SCGs over the underlying limb. Limb circumferential measurement affects the pressure induced by SCGs over the underlying limb. Composition of different fabrics with various tensile properties, within one garment, affects the pressure induced by SCGs over the underlying limb. Interface pressure induced by SCGs can be predicted with known fabric tensile properties and limb circumference. The physiological comfort properties of fabrics composing SCGs can be measured and evaluated. The effect of fabric strain on physiological comfort properties of fabrics composing SCGs can be measured. A protocol for generation of lower-body measurements relative to SCGs for 3D body-scanner can be developed.

In this research, the focus was on the lower-body of the human and on one type of commercially available sport compression tight, comprising of two different fabrics. It was assumed that the limb of the human has a cylindrical cross-section.

3.3. Methodology

To achieve the above mentioned aim, the proposed research reviewed the existing knowledge and carried out a preliminary experiment on the construction and pressure profile of a commercially available SCG. A suitable test method for determination of various properties of fabrics used in SCGs, especially their tensile properties was chosen/developed. During the course of this research, fabrics composing commercially available SCGs were assessed in terms of physical parameters such as stitch density, mass per unit area, thickness and optical porosity, as well as tensile performance including tension, tension decay and residual extension. Theoretical pressure induced by SCGs was predicted and compared with measured pressure, and validated. The reliability of pressure-measuring device used was evaluated before the pressure validation. Physiological comfort properties of fabrics comprising SCGs was analysed in terms of porosity, air permeability, moisture management, thermal and water-vapour resistance in relaxed and strained formation, and tactile comfort properties again in both relaxed and strained formation as well as dry and moist conditions. Last but not least, lower-body measurement method and 3D body-scanning protocol applicable to the SCGs was developed. Human models were scanned and their body measurements were analysed in respect to the application under investigation. The results were analysed and assessed.

Research's methodology is as followed:

- **Preliminary experiments**
    - Determination of construction and pressure profile of commercially available SCGs
    - Determination of a suitable method for testing of fabrics composing SCGs for tensile properties
        - Practical elongation
        - Tension at specified extension
            - Tensile properties in strip and loop formation specimens
            - Effect of fabric composition on its tensile properties
        - Tension decay
        - Residual extension
- **Experimental**
    - Physical parameters of the fabrics comprising SCGs
        - Determination of stitch density
        - Determination of thickness
        - Determination of mass per unit area
        - Determination of optical porosity
    - Pressure induced by SCGs
        - Determination of theoretical pressure generated by SCGs – Law of Laplace
        - Determination of reliability and calibration of a pressure-measuring device
        - Determination of measured pressure – cylinder experimental rig
        - Validation of pressure – theoretical and measured
    - Performance of the fabrics comprising SCGs in terms of physiological comfort properties
        - Determination and assessment of porosity, air permeability and optical porosity
        - Determination and assessment of thermal and water-vapour management
        - Determination and assessment of moisture management

- Determination and assessment of tactile comfort properties

- 3D body-scan and body measurement
  - Development of lower-body measurement method and scanning protocol
  - Acquisition of body measurement with 3D body-scanning
- Results analysis and assessment

3.4. Materials and Methods

Materials used in this study were fabrics commercially used in sport compression tights (SCTs). Fabrics A, B, C and D were evaluated in this research. All fabrics were weft knitted of single jersey construction containing elastane fibre in their fibre composition.

The SCT under investigation was composed of two different fabrics with different physical attributes (Figure 3.1).

(a) (b)

Figure 3.1 SCT construction – (a) front and (b) back of the garment

The composition of the two fabrics varied along the length of the garment. At the lower end of the tight, fabric A (at the back of the SCT) made up a bigger percentage of the circumference of the garment leg while towards the upper end of the tight, this composition reversed and fabric C (at the front of SCT) made up for a bigger percentage in the garment leg. Later on in the research, SCT with same construction was investigated where fabric A was replaced by fabric D.

Samples composed of the two fabrics in strip formation were prepared: samples composed of fabrics A and C, joined by flat-lock seam, in weft and warp directions (Figure

3.2). As per garment styling, seams ran in the length of the tight, which was approximately aligned with the warp direction of fabrics composing the garment; hence the fabric samples in the weft direction, simulating the width of the garment, had the two fabrics joint by seam in warp direction (Figure 3.2a), and the fabric samples in warp direction, simulating the length of the garment, had the two fabrics joint by seam in the same direction (warp) (Figure 3.2b).

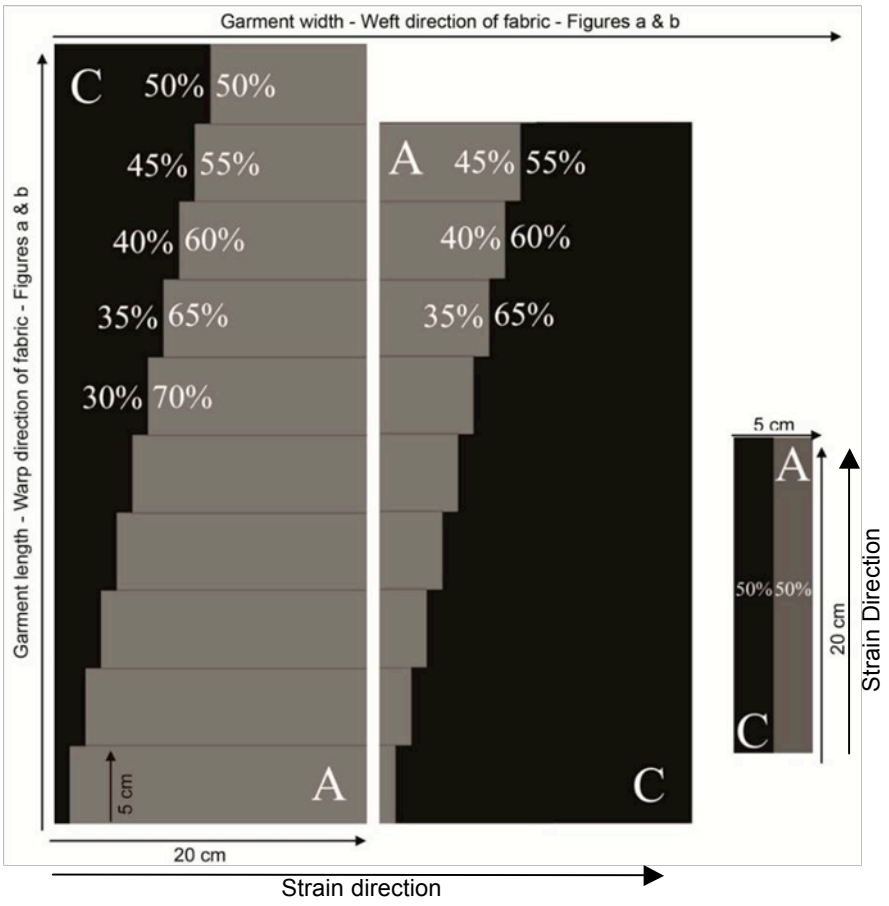

(a) (b)

Figure 3.2 Samples compositions in strip formation: (a) weft and (b) warp direction

Samples composed of the two fabrics in strip formation were prepared: samples composed of fabrics A and C, joined by flat-lock seam, in weft and warp directions (Figure 3.2). As per garment styling, seams ran in the length of the tight, which was approximately aligned with the warp direction of fabrics composing the garment; hence the fabric samples in the weft direction, simulating the width of the garment, had the two fabrics joint by seam in warp direction (Figure 3.2a), and the fabric samples in warp direction, simulating the length of the garment, had the two fabrics joint by seam in the same direction (warp) (Figure 3.2b).

Samples in weft direction were composed of fabrics A and C, with the compositions provided in Table 3.1 and Figure 3.2a.

Table 3.1 Samples compositions - composed of fabrics A and C- in weft direction

Composition no.	Fabric A	Fabric C	Composition no.	Fabric A	Fabric C
	%	%		%	%
0	0	100	11	55	45
1	5	95	12	60	40
2	10	90	13	65	35
3	15	85	14	70	30
4	20	80	15	75	25
5	25	75	16	80	20
6	30	70	17	85	15
7	35	65	18	90	10
8	40	60	19	95	5
9	45	55	20	100	0
10	50	50			

Samples in warp direction were composed of the same fabrics (Table 3.2 and Figure 3.2b). The direction of the seam within the samples was the same as the actual garment.

Table 3.2 Samples compositions - composed of fabrics A and C- in warp direction

Composition no.	Fabric A	Fabric C
	%	%
P1	0	100
P2	50	50
P3	100	0

There was one specimen per each sample composition in each of the weft and warp direction.

Table 3.3 Fabric sleeve composition – fabrics C and D

Composition no.	Fabric C	Fabric D	Composition no.	Fabric C	Fabric D
	%	%		%	%
0	0	100	6	60	40
1	10	90	7	70	30
2	20	80	8	80	20
3	30	70	9	90	10
4	40	60	10	100	0
5	50	50			

Fabric sleeves were made of 100% fabric C, 100% fabric D, and a combination of fabrics C and D, providing variable weft strains. Fabric sleeves were prepared providing 25%, 50% and 75% strain around the circumference of the cylinders of 90, 130 and 160 mm in diameter (Appendice 1). Fabric sleeves were 450 mm in length and 20 mm wider

than the width required for each strain, where they were sewn along the length with an overlock stitch (Figure 3.3).

Fabric sleeves were made from variable compositions of fabrics C and D (Table 3.3). The fabric sleeves provided 50% and 75% strain in weft direction over cylinder with 90 mm diameter.

There were three specimens per each cylinder/strain combination for sleeves made of 100% fabric C and 100% fabric D, and one specimen per each strain for each composed sleeves.

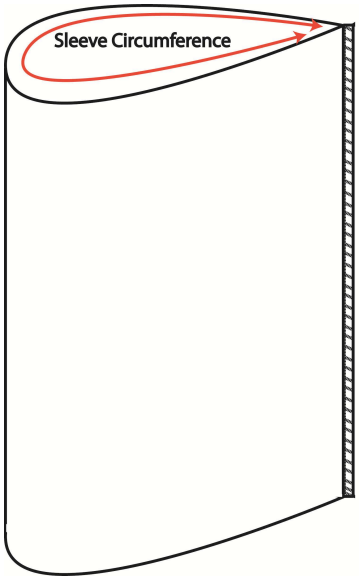

Figure 3.3 Fabric sleeve

All fabrics and garments were conditioned and tested in standard temperature atmosphere of 20 ±2°C and 65 ±2% relative humidity, as per AS 2001.1-1995 (AS 1995).

3.4.1. Preliminary investigation

In this section, preliminary investigation is carried out on the commercially sourced SCTs, on their construction and pressure profile. Physical attributes of fabrics composing SCTs is measured. Furthermore, a suitable method for testing of fabrics comprising SCTs for their tensile properties is developed.

3.4.1.1. Preliminary investigation of SCGs

Preliminary investigation was carried out on commercially available SCTs for men in sizes Medium and Large. All measurements were carried out on the right leg of the tights.

The tights were measured for length and various important circumferential measurements. They were laid flat on the table, relaxed and were under no strain. Length

measurements from leg opening (hem) to crotch and to waist, inseam and outseam were recorded.

Circumferential measurements were measured on tights at leg opening (hem) and also at measuring points B to G. In order to measure the circumferences at measuring points B to G, tights were worn on Salzmann wooden legs. Salzmann wooden legs (Figure 3.4) had different sizes (9, 12 and 14) with varying circumferences relating to various body sizes (Medium, Large, etc.) and they were marked at measuring points B to G relating to important medical pressure-measuring points and Salzmann sensor points. The tight for men in size Medium relates to Salzmann wooden leg 9 and the tight for men in size Large to wooden leg 12. Measuring points B to G were marked on the tights using a marker when worn on relative wooden legs. The tights were then removed from the wooden leg and were allowed to relax on a flat surface for 2 hours. Then the widths at marked measuring points were measured and the circumferences at each point were calculated.

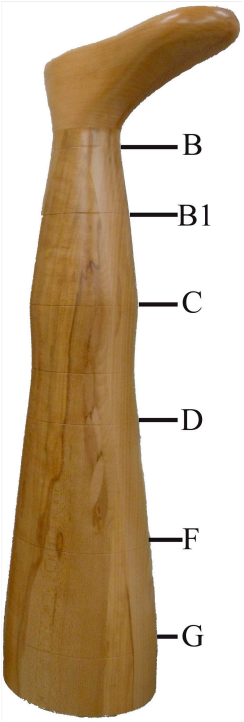

Figure 3.4 A Salzmann wooden leg and measuring points B to G

The circumferences of the tight at measuring points B to G when worn on the wooden legs were equal to the wooden leg circumferences at each point. Wooden leg circumferential measurements at measuring points B to G are provided in Appendice 2. Wooden leg measurements were used to calculate the strain in width direction for each tight when worn on relative wooden leg, Eq. (4):

$$S_{weft} = \frac{\left(C_w - C_g\right)}{C_g} \times 100 \quad (4)$$

where S_{weft} is the strain in width (%), C_W is the circumference of the wooden leg (mm), and C_g is the circumference of the relaxed garment (mm).

Each garment was worn on the relative wooden leg and one size bigger (tight in size Medium worn on legs 9 and 12 and tight in size Large on legs 12 and 14). The pressure generated by tights was measured on the side and back of the tight using Salzmann pressure-measuring device and two long probes: one placed on the side and one at the back of the wooden leg. The pressure at each site was measured four times and the mean results were reported and analysed between the garments, leg sizes and measuring sites.

3.4.1.2. Determination of physical attributes of fabrics

Physical attributes of fabrics A, B, C and D such as stitch density, mass per unit area, thickness and optical porosity are measured.

Stitch density is calculated as per standard method BS EN 14971:2006 (BS 2006) and mass per unit area is measured according to standard method AS 2001.2.13-1987 (AS 1987). Thickness is measured as per standard method AS 2001.2.15-1989 (AS 1989), as the distance between the reference plate and parallel presser foot of a thickness measuring device.

Optical porosity of fabrics is calculated as the percentage of fabric surface not covered by yarns in its relaxed state. Microscopic images are taken from fabrics using Motic microscope and the optical porosity is calculated using Image Tool UTHSCSA, Version 3, by calculating the percentage of black and white pixels representing yarn and pores, respectively, within the fabric area.

Each parameter was measured for five specimens and mean results were reported and evaluated.

3.4.1.3. Development of a method for evaluation of tensile performance attributes of fabrics comprising SCGs

The tensile properties of fabrics can be determined from specimens in strip and loop formation, which according to the British Standard 4952:1992 (BSI 1992), would not necessarily give the same results; the fabrics are tested in strip formation when testing to British Standard 4952:1992 (BSI 1992). Specimens in strip formation are 50x200 mm, providing 100 mm nominal gauge length. In the application under investigation, weft-directional stress and strain has more importance; the extensibility in warp direction, however, was investigated as well, as it affects the fit and ease of movement of the garment (Saville 1999). Tests were carried out with use of an Instron tensile strength tester, Model No. 5565A, and 5 kN load cell capacity.

Fabrics were tested according to British Standard 4952:1992 (BSI 1992), ‘Method of test for Elastic Fabrics’. Extension at specified force is determined by cycling the specimen once and then recording the strain under 20 N stress on the second cycle. Tension decay is determined by cycling the specimen twice and then extending the specimen to 25% strain, holding it for 5 minutes, after which time the stress is re-recorded.

Residual extension is determined by measuring the length of the specimen after 1 minute of relaxation from 25% strain. Extension at specified force, tension decay, and residual extension of all fabrics were determined, with five specimens for each fabric, and the mean results were calculated and reported.

For determination of extension at specified force, the specimen is clamped under no stress and then a pre-stress of 2 N is applied. The specimen is then cycled twice between zero and 20 N stress at a constant rate of extension/retraction of 500 mm/min and the strain versus the stress is plotted. The stress of 20 N is considered to be standard for testing of elastomeric fabrics; however, measurement of the extension at specified force was also carried out at 30 N stress. For determination of tension decay, the specimen is clamped and cycled twice between zero and 20 N stress at same constant rate. Without a pause, the specimen is then strained and held at 25% strain for 5 minutes where the stress is recorded at the beginning and the end of 5 minutes cycle. For the determination of residual extension, the test is carried out in the same way as for the determination of extension at specified force: the cycled specimen is laid flat on a smooth surface after the test for 1 ±0.1 minute, when the gauge length is remeasured and the residual extension is calculated and recorded.

Five specimens in strip formation (Figure 3.5) were tested to British Standard 4952:1992 (BSI 1992), and the mean results were calculated and evaluated.

Figure 3.5 Clamped specimen in strip formation

As the practical stress relative to the garments under investigation are usually lower than 20 N (Troynikov et al. 2010), modified test methods based on BS 4952:1992 method (BSI 1992) were used, so that the fabric deformation conditions would be closer to those under which the SCGs are used. According to the modified method, a range of strains and stresses were chosen for testing of tensile properties of fabrics. Fabrics were tested to the modified method and the results were compared to the results of the standard test method of determination of extension at specified stress under 20 and 30 N stress, with the

purpose of determination of the most suitable method for testing of fabrics for the calculation of theoretical pressure generated by SCGs.

Fabrics A and C were tested for determination of strain at specified stress and determination of stress at specified strain. During the modified method the specimens were cycled twice to the specified strain or to the specified stress and then extended to a specified strain/stress where the results were recorded. The results of the modified method were then compared to the results at a given stress recorded from the standard method. Each fabric was tested in weft direction in strip formation, and the mean results of five specimens per each fabric were calculated.

In the modified method the strain of fabrics was determined at 5, 10 and 15 N stress and the stress was determined at 25%, 50%, 75%, 100% and 200% strain in strip formation.

Fabrics A and C were also tested in loop formation for determination of stress at 100% strain in weft direction, in order to compare the results to specimens in strip formation. Specimens in loop formation are 75x250 mm, which are sewn at 25 mm at each end from short dimension of the specimen to form the loop, providing 200 mm circumferential nominal gauge length. Taking into account the circumferential gauge length of specimens in loop formation, their resultant stresses were divided by two. The loop test requires special grips (Figure 3.6), where the specimen in loop formation is placed around. The grips are adjustable to provide the desired circumferential gauge length, taking into account the thickness of the grips.

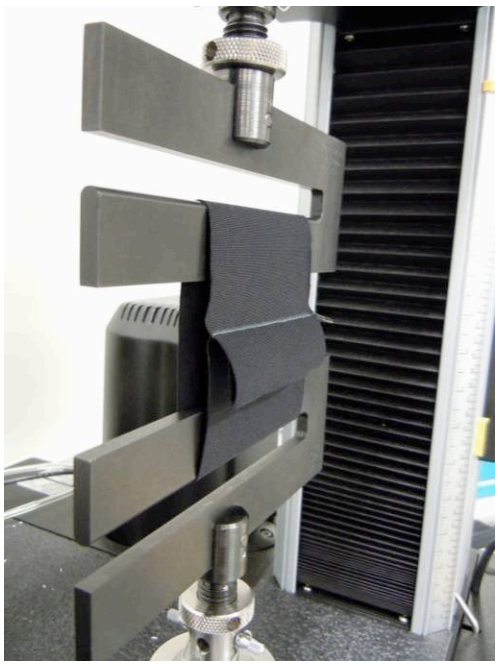

Figure 3.6 Specimen in loop formation on special grips

Samples composed of the two fabrics (fabrics A and C) in strip formation were tested for determination of stress at specified strain of 100% (modified method) in both warp and weft directions. The two fabrics were sewn with flat-lock seam (Figure 3.2). With testing the composed samples in weft direction the influence of different fabric compositions on

tensile properties, its stress and thus pressure generation over a limb, was determined, and with testing the composed samples in warp direction the influence of seam along the length of the garment, where the two fabrics were joined together, and the ease of movement and fit of the garment was evaluated. Two specimens for each composition of fabrics in strip formation were tested and the mean results were calculated and analysed.

3.4.2. Compression calculation and validation

Theoretical pressure is calculated using Law of Laplace and validated with pressure readings from Salzmann pressure-measuring device MST MK IV (Figure 3.7) and Salzmann MST 2007 software.

In order to eliminate the complexity of the human leg in terms of geometrical shape and bone/tissue composition and its effect on pressure measurement, pressure inserted from variable fabric sleeves were measured on three rigid cylinders. Cylinder circumferences were comparable to the circumference of important measuring points on Base Model lower limb. The rigid cylinders measured 90, 130 and 160 mm in diameter and were 300 mm long. The lower-body measurements of Base Model were derived from 3D body-scanning (section 4.4.2): ankle, calf and mid-thigh measuring 263, 398 and 532 mm. In this research, from this point onward, rigid cylinders are referred to as cylinder 90, 130 and 160, where figures represent cylinder diameter.

Figure 3.7 MST MK IV

Meanwhile, three weft strains were chosen in accordance to practical elongation of the SCT for men in size Medium on lower-body of Base Model (Table 3.4).

Table 3.4 Practical elongation on Base Model – SCT in size Medium

Measuring point	Practical elongation - weft strain %
Mid-thigh	35
Knee	21*
Calf	56*
Ankle	64*

*selected values for variable weft strains

Practical elongation was calculated using Eq. (5):

$$PE = \frac{(C_l - C_g)}{C_g} \times 100 \quad (5)$$

where *PE* is the practical elongation (%), C_l is the limb circumference (mm) and C_g is the garment circumference (mm).

From Table 3.4, strains of 25%, 50% and 75%, covering wide range of practical elongations in weft direction were chosen for theoretical pressure calculation, measurement and validation.

3.4.2.1. Theoretical pressure calculation – Law of Laplace

Fabrics C and D were tested for stress to 100% strain in weft direction (direction where the pressure is generated over the limb). Five specimens in strip formation were tested according to section 3.4.1.3 and the mean results were used in theoretical pressure calculation. The pressure was calculated for 25%, 50% and 75% strain in weft direction over cylinders 90, 130 and 160, using Eq. (2). The stresses from testing the fabrics were recorded as N/5cm in strip formation, which was converted to N/cm for theoretical pressure calculations.

Theoretical pressure were also calculated for composition samples, composed of fabrics C and D, in various compositions, same as compositions for fabrics A and C (Figure 3.2a and Table 3.1). The theoretical pressure was calculated for 50% and 75% strain on cylinder 90.

3.4.2.2. Salzmann sensor calibration

One method for sensor calibration is using a sphygmomanometer to induce the known pressure over the sensor measuring point and comparing between the known and measured pressure; however, there are four and six measuring points on Salzmann short and long probe, respectively; generally, the sphygmomanometer width is greater than the distance between the measuring points (Figure 3.8); thus, the sphygmomanometer sleeve placed on adjacent measuring points would fall over each other and induce extra pressure at each measuring point. For this reason and in this research, the usage of a sphygmomanometer was eliminated for sensor calibration.

For sensor calibration, equal known weights were placed over each of the short sensor measuring points (B to D) (Figure 3.8) and the pressure was measured with the MST Salzmann pressure-measuring device and were compared to calculated pressure generated by weights. The calculated pressure generated by weights are defined as force per unit area (Serway & Jewett 2010). Four series of weights were chosen, called ‘Base’, ‘Base+1’, ‘Base+2’ and ‘Base+3’, with increasing weights. The weights assembly were chosen so that the base of each series of weight would only be placed over the sensing area of each measuring point, which has a circular area of 10 mm in diameter. The pressure induced from the weights over the sensor area are calculated, Eq. (6):

$$P = \frac{F}{A} \tag{6}$$

where P is the pressure (N/m^2), F is the applied force (N) and A is the area (m^2) where the force is applied.

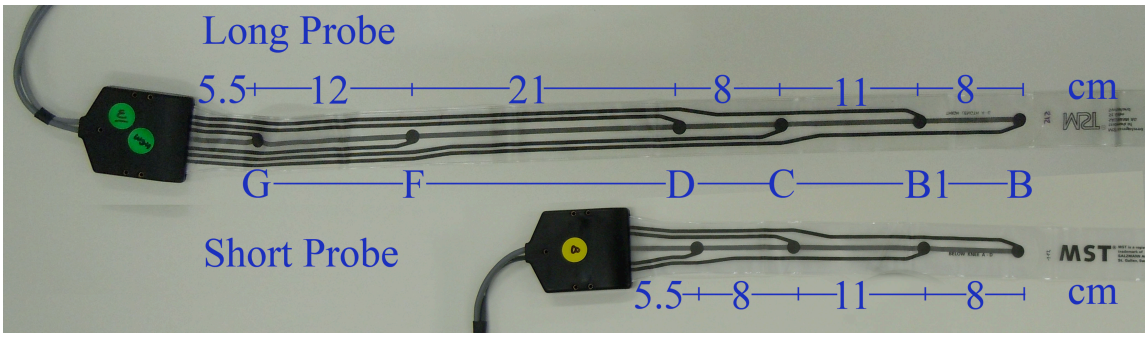

Figure 3.8 Salzmann short and long probes with sensor measuring points and distances in cm

Weights were placed on a cork bumper, covering just the sensing area of each measuring point, starting only with 'Base' (Figure 3.9a) and following with second row of weights 'Base+1' (Figure 3.9b).

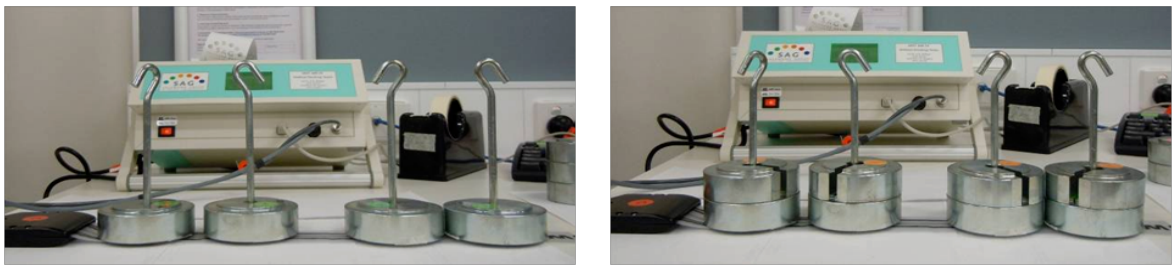

(a) (b)

Figure 3.9 Calibration (a) step 1 with 'Base' and (b) step 2 with 'Base+1'

(a) (b)

Figure 3.10 Calibration (a) step 3 with 'Base+2' and (b) step 4 with 'Base+3'

The test was continued with ‘Base+2’ and ‘Base+3’ (Figure 3.10a and b). The mass of each series of weights are provided (Table 3.5).

To the extent possible, the weights were not touching the adjacent ones or the table top, and the measurements were taken with the Salzmann pressure-measuring device. After each measurement was taken, the air was pushed out of the sensor sleeve with the help of fingers squeezing it out and the weights were placed back over the sensor point and balanced over the cork bumper, for the next measurement to be taken.

Table 3.5 Weights used for each series and measuring point

Weight series	Measuring points				STDEV	Mean weight
	B	B1	C	D		
	grams					
Base	860	859	860	859	0.35	860
Base+1	1545	1545	1546	1530	8.00	1542
Base+2	2230	2229	2232	2215	7.84	2227
Base+3	2917	2916	2919	2901	7.96	2913

Thirty measurements were taken from each series of weights at each measuring point.

3.4.2.3. Validation of theoretical pressure calculation - cylinder experimental rig

Pressure induced by fabric sleeves were measured for validation of theoretical pressure.

Three fabric sleeves were made of fabric D, which covered the rigid cylinders 90, 130 and 160 and provided 25%, 50% and 75% strain around the circumference of the cylinders. The fabric sleeves made of fabric D were made out of fabric taken closely to samples tested for theoretical pressure calculation in section 3.4.1.3, in order to eliminate the fabric variation within one roll of fabric. The fabric sleeves fully covered length of the rigid cylinders. The circumference of fabric sleeves are calculated (Appendice 1), using Eq. (7):

$$C_s = \frac{C_c}{(1+\frac{S_{weft}}{100})} \tag{7}$$

where C_s is the fabric sleeve circumference (mm), C_c is the cylinder circumference (mm) and S_{weft} is the weft strain (%).

Salzmann MST MK IV pressure measurement device and Salzmann MST 2007 software was used for pressure measurement and recording. Normal pressure-measuring speed of the device is 1 mmHg/sec; however, for pressures of lower than 15 mmHg, the pressure is measured at lower speed of 1 mmHg/4sec (Salzmann MST MK IV User Manual, St. Gallen).

Before taking the pressure measurements, the device is calibrated by the method recommended by the manufacturer: the air connector for the measuring probe is connected to a pressure gauge (manometer) and the device is calibrated to two values of zero and 100% air pressure, which equals to zero and 75 mmHg. The measured pressure is calculated on the basis of the ramp generated from the two calibration values.

The rigid cylinder was assembled with a short sensor probe attached along its length, using adhesive tape, with measuring point B at top of the cylinder (Figure 3.11).

(a) (b)

Figure 3.11 (a) Cylinder and Salzmann probe set-up and (b) fabric sleeve worn over cylinder

Ten measurements were taken from each fabric sleeve, which made a total of thirty measurements per each strain/cylinder. The first measurement of each fabric sleeve was taken 90 seconds after the fabric sleeve was set over the cylinder and the sensor probe, and there was a 90 seconds gap before the next pressure measurement was taken, in order to allow time for the air to be pumped out of the sensor probe.

Fabric sleeves made from fabric C had higher variation to the specimens tested for stress at 100% strain for theoretical pressure calculation. Unlike fabric D, the specimens from fabric C were not cut closely from the specimens used for fabric sleeves, yet all specimens were provided from the same roll of fabric. Furthermore, two sensor probes were used in pressure measurements over the cylinders and three pressure measurements were recorded per each fabric sleeve/probe, providing eighteen pressure recordings per each combination of strain/cylinder. This method allowed analysis of the fabric variation on pressure validation.

The pressure induced from composed fabric sleeves, made from fabrics C and D, was measured over cylinder 90 (Table 3.3). The pressure was measured at three positions along the cylinder circumference. One probe was positioned under the fabric with smaller sample composition, and two probes measuring the pressure of the other fabric within the sleeve along the length of the cylinder: for example, in composition no. 3, one probe measured the pressure induced from fabric C, comprising 30%, and two probes measured the pressure induced from fabric D, comprising 70% of the fabric sleeve composition. The pressure was measured three times per each probe.

The pressure induced by combination of strains in both weft and warp directions was measured using Salzmann pressure-measuring device over the same rigid cylinders. The warp extension was comparable to the warp strain calculated from the garment in size Medium on Base Model (Table 3.6).

Table 3.6 Practical warp strain on Base Model – SCT in size Medium

Measuring point	Warp Strain %
Inseam	28
Knee - Mid-thigh	7*
Calf - Knee	9
Ankle - Calf	33*

* selected values for variable warp strains

(a) (b) (c)

Figure 3.12 (a) Cylinder and probe set-up, (b) 0% strain in warp direction and (c) sleeve held strained to provide warp strain

One fabric sleeve made of fabric C, providing a combination of 25%, 50% and 75% weft strain and zero, 10% and 30% warp strain was tested on each cylinder, where three measurements were recorded per strain combination/cylinder diameter. The pressure induced by strain in weft direction was recorded when the sleeve was placed over the cylinder and the strain in warp direction was kept at zero. Then the fabric sleeve was extended to provide 10% and 30% of additional strain in warp direction and the pressure was recorded for each combination of weft and warp strains. The first measurement was taken 45 seconds after the sleeve was first put on the cylinder. The following pressure measurements were recorded 30 seconds after each measurement was taken. The air within the sensor sleeve was squeezed out between each pressure measurements.

The strain in warp direction was achieved by fixing the sleeve at one end of the cylinder set-up using cable ties (top end) and stapling the other end to a wheel fixture (bottom end) (Figure 3.12). Long sensor probe was used in this part of the research, due to longer length of the set-up; therefore, the pressure induced only by weft strain was remeasured over the cylinders with the long probe, to eliminate any possible variations in pressure recordings between short and long sensor probes. The fabric sleeve induced pressure only over the first four measuring points (B to D).

The pressure readings from each point of the sensor probe were analysed and compared to theoretical pressures calculated per each strain/cylinder composition.

3.4.3. Testing of fabrics comprising SCGs for physiological comfort properties

In this section, the methods of measurement of porosity, air permeability and optical porosity of fabrics are explained. These parameters as well as physical attributes of fabrics influence their physiological comfort properties. Then, the methods for evaluation of thermal and water-vapour management, moisture management and tactile properties of fabrics are discussed.

3.4.3.1. Porosity, air permeability and optical porosity

The porosity of fabrics C and D, representing the amount of air space as a percentage of a total volume of fabric is calculated. The air space within the fabric is calculated from the difference of total volume of fabric and total volume of fibre (Skinkle 1940), Eq. (8):

$$P = 100 \times \left(1 - \frac{W}{ADT}\right) \tag{8}$$

where P is the porosity (%), W is the weight of the specimen (g), A is the area of the specimen (cm^2), D is the fibre diameter (g/cm^3) and T is the specimen thickness (cm).

In case of fabrics C and D, where the fabrics were made of composition of fibres, the weighted average of fibre density was calculated and used for porosity calculations.

Air permeability measure, which is the resistance of fabric to the passage of air through the fabric, is tested for fabrics C and D; air permeability measurement is carried out as per standard method ISO 9237:1995 (ISO 1995) with ATLAS Air Permeability Tester. The air inlet orifice is 2.5 cm in diameter. Five specimens of 3.5x3.5 cm^2 were prepared from each fabric. The specimen is clamped over the air inlet orifice with outer face towards the air inlet, making sure there is no air leakage at the edges of the fabric. The air supply is turned on with the pressure reading of zero in the manometer tube. The relative valve (valves C and D) are closed, and the vacuum pump unit is turned on. Flow tube switch was selected as Tube no. 3. Valve C was opened gradually until the pressure drop of 100 Pa is achieved across the test area of the fabric. The rate of air flow is recorded by reading from the top of the float within the tube, when steady condition is reached, and air permeability is calculated, Eq. (9):

$$R = \frac{\bar{q}v}{A} \times 167 \tag{9}$$

where R is the air permeability (mm/s), $\bar{q}v$ is the arithmetic mean rate of air flow (l/min), A is the area of fabric under test (cm^2), and 167 is the conversion factor.

Air permeability was calculated for five specimens per each fabric and the mean results were evaluated.

Optical porosity of fabrics C and D in relaxed formation are calculated in section 3.4.1.2. Porosity and optical porosity was also calculated for fabric D in various strains in weft direction (13%, 26%, 41%, 56%, 69% and 82% strain). Optical porosity was measured and calculated as explained in section 3.4.1.2, using Motic microscope and Image Tool UTHSCSA, Version 3, where fabrics were strained over a perspex plate to relative weft strains and the image was taken and optical porosity was calculated.

Mass per unit area, number of courses and wales per unit length, stitch density and thickness of fabric D was also measured in various strains in weft direction mentioned above. The mass per unit area of the specimens were measured by weighing a fabric sample in a size that when it would be strained to relative strain in weft direction would cover a 100 cm^2 area. Thickness of specimens in strained formation was measured by stretching a fabric sleeve over a perspex plate providing relative strains in weft direction and measuring the thickness of the assembly. Thickness of one layer of fabric was then calculated as half of the measured thickness, having subtracted the thickness of perspex plate. Thickness and mass per unit area of the fabric in strained formation were used in calculation of porosity in various strains in weft direction.

3.4.3.2. Thermal and water-vapour management

Fabrics C and D are tested for thermal and water-vapour resistance using sweating guarded hotplate in relaxed formation as per standard method ISO 11092:1993(E) (ISO 1993) and were tested in relaxed and strained formation as per a developed method based on the same standard. Thermal resistance (R_{ct}) is the thermal difference between the sides of the fabric divided by the resultant heat flux per unit area in the direction of the

gradient. Thermal resistance (m^2.K/W) is the dry heat flux across a given area in response to a steady applied temperature gradient (ISO 1993). Water-vapour resistance (R_{et}) is the water-vapour pressure difference between the two sides of the fabric divided by the resultant evaporative heat flux per unit area in the direction of the gradient. Water-vapour resistance (m^2.Pa/W) is the 'latent' evaporative heat flux across a given area in response to a steady applied water-vapour pressure gradient (ISO 1993).

Thermal resistance of the fabrics are tested as per standard method ISO 11092:1993(E) (ISO 1993), where the measuring unit temperature (T_m) is set at 35°C ±0.1 K, air temperature (T_a) at 20°C ±0.1 K and relative humidity (R.H.) at 65 ±3% with air velocity (v_a) of 1 ±0.05 m/s.

Water-vapour resistance of the fabrics is tested as per standard method ISO 11092:1993(E) (ISO 1993), where the measuring unit temperature (T_m) and air temperature (T_a) are set at 35°C ±0.1 K and relative humidity (R.H.) at 40 ±3% with air velocity (v_a) of 1 ±0.05 m/s. A water-vapour permeable and liquid-water impermeable cellophane membrane is fitted on the measuring unit prior to the water-vapour resistance measurement, and the measuring unit is kept constantly moist during the test.

Each specimen is 30x30 cm^2, laid flat in relaxed state completely covering the surface of the measuring unit and thermal guard, held by adhesive tape, where air flows across and parallel to the upper surface of the fabric. The thermal and water-vapour resistance of the measuring unit itself and its boundary air layer adhering to the surface of the test specimen in the same conditions are determined as 'bare plate' values at steady state (R_{ct0} and R_{et0} for thermal and water-vapour constants, respectively), before testing of specimens, and are incorporated in the results. The results are the arithmetic mean of three 'power meter' readings based on a 15 minutes integration after steady state is reached.

The fabrics were also tested for thermal and water-vapour resistance in strained formation, with 25% strain in weft direction and zero strain in warp direction according to a developed method based on standard method ISO 11092:1993(E) (ISO 1993). As per developed method, the testing conditions were the same as the standard method, yet the fabrics were strained and held on a wooden frame using staples (Figure 3.13). The wooden frame was 25.4x25.4 cm^2 and 3.5 cm high. Since the height of the wooden frame had potential influence on the air flow and boundary air layer over the measuring plate, the bare plate values and also the thermal and water-vapour resistance of the relaxed fabrics were also tested with the wooden frame placed over them, in order to eliminate any difference in air flow conditions and boundary air layer and to have the identical conditions (same air flow) as the strained fabrics.

To test the fabrics in strained formation, the fabric was strained and secured on one side of the frame in a way that fabric laid flat on the measuring unit. As the wooden frame covered with fabric was slightly bigger than the area of the measuring unit, the strained fabric was covering the whole surface of the measuring unit and the thermal guard; adhesive tape was used at the edges of the frame to ensure there was no air passing through the edges, the same as for relaxed fabrics (Figure 3.14).

(a) (b)

Figure 3.13 (a) wooden frame and (b) fabric extended on the wooden frame

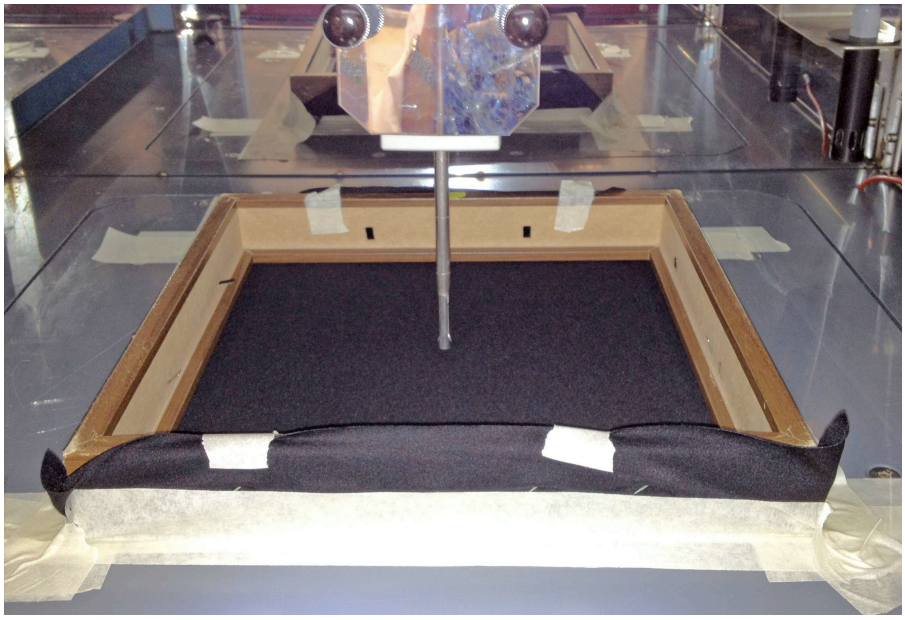

Figure 3.14 Strained fabric on the wooden frame, placed over the measuring unit

The air temperature and air flow is measured at 15 mm above the measuring table. Due to the height of the frame and its potential affect on the air flow over the surface of the fabric, the 'bare plate' values of boundary air layer (R_{ct0} and R_{et0} for thermal and water-vapour constants, respectively) with the wooden frame over the measuring unit were incorporated in the results when wooden frame was used along with fabrics in both relaxed and strained formations.

The fabrics and the wooden frame were conditioned in the same temperature and relative humidity as per dry and wet test according to ISO 11092:1993(E) (ISO 1993) for both standard and developed method. Three specimens per each fabric were tested and three readings were recorded per specimen in steady state and mean results were reported and analysed.

Results for relaxed fabrics were compared between fabrics C and D. Separate paired t-tests were carried out between relaxed fabrics with and without the frame, and between the relaxed and strained fabrics both with the frame, for fabrics C and D. The significance

of the introduction of wooden frame and strain in weft direction on thermal and water-vapour resistance were analysed.

3.4.3.3. Moisture management properties

Moisture management properties of fabrics C and D are tested on their technical back (next-to-skin side) according to AATCC TM 195:2009 (AATCC 2009) with SDL ATLAS Moisture Management Tester (MMT).

Specimens are 8x8 cm^2 and placed with their technical back facing up (top surface) between two horizontal electrical sensors with seven concentric pins. Test solution of amount of 0.22 cc (conductive medium prepared as per same standard method) is dropped on the centre of top surface of the fabric during 20 seconds. The electrical conductivity of the fabric due to test solution and its moisture management properties are measured for 120 seconds from when the solution started pumping. The test solution is dropped on the technical back of the fabric, mimicking the sweat water present on human skin surface being exposed to the garment worn next to the skin.

Radial spreading of water on top surface, movement of water through the fabric from top surface to bottom (from skin side to outer surface) and radial spreading of water on bottom surface of the fabric is measured through change in electrical resistance on both sides of the fabric. Fabric liquid moisture content changes cause electrical resistance readings, which are used to quantify dynamic liquid moisture transport behaviour in multiple directions (outwards on both surfaces and through the fabric). The following predetermined indices are used in grading the liquid moisture management of fabrics (AATCC 2009): Wetting time (WT_T and WT_B) is the time in seconds when the top and bottom surfaces of the fabric begin to be wetted after the test is started. Absorption rate (AR_T and AR_B for top and bottom surface, respectively) is the average speed of liquid moisture absorption for the top and bottom surfaces of the fabric during initial change of water content during a test. Maximum wetted radius (MWR_T and MWR_B) is the greatest ring radius measured on top and bottom surfaces. Spreading speed (SS_T and SS_B) is the accumulative rate of surface wetting from the centre of the fabric, where the test solution is dropped to the maximum wetted radius. Accumulative one-way transport capability (R) is the difference between the area of the liquid moisture content of the top and bottom surfaces of the fabric with respect to time and overall (liquid) moisture management capability (OMMC) is an index of the overall capability of the fabric to transport liquid moisture, as calculated by combining three measured attributes of performance, Eq. (10): AR_B, R and SS_B.

$$OMMC = C_1 * AR_{B\_ndv} + C_2 * R_{ndv} + C_3 * SS_{B\_ndv} \quad (10)$$

where C_1, C_2 and C_3 are the weighting values * for AR_{B_ndv}, R_{ndv}, and SS_{B_ndv}, AR_B is the absorption rate, R is the one-way transport capability, and SS_B is the spreading speed.

Five specimens were tested per each fabric and mean results were analysed.

3.4.3.4. Tactile comfort properties

Fabrics A to D are tested for surface properties such as surface friction and surface roughness properties on technical back (next-to-skin side) in dry state, using Kawabata Evaluation System FB4, which is an automatic surface tester used for measuring the former mentioned values. There are two probes, one measuring the surface roughness and the other surface friction, in two sliding movements in opposite direction for 30 mm horizontally with a constant speed of 0.1 cm/sec; however, the measurements were taken from only 20 mm of the travelled distance, omitting 5 mm at both ends.

The surface roughness is measured by 5 mm length contact sensor with vertical load of 10 gf moving in a 'go-stroke' and 'return stroke', and the surface friction (kinetic coefficient of friction - MIU) is the average of frictional coefficient measured by a contact probe of 10 mm^2 with vertical load of 50 gf. Surface roughness mean deviation (SMD) is obtained, Eq. (11):

$$SMD = \frac{1}{L\max}\int_0^{L\max} \left| Z - Z \right| dL \tag{11}$$

where *Lmax* is the maximum distance of movement, *Z* is the vertical deformation of the sensor from a standard position (cm), and *L* is the distance of sensor that moves on fabric surface.

Frictional coefficient (MIU) is calculated, Eq. (12):

$$MIU = \frac{F}{P} \tag{12}$$

where *MIU* is the coefficient of friction, *F* is the frictional force, *P* is the standard load of sensor pressing the fabric.

The mean frictional coefficient (MMD) represents the variation of friction in the direction of travel, which could be sensed by human fingers running on the surface of the fabric, while SMD represents the geometry of the surface.

The roughness and friction measurements are carried out three times in 12 mm distances apart, in both warp and weft directions. All four fabrics tested in relaxed state were held under 20 gf/cm tension, to provide 0% strain and flat surface.

Fabric D was also tested in various strains in weft direction in dry condition for surface friction and surface roughness and the results were compared to relaxed state.

To test the fabric in various weft strains, a perspex plate with smooth edges measuring 145 mm in width, 175 mm in length and 2 mm in thickness was sourced (Figure 3.15a); the circumference of the plate in its width direction, taking into account the thickness, was 294 mm.

Fabric sleeves were made so that when strained over the plate would provide 13%, 26%, 41%, 56%, 69% and 82% strain in weft direction (Appendice 3). The length of 20 mm was allowed at the both ends of the plate to ensure that the fabric was under no warp

strain and the weft strain was distributed evenly along the width of the plate when tested (Figure 3.15b).

(a) (b)

Figure 3.15 (a) Perspex plate and (b) fabric sleeve stretched over it

Fabric D was also tested for surface roughness and surface friction properties in various weft strains and in moist conditions. A developed method was used to test the fabrics in moist conditions. Fabric sleeves were first dried out to 0% moisture content to determine their dry weight. They were then wetted out thoroughly by immersion in tap water for 1 minute. A padder was then used to squeeze out the excess water by passing the wetted fabric sleeve twice between squeezing rollers with a consistent pressure and speed (Figure 3.16). The fabric sleeve was then wet but not dripping. The fabric sleeves were weighed again to determine their wet pick-up as a percentage of their initial dry weight. The wetted out fabric sleeves were then kept in a polyethylene zipped bag to avoid any loss of moisture until the test for surface characteristics was carried out. With this method, the fabric sleeves represent a fabric next to the skin saturated with perspiration of the wearer.

Figure 3.16 Squeezing padder

Microscopic images were taken from all four fabrics and also from fabric D strained to various strains in weft direction, using Motic microscope and Image Tool UTHSCSA,

Version 3. The microscopic images were used to further study the surface characteristics of fabrics.

3.4.4. 3D body-scanning

NX-16 3-Dimensional Scanner was used for scanning and generation of true to scale body-model (TC2 Website, 2011). The 3D body-scan raw data is in the form of point cloud, which is processed into a 3D body-model (Figure 3.17).

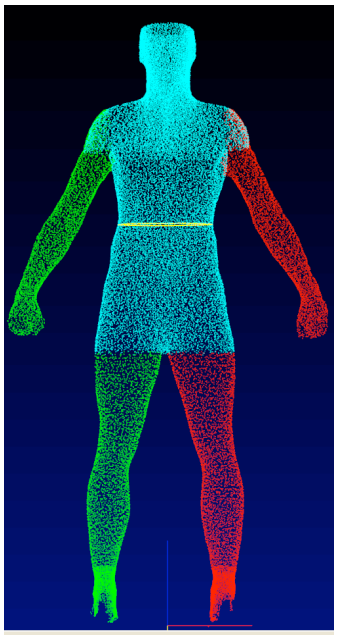

Figure 3.17 3D body-model

Various body measurements, including standard and customized body measurements from $[TC]^2$, could be automatically extracted from the 3D body-model using the $[TC]^2$ Measurement Extraction Profile (MEP). $[TC]^2$ measurement extraction software has predefined measurement points already included in the program. It also allows the user to define new measurement points, which are modifications to the predefined measurement points in the program. The MEP File was modified according to important measurement points identified for the application under investigation and the body measurements were extracted and used subsequently in this research.

A group of thirteen male and thirteen female healthy volunteers were selected, belonging to a range of sizes for a selected brand of sport compression apparel, so that the participants were a cross-section of sizes from Extra Small to Large for males and from Small to Large-Tall for females, respectively. The mean ages were 36.8 (from 23 to 51) and 32.9 (from 22 to 60) years old for male and female participants, respectively. All participants were active in some type of sport or fitness activity, and they wore or considered wearing SCTs in their activities. Approval from RMIT University's Ethics Committee was obtained (Register Number CHEAN AB-2000413-10/10) and the participants gave their written consent to voluntarily take part in this research.

Participants were asked to wear the SCT in their size according to the sizing chart of the brand. The sizing mechanism of the brand allocated the sizes according to height and weight (Figure 3.18).

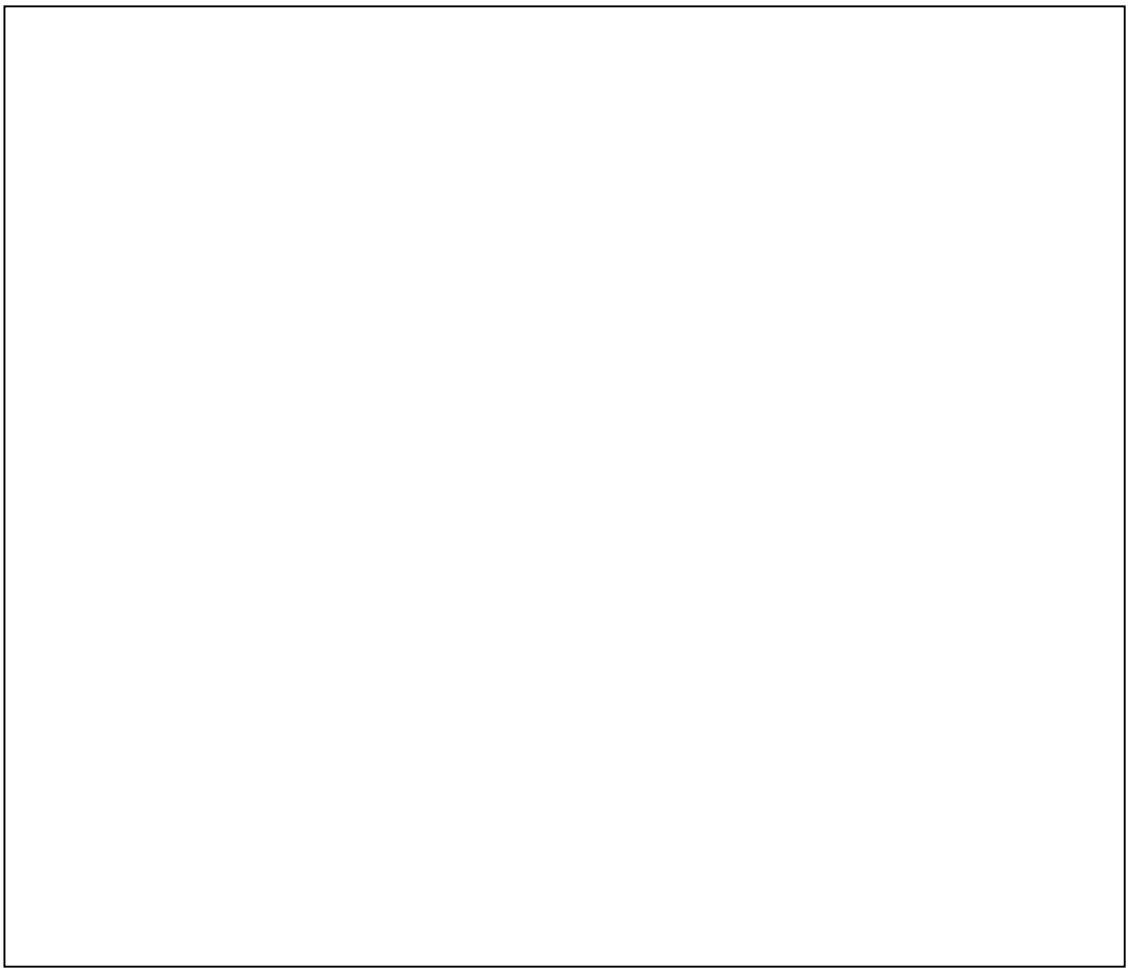

Figure 3.18 SCT Size Chart (2XU Website 2012)

Body mass and stature of participants were measured and recorded prior to the 3D body-scanning. A calibrated scale is used and tare button is pressed prior to each measurement. Participants are then directed to stand in the centre of the platform with the mass being recorded to the nearest 0.01 kg. Stature of participants are recorded, where the participant is directed to stand erect with heels, buttocks and shoulders pressed against the vertical wall. The heels are touching and the arms are hung by the sides in a natural manner. Participants are instructed ‘to look straight ahead and take a deep breath’ and to gently but firmly stretch the vertebral column. The measurement is read from the measuring ruler attached to the wall and recorded. The postures of participants were recorded, having their written consent, with photographs at front and side views with the participants wearing the SCT and an own top. Participants were directed to stand with feet at a specific distance apart marked on a mat, with hands in straight line apart from their body; this is the same position in which they are later scanned (Figure 3.19).

Landmarks were put on specific points on the body of each participant. Knee, at centre of Patella (Figure 3.21b), was marked with a marker. To identify this point, the participants

were asked to bend their knees, where the patella was more recognizable by touch, and the centre of patella was marked using a marker. As the body shape and size would influence the position of the top of the garment in the waist area, the top front and back, and also the bottom edge of each tight were marked on the body of participants, when the SCT was worn. As the participants were scanned in their underwear with bare lower limbs, the specific recognisable scanning paper landmarks were placed on the marks at the points marked with a marker after removal of SCTs and before the scanning process. Landmarking sites were rechecked, since the movement of the skin over the skeleton may alter the relative position of the mark when pressure is released.

(a) (b)

Figure 3.19 3D body-scanning foot position and posture form – (a) front and (b) side views

Participants were scanned six times (according to 3.4.4.2), wearing only their underwear and the landmarks placed on their body.

3.4.4.1. Development of scanning protocol

The measuring points of importance recognized for MCGs (BSI 1985, 1999; RAL 2008) and other anatomical measuring points critical for application under investigation were chosen to design the MEP File.

Measuring points B, B1, C, D, F and G were derived from medical compression hosiery standards such as RAL-GZ (RAL 2008), BS 6612:1985 and BS 7563:1999 (BSI 1985, 1999). B was horizontal circumference at 2 cm above the Ankle (Ankle was defined at

average height between Lateral and Medial Malleolus) (Figure 3.21a), and B1, C, D, F and G were 8, 19, 27, 48 and 60 cm distant apart from point B, respectively. These distances are according to sensor measuring points on Salzmann sensor probe (Figure 3.8).

Figure 3.20 demonstrates the measuring protocol consisting of circumferential and length measurements of the lower limb.

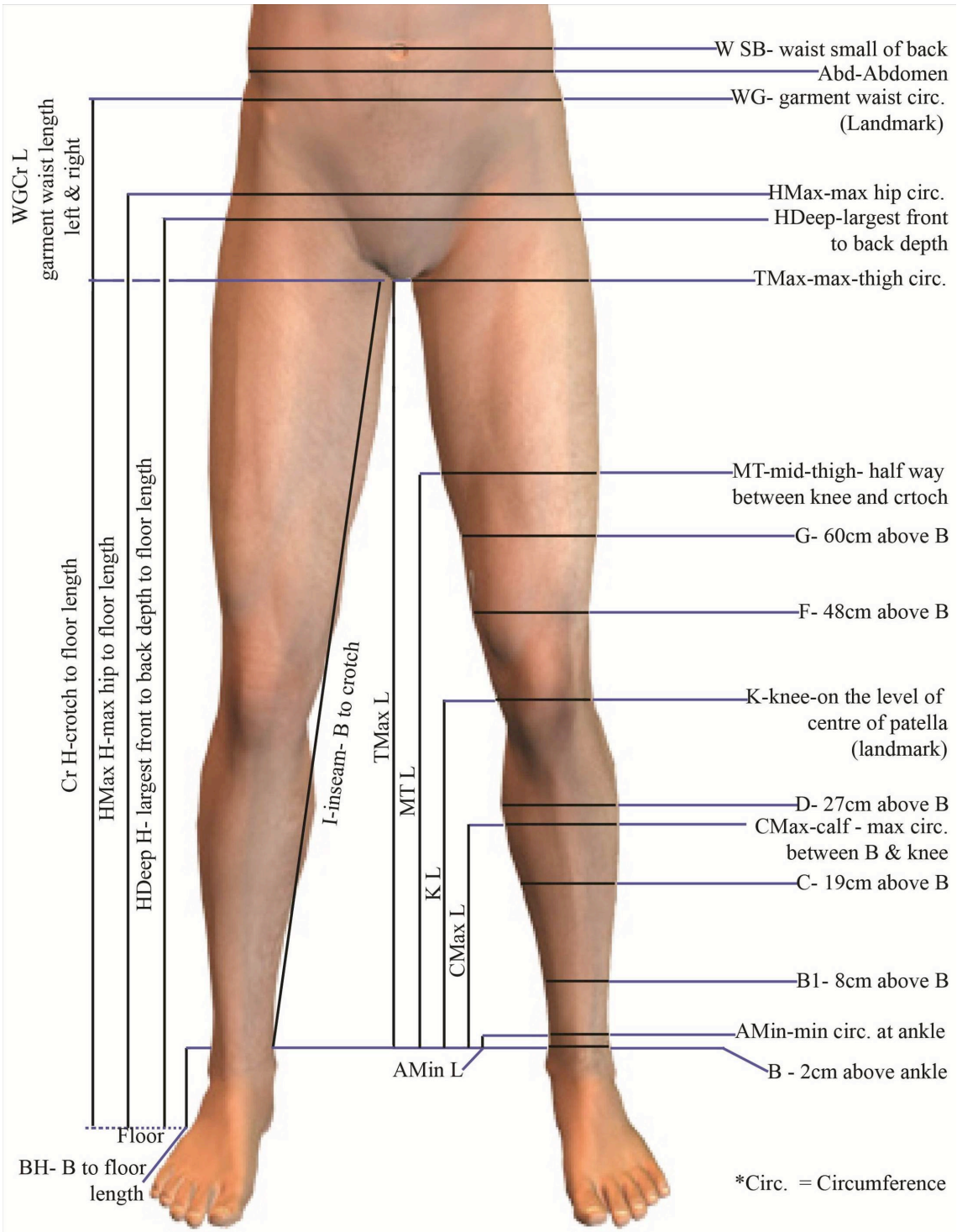

Figure 3.20 Measurement protocol for 3D body-scanning – lower-limb

There were other measuring points added to the protocol: some were critical anatomical points such as patella centre and posterior prominence of the buttocks (Yu 2004b) and some were joints, minimum or maximum circumferences along the limb, which were also required for referencing and investigation of fabric strain, performance and garment fit. AMin was minimum circumference at the ankle. CMax (calf) was the maximum circumference between point B and knee. K (knee) was the circumference at centre of Patella (Figure 3.21b). MT (mid-thigh) was circumference half way between the knee and crotch, and TMax (thigh-max) was the maximum circumference on the thigh. HDeep or Hip Deep was the largest front to back depth between the crotch and W SB (waist small of back), HMax (hip-max) was maximum hip circumference and Abd was the abdomen in reference to W SB. Knee (K) was defined differently within the 3D body-scanner software to the definition relative to this application; thus, it was landmarked on the body before the 3D body-scanning and was edited to match the landmark placed on the body (Figure 3.22).

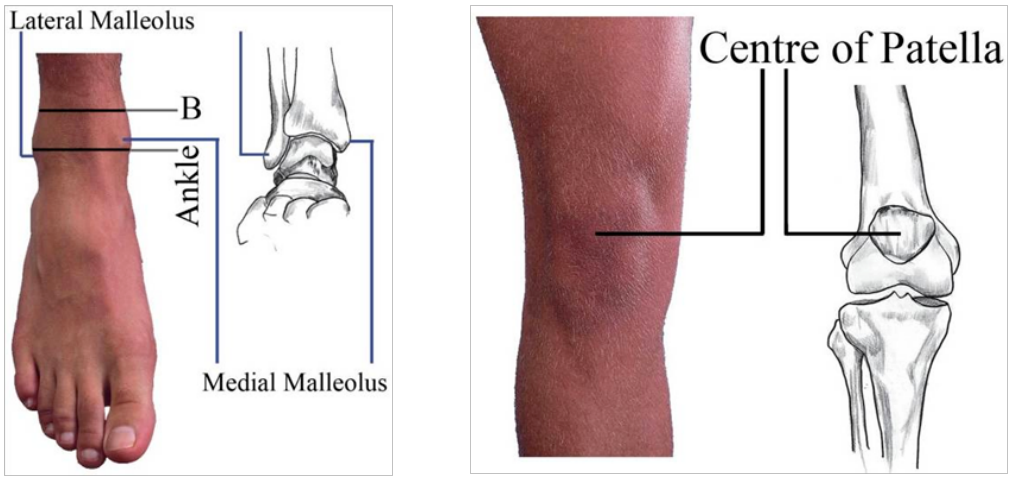

(a) (b)

Figure 3.21 (a) Right ankle – Medial Malleolus and (b) right knee – centre of Patella (Field & Hutchinson 2008)

Body shape and size would influence the position of the top of the tight in the waist area; for this reason, the waist of the garment (WG) was also landmarked in front and back of the body to reference the position of the top of tight on the body. These points were also edited after the 3D body-scanning, to match the landmarks.

In the MEP File, measuring points such as ankle, calf, abdomen, hip and waist were defined by the program. Yet points such as B to G were defined using anchor points such as the measurement points recognised by the software; for instance, B and B1 circumferences were defined as the circumferential measurement at 2 and 10 cm above the position where the ankle was recognised by the program, respectively. Mid-thigh circumference was defined as the leg circumference at 50% height between knee and crotch and max-thigh circumference was defined as the largest circumference between knee and crotch.

Due to software limitations, the vertical distance between all the extra measuring points and point B were manually calculated after the measurements were extracted, by

subtracting the BH (B to floor length) from the height of these points from the floor. The length of the waist of the garment and the crotch in right and left (WGCr L) and inseam (I) which was the distance between the crotch and B was also manually extracted. These measurements provide the references to warp strain of the garment over the body. Furthermore, Cr H (crotch height), Hmax H and HDeep H (height) to the floor were recorded. The extra measurements provide the data of the overall measurement and size of the wearer. Also, they were used in analysis of the garment construction, fit and sizing.

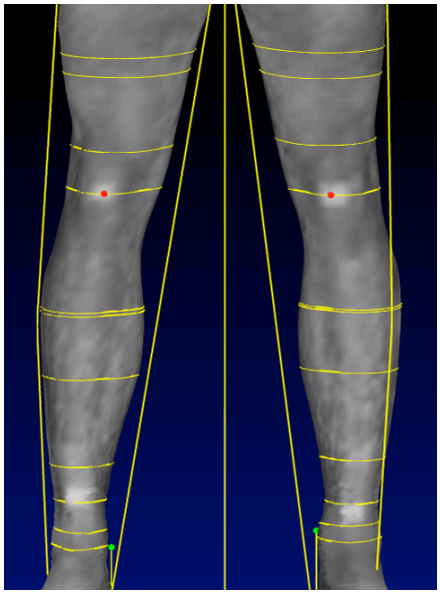

Figure 3.22 Knee edited to match the landmark placed on leg

Figure 3.23 Base Model wearing SCT

A male fit model selected by the sport compression brand was used as a Base Model for this research, where further 3D body-scans were recorded wearing the SCT. Base Model was an athlete, who weighed 84 kg and his height was 184.5 cm (Figure 3.23). The model fitted size Medium according to sizing mechanism of the SCT under investigation (Figure 3.18) and represented the customers of the brand fitting this size.

Base Model was scanned wearing his underwear, to form the all over body measurement reference, as per other participants. He was then scanned wearing the SCT in sizes Small, Medium and Large. Measurements extracted from the second set of scans enable calculation of garment strain in both weft and warp directions. This provided the information on practical elongation of the garment over the limb used in 3.4.2. Additionally, body deformation due to wearing SCT was analysed by comparison of body-models in relative points in underwear with bare limbs and with the SCT being worn.

3.4.4.2. Reliability and validity of instrument

As mentioned in 2.4.2, the accuracy and reproducibility of 3D body-scans require further investigation. According to ISO 20685:2010 (ISO 2010), to ensure the repeatability of the 3D body-scanner, at least three scans must be acquired from each subject, to check the location of points at least in the centre of scanning volume. To test the reliability and repeatability of 3D body-scanner used in this research, two female participants (participant 1 aged 27, 49 kg and 160 cm and participant 2 aged 23, 53 kg and 160 cm) were scanned with $[TC]^2$ 3D body-scanner and their body measurements were extracted using ASTM SizeUSA MEP File. Thirty consequent scans were recorded from each participant, in order to eliminate any external variations resulting from time. The extracted measurements were studied statistically for each participant, in order to decide on number of 3D body-scans required to be taken from each participant to achieve statistically significant results.

ASTM SizeUSA MEP File extracts whole-body measurements in length and circumference: it measures bust, waist, high hip, hips, mid-neck, neck base, armscye, upper arm, elbow, wrist, thigh-max, thigh mid, knee, calf, ankle, centre trunk, crotch length total, cervical height, waist height, high hip height, hips height, crotch height, knee height, ankle height, waist height, across shoulder, cross back width, shoulder length, shoulder slope arctan, arm length, bust pt to bust pt, neck to bust and scye depth. Considering the accuracy of the $[TC]^2$ 3D body-scanner which is ≤ 3 mm in circumference ($[TC]^2$ n.d.), the data points were analysed relative to the body scanner resolution.

For measure of reliability, mean, median and mode of body measurements were considered. A body with mean measurements does not exist in reality and as the number of data points were even, median was the mean of two different 3D body-scans as well; thus, mean and median were not a good measure. While mode was actual body measurements from one 3D body-scan; for this reason, mode was a better measure and was used in this analysis. In order to calculate the mode, the data points were rounded to one decimal place. If absolute difference of each data point and mode was equal or smaller than the specified error (≤ 3 mm in circumference), the data point was considered acceptable. Each set of scans were then ranked from the highest number of data points

within the specified error range. The percentage of data points within the range and the percentage of each data set within the range were also calculated. The 3D body-scan which was ranked the highest within the tolerance was used for the investigation.

3.4.5. Statistical analysis

The following statistical analysis is carried out in this research:

Descriptive statistics such as mean, mode, minimum, maximum, range, standard deviation (STDEV) and mean absolute differences (MAD) were used to summarise the differences between measured values; Pearson's correlation analysis was conducted to evaluate whether there were significant relationships between variables; Paired t-tests were carried out to analyse whether properties of fabrics differed significantly following the introduction of a new parameter; and linear regression models were derived to predict measured pressure from theoretical predicted pressure for fabrics.

Statistical analysis was carried out using Microsoft Excel and PASW Statistics 18 software. All analysis incorporated 95% confidence limits, with statistical significance being accepted at $p < 0.05$.

3.4.6. Study limitations

Limitations of this study are as followed:

In preliminary investigation, the interface pressure of SCTs was measured without any extra calibration procedure of sensors, except for the calibration procedure recommended by the manufacturer of the device.

Due to material constraints, three specimens per each cylinder diameter/strain combination for sleeves and one specimen in various compositions in strip formation was prepared and tested. The pressure from combination sleeves was only measured for 50% and 75% strain in weft direction and only on cylinder 90.

Due to design and pressure measurement mechanism of the pressure sensor, it was difficult to source suitable weights, covering the small surface area of the sensor point and providing sufficient mass; thus, the calibration with weights was under the influence of off-balanced weights. Furthermore, due to funding limitation, calibration of sensor probes were not carried out any further than what was explained in section 3.4.2.2.

Similar to the methods employed by other researchers mentioned in section 2.2, some of the variables affecting the induced pressure by CGs was reduced and/or eliminated throughout this research, to be able to study other factors in more depth. In this research, the human limb was considered to be cylindrical and non-compressive.

Due to configuration of air permeability tester, air permeability could not be tested in strained formation.

Last but not least, due to small space within the MMT device and the fact that the fabrics were placed between the top and bottom sensors, testing of fabrics in strained formation for moisture management properties was not possible.

4. Results and discussion

The aim of this research was to predict, measure and validate pressure generated by SCGs on the underlying tissue of human and to evaluate the physiological comfort performance of the garments. All the materials were prepared, and tests and evaluations were carried out as detailed in section 3.4. In this chapter, the results from experiments are reported, analysed and discussed.

4.1. Preliminary analysis of SCGs and fabrics comprising them

Due to lack of scientific knowledge available on SCGs, and their construction and pressure profile, preliminary investigation was carried out on commercially sourced SCTs for men in sizes Medium and Large. Physical attributes of fabrics comprising SCTs were investigated such as mass per unit area, stitch density, thickness and optical porosity, in order to have a basic understanding of the fabrics. Meanwhile, a widely acceptable method for evaluation of tensile performance of fabrics used in CGs was not available; thus, a suitable method was developed based on a standard test method for evaluation of tensile properties of elastomeric fabrics, which was used in theoretical pressure calculations in section 4.2.

4.1.1. Construction and pressure profile of SCGs

SCTs under investigation were composed of two fabrics with different properties, analysed in detail later in sections 4.1.2 and 4.1.3. The tights were composed of approximately 48% of one fabric (fabric C) in the front and 52% of another fabric (fabric D) in the back of the tight, eliminating the gusset (Figure 3.1).

Various length and circumferential measurements were obtained from tights in both sizes of Medium and Large (Appendice 4). It was observed that the tight in size Large was equal in inseam and in height from hem to crotch measurement, but slightly longer in outseam measurement (by 2%). This means that the tight in size Large was mainly longer in the seat area and not the actual leg length of the tight in comparison to tight in size Medium.

Figure 4.1 reveals that the circumferential measurements increased from measuring point B to G in each tight. Furthermore, tight in size Large was slightly wider in circumferential measurements along the leg length in comparison to the tight in size

Medium, by 3%, 4%, 4%, 7%, 6% and 3% at measuring points B to G, respectively and that the increase in circumferential measurements was mainly greater in thigh area.

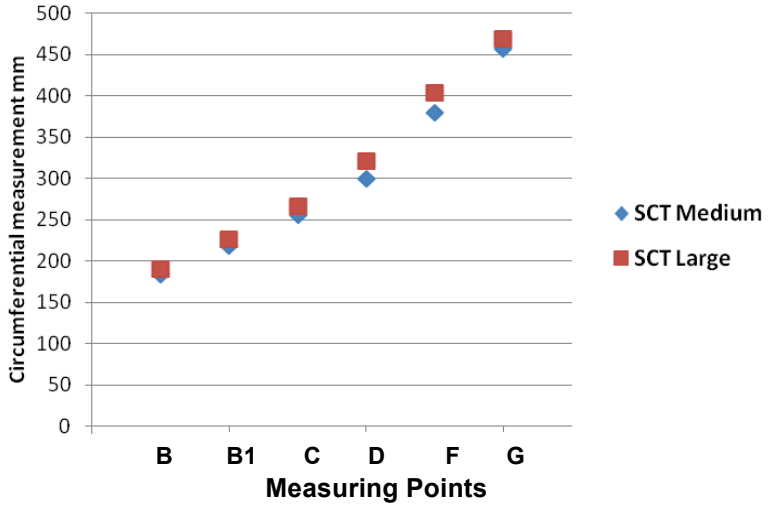

Figure 4.1 Circumferential measurements of SCTs at measuring points B to G – sizes Medium and Large

The composition of the fabrics (fabrics C and D) along the circumference of the tight varied along its length (Figure 3.1). Fabric D had a greater percentage within the tight circumference from the bottom (measuring point B) to measuring point D (mean of 81% and 79% in sizes Medium and Large, respectively) and this composition was inversed from point D onwards (mean of 27% and 25% in sizes Medium and Large, respectively). Percentage of each fabric along the circumference of the tight at measuring points B to G is shown in Figure 4.2. Since the fabrics had different properties, this would potentially influence the strain, and hence the pressure generated by the tight; this is investigated further in this research.

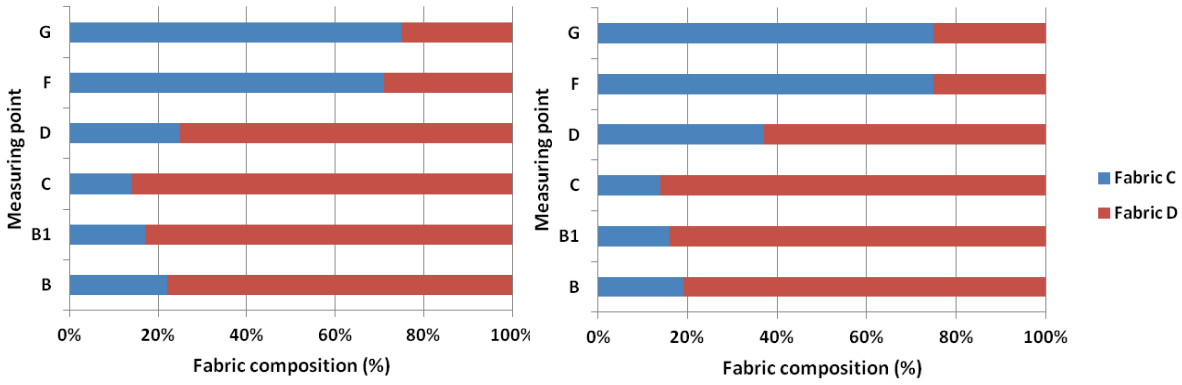

(a) (b)

Figure 4.2 Fabric composition (%) at measuring points B to G in tights (a) Medium and (b) Large

Strain in width (weft) direction of the tights is important as it influences the pressure generated by the tight on the underlying limb. The strains in width (weft) direction on

Salzmann wooden legs at each measuring point were calculated using Eq. (4), for both tights (Figure 4.3).

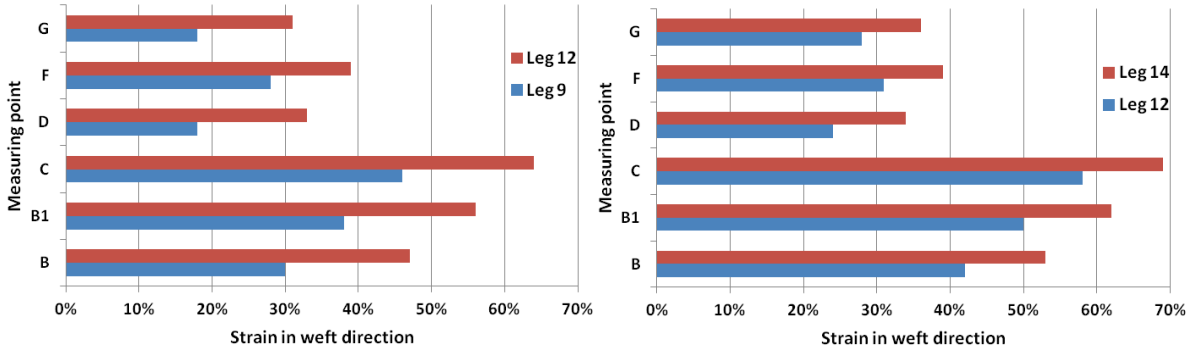

(a) (b)

Figure 4.3 Strain in weft direction of SCTs in sizes (a) Medium and (b) Large on Salzmann wooden legs

As expected and evident in Figure 4.3, increase in leg size (increase in leg measurement at each measuring point) noticeably increased the strain in weft direction of the tights. The increase in strain, however, was not proportional to increase in wooden leg measurements. The cross-section of the wooden legs at each measuring point was circular, yet the overall shape of the leg along its length was not cylindrical and it mimicked an actual leg; there was a decrease in wooden leg circumference at measuring point D from point C, which is generally consistent with a human leg measurements (around the knee). As mentioned earlier, however, the circumferential measurements increased from measuring point B to G in each tight. As a result, the strain in tights increased from point B to C; the decrease in wooden leg circumference and increase in tight circumference resulted in decrease in strain at point D from point C. Furthermore, the strain at measuring point C was relatively high for both tights, especially on the bigger wooden leg. Measuring point C is close to calf area and depending on fabric tensile properties, high strain at this measuring point could lead to high stress and result in very high pressure, which could potentially reverse the gradient pressure required from CGs.

Interface pressure on side and back of SCTs were measured on Salzmann wooden legs (Appendice 5). The measured pressure on the side was lower than the measured pressure from the back on both tights. This could be due to the varied fabric composition of the tight on the side and back. At the back of the tight the sensor was only covered by one fabric (fabric D), while on the side there were two fabrics present, attached via flat-lock seam. On human leg major veins are positioned on the back of the leg; therefore the pressure on the back is more important than the side of the leg and is evaluated further in this research.

Mean interface pressures measured on back of SCTs on Salzmann wooden legs are plotted (Figure 4.4). As expected and can be identified in Figure 4.4, the pressure measured from each tight was higher on the bigger wooden leg; the reason is, as mentioned earlier, increase in leg size noticeably increased the strain in weft direction of the tights. The pressure measured on same sized leg (leg 12) from tight in size Large was lower at relative measuring points in comparison to tight in size Medium; as discussed

previously, this is due to the fact that tight in size Medium was smaller in circumferential measurements than tight in size Large and hence under higher strain (seen in Figure 4.3), recording higher pressure.

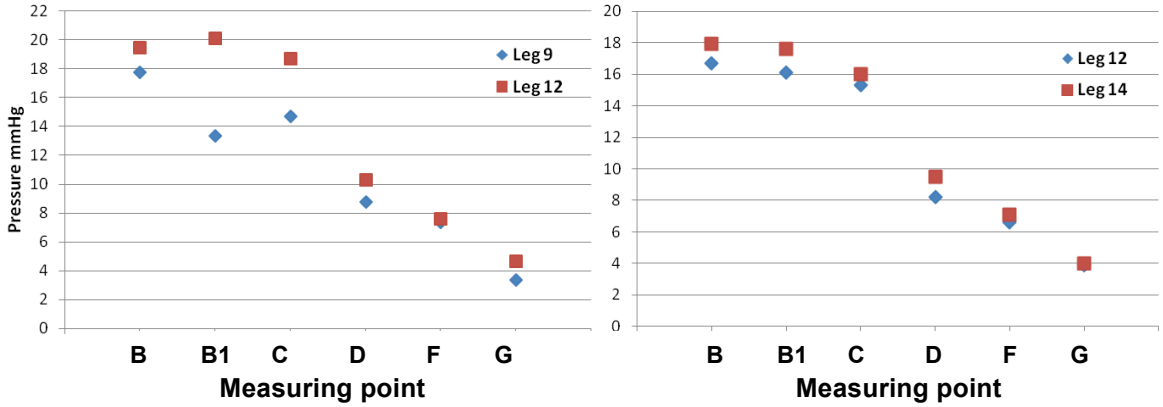

(a) (b)

Figure 4.4 Pressure measured on back of wooden legs from SCTs in sizes (a) Medium and (b) Large

The pressure generally dropped from measuring point B towards measuring point G. It is ideal to achieve gradient pressure from point B to G, which means that pressure is at its highest at point B (close to the ankle) and it gradually decreases towards point G (close to the thigh). In some cases, such as tight in size Medium on back of leg 12, there was 3% increase in pressure from point B to B1. The reason could be that the difference in circumferences between the leg 12 and the tight in size Medium was greater at point B1 in comparison to point B, resulting in higher strain and thus higher pressure. This decrease in pressure reversed the gradient pressure of the tight in size Medium on leg 12. For both sizes, there was a higher drop in pressure from point C to D. Interestingly, even though the measured pressure from tight in size Large was higher on the bigger leg (leg 14), yet the drop in gradient pressure was similar on both legs; while this was not the case for tight in size Medium, where gradient pressure was disrupted at point B1 on both legs.

4.1.2. Physical attributes of fabrics comprising SCGs

Physical parameters of the fabrics under investigation are listed in Table 4.1. All four fabrics were of single jersey construction (Figure 4.5).

Fabric A had highest mass pet unit area and second highest stitch density, resulting in lowest optical porosity. Fabric B had highest thickness and stitch density, which made it a more tightly knitted fabric (due to finer yarn and a higher machine gauge), while it interestingly had second highest optical porosity; even though the stitch density of fabric B was higher than the rest of the fabrics, yet finer yarns allowed the light to pass through the fabric more easily. Fabric C was the lightest with lowest thickness in comparison to other fabrics with third lowest stitch density, resulting in second lowest optical porosity. Last but not least, fabric D had lowest stitch density of all, which led to highest optical porosity.

Table 4.1 Physical attributes of sourced fabrics

Fabric label	Fibre composition	Fabric construction	Mean stitch density	Mean mass per unit area	Mean thickness	Mean optical porosity
			per cm^2	kg/ m^2	mm	%
A	Nylon, Elastane	Single Jersey	848	0.246	0.504	1.5
B	Nylon, Elastane	Single Jersey	918	0.237	0.507	2.8
C	72% Nylon, 28% Elastane	Single Jersey	820	0.226	0.431	2.2
D	65% Nylon, 35% Elastane	Single Jersey	798	0.240	0.445	3.3

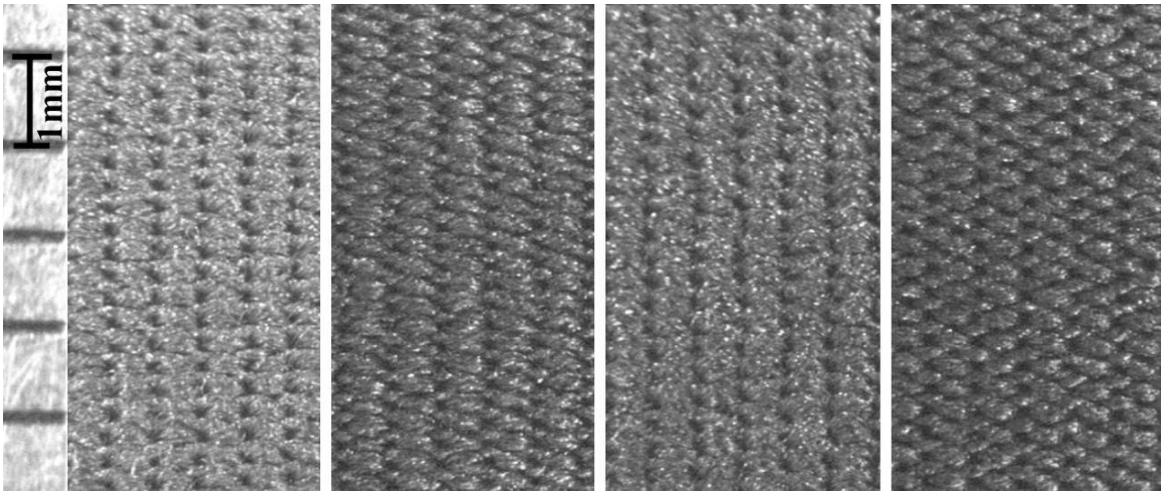

Figure 4.5 Microscopic images of fabrics A to D from left to right - technical back

Average differences between these properties to the highest values were approximately 5%, 9%, 10% and 35% for mass per unit area, thickness, stitch density and optical porosity, respectively. Some of the differences in physical attributes are statistically significant and some are insignificant; yet they contribute to comfort properties of fabrics, such as thermo-physiological and tactile properties. These parameters are evaluated further in regards to comfort properties of fabrics in section 4.3.

4.1.3. Tensile performance attributes of fabrics comprising SCGs

The mean results of testing the fabrics for tensile properties according British Standard 4952:1992 (BSI 1992) in strip formation are listed in Table 4.2.

Even though it is expected from the fabric construction that the fabrics have higher extensibility in weft direction compared to warp direction, fabrics A, B and D recorded higher extensibility in warp direction at 20 N stress. Under the same stress of 20 N, fabric D exhibited the least strain in weft direction followed by fabrics B, C and A. The difference

in stress in fabrics directly translates into the difference in pressure when other properties impacting the pressure remain constant; for instance making the same garment from fabric D would result in 7% to 8% higher pressure on the same limb circumference compared to fabrics B and C. While the same garment from fabric D would result in 60% higher pressure on the same limb circumference compared to same garment from fabric A, which is substantially higher.

Table 4.2 Tensile performance attributes according to BS 4952:1992 - strip formation

Fabric label	Direction	Strain at 20 N stress	Residual extension	Tension decay
		%	%	%
A	Warp	191.7	6.6	0.0
	Weft	186.2	5.4	-7.9
B	Warp	170.7	7.4	6.1
	Weft	124.7	3.6	-0.9
C	Warp	112.1	2.6	-0.8
	Weft	127.1	3.8	0.0
D	Warp	120.5	4.2	-3.5
	Weft	116.8	2.2	-4.6

Fabric C recorded the least strain in warp direction under 20 N stress, followed by fabrics D, B and A. Fabrics A, C and D demonstrated ‘square’ stretch, also known as balanced in terms of their tensile performance; square stretch improves the ease of movement in the resultant garment. Pressure induced by CGs, however, mostly results from stress in weft direction; thus the strain in warp direction is a secondary consideration. In theoretical pressure calculations in this research, the influence of fabric stress in warp direction was not considered; it is important, however, to note that stress in warp direction could potentially influence the generated pressure and will certainly affect fit of the garment and ease of movement. Amongst the fabrics tested, fabric D was the most ‘powerful’ amongst all and would generate highest pressure in equal conditions.

Tension decay was measured at 25% strain, which is a common practical elongation in CGs. The fabrics under investigation were under little or no stress at 25% strain; hence the tension decays measured were almost zero for all but fabric B in warp direction. Fabric B recorded 6% decay in tension. The loss of stress in fabric over time results in the loss of generated pressure, which is undesirable; yet 6% loss in fabric stress is fairly small. In summary, the tension decay results were irrelevant at this point of research as the percentage strain under investigation was too low for the fabrics under investigation. Nevertheless, fabric D showed good performance in the aspect of remaining its stress over time.

All four fabrics exhibited residual extension after 1 minute of relaxation. The most residual extension was recorded for fabric B in warp direction, followed by fabric A in both warp and weft directions. Fabric C had the least residual extension of 3.8% and 2.6% in weft and warp directions, respectively. Residual extension over time would cause lower stress in the fabric which would result in lower generated pressure. Fabric D

demonstrated the least residual extension in weft direction amongst all fabrics and better results than fabrics A and B in warp direction. This research represents only a preliminary attempt to evaluate the tension decay and residual extension of fabrics comprising SCGs and the investigation must be further carried out under suitable strain-stress relative to tensile performance of fabrics.

Fabrics A and C were tested to standard and modified methods in weft direction and strip formation, in order to determine the suitable method of testing for tensile properties of fabrics comprising SCGs.

Figure 4.6 demonstrates the results of determination of strain at various stresses of 5, 10 and 15 N (modified method) for fabrics A and C in weft direction compared to the strain at 20 and 30 N stresses (standard method) in strip formation. The stress values plotted in Figure 4.6 are in N/5cm, where 5 cm is the width of the tested specimen. All strains recorded from modified method under specified stresses of 5, 10 and 15 N were lower than relative strains from standard method for both fabrics in weft direction. Fabrics tested under 30 N stress had a similar trend and slightly higher strain compared to fabrics tested under 20 N stress. The reason for this difference was that in standard method the fabrics were tested to a higher strain and they lost some of the 'power' within the fabric due to cycling under relatively higher stress.

It is interesting to note that in the modified method, when the stress under which fabrics were tested increased, the differences in strain to standard method decreased; as the conditions of testing became closer (tested under higher strain).

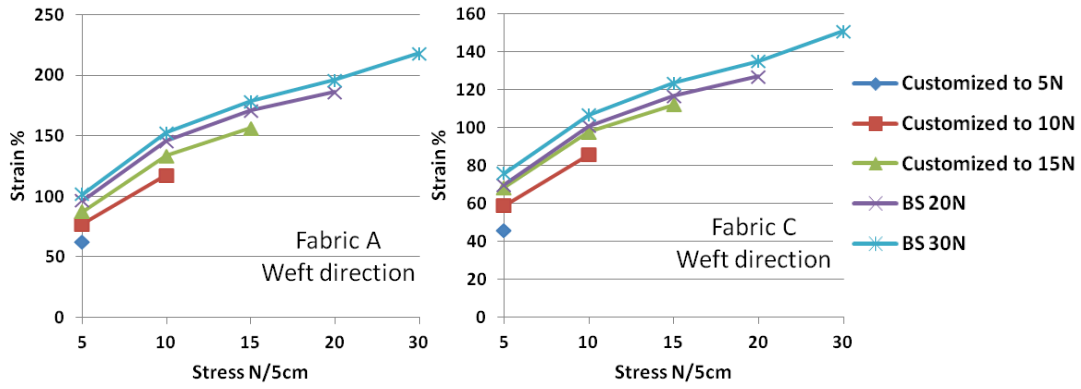

(a) (b)

Figure 4.6 Strain (N/5cm) at specified stress - standard vs. modified method – fabrics (a) A and (b) C in weft direction and strip formation

Figure 4.7 plots the results of determination of stress at various strains of 25%, 50%, 75%, 100% and 200% (modified method) for fabrics A and C compared to the strain recorded at 20 N stress (standard method) in weft direction and strip formation. In Figure 4.7, the stress values plotted are also in N/5cm, where 5 cm is the width of the tested specimen.

The strain-stress curve followed a similar trend from both test methods; the difference in measured stress, however, became greater as the strain increased. The stress recorded from the modified method to 200% strain was invariably lower than other methods; the

same reasoning as above applied: when the fabric was extended to higher strain/stress, some of the power was lost and it was relatively easier to extend the fabric to higher strain.

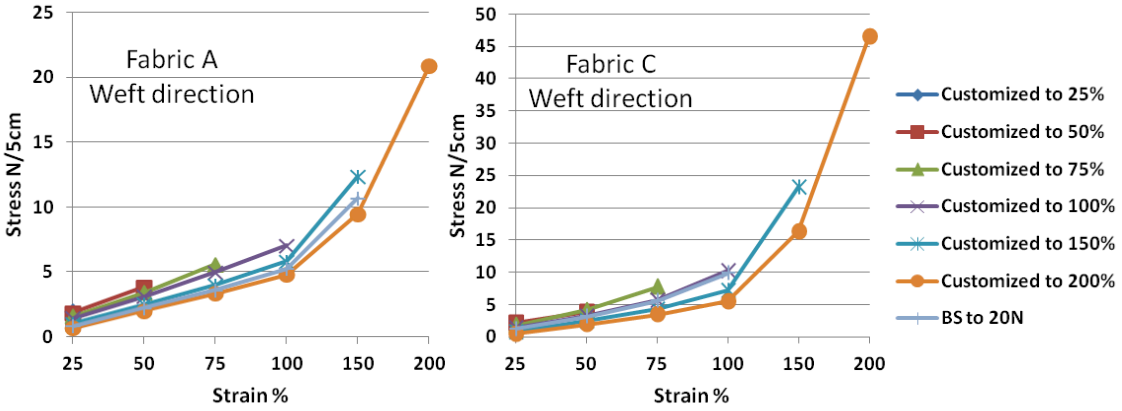

(a) (b)

Figure 4.7 Stress (N/5cm) at specified strain - standard vs. modified method – fabrics (a) A and (b) C in weft direction and strip formation

It must also be noted that fabric A was under lower stress in weft direction compared to fabric C and that the differences in results between methods were greater at higher strain/stress. For this reason, fabric A (Figure 4.7a) demonstrated closer results from both customised and standard methods in comparison to fabric C;

The difference in stress recorded at various strains from modified and standard methods decreased with increase in strain; the difference of stress in modified method to standard method was lower in comparison to stress tested to 200% strain. This suggests that the closer the conditions of testing between modified and standard method are, the smaller the differences in stress become.

A wide range of strains is achieved when the garment is worn over the body. Relatively, a more comprehensive set of results is achieved when the fabrics are tested under a high strain-stress. It is, however, difficult to determine a stress value that would provide the range of strains required for all fabrics, as fabrics differ in terms of their tensile performance. Meanwhile, when the fabric is tested for determination of stress at a specified strain, the range of strains required for the application is produced. Thus, the suitable method of testing of fabrics for the tensile performance was chosen to be determination of stress at specified strain. The strain under which the fabrics were tested was chosen according to the application under investigation and from the preliminary studies (Troynikov et al. 2010): a range of practical elongations expected from SCGs were within the range of 20% to 70%. For above mentioned reasons, it was decided to test the fabrics for determination of stress at 100% strain.

Furthermore, the cycling of the fabrics in BS 4952:1992 method (BSI 1992) is a good representative of how the garments are worn over the body, as the garments would normally get stretched to higher strains than practical elongation when donning, and they relax back to practical elongation over the limb; in the same standard, the fabrics are pre-cycled and the measurements are recorded from the second cycle, where the donning

effect is somewhat mimicked by the pre-cycling to a higher strain. Thus the fabrics are cycled once to a little over the maximal practical elongation (strain) expected, which is not likely to exceed 100% strain. This allows for the donning effect and a little extra strain if necessary. Then from the second cycle of extension, the strain-stress was recorded and used subsequently in section 4.2.1.

In order to choose the suitable specimen formation, fabrics A and C were tested to the chosen modified method, determination of stress at 100% strain, in both strip and loop formations in weft direction. The strain-stress for both fabrics and formations is plotted (Figure 4.8). From this point onwards, the stress plotted/reported is in N/cm, for comparison of stress at relative strains and also for theoretical pressure calculations. The stress recorded from testing was divided by 5 and 7.5 for strip and loop formations, respectively, to be able to compare the stress at relative strains for both specimen formations.

Figure 4.8 illustrates that the strain-stress curves almost match for both strip and loop formations for each of the two fabrics. For fabric A, the curves separated at 50% strain to 100%. The difference in stress at 100% strain between strip and loop formation in fabric A was 0.1 N (11%) in weft direction; this is somewhat significant in terms of pressure generation, however, 100% strain is considerably high in SCGs. While the strain-stress curves for fabric C matched consistently up to 100% strain. It should be noted that the seam (plain stitch) used in construction of loop formation specimens acted in similar way to the grips which held strip formation specimens in place and it differed to the seams within the garment (flat-lock stitch). In conclusion, the difference in results between strip and loop formations was insignificant at lower end of strain range (below 60%); this lower range is most expected in terms of practical elongation in SCGs. Therefore, it was decided to test the fabrics in strip formation, which is also more common in textile testing.

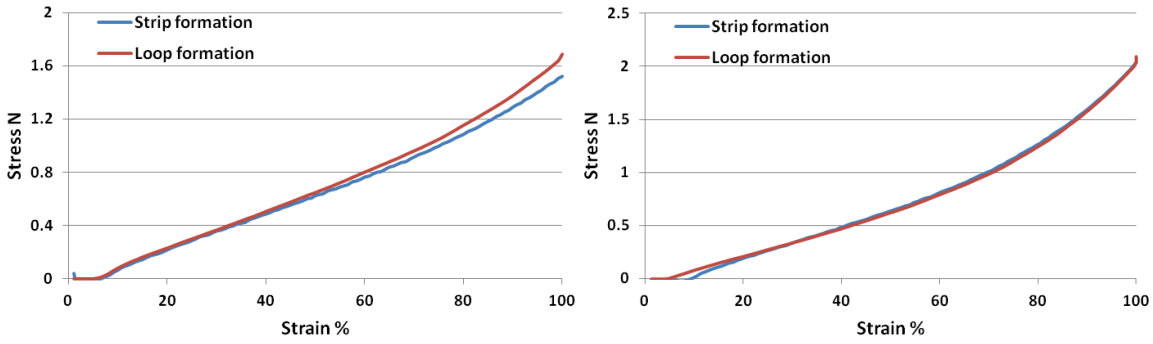

(a) (b)

Figure 4.8 Stress at 100% strain - strip vs. loop formation – fabrics (a) A and (b) C in weft direction

STDEV of all four fabrics tested to BS 4952:1992 (BSI 1992) for determination of extension at specified force were analysed (Appendice 6); it was revealed that the STDEVs for five, three and two specimens were relatively small; therefore, due to time and materials constraints and the low variability displayed amongst specimens, the number of specimens for each fabric was reduced from five to two in testing for tensile properties of composed samples from this point onwards.

Samples composed of fabrics A and C, with compositions listed in Table 3.1, were tested for determination of stress at 100% strain in weft direction and strip formation (Appendice 7). Strain-stress curves of composed samples are plotted in Figure 4.9.

Referring to analysis made earlier in this research, fabric C was more powerful than fabric A; thus higher stress was required to extend it to a same strain. Furthermore, according to testing observation and also logic, when a sample is composed of two fabrics with different tensile properties, the sample would extend more within the section of the less powerful, and less in the section of the more powerful fabric. As shown from Figure 4.9, as the percentage of fabric C within the sample composition decreased, so did the stress required to extend the sample to 100% strain. When a sample is composed of two fabrics, the more the percentage of the less powerful fabric within the sample composition, the lower the stress required in achieving a specified strain and the more the percentage of the more powerful fabric, the higher the stress required in achieving the same strain.

From 0% to 50% strain, the stress recorded from different compositions was almost equal; from 50% to 100% strain, however, the influence of sample compositions surfaced: for example, the difference in recorded stress at 60% strain was much lower than at higher strains such as 100%; the mount of strain the sample was under brought about the differences in recorded stress. When the sample is strained, the extensibility is first achieved by movement of yarns within the loops and as the strain increases, true tensile properties of fabric such as yarn extension surfaces. At higher strains, the difference in tensile properties of each fabric within the sample composition was revealed, causing higher variation in recorded stress.

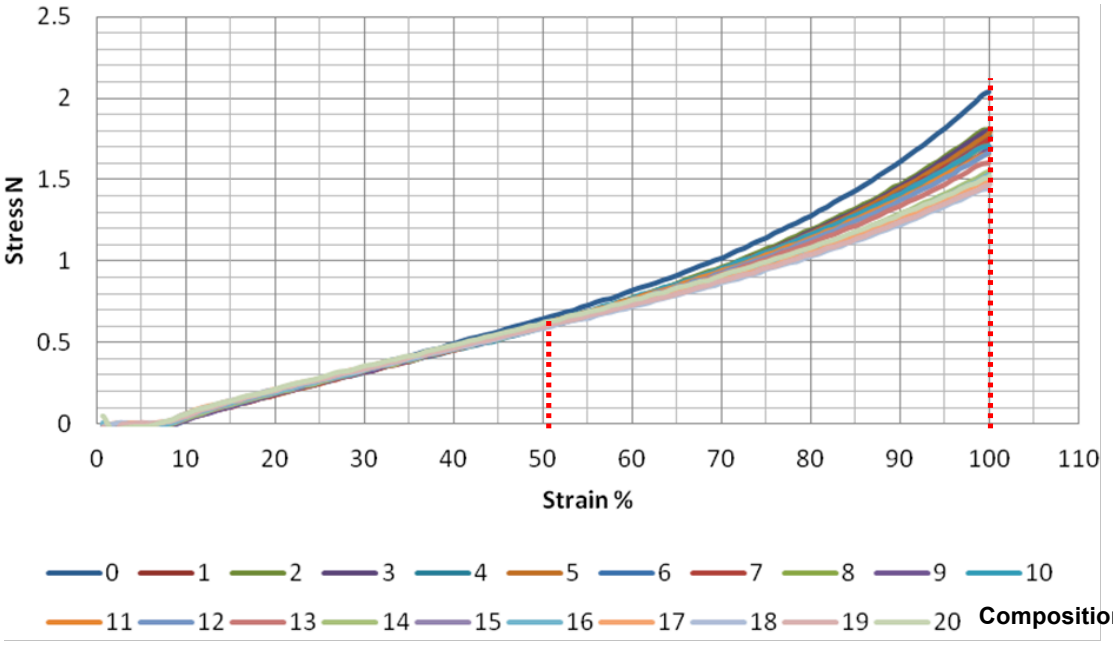

Figure 4.9 Stress at 100% strain – composition of fabrics A and C in weft direction and strip formation

This is demonstrated more clearly in Figure 4.10 and Appendice 8, where stress recorded at various strains is plotted in relation to the percentage of fabric A within sample composition.

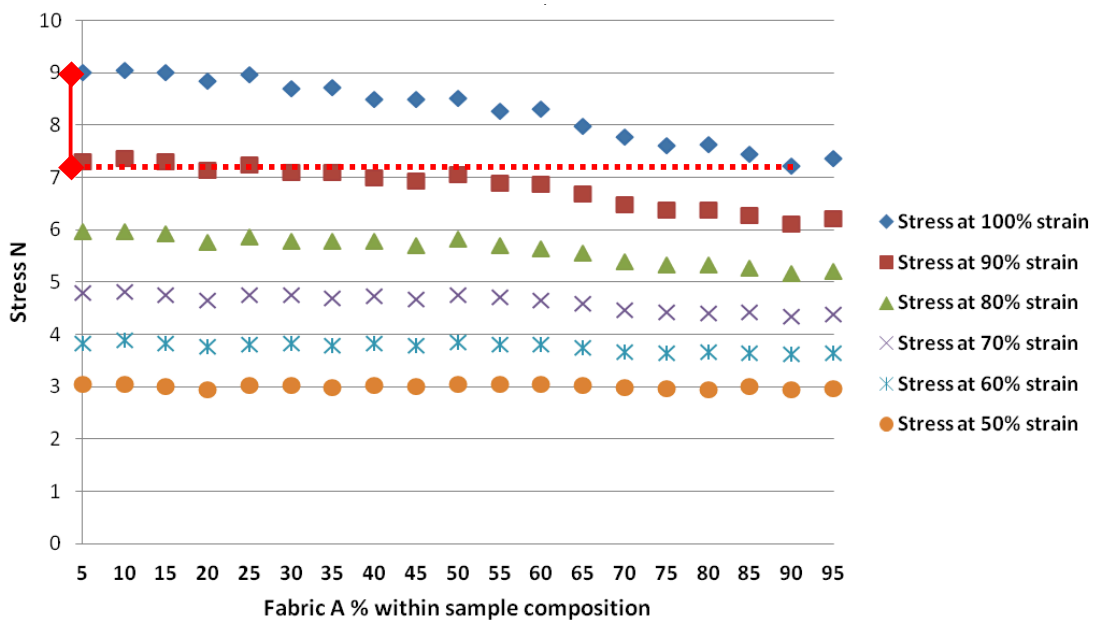

Figure 4.10 Stress at 50 to 100% strains in relation to percentage of fabric A within sample composition in weft direction and strip formation

It can be observed that the stress variation recorded at 50% strain at different compositions was negligible (0.02 N); however, at 100% strain, when fabric A composed 10% of the sample composition, maximum stress of 1.81 N was recorded in the stress range (plotted in red-dotted line in Figure 4.10); while in comparison to recorded minimum stress of 1.45 N in recorded stress range when fabric A composed 90% of the sample composition, the difference in generated pressure would be 36%. Pressure variation of 36% is significant and should be taken into consideration when evaluating tensile properties of composed samples, as the generated pressure could fall out of the acceptable pressure range. Yet it should be noted that 100% strain is very high and unlikely to exist in reality when SCGs are worn. Interestingly, the influence of the percentage of fabric A within sample composition on recorded stress at strains of 50% to 100% was highly significant ($p < 0.001$, 2-tailed), and the correlation was at its highest at 100% strain ($r = -0.976$) and decreased towards 50% strain ($r = -0.507$). This could be explained by the fact that at higher strains, the fabrics comprising the sample and the seam have moved and adjusted fully to the strained state.

It could be concluded that the influence of sample composition became greater at higher strains, which meant at strain ranges of 50% and lower, the percentage of fabrics within one sample did not have great influence on tensile properties of the composed sample (note that it remained different to one fabric within the sample due to existence of seam), and from 80% strain and higher the influence of percentage of each fabric (powerful or weak) within composed sample was substantial and must be taken into consideration.

The stress at 100% strain of samples composed of fabrics A and C in warp direction are plotted (Figure 4.11 and Appendice 9).

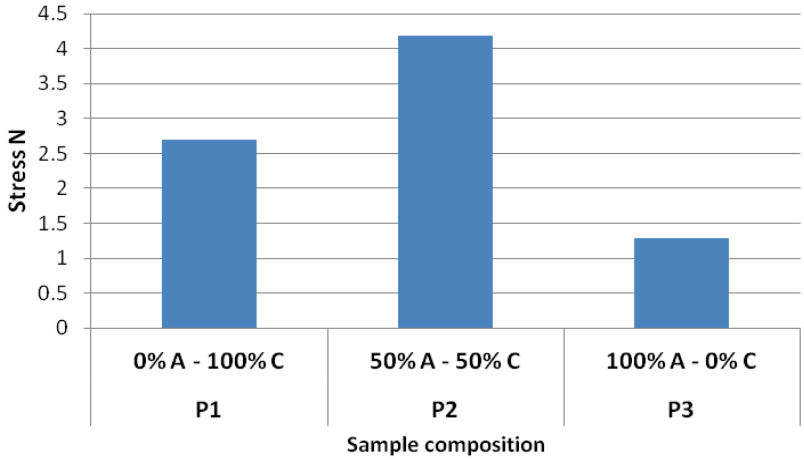

Figure 4.11 Stress at 100% strain – composition of fabrics A and C in warp direction and strip formation

Figure 4.11 indicates that the stress required to extend the sample to 100% strain in warp direction was much higher when the sample was composed of two fabrics joint with seam. As demonstrated earlier in Figure 3.2b, the seam in the composed sample tested in warp direction ran along its length and it impeded the sample to strain in warp direction.

Figure 4.12 plots the strain-stress curves when the composed samples were tested to 100% strain in warp direction and strip formation.

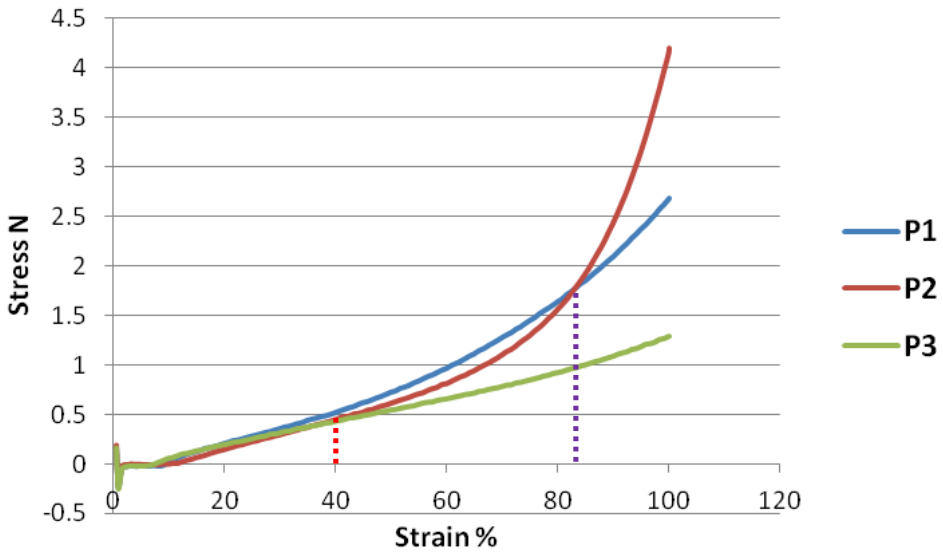

Figure 4.12 Stress at 100% strain – composition of fabrics A and C in warp direction and strip formation

Samples behaved similarly up to around 40% strain (plotted in red-dotted line in Figure 4.12). After this point, there was a great rise in stress; sample P1 (100% fabric C) recorded higher stress at relative strains up to 85% strain, followed by sample P2 (50% fabric A - 50% fabric C) and sample P3 (100% fabric A), respectively. Sample P1 (fabric

C) was more powerful in comparison to P3 (fabric A) in warp direction (as seen in Table 4.2). Yet the extensibility of sample P2 in warp direction was affected due to existence of seam. The stress required to strain sample P2 was lower than sample P1 and higher than sample P3 from 40% strain and higher, yet it increased with a higher slope. From approximately 70% strain, the strain-stress ratio of sample P2 changed and from 85% strain and higher, the stress required to strain sample P2 became greater than other samples. This demonstrated that the seam within the sample was capable of being strained and the fabrics within the composed sample repositioned within the seam, and from around 70% strain onwards, there was less allowance for further strain, and more and more stress was required to achieve higher strains. The stress difference between samples P2 with P1 and P3 was approximately 16% and 30% at 70% strain, 5% and 50% at 85% strain and it reached 36% and 69% at 100% strain, respectively.

Logically and from observation, the strain in warp direction is mostly expected at the anterior side of the knee section of the garment where according to the garment construction (seen in Figure 3.1), no seam existed in that section. Even though the stress of the sample varied from 40% strain and higher, yet the garment is allocated to each size according to height and weight; hence, the expectancy of the warp strain is relatively low. Garments with longer inseam are produced for longer legs, which eliminates the great strains in warp direction of the garment. This was why the influence of the seam on warp strain was not investigated further in this research.

4.1.4. Discussion and conclusions

The SCTs under investigation consisted of two fabrics with different physical attributes, with varied composition along the leg length. Tights in sizes Medium and Large were each worn on two Salzmann wooden legs, and the strains in width (weft) direction of the tight were calculated at each measuring point and the interface pressure was also measured. SCTs recorded interface pressure of 18 to 3 mmHg and 17 to 4 mmHg, at points B to G on the back of the leg, for sizes Medium on leg 9 and Large on leg 12, respectively. Gradient pressure was achieved from tight in size Large on both leg sizes, while the gradient pressure was disrupted at measuring point B1 for tight in size Medium. Liu & Little (2009) suggested that light or mild pressure is expected from a one layer SCG. This is in comparison to German standard RAL-GZ for medical compression hosiery 387:2000 (RAL 2008), where the measured interface pressure from the above SCTs just provided compression class I with low intensity compression.

The physical attributes of four fabrics used in manufacture of SCTs were analysed. Highest mass per unit area and relatively high stitch density resulted in lowest optical porosity amongst the four fabrics. Interestingly, one of the fabrics with highest thickness and stitch density had the second highest optical porosity, due to finer yarns; the fabric with lowest stitch density of all, recorded the highest optical porosity. Some of the differences between fabrics were statistically significant and some were not significant, yet these features contribute to the comfort properties of fabrics, such as thermo-physiological and tactile properties, which makes them important.

In this research, fabrics were tested for tensile performance attributes according to British Standard 4952:1992 (BSI 1992) under 20 N stress. One of the fabrics was found to be particularly powerful, and generated the highest pressure under similar conditions. Different standard and non-standard methods has been used to determine the tensile properties of fabrics comprising CGs, demonstrating a lack of agreement on the most suitable method of testing of such fabrics. Similarly variable stress levels and variable strains had been used, such as 25%, 100%, to 'maximum circumference' and 'light overstretch' by cycling the samples two to six times (Ghosh, S et al. 2008; Macintyre, Baird & Weedall 2004; Partsch, Partsch & Braun 2006; Thomas & Fram 2003; van der Wegen-Franken et al. 2006).

In this research, fabrics were tested to modified methods based on British Standard 4952:1992 (BSI 1992) and it was decided that determination of stress at 100% strain was most suitable for testing of fabrics comprising SCGs for tensile properties. In this modified method, a wide range of strain-stress relative to CGs was produced and the donning of the SCGs was mimicked by pre-loading and cycling of the fabric before recording the results. Furthermore, little difference was found between the results of specimens tested in strip and loop formation; thus, strip formation, which is most common in textile testing, was chosen.

It was important to evaluate the varied fabric composition at different sections of the garment and determine its influence on the tensile properties of the composed sample. In samples composed of two fabrics, the less powerful fabric had a greater impact on the resultant stress in weft direction at strains of 80% and higher. Furthermore, the existence of seam in warp direction influenced the extensibility of the composed sample at high strains, which is unlikely to exist in CGs.

This preliminary investigation, gave an idea of the range of pressure induced from each tight on different leg sizes. The pressure generated by SCGs are dependent on various properties such as the construction of the garment, the limb measurements, the measuring site, pressure-measuring device and last but not least, the tensile properties of fabrics comprising SCGs; therefore, it was important to found a suitable method for testing of tensile properties of fabrics. A more detailed investigation on pressure generation of SCTs is carried out in section 4.2.

4.2. Compression calculation and validation

Theoretical pressures generated by fabrics comprising SCTs at variable strains in weft direction were predicted on variable cylinder diameters, in non-composite and composed samples. Salzmann sensor probe calibration was attempted. The theoretical predicted pressures were validated by measured interface pressure on cylinders and the influence of composed samples and also combination of strains in both weft and warp directions on measured pressure were analysed.

4.2.1. Theoretical pressure generated by fabrics comprising SCGs

The theoretical pressures induced by fabric D over cylinders 90, 130 and 160 is plotted (Figure 4.13 and Appendice 10).

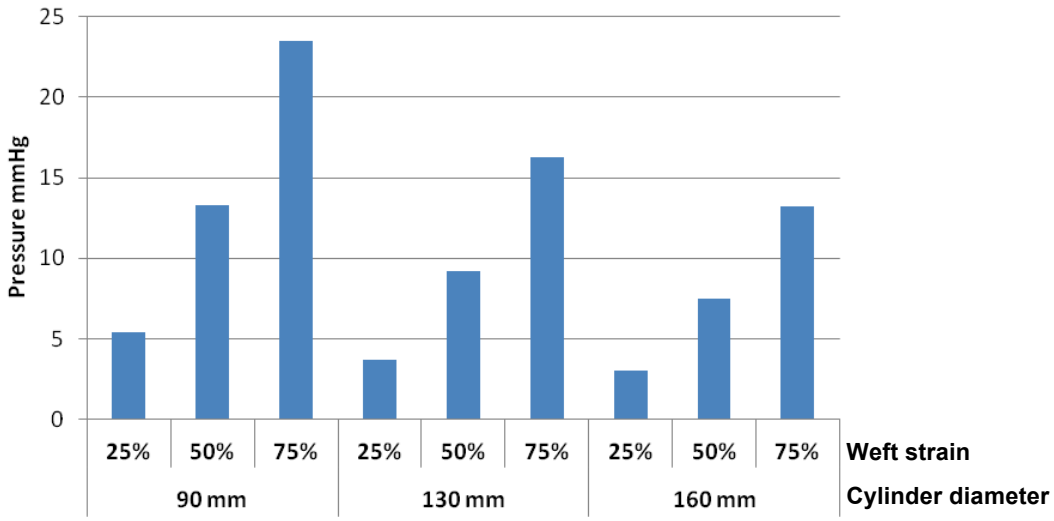

Figure 4.13 Theoretical pressure induced by fabric D at variable weft strains and cylinder diameters

As expected and demonstrated in Figure 4.13, the pressure increased with increase in strain in weft direction, as the fabric was under higher stress, resulting in higher pressure. Furthermore, the pressure generated by fabric D at each strain decreased with increase in cylinder diameter; this confirms that pressure is inversely proportional to cylinder diameter/circumference.

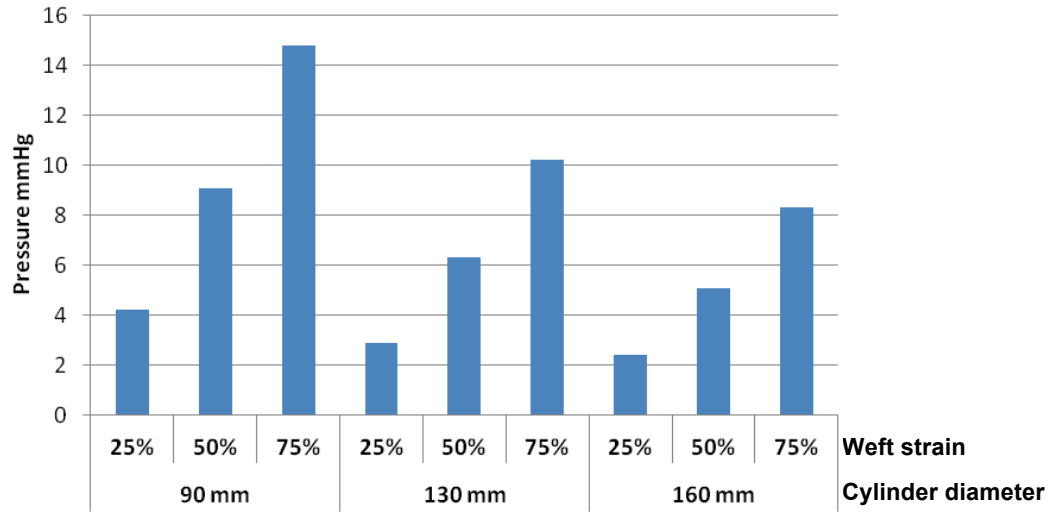

Figure 4.14 Theoretical pressure induced by fabric C on variable weft strains and cylinder diameters

The theoretical pressure induced by fabric C over cylinders 90, 130 and 160 is plotted (Figure 4.14 and Appendice 11). Once again, the relation of pressure to stress and cylinder diameter is observed in Figure 4.14. The pressure decreased with increase in cylinder diameter and the pressure increased with increase in strain due to higher stress.

The theoretical pressure from fabric C was on average lower than fabric D at relative strains/cylinder diameters. This was due to different tensile properties of fabrics: as explained earlier in section 4.1.3, fabric D was more powerful than fabric C and thus it was under higher stress at relative strains in comparison to fabric C. For this reason, in theoretical pressure calculations at similar strains and cylinder diameters, the theoretical pressure induced by fabric D was higher than fabric C. Furthermore, the difference in theoretical pressure amongst fabrics C and D increased with increase in strain: from 21% at 25% strain to 37% at 75% strain. This highlights that the difference in power of fabrics became greater and more significant at higher strains.

Theoretical pressure induced by samples composed of fabrics C and D are shown (Figure 4.15 and Appendice 12).

As demonstrated in Figure 4.15, the theoretical pressure dropped with increase in percentage of fabric C (less powerful) within sample composition at each strain. This is in line with the results found from testing samples composed of fabrics A and C for tensile properties (seen in Figure 4.9), where with increase of the percentage of less powerful fabric within sample composition, the stress generated by the composed sample decreased. With decrease in stress, while other parameters were constant, the theoretical pressure decreased as well.

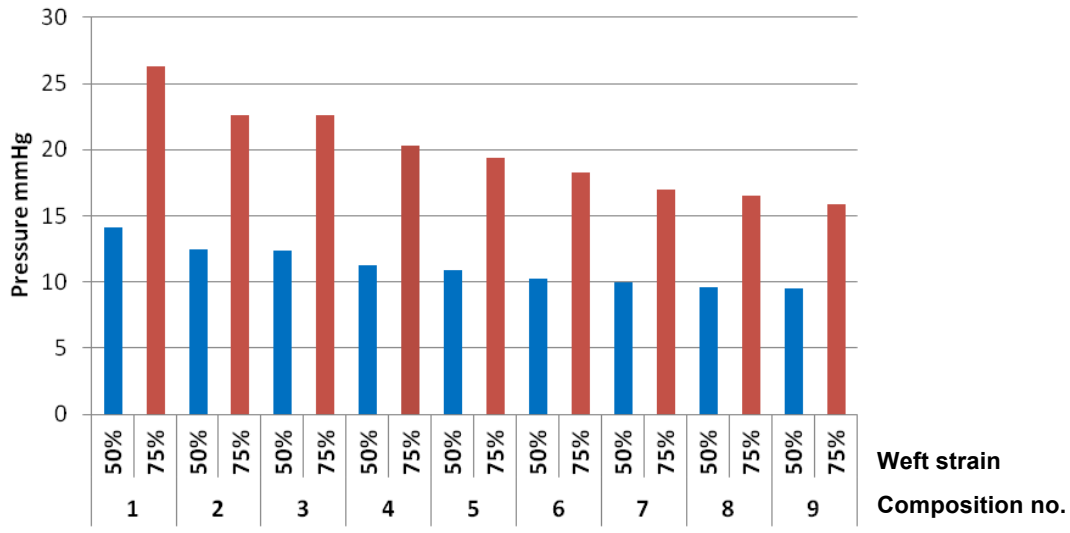

Figure 4.15 Theoretical pressure from composition of fabrics C and D on cylinder 90 at 50% and 75% strain in weft direction

The effect of more and less powerful fabric on stress within the composed sample is directly translated into theoretical pressure at relative strains. The stress and thus theoretical pressure generated by composed samples are mostly higher than the stress and theoretical pressure generated by the sample made only of less powerful fabric and

lower than the sample made only by more powerful fabric. The reason is that introduction of less powerful fabric decreased the overall stress and theoretical pressure within the composed sample in comparison to sample made only by more powerful fabric and that introduction of more powerful fabric increased the overall stress and theoretical pressure within the composed sample in comparison to sample made only by less powerful fabric. In conclusion, the theoretical pressure calculated for samples composed of fabrics with different tensile properties was mostly influenced by the amount of each fabric within the sample composition and this influence was more significant at higher strains due to higher stress variations recorded.

4.2.2. Salzmann sensor calibration

The theoretical pressure induced by each series of weights (provided earlier in Table 3.5) was calculated using Eq. (6), and the units were converted to calculate the pressure in millimetres of mercury (mmHg) (Figure 4.16 and Appendice 13).

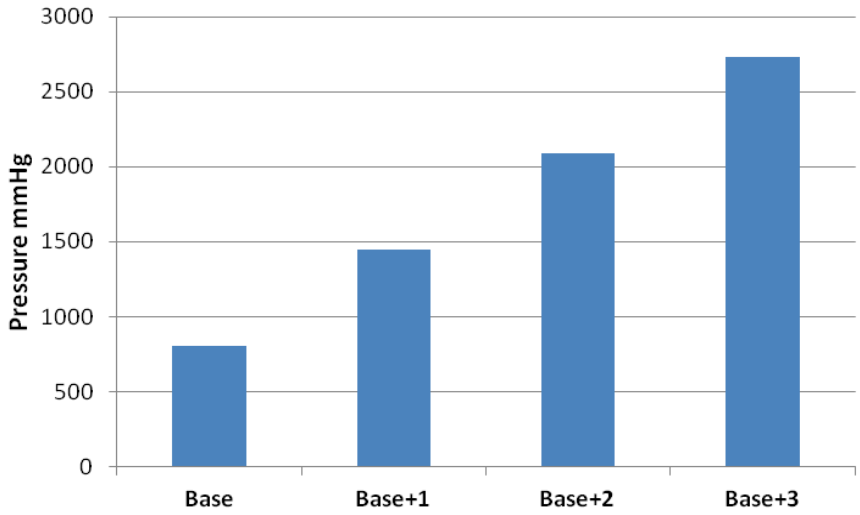

Figure 4.16 Theoretical calculated pressure from 'Base' to 'Base+3'

It was surprisingly difficult to find weights which would cover the relatively small sensing area of the measuring point on the sensors, to provide the required mass and not to touch the adjacent weights. The sourced weights did not provide exactly the same mass, yet the difference in their mass was negligible in terms of pressure generation. As the air was pumped in the sensor sleeve for pressure measurement, the weights became off balanced to some extent, due to high mass to base ratio and touched the weight on the adjacent sensor point or the table top. This issue became greater in 'Base+2' and 'Base+3', as the height of the weight assembly was higher and was less stable on the small surface area of the sensor point. This was the study limitation which was considered when analysing the data, as the off balanced weights did not have the whole weight distributed only on the sensing area of the measuring point and influenced the measured pressure.

As expected and shown in Figure 4.16, the theoretical pressure calculated from each series of weights increased as the mass increased. This was the case for measured

pressure from each series of weights as well (Figure 4.17 and Appendice 14). There was a high discrepancy, however, between theoretical and measured pressure at each series of weights and the calculated pressures were very high in terms of pressure range expected to be induced by CGs. In practice, lower mass than the one used in 'Base' measured very low pressures, which was not sufficient for obtaining a wide range of pressures for calibration of the device. It was inspected that the reason was the way the weights were assembled over the small sensing area of each measuring points and pressure measurement mechanism of the sensor, that such theoretically high pressures were measured much lower from 'Base' to 'Base+3'.

Mean measured pressure from thirty measurements from each series of weights is plotted (Figure 4.17).

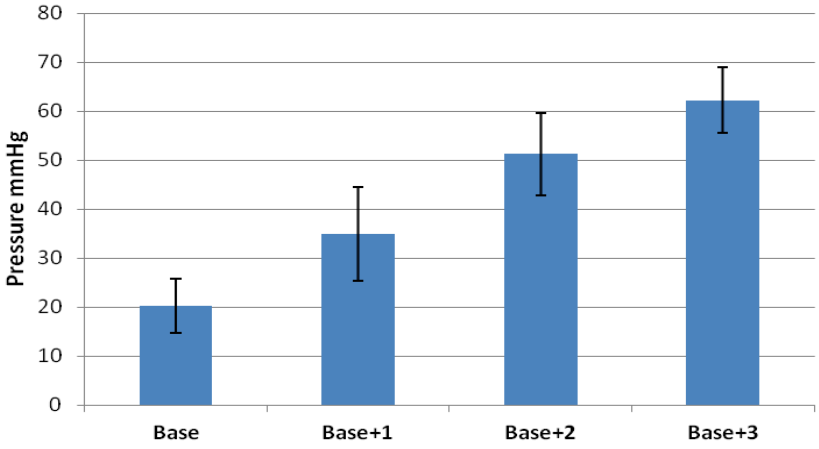

Figure 4.17 Measured pressure from 'Base' to 'Base+3'

Relatively high STDEV for measured pressure were caused due to difficulty in measuring the pressure precisely from each series of weights; thus, the pressure readings which fell out of the range of 10 to 90th percentiles were eliminated for each measuring point of B to D in each series and the results with 95% confidence interval were analysed at sensor measuring points B to D, plotted along with interpolation lines working through mean of measured pressures for each series of weights in Figure 4.18.

As evident in Figure 4.18, the measured pressures at each point of B to D were not equal when that same mass were placed over them at each series of weights ('Base' to 'Base+3'). Measuring point B measured higher pressure at each step followed by measuring point D, C and B1; this was also shown with interpolation line for each series of weights. The difference in recorded pressure at each measuring point could be explained from the design of the sensor and pressure measurement mechanism of the device. The air is pumped in the sensor sleeve from one end of the sensor sleeve (measuring point D); when the air pressure within the sleeve is equal and slightly over the pressure inserted over each measuring point, the two sides of the sensor point lose contact and that is when the pressure is recorded. The pressure is recorded from the lowest pressure amongst the measuring points to the highest.

The measuring point B is at the farthest end of the sensor; due to the design of the sleeve (seen in Figure 3.8) and with weights placed over other measuring points impeding

the air flow to readily reach point B, more air pressure was required for inflation and pressure measurement at point B. Measuring point B1 and C are situated in the middle of the sensor with more similar situations along the sensor sleeve, where the air is more readily pumped in and the recorded pressure at each series of weights were closer at these points in comparison to other measuring points. While measuring point D is closer to end of the sensor sleeve, where the air is pumped in with only 5.5 cm distance to the fixture, where wires and air tube are attached to the sensor. This also affects how the air passes from the measuring point D and how the weights were balanced. Due to difficulties encountered, the conditions where the pressure was measured at each series of weight were less than ideal and inevitable, especially as the series of weights became heavier.

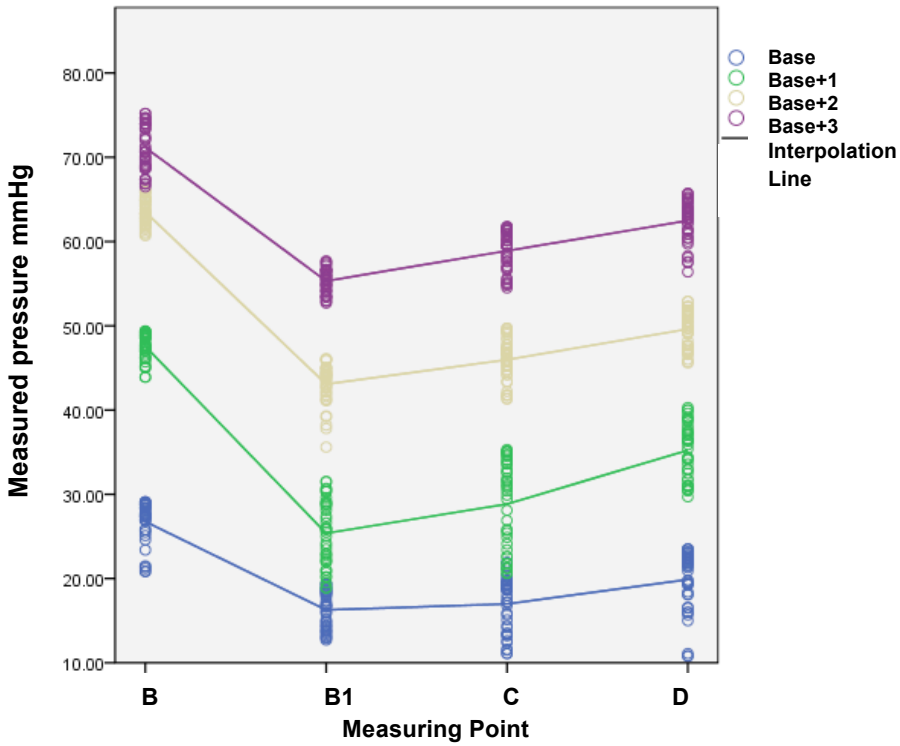

Figure 4.18 Measured pressure from 'Base' to 'Base+3' at measuring points B to D

The measuring point B is at the farthest end of the sensor; due to the design of the sleeve (seen in Figure 3.8) and with weights placed over other measuring points impeding the air flow to readily reach point B, more air pressure was required for inflation and pressure measurement at point B. Measuring point B1 and C are situated in the middle of the sensor with more similar situations along the sensor sleeve, where the air is more readily pumped in and the recorded pressure at each series of weights were closer at these points in comparison to other measuring points. While measuring point D is closer to end of the sensor sleeve, where the air is pumped in with only 5.5 cm distance to the fixture, where wires and air tube are attached to the sensor. This also affects how the air passes from the measuring point D and how the weights were balanced. Due to difficulties encountered, the conditions where the pressure was measured at each series of weight were less than ideal and inevitable, especially as the series of weights became heavier.

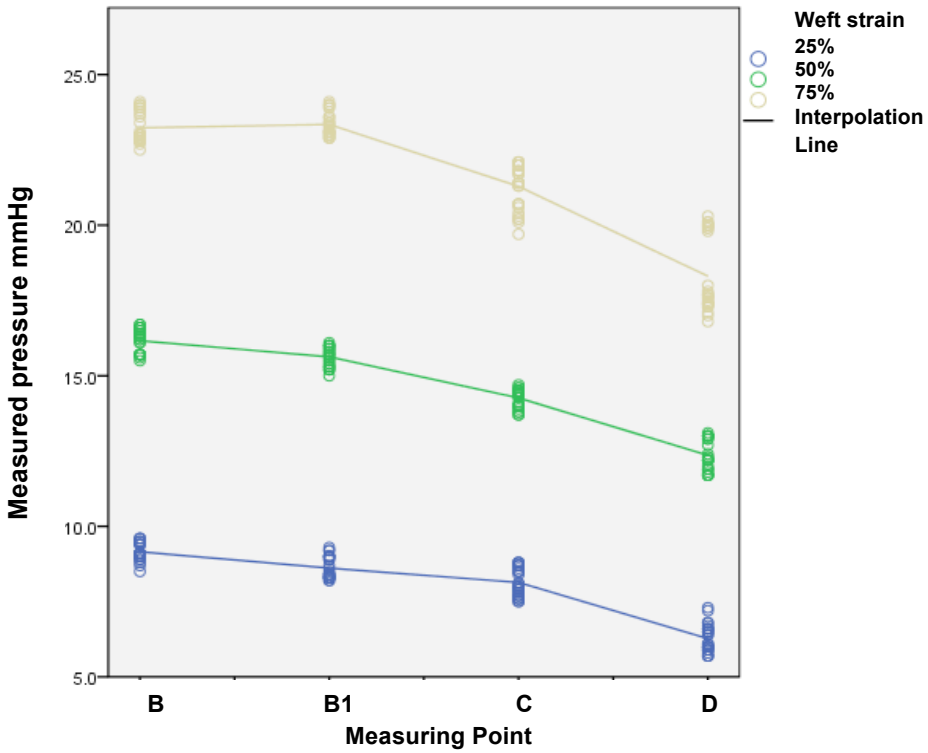

Figure 4.19 Measured pressure from fabric sleeve D over cylinder 90 at 25%, 50% and 75% strains in weft direction and measuring points B to D

For this reason and to demonstrate the trend under which the pressure-measuring device recorded the pressure at each measuring point, the pressure induced by fabric sleeves providing constant strain along the length of a rigid cylinder was measured using the device. Same strain within the fabric sleeve and constant cylinder diameter induced the same pressure along the length of the cylinder; however, when the pressure induced by fabric sleeves was measured, the recorded pressure was different at each measuring point similar to the experiment with series of weights. This method is explained in more detail in section 4.2.3, yet a summary of the data recorded from the pressure measurement from fabric sleeves is provided for reference in Figure 4.19.

The practical error when measuring the pressure from fabric sleeves was much lower than the method with series of weights. Interpolation line working through mean pressure measurements demonstrate the way same pressure was recorded differently within each pressure ranges (due to variable fabric strain in weft direction for different fabric sleeves). The device recorded the highest pressure at measuring point B for each weft strain except for pressure measured at measuring point B1 in 75% strain, which was slightly higher than pressure recorded at measuring point B. This slight increase could have been a practical error. The pressure dropped towards measuring point D; this demonstrates that the error in pressure measurement at each measuring point is systematic. When the pressure induced by fabric sleeves was measured over rigid cylinders, there was a difference between measuring points conditions along the cylinder. Measuring point B was at the top edge of the cylinder; while top edge of the cylinder did not affect the pressure reading as the top end of the sensor matched the edge of the cylinder and the pressure recorded was only under the influence of the sensor design. Measuring points B1 and C had similar

conditions along the length of the cylinder, but measuring point D was close to the bottom edge of the cylinder. Being close to the edge of the cylinder could have also affected the way the air is pumped in the sensor sleeve and affected the resultant pressure.

As the practical error was relatively high and inevitable when series of weights were used, a correction could not be derived from the data between the calculated pressure from the weights and measured pressure. The pressure measurement using fabric sleeves demonstrated the pressure measurement trend between points B to D, and confirmed the hypothesis about the measuring points; yet, correction factor could not be concluded from sleeves either, since the theoretical pressure from fabric sleeves required validation itself.

From the investigation above, a correction factor was not derived for the sensor points, yet an obvious pressure measurement trend was observed amongst measuring points B to D. The measuring point B measured higher pressure than other measuring points due to the sensor sleeve design and pressure measurement mechanism. Measuring points B1 and C performed relatively similarly, yet their accuracy was not confirmed at this stage. And last but not least, measuring point D was relatively less accurate compared to points B1 and C, due to its position close to where the air is pumped into the sensor sleeve.

It was concluded that measuring points B1 and C were more reliable due to their position along the length of the sensor sleeve, were under less influence of sensor design and in case of the experiment with cylinders, under less influence of positioning close to the edges of cylinders; hence, the pressure recorded on measuring points B1 and C is investigated in more detail throughout the rest of the research.

4.2.3. Validation of theoretical pressure calculation

The pressure was measured over rigid cylinders with three fabric sleeves made of fabric D per each weft strain/cylinder diameter, providing thirty pressure readings per each combination (Appendice 15 to Appendice 17). STDEV of measured pressures were lower than the resolution of the device for all but 2 out of 36 combinations of weft strain/cylinder diameter; Salzmann pressure-measuring device resolution is 1 mmHg, confirmed by email by Ms M. Wüst (Salzmann AG Laboratory Manager) on 23 November 2011.

Fabric sleeves provided consistent strain along the length of the cylinders, providing consistent pressure on all four measuring points; while as demonstrated in Figure 4.20, the pressure readings differed between measuring points B to D for each set of weft strain/cylinder diameter, also referred to in Salzmann calibration experiment with cylinders and fabric sleeves (section 4.2.2).

The pressure recordings were generally at their highest at measuring point B and the pressure dropped towards point D. Low STDEV of pressure recordings suggested that sensor probes performed consistently per each measuring point and that the device measured the pressure at various points with systematic error. When compared to theoretical pressure calculated for fabric D at relative strains discrepancies were found between theoretical and measured pressure (Appendice 18). The theoretical pressure

was generally lower than measured pressure for all measuring points at 25% strain on all cylinders, while with increase in strain, theoretical pressure was higher than measured pressure at some measuring points.

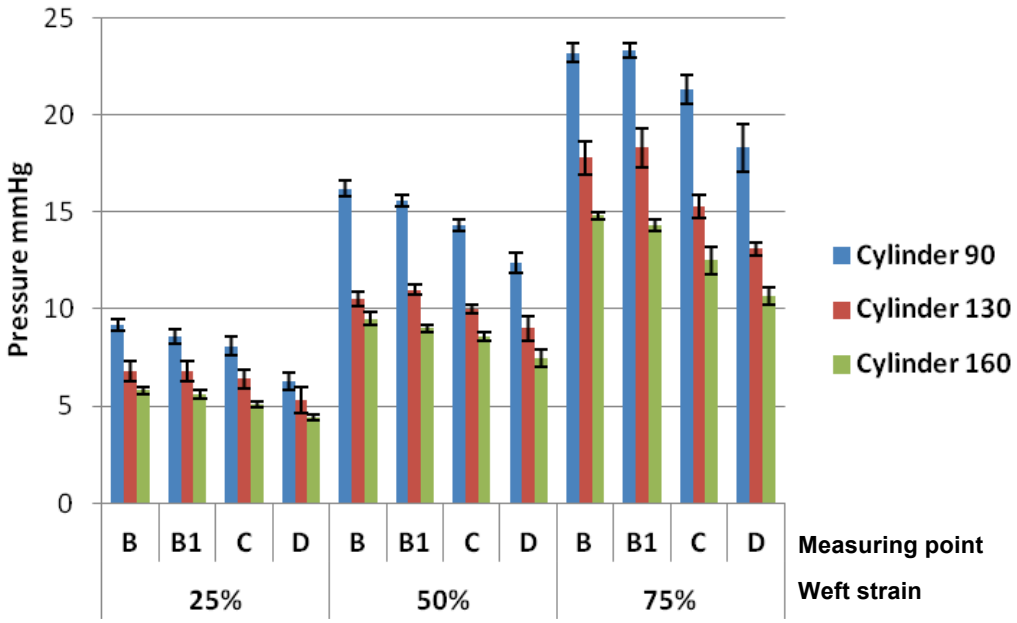

Figure 4.20 Measured pressure on variable cylinder diameters and strains – fabric D

The pressure recordings were generally at their highest at measuring point B and the pressure dropped towards point D. Low STDEV of pressure recordings suggested that sensor probes performed consistently per each measuring point and that the device measured the pressure at various points with systematic error. When compared to theoretical pressure calculated for fabric D at relative strains discrepancies were found between theoretical and measured pressure (Appendice 18). The theoretical pressure was generally lower than measured pressure for all measuring points at 25% strain on all cylinders, while with increase in strain, theoretical pressure was higher than measured pressure at some measuring points.

Measured pressure over rigid cylinders were analysed further in regards to theoretical pressure from data derived from fabric D tested for tensile properties in strip formation. Regression analysis was carried out for results on fabric D for measuring points B to D separately, with theoretical pressure being the independent value (Appendice 19). The theoretical and measured pressure had very strong correlation at all measuring points (R^2 had a range of 0.970 to 0.982, and *Beta* had a range of 0.985 to 0.991 for all measuring points); the strongest correlation, however, was found between theoretical and measured pressure at measuring point B1.

Measuring points B1 and C were found more reliable than other measuring points in section 4.2.2 and from regression analysis, measuring point B1 had strongest relation to theoretical pressure. For this reason, pressure at measuring point B1 is investigated in more detail; the measured pressure at point B1 is plotted along with the theoretical pressure from data derived from fabric D in strip formation (Figure 4.21).

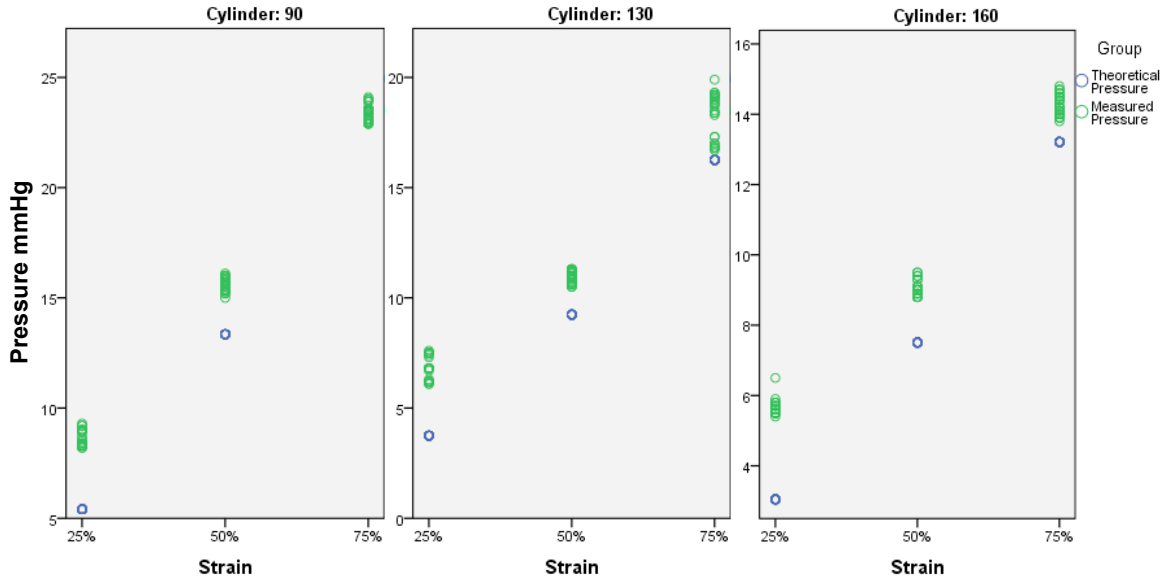

(a) (b) (c)

Figure 4.21 Measured and theoretical pressure at measuring point B1 – cylinders (a) 90, (b) 130 and (c) 160 and variable strains in weft direction – fabric D

As can be seen in Figure 4.21, the theoretical pressure at measuring point B1 was lower than measured pressure over cylinders except for 75% strain in weft direction on cylinder 90, which could be due to practical error. The difference between measured and theoretical pressure decreased with increase in strain in weft direction on all cylinders. It could be inferred that the measured pressure at higher strains which resulted in higher pressure ranges could be more accurate than lower pressure ranges derived from lower strains.

From analysis mentioned above, measured pressure at point B1 from fabric D ($MP_{B1,D}$) could be predicted with great accuracy (*Beta* = 0.991, $p < 0.001$) from its theoretical predicted pressure ($TP_{Strip,D}$). A linear regression model was derived, with the strongest correlation between measured and theoretical pressure found for measuring point B1, Eq. (13):

$$MP_{B1,D} = (0.872 \times TP_{Strip,D}) + 3.281 \quad (13)$$

The intercept in Eq. (13) is greater than zero. This meant that even when the theoretical pressure was zero, there was approximately 3 mmHg of predicted measured pressure. This could be explained by contact pressure between the sleeve and the sensor.

Even though there was a strong relationship between theoretical and measured pressure at measuring point B1, further statistical analysis was carried out on the data in accordance to weft strain (Appendice 20). When data were divided into groups by strain in weft direction and further analysed, the power of predictability of the model slightly decreased at 25% strain (R^2 decreased by 8%), yet the model remained strong (lowest R^2 = 0.898 and *Beta* = 0.948 at 25% strain).

The fabric sleeves were slightly over strained to be placed over the cylinders and sensor and all the pressure measurements were taken consecutively. Low STDEV of the measured pressure indicates that the possible loss of power within the fabric sleeve, while the pressure is being recorded, was minimal. When the fabric variation was kept to minimum, by sourcing the specimens tested for strain-stress and the fabric sleeves per each cylinder/strain as close as possible to one another and from the same roll of fabric, there was a strong relationship and power of predictability of measured pressure from the theoretical pressure at various strains of 25% to 75% in weft direction for fabric D. Meanwhile, same analysis was carried out for fabric C, yet with higher variation and lower number of data and the outcome was compared to fabric D with lower variation and higher number of data.

The pressure was measured using two sensor probes and three times per each fabric sleeve made of fabric C (total of three fabric sleeves per cylinder/strain), providing eighteen measurements per each combination (Figure 4.22). Descriptive statistics of measured pressure from fabric C is summarised (Appendice 21 to Appendice 23).

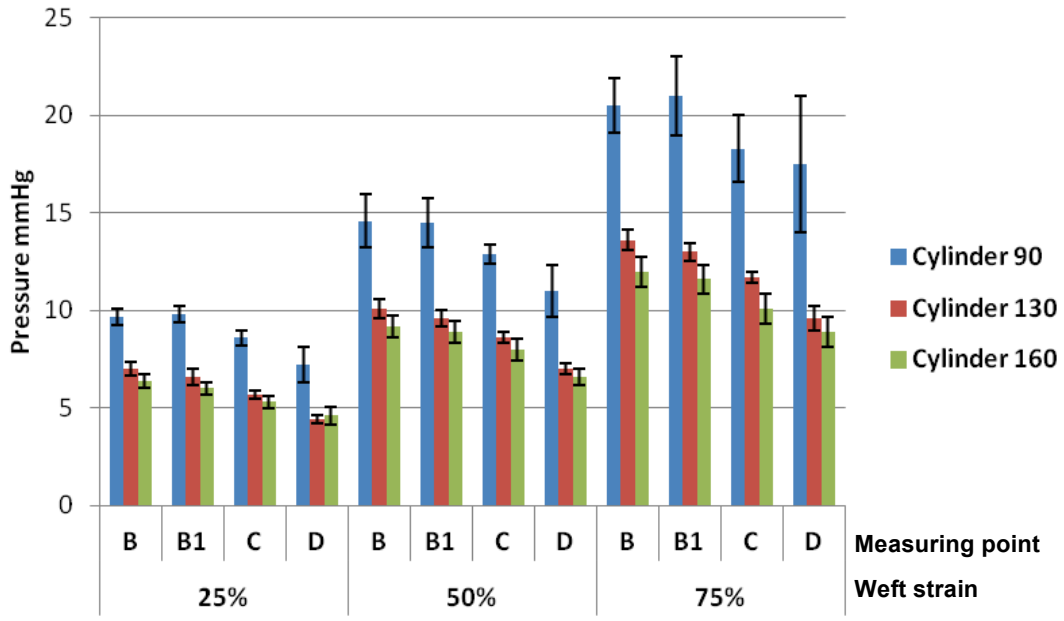

Figure 4.22 Measured pressure - variable cylinders and strains – fabric C

Unlike fabric D where fabric variation was kept to minimum and as expected, the variation amongst the data for measured pressure on fabric C was higher; for fabric C, specimens used for testing of strain-stress of the fabric were not sourced exactly close to the fabric used for pressure measurement from the fabric sleeves. This demonstrates the fabric variation within one roll of fabric. STDEV of the data were higher at each measuring point, especially on cylinder 90; they remained, however, relatively low (worse case had a maximum STDEV of 3.5 mmHg on cylinder 90, 75% weft strain and at measuring point D).

As observed in Figure 4.22 and similar to pressure measured from fabric sleeves made of fabric D, the measured pressure dropped from point B to D for fabric C. Similar analysis carried out on fabric D in regards to theoretical pressure at relative cylinder diameters/strains in respect to measuring point B1 which was found to have highest

correlation was performed on fabric C. The relationship between measured pressure at point B1 and theoretical pressure for fabric C was not as strong as fabric D (R^2 decreased by 8%), due to higher variation within the specimens and also smaller sample size (by 40%). Yet the theoretical pressure remained 90% responsible for the measured pressure at B1 in fabric C (Appendice 24) and the remaining 10% could be explained by higher variation within the data and fabric.

Measured pressure at measuring point B1 from fabric C ($MP_{B1,C}$) could be predicted with high accuracy (*Beta* = 0.953, $p < 0.001$) from its theoretical predicted pressure ($TP_{Strip,C}$). A linear regression model was derived, between measured and theoretical pressure found for measuring point B1, Eq. (14):

$$MP_{B1,C} = (1.124 \times TP_{Strip,C}) + 3.376 \quad (14)$$

Using Eq. (14), the measured pressure from fabric sleeves made of fabric C could be predicted with high accuracy from theoretical pressure, at stains of 25% to 75% in weft direction and over cylinder diameters 90 to 160 mm.

Pressure was also measured from fabric sleeves composed of fabrics C and D on cylinder 90, providing 50% and 75% strain in weft direction. Descriptive statistics of measured pressure at measuring point B1 split by weft strain at various compositions is summarised (Appendice 25).

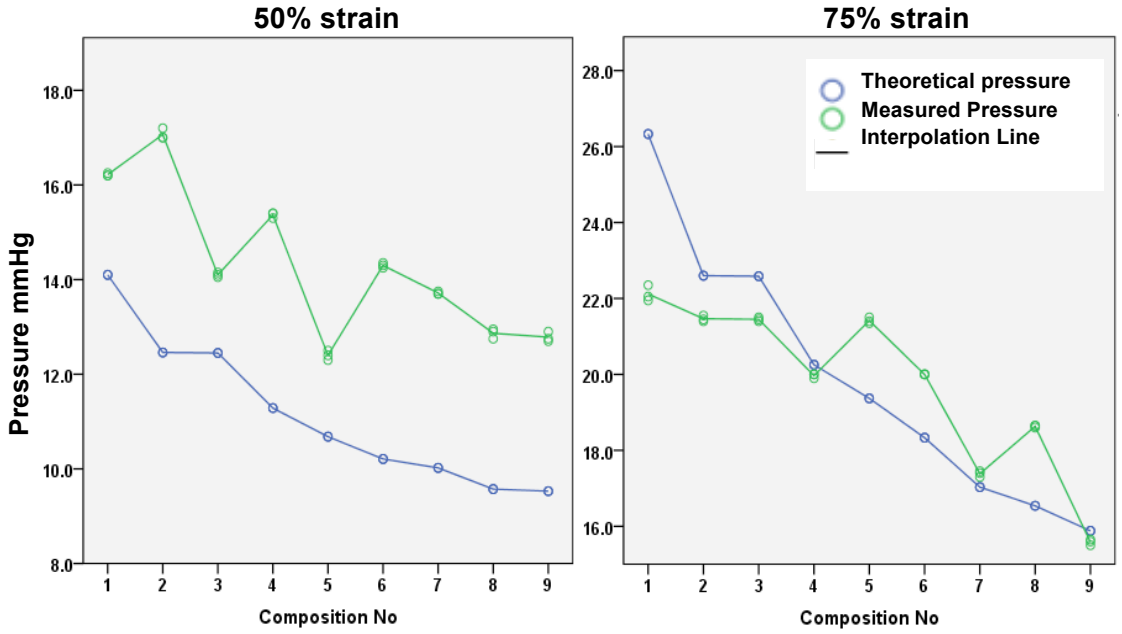

(a) (b)

Figure 4.23 Measured and theoretical pressure at measuring point B1 – samples composed of fabrics C and D at (a) 50% and (b) 75% strain in weft direction

The theoretical pressure calculated from composed samples followed relatively consistent trend where the pressure decreased from composition 1 to 9, whereas greater

variation in measured pressure was recorded between compositions at various strains (Figure 4.23 and Appendice 26).

This was a result of variation in fabric sleeves, smaller sample size and pressure measurement error. A general trend, however, was found by elimination of variations in measured pressure; generally, the measured pressure decreased similar to theoretical pressure from composition 1 to 9, explained by differences in power of fabrics composing the samples and their percentage within the sample composition.

The small percentage change within sample composition (10% interval change for each fabric) did not result in significant differences on pressure; thus, the data for all compositions were analysed as one group and the correlation between the measured pressure and theoretical pressure derived from composed samples in strip formation were investigated.

Regression analysis was carried out on measured pressure and theoretical pressure predicted for samples composed of fabrics C and D in strip formation at measuring point B1 (Appendice 27). The linear model derived from the regression analysis was not as strong as the non-composite samples in terms of power of predictability; the reason was higher fabric variation within the roll of fabric, smaller sample size and extra variation from the seam attaching fabrics C and D together; yet the model remained relatively strong (R^2 = 0.884). Therefore, measured pressure at measuring point B1 ($MP_{B1,comp}$) could be predicted with accuracy (*Beta* = 0.943, $p < 0.001$) for composed samples from its theoretical predicted pressure ($TP_{Strip,comp}$). A linear regression model is derived, between measured and theoretical pressure found for measuring point B1, Eq. (15):

$$MP_{B1,comp} = (0.611 \times TP_{Strip,comp}) + 7.721 \quad (15)$$

Regression analysis was carried out for various compositions relative to strain in weft direction, as the tensile performance of composed samples changed at higher strains in weft direction (Appendice 28). Interestingly, the greater loss of power of predictability was reported for 50% strain in weft direction in comparison to 75% strain; this could be due to the fact that the composed samples did not show their true tensile performance at lower strains, also mentioned in section 4.1.3. The linear regression model derived from composed samples was not statistically significant (R^2 = 0.593 for 50% and R^2 = 0.724 for 75% strain in weft direction) and could not accurately predict the measured pressure from theoretical pressure due to small sample size and high variation within the data.

The analysis concluded that the measured pressure could be predicted with high accuracy from theoretical pressure from data derived from specimens in strip formation, within the range of cylinder diameters and strains in weft direction investigated; variation within the roll of fabric and decrease in sample size, however, reduced the power of predictability of the model.

Measured pressure induced by fabric sleeves made from fabric C with variable strains in weft and warp directions on cylinders 90 and 160 is plotted Pressure (Figure 4.24 to Figure 4.26). Achieving 30% strain in warp direction on fabric sleeves was difficult, especially at higher strains in weft direction, as the fabric sleeve would slip from within the cable grip, and also would tear at the staple insertion points; for this reason, the pressure

readings which were obviously incorrect due to fabric slippage were eliminated and three pressure recordings with lower variations were used for further analysis.

As demonstrated in Figure 4.24 and Figure 4.25, the pressure recorded due to 10% strain in warp direction at 25% and 50% strain in weft direction on cylinders 90 and 160 were very close to pressure recorded where strain in warp direction was kept at zero. Yet the difference in pressure at 75% strain in warp direction became more significant (Figure 4.26); for instance, 28% pressure increase was recorded at measuring point B1 over cylinder 160 at 75% and 10% strain in weft and warp directions, respectively. At 30% strain in warp direction, the pressure recorded over cylinders was greater at cylinder 160 in comparison to cylinder 90.

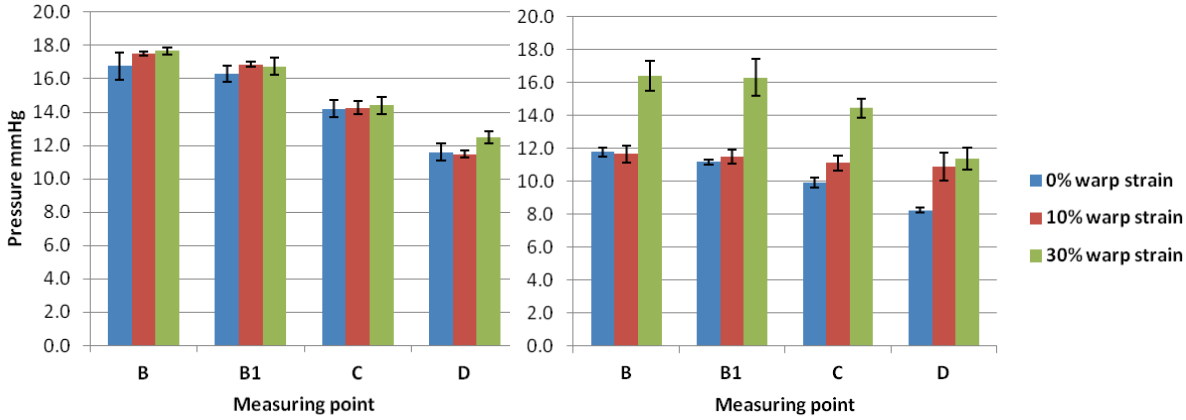

(a) (b)

Figure 4.24 Measured pressure at variable strains in warp direction and 25% strain in weft direction - cylinders (a) 90 and (b) 160 – fabric C

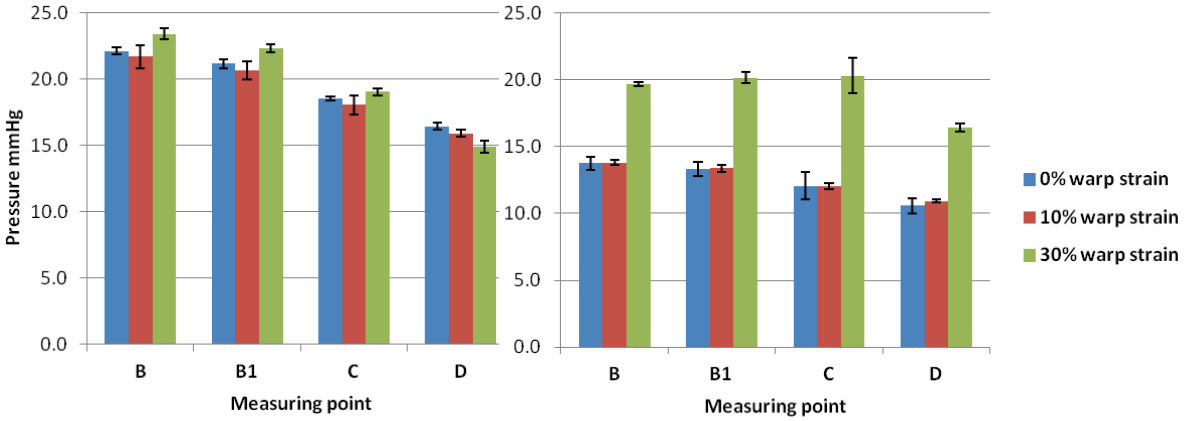

(a) (b)

Figure 4.25 Measured pressure at variable strains in warp direction and 50% strain in weft direction - cylinders (a) 90 and (b) 160 – fabric C

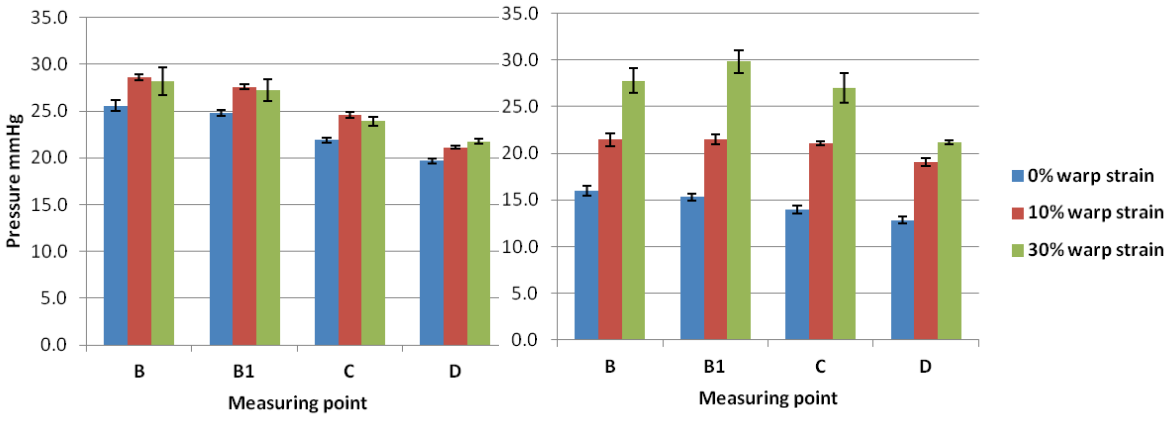

(a) (b)

Figure 4.26 Measured pressure at variable strains in warp direction and 75% strain in weft direction - cylinders (a) 90 and (b) 160 – fabric C

As explained in section 4.1.3, fabric C was less powerful in warp direction compared to weft direction by 12% under 20 N stress; this meant that less stress was generated by the fabric under similar strain in warp direction. The strains in warp direction induced on CGs are relatively low, so the pressure generated by warp direction would be lower at similar conditions.

In conclusion, the combination of strains in weft and warp directions increased the overall measured pressure on the cylinders, yet the significance of this effect depends on other variables such as the cylinder diameter and the amount of strain applied in each of weft and warp directions.

Separate paired t-test analysis was carried out on the pressure induced on measuring point B1, by strain in weft direction along with 10% and 30% strain in warp direction on different cylinders (Appendice 29). The results revealed that the effect of 10% warp strain in combination to variable weft strains was insignificant for all but three out of nine combinations of strains/cylinders (cylinder 90 and 75% weft strain, cylinder 130 and 50% weft strain and cylinder 160 and 75% weft strain); this could be due to variations in pressure measurement and the fact that achieving and maintaining consistent warp strain was difficult. In case of 30% strain in warp direction in combination to variable weft strains, the influence of warp strain was significant ($p < 0.05$, 2-tailed) for all combinations and cylinders but cylinder 90 and 75% weft strain. 30% strain in warp direction, however, was rather extreme. On the cylinder set-up, the fabric sleeves were held by staples and cable grips and were torn due to high strain; while when SCGs are worn over the body, they may ride up the leg as they are not held in place similar to fabric sleeves over the cylinder.

This investigation suggested that the effect of warp strain on measured pressure became significant at higher strain in warp direction; due to difficulty of this method, however, the pressure was only recorded from one sleeve per each combination of strains/cylinders. Greater number of data could eliminate the variations and increase the certainty of the effect of warp strain on the measured interface pressure, especially at low warp strains such as 10%.

4.2.4. Discussion and conclusions

The theoretical pressures generated by non-composite and composed samples were calculated, using Law of Laplace and data derived from testing the fabrics for tensile properties in strip formation. The theoretical pressure was confirmed to be directly proportional to fabric stress; hence all analysis and conclusions regarding fabric tensile properties, carried out in section 4.1.3, was applicable to theoretical pressure calculated for same fabrics. Furthermore, the theoretical pressure increased at higher strains as the fabric was under higher stress and decreased at greater cylinder diameters, as expected from Law of Laplace and reported by other researchers (Macintyre, Baird & Weedall 2004; Ng, SF, Parkinson & Schofield 1999). On the other hand, the theoretical pressure calculated for samples composed of fabrics with different tensile properties was mostly influenced by the amount of each fabric within the sample composition; this influence was greater at higher strains due to higher stress variations. There was no existing literature on this topic; yet, as sourced SCTs under investigation were made with fabrics with varied tensile properties, it was important to predict and validate the theoretical pressure of composed samples.

Calibration of Salzmann MST MK IV Device and its sensor probes was attempted. Previous reports on consistency of the Salzmann MST Device led some of the researchers to not investigate its calibration and performance any further; while, Flaud, Bassez & Counord (2010) thoroughly investigated the performance of the device. They explained that measurement error to flexion was due to the mechanism of the sensor probe. However, the drop in measured pressure, from measuring points B to D when under the same pressure, was never reported by any researchers. This was confirmed in this research by various experiments (using series of weights and fabric sleeves over rigid cylinders providing in section 4.2.2). From analysing the sensor probe design and pressure measurement mechanism, measuring points B1 and C were found to be more reliable due to their positioning towards the middle of the sensor probe.

In this research, the theoretical pressure could not have been validated by comparison to measured pressure. The reason for this was systematic error of the pressure sensors and difficulties encountered in calibration process. Thus, the validation was carried out through linear regression analysis.

With the linear regression model, the measured pressure at measuring point B1 was predicted with high accuracy from the theoretical pressure derived from testing a known fabric for tensile properties in strip formation within the range of cylinder diameters and strains in weft direction investigated. However, the power of predictability of the model depends on statistically significant sample size and also low variation within the material. In the regression model, some predicted measured interface pressure was observed while the theoretical pressure was zero; the contact pressure between the fabric and the sensors resulted in interface pressure even when the fabric was under no strain, also reported by S.F. Ng, Parkinson & Schofield (1999).

On the other hand, the composed samples introduced high variations in data due to small sample size as well as possible variations caused by the seam attaching the two fabrics together. Further investigation is required in order to achieve a linear regression

model to accurately predict the measured pressure from theoretical pressure similar to non-composite samples.

Strain in the warp direction of garments is mainly investigated in regards to fit and comfort of the garments and not to analyse its effect on resultant interface pressure. It was found that introduction of warp strain increased the overall measured interface pressure, and that the influence of higher strains in warp direction (30%) was statistically significant on resultant measured pressure. A greater sample size would enable more accurate analysis of effect of strain in warp direction on the pressure, especially at lower strains.

As in previous research, the theoretical pressure was validated on rigid cylinders, eliminating the complexities of the human leg. From previous investigations, however, it is known that human limb geometry and body posture cause variations on measured interface pressure (Liu et al. 2005; Partsch, Partsch & Braun 2006; Wildin et al. 1998). These parameters must be taken into account in validation of theoretical pressure; as in real life, the human limb is not cylindrical, nor it is rigid and the human body is not generally in a static position when SCGs are worn.

4.3. Performance of fabrics comprising SCGs in terms of physiological comfort properties

Physical attributes of fabrics contribute to the physiological comfort properties of the garments. Some of these physical attributes are analysed previously in section 4.1.2 and are further analysed along with physiological comfort properties such as thermal and water-vapour management, moisture management and tactile comfort properties according to standard testing methods in this section. Where possible, the fabric physical attributes and physiological performance were also assessed to modified methods mainly based on standard testing methods, though in conditions close to the application of SCGs; that involved assessment in strained and/or moist conditions.

4.3.1. Porosity, air permeability and optical porosity properties

Porosity of fabrics C and D are calculated using Eq. (8). Fibre density of nylon is 1.14 g/cm^3 (Skinkle 1940) and elastane has a range of 1.20 to 1.25 g/cm^3 (Ghosh, P 2004). The weighted average of fibre density for fabrics C and D was calculated as 1.16 and 1.17 g/cm^3, respectively, which was used in porosity calculations.

Porosity and optical porosity of fabric fabrics C and D are plotted in Figure 4.27a and b. As porosity is derived from calculations, there are no STDEVs plotted in the graph; whereas relatively high STDEVs for optical porosity were due to unevenly distribution of gaps within the fabric.

Porosity is the air space within the fabric (inter and intra yarn) while optical porosity is the visible air gaps within the fabric. Fabric C had slightly higher porosity than fabric D (by 2%), while it had significantly lower optical porosity (by 52%). Fabric C was lighter by 6% and thinner by 3% in comparison to fabric D, but as its weighted average fibre density was lower, the resultant porosity was slightly higher. This meant that there was slightly more air space within the fabric C in comparison to fabric D. Even though the porosity of fabrics was very similar, yet the distribution of pores was very different between the two fabrics, resulting in much higher optical porosity in fabric D.

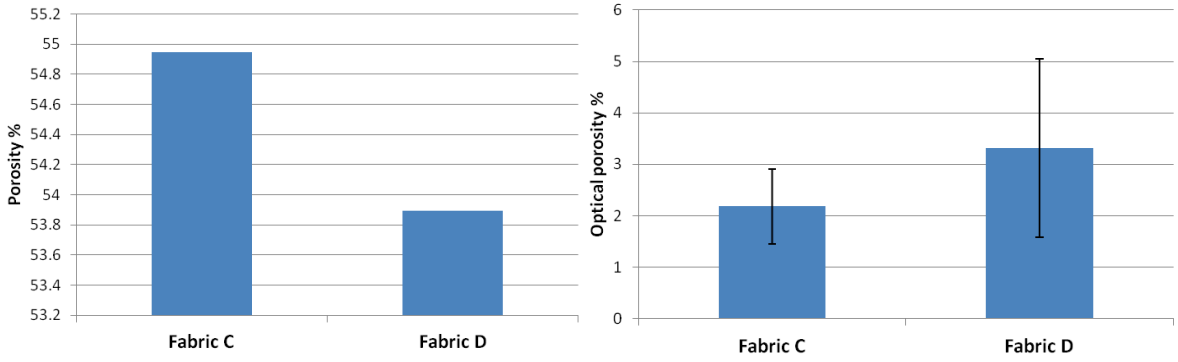

(a) (b)

Figure 4.27 (a) porosity and (b) optical porosity – fabrics C and D

There was a small difference in stitch density (2%) between the two fabrics; yet slightly lower number of yarns inter-looped per surface area in fabric D and possible difference in yarns between the fabrics and difference in distribution of pores, resulted in higher optical porosity in fabric D. The differences between fabrics were not all significant (for instance 2% difference in porosity and stitch density), but these small differences may affect the physiological performance of fabrics which makes them important. Since the fabrics analysed were commercially sourced, there were some undefined parameters regarding their raw material and manufacturing process and each of these unknown parameters could influence the measured properties to a certain extent; thus the analysis was carried out referring to known and measured parameters of the fabrics.

Air permeability of fabrics C and D are measured and calculated using Eq. (9). Fabric D had higher air permeability than fabric C by 27% (54.5 ±0.2 and 74.5 ±0.3 mm/s for fabrics C and D, respectively). Despite having higher mass per unit area and higher thickness, fabric D had lower stitch density (as listed in Table 4.1) and higher optical porosity, which meant greater pore size and resulted in higher air permeability.

Since SCGs have a negative fit over the body of the wearer, the strain could have potential effect on physical fabric attributes. For this reason and in this research, porosity and optical porosity of fabric D was measured both in relaxed and in various strains in weft direction. Air permeability could not be tested when fabric was strained.

Thickness and porosity, stitch density and optical porosity of fabric D in relaxed formation (0% strain) and various strains in weft direction are presented in Figure 4.28 and Figure 4.29. Mass per unit area, thickness, and number of courses and wales per unit

length of fabric D at various strains in weft direction were also measured for calculation of stitch density and porosity (Appendice 30).

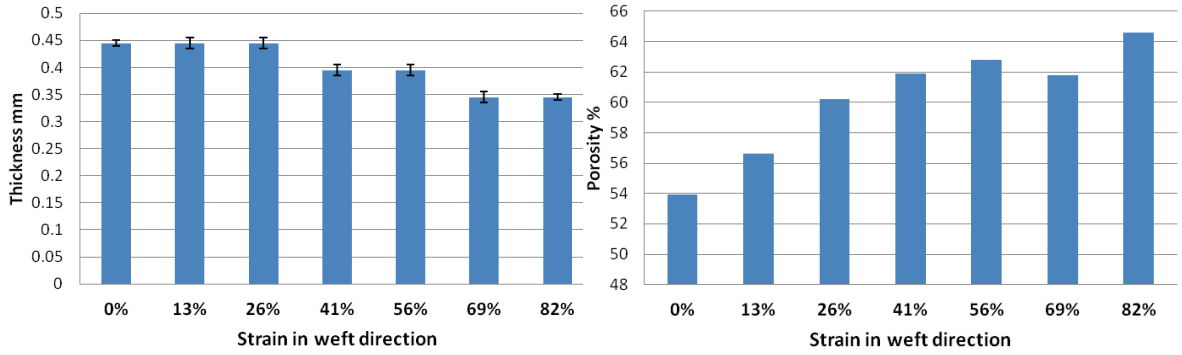

(a) (b)

Figure 4.28 (a) Thickness and (b) porosity of fabric D in relaxed and strained state

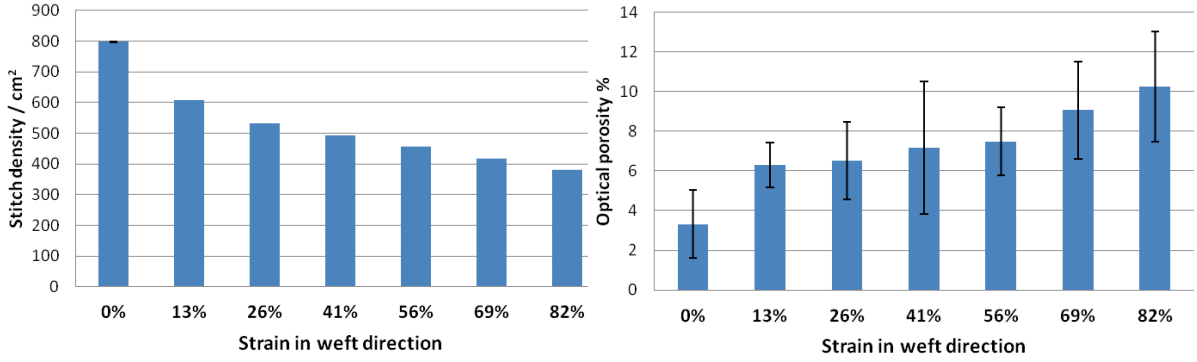

(a) (b)

Figure 4.29 (a) Stitch density and (b) optical porosity of fabric D in relaxed and strained state

When fabrics diverged from their relaxed state (0% weft strain) to various strains in weft direction (13% to 82%) physical parameters changed, ultimately affecting porosity and optical porosity. STDEVs of measured values (thickness, stitch density and optical porosity) are plotted in the graphs. Stitch density of the fabric at each strain were very close, therefore the error bars are not visible. STDEV of thickness values were very low, while it was higher for optical porosity. As explained earlier, the reason was unevenly distributed gaps within the fabric.

As the amount of strain increased the fabric structure changed, resulting in lower mass per unit area, wales per unit length and thickness. The decrease in stitch density was mainly due to decrease in number of wales per unit length, as the warp strain of fabrics was avoided and thus the number of courses per unit length remained the same. The effect of strain in weft direction was significant on thickness and stitch density ($p < 0.05$, 2-tailed). These changes resulted in higher porosity and optical porosity. The influence of change in thickness and stitch density was highly significant on porosity of fabric D ($p <$

0.001, 2-tailed). This revealed that the air space in fabrics increased with increase in strain in weft direction.

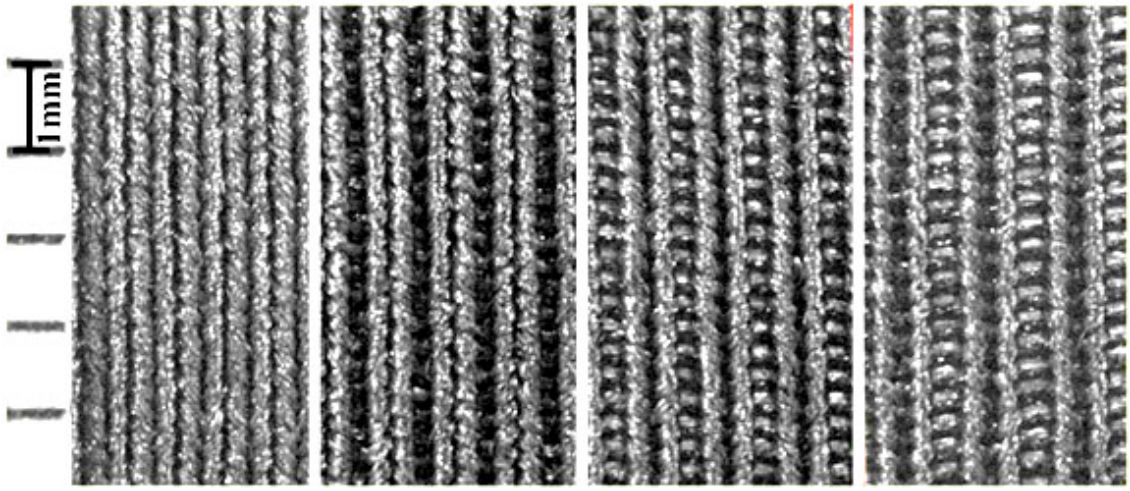

Figure 4.30 Microscopic images of 0%, 26%, 56% and 82% strain in weft direction from left to right – technical face of fabric D

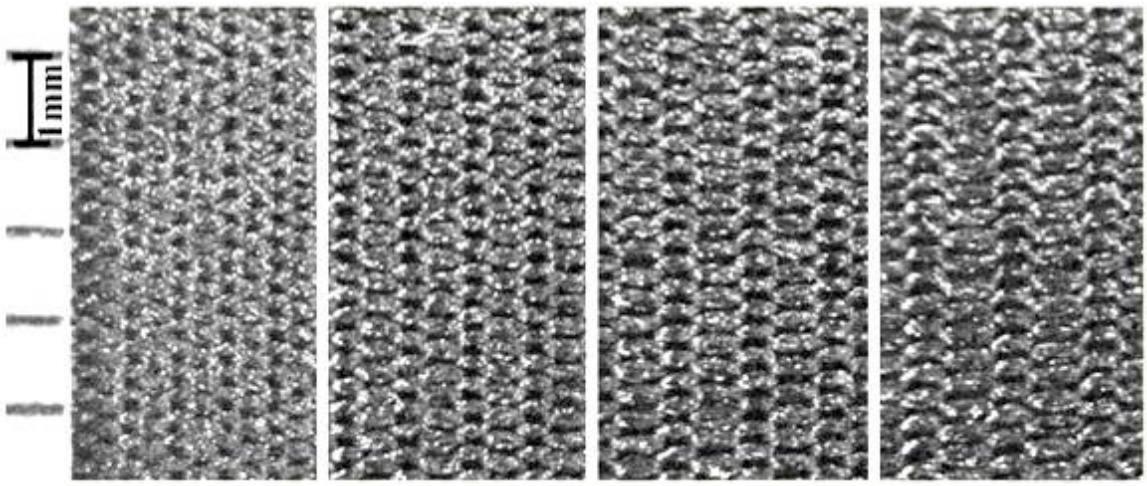

Figure 4.31 Microscopic images of 0%, 26%, 56% and 82% strain in weft direction from left to right – technical back of fabric D

Since in strained fabrics there were less yarns (wales) available to cover the same area as the relaxed fabric, the fabric under strain became more porous compared to its relaxed state, also visible in Figure 4.30 and Figure 4.31, where more pores/air gaps were available within the fabric area under strain.

Stitches were stretched approximately uniformly across the surface of the fabric, resulting in decreased stitch density; the influence of change in stitch density on optical porosity was highly significant ($p < 0.001$, 2-tailed).

Since fabrics C and D were very similar in terms of construction and basic physical parameters, it is expected that strain in weft direction in fabric C would have similar influences on above parameters as for fabric D.

Porosity, air permeability and optical porosity affect the thermal resistance, water-vapour resistance and moisture management of fabrics and overall physiological comfort of the wearer, which are addressed in the following sections (4.3.2 and 4.3.3).

4.3.2. Thermal and water-vapour management

Thermal resistance of fabrics C and D in relaxed, relaxed with frame and with 25% strain in weft direction with frame are displayed in Figure 4.32.

Low STDEV for each fabric suggests low variation between the specimens. The STDEV was slightly higher in strained fabrics, possibly due to variations caused by strain across the fabric.

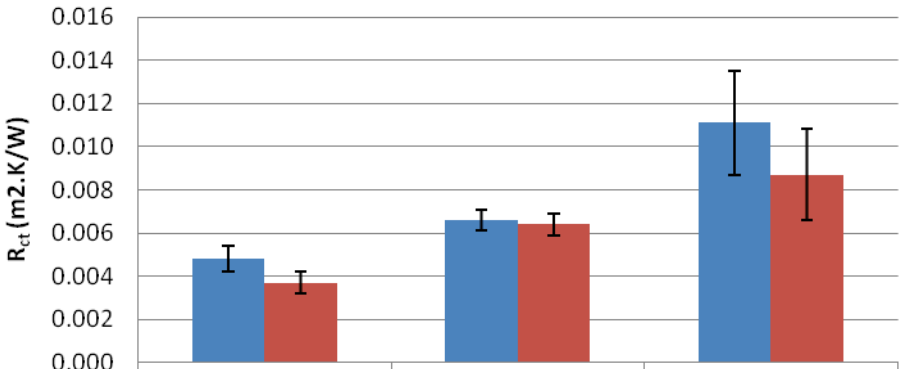

	Relaxed	Relaxed with frame	25% strain in weft direction with frame
Fabric C	0.0048	0.0066	0.0111
Fabric D	0.0037	0.0064	0.0087

Figure 4.32 Thermal resistance (R_{ct}) – fabrics C and D

Fabric D had lower thermal resistance than fabric C in relaxed formation by 29%. This difference is explained by higher optical porosity, air permeability of fabric D and higher porosity of fabric C. Porosity is a static, while air permeability is a dynamic fabric parameter. High porosity demonstrates the existence of more air within the fabric structure, while high air permeability explains the passage of air (and thus the heat transfer by convection) through the fabric. When the air permeability of the fabric is higher, more air penetrates the fabric and results in more convective heat transfer and lower thermal resistance.

The fabrics were tested in relaxed formation with air flow of 1 ±0.05 m/s. The thermal resistance of both fabrics in relaxed formation increased with introduction of wooden frame; introduction of wooden frame disrupted and reduced the air flow in comparison to testing for thermal resistance of fabrics in relaxed formation without the frame. The reduced airflow over the measuring plate increased the thermal resistance of both fabrics in relaxed formation (by 27% for fabric C and 42% for fabric D), as heat transfer by convection was reduced (Figure 4.32). The higher influence of introduction of wooden frame on R_{ct} of fabric D could be explained by the fact that fabric D had higher

concentration of pores (higher optical porosity and air permeability), thus reduced air velocity had greater influence on its thermal resistance than fabric C. The influence of introduction of wooden frame on thermal resistance of the fabric in relaxed formation was significant ($p < 0.05$ for fabric C and $p < 0.001$ for fabric D, 2-tailed).

Between the two fabrics tested with wooden frame, the introduction of strain in weft direction increased the thermal resistance of the both fabrics as well (Figure 4.32). The reason was increased porosity due to strain.

The introduction of strain in weft direction on the thermal resistance, with presence of wooden frame, was also significant ($p < 0.001$ for fabric C and $p < 0.05$ for fabric D, 2-tailed).

The approximate thermal resistance of strained fabrics without the influence of frame could be calculated by subtraction of percentage influence of wooden frame on thermal resistance of relaxed fabrics from the measured thermal resistance of strained ones, using Eq. (16):

$$R_{ct,a,s} = R_{ct,m,s} - (R_{ct,m,s} \times \frac{W_{ct}}{100}) \quad (16)$$

where $R_{ct,a,s}$ is the approximate R_{ct} strained without the influence of wooden frame (m^2.K/W), $R_{ct,m,s}$ is the R_{ct} measured strained under the influence of wooden frame (m^2.K/W) and W_{ct} is the influence of wooden frame on R_{ct} of relaxed fabric (%).

From above calculations, the approximate thermal resistance of fabrics C and D in strained formation without the influence of wooden frame are provided (Table 4.3).

Table 4.3 Thermal resistance (R_{ct}) of fabrics C and D with 25% strain in weft direction without the influence of wooden frame

Fabric label	Influence of wooden frame	Relaxed	25% strain in weft direction
	%	m^2.K/W	
C	27	0.0048	0.0081
D	42	0.0037	0.0051

From this approximate thermal resistance values for fabrics strained in weft direction, it could be inferred that the 25% strain in weft direction increased the thermal resistance of fabrics tested, by average 34% (41% for fabric C and 27% for fabric D). The difference in results between fabrics was due to difference in their physical parameters; fabric C was more porous than fabric D in relaxed formation, and the porosity was further increased due to strain in weft direction (explained in section 4.3.1). The increase in porosity means that there is more air within the fabric, which increased the air insulation and resulted in higher thermal resistance. Yet it should be noted that the thermal resistance of strained fabrics were tested with lower air flow across the fabrics which decreases the sensitivity of the measuring plate and that the thermal resistance for strained fabrics in Table 4.3 are approximations.

The thermal resistance of fabrics were tested under steady state and the thermal resistance of strained fabrics were higher than relaxed fabrics in case of the fabrics investigated in this research. Increased volume of air within fabric structure under low air speed, results in higher thermal resistance due to lower thermal conductivity of air in comparison to fibres. However, it is expected that in active situations, higher air velocity is present, increasing the air ventilation through the fabric, enhancing the heat transfer through convection and reducing the resultant thermal resistance of fabrics. It is expected that under higher air velocity, the increased size of pores within the fabric structure would decrease the thermal insulation of the fabric.

Water-vapour resistance of fabrics C and D in relaxed, relaxed with frame and with 25% strain in weft direction with frame are illustrated in Figure 4.33. Similar to thermal resistance of fabrics C and D analysed above, low STDEV suggests low variation between specimens.

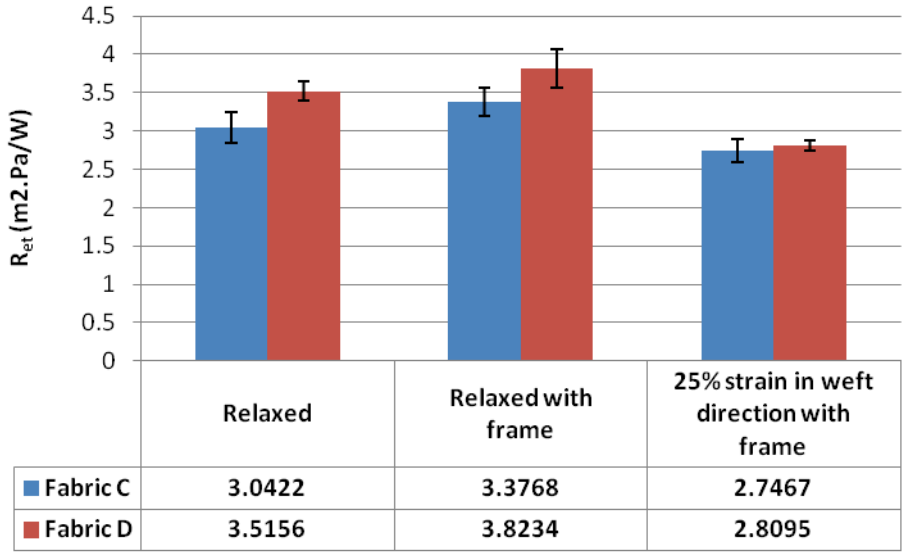

Figure 4.33 Water-vapour resistance (R_{et}) – fabrics C and D

Yet unlike thermal resistance, fabric D had higher water-vapour resistance than fabric C by 13% which was not high but not negligible either. Both fabrics were made of nylon and elastane fibres, which are hydrophobic and were conditioned similarly prior to testing; therefore, their influence on water-vapour resistance, such as water content, was similar and negligible. Thickness and mass per unit area of fabrics affected their water-vapour resistance; fabric D was thicker and heavier than fabric C (seen in Table 4.1), which explained the higher water-vapour resistance.

The introduction of wooden frame when fabrics were tested in relaxed formation increased water-vapour resistance, due to disruption of air flow. The water-vapour resistance of strained fabrics, however, was lower than the water-vapour resistance of relaxed fabrics tested with frame.

As explained earlier in section 4.3.1, thickness and mass per unit area of fabric D decreased with increase in strain in weft direction, which should be similar for fabric C; hence, lower thickness and mass per unit area of the strained fabrics enhanced the water-vapour transmission and resulted in lower water-vapour resistance.

Again the significance of the introduction of wooden frame and strain in weft direction on water-vapour resistance of fabrics were analysed. The influence of introduction of wooden frame on water-vapour resistance of the fabric in relaxed formation was significant ($p < 0.001$ for fabric C and $p < 0.05$ for fabric D, 2-tailed) and when the frame was present, the introduction of strain in weft direction on the water-vapour resistance was highly significant as well ($p < 0.001$ for both fabrics, 2-tailed).

The introduction of wooden frame resulted in 10% and 8% increase of water-vapour resistance of fabrics C and D in relaxed formation, respectively. The approximate water-vapour resistance of strained fabrics without the influence of frame could be calculated by subtraction of percentage influence of wooden frame on water-vapour resistance of relaxed fabrics from the measured water-vapour resistance of strained ones, using Eq. (17):

$$R_{et,a,s} = R_{et,m,s} - \left(R_{et,m,s} \times \frac{W_{et}}{100}\right) \quad (17)$$

where $R_{et,a,s}$ is the approximate R_{et} strained without the influence of wooden frame (m^2.Pa/W), $R_{et,m,s}$ is the R_{et} measured strained under the influence of wooden frame (m^2.Pa/W) and W_{et} is the influence of wooden frame on R_{et} of relaxed fabric (%).

From above calculations, the approximate water-vapour resistance of fabrics C and D in strained formation without the influence of wooden frame are provided (Table 4.4).

Table 4.4 Water-vapour resistance (R_{et}) of fabrics C and D with 25% strain in weft direction without the influence of wooden frame

Fabric label	Influence of wooden frame	Relaxed	25% strain in weft direction
	%	m^2.Pa/W	
C	10	3.0422	2.4720
D	8	3.5156	2.5848

From this approximate water-vapour resistance values for fabrics strained in weft direction, it could be concluded that the 25% strain in weft direction decreased the water-vapour resistance of fabrics tested, by average 30% (23% for fabric C and 36% for fabric D). As explained earlier, the decrease in thickness and mass per unit area of strained fabrics decreased the water-vapour resistance. Again, it should be noted that the water-vapour resistance of strained fabrics were tested with lower air flow across the fabrics and the water-vapour resistance of strained fabrics in Table 4.4 are approximations.

In conclusion, in regards to transmission of water-vapour, fabrics performed better when strained. Yet it should be mentioned that the fabrics were tested under steady conditions. While in activity, changes in temperature and/or humidity may influence the water-vapour transmission of fabrics in both relaxed and strained formation; therefore the water-vapour resistance of fabrics must be evaluated in transient conditions as well.

4.3.3. Moisture management properties

Fabrics C and D were very similar in terms of moisture management properties. The water dropped on the top surface of the fabrics was absorbed by neither of the fabrics and it beaded up on the top surface. The fabrics did not get wet, up to the end of the test period.

Low surface energy of fibres (interfacial tension), tight construction of the fabrics, and high stitch density did not allow for the liquid-water to penetrate the fabrics and be transferred through the pores within the fabric structure. As the fabrics under investigation were commercially sourced, there was no information regarding application of hydrophilic finishes. Indices resultant from testing of fabrics C and D for moisture management properties on MMT are listed in Table 4.5.

Table 4.5 Liquid moisture management properties – fabrics C and D

Fabric label		Wetting time		Absorption rate		Max wetted radius		Spreading speed		Accumulative one-way transport Index	OMMC
		WT_T	WT_B	AR_T	AR_B	MWR_T	MWR_B	SS_T	SS_B	R	
		sec		%/sec		mm		mm/sec		%	
C	Mean	8.3	120	287	0	5	0	0.6	0	-823.0	0
	STDEV	1.2	0	141	0	0	0	0.1	0	45.6	0
D	Mean	8.1	120	165	0	5	0	0.6	0	-777.1	0
	STDEV	0.7	0	24	0	0	0	0.1	0	31.58	0

The water content measured on the top surface of the fabric was mainly due to existence of water beads (droplets) sensed by the sensors, which reached 5 mm from the centre on top surface for both fabrics without being absorbed. The reported absorption rate, which is the initial change in water content, was mainly due to existence of water on top surface and not the change in water content within the fabric. The water content at the bottom of the fabric did not change, since the water did not reach the bottom surface throughout the testing period (120 seconds).

To sum up, poor overall moisture management property of fabrics results in liquid sweat to remain on the inside of the garment and lead to uncomfortable feeling of wetness for the wearer. Fabrics with ideal moisture management properties must have medium to fast wetting, medium to fast absorption, and large spread at bottom surface and good to excellent one-way transport. This allows for the garments worn next to the skin to quickly absorb the water dropped on them and pass the water from the top to the bottom surface where it spreads out and enables its evaporation to the surrounding environment. This will eliminate the feeling of dampness and clinginess of the moist fabric next to skin and impedes the cool chill of the wet fabric next to the skin.

On the other hand, the fabrics were tested in relaxed formation. Yet when SCGs are worn, they are strained over the body; the change in fabric physical parameters due to strain could have possible effect on moisture management properties, as the stitch density, thickness and pore size within the fabric change. Furthermore, in reality, due to the negative fit of the garments, the perspiration is not dropped on the fabric; the stretch

and constant contact pressure between the garment and the body influences the way the perspiration comes into contact with fabric. The pressure induced between the body and the garment on the perspiration drop changes its interaction with the fabric and could influence the absorption, spreading speed and water transport from skin side to outer surface of the fabric.

4.3.4. Tactile comfort properties

Coefficient of friction (MIU) of the fabrics A to D in relaxed state is plotted in Figure 4.34.

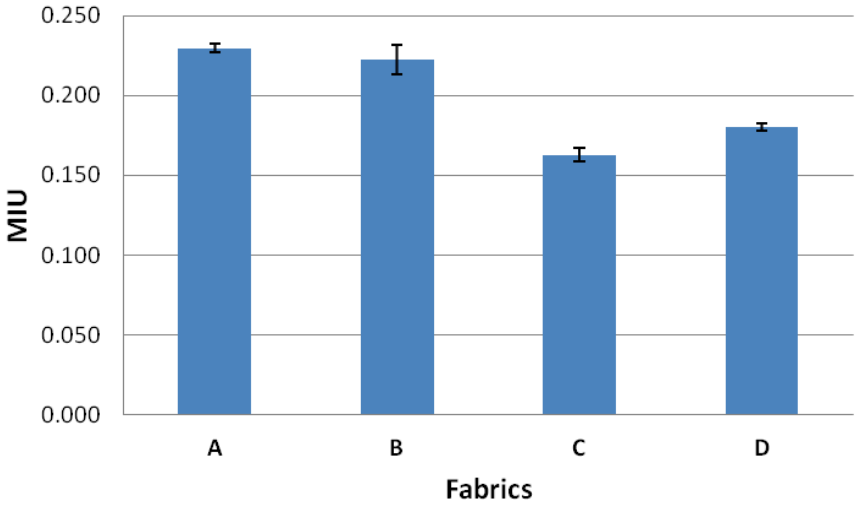

Figure 4.34 Coefficient of friction – fabrics A to D in relaxed state

All four fabrics had relatively low friction (below 0.25) on their next-to-skin side due to their fine micro-structure, as also seen in Figure 4.5. Fabrics A and B were only different by 3% in terms of coefficient of friction, since their construction and stitch density were similar (as detailed in Table 4.1). The coefficient of friction (MIU) was lower in fabrics C and D in comparison to fabrics A and B. The reason would be lower stitch density (Table 4.1), which meant that there were fewer yarns present per unit area and there would be fewer contact points between the fabric and the sensor and hence the skin. Meanwhile, all four fabrics would present a smooth sensation due to fine structure and low coefficient of friction.

Surface roughness mean deviation (SMD) of four fabrics is plotted in Figure 4.35. In roughness measurement with KES-FB4, the force and the displacement speed of the probe on the fabric are constant; thus, the difference in the measured roughness is mainly due to ridges width and their distribution on fabric surface.

Smooth fabrics have lower, while rough fabrics have relatively higher MMD and SMD. The fabrics tested had relatively homogeneous surface topography on their next-to-skin side (also observed in Figure 4.5), which resulted in relatively low SMD of maximum 4. Fabric D had lowest asperity height, 45% lower than the maximum SMD measured on fabric B; the difference could be due to difference in stitch density and yarn bulkiness. When the stitch density is higher, more yarns are available per unit area causing fewer

areas without yarn; also when the yarns are bulky, fewer surface irregularities are present, and therefore the surface roughness becomes lower. In total, all four fabrics had low friction and regular surface next to the skin.

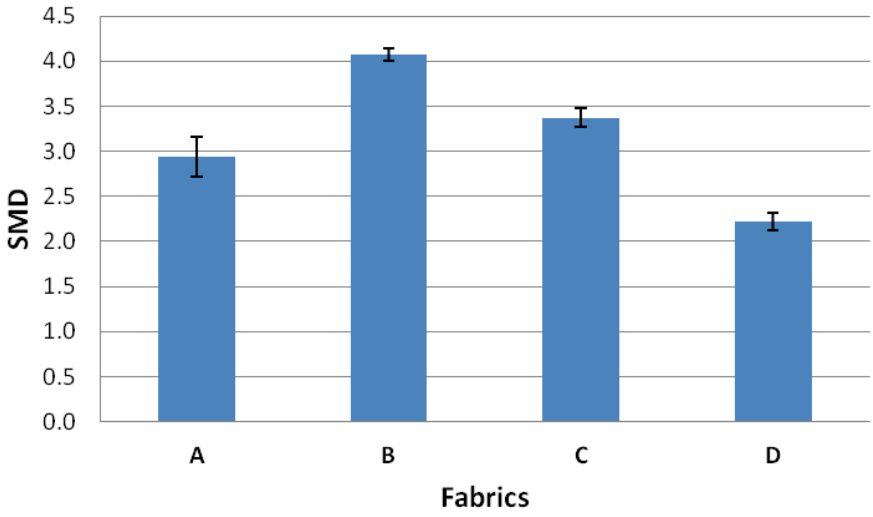

Figure 4.35 Surface roughness mean deviation – fabrics A to D in relaxed state

In general, in order to evaluate the tribological properties of fabrics, fabrics are evaluated in relaxed dry state; however, in many applications such as garments which are worn next to the skin with a negative fit, the fabrics are strained over the body when garments are worn; furthermore, in sport applications, a considerable amount of moisture from the sweat and in some cases from the environment is present in the garment. For these reasons, fabric D was tested for surface friction and surface geometry on various strains applied in weft direction in both dry and wet conditions.

Fabric sleeve dimensions for fabric D, for evaluation of tribological properties in strained state at various weft strains, are listed in Appendice 3. The fabric sleeves were 200 mm in length to eliminate any warp strain, where the number of courses per unit length was not changed from relaxed state (visible in Appendice 30).

It was expected that change in physical parameters due to strain in weft direction (as observed in Figure 4.30, Figure 4.31 and Appendice 30), would lead to the considerable change in the fabric surface topography that would influence the surface characteristics relevant to human tactile comfort; there was a clear difference observed in the change of the fabric topography under strain on the technical back (next-to-skin side) and technical face (outside the garment). Fabric changed from its homogeneous surface in its relaxed state to ribbed appearance under various strains in weft direction. The topography of technical back of the fabric under strain changed but remained considerably more homogeneous compared to the technical face (evident from Figure 4.30 and Figure 4.31).

The wet pick-up of fabric D in relaxed and strained formation ranged between 32% and 38% of the dry weight of the fabrics (Appendice 31). The difference in wet pick-up was insignificant and it did not influence the results for surface characteristics of the fabrics.

MIU and SMD of fabric D in relaxed and various strains in weft direction are illustrated in both dry and wet state (Figure 4.36 and Figure 4.37).

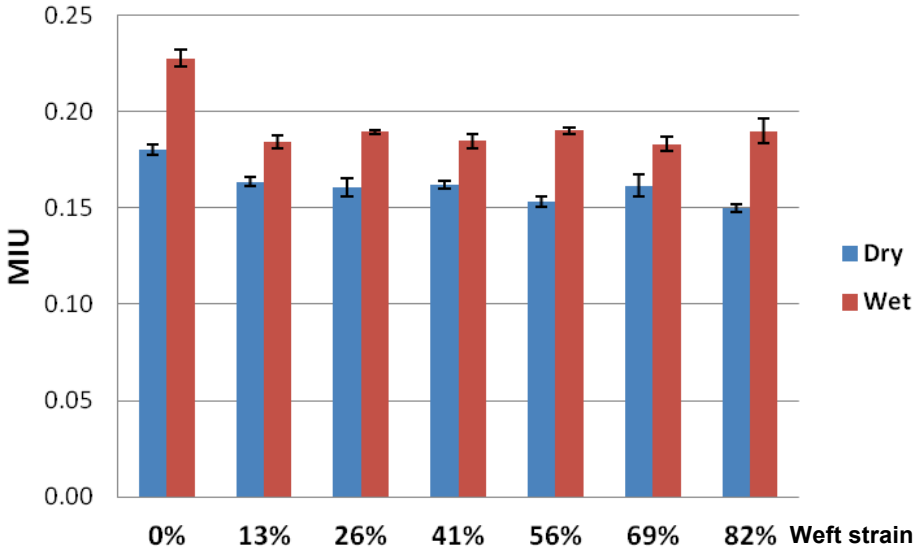

Figure 4.36 Coefficient of friction – fabric D in dry and wet states at various strains in weft direction

Fabric D, at various weft strains in both dry and wet state, had low MIU (below 0.25). Friction of fabric D under strain became lower on the technical back of the fabrics in comparison to relaxed fabric (0% Strain) by an average of 12%; fewer yarns available per surface area resulted in less contact points in the fabric surface and led to the lower coefficient of friction. However, since the coefficient of friction was low, the difference in friction caused by the strain did change the tactile comfort of the fabrics to a large extent. Except for a drop in friction in fabric strained to 56%, the coefficient of friction decreased with increase in strain. The obvious change in surface geometry is demonstrated in the results and the effect of strain on MIU in dry condition was statistically significant ($p < 0.05$, 2-tailed).

On the other hand and as expected, the friction due to moisture was increased in comparison to dry fabrics. It was observed that the introduction of moisture was highly significant on MIU as well ($p < 0.001$, 2-tailed); however, the correlation between the strain in weft direction and MIU in wet conditions was not statistically significant ($r = -0.562$).

As mentioned earlier, the fabric had relatively homogenous surface geometry on the technical back even when strained; hence, low variation in surface roughness was recorded when fabric D was strained in both dry and wet states (seen in Figure 4.37). Yet the surface roughness of wet fabric were generally lower than dry fabric with exception of 4% increase in fabric strained to 13% strain in weft direction, which is negligible. The presence of moisture had swollen the yarns and the fabric, reducing the asperity height of the fabric surface; for this reason, lower surface irregularities in wet fabric were recorded in comparison to dry fabric, by average of 9%.

The effect of strain in weft direction on SMD was statistically significant on dry fabric ($p < 0.05$, 2-tailed), while the effect of moisture on SMD was insignificant ($p = 0.106$, 2-tailed).

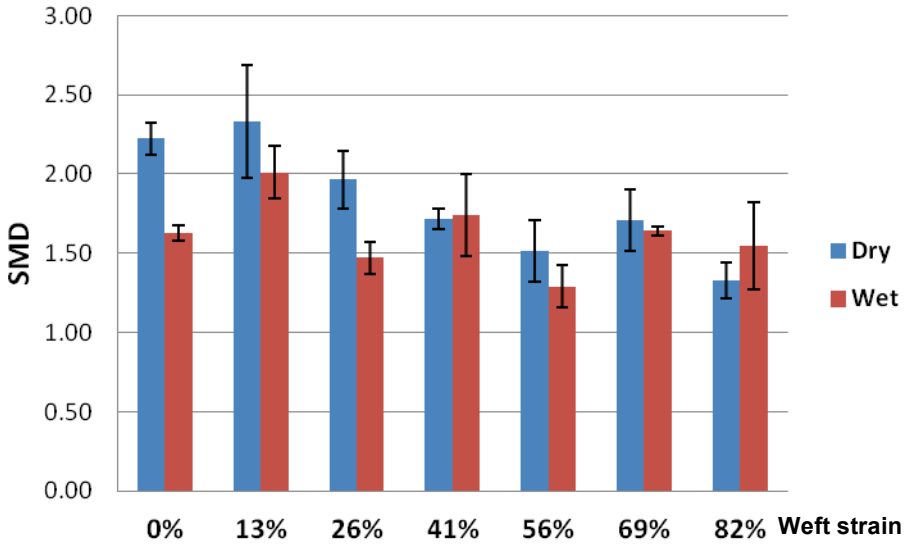

Figure 4.37 Surface roughness mean deviation - fabric D in dry and wet states at various strains in weft direction

Change in structure of the fabric due to weft strain, also changed the surface characteristics of fabric. The loops became widened and there were larger spaces between the rows of wales. This affected the contact points of the fabric as well as the asperity height of its surface, also revealed in coefficient of friction and surface roughness mean deviation, respectively.

The study of effect of various strains on fabric friction suggests that the coefficient of friction was lower in strained fabric; as the loops were widened due to strain, there were less contact points between the fabric and the skin, which meant that the fabric would feel smoother next to the skin compared to its relaxed state. As demonstrated in the microscopic images, the surface geometry of fabrics was changed due to strain. The asperity height of the surface of fabric was decreased as a result of weft strain and the surface roughness was decreased in strained fabric. Both MIU and SMD were decreased with increase in weft strain.

The presence of moisture increased the friction and the feeling of fabric clinging to the skin. This reduced the pleasantness of the fabrics. Even though the friction of wet fabric was higher than the dry, yet in case of fabric D, the fabric remained objectively smooth next to the skin. The process of wetting out the fabrics and the presence of moisture had affected the surface roughness of the fabric; the fabric was smoothed out and it was less irregular on surface.

It could be speculated that similar results would be found for fabrics with similar fibre blend, yarn, construction and physical attributes as the one tested in this research. However, the effect of the strain and moisture may be different for fabrics with different fibre blend, yarn and/or construction, which requires further investigation.

4.3.5. Discussion and conclusions

Porosity, air permeability and optical porosity of two fabrics were tested in a relaxed formation. Additionally, the porosity and optical porosity of one of the fabrics were tested in various strains applied in weft direction. Differences in the distribution of pores within the fabric resulted in slightly higher porosity and much lower optical porosity amongst the fabrics investigated.

Unlike reports by Majumdar, Mukhopadhyay & Yadav (2010), lower mass per unit area and thickness did not result in higher porosity; as porosity also depends on the ratio of mass per unit area to thickness as well as fibre diameter. Despite having higher thickness and mass per unit area, lower stitch density and higher optical porosity of one of the fabrics indicated greater pore size; greater pore size results in higher air permeability.

Strains in weft direction applied to the fabric had significant effect on its thickness and stitch density, and thus on its porosity and optical porosity, respectively. Increase in strain in the weft direction applied to the fabric decreased its thickness and stitch density, and resulted in higher porosity and optical porosity.

One of the fabrics under investigation performed better in terms of heat transmission (lower thermal resistance) by 29%, but it performed slightly worse in terms of water-vapour transmission (higher water-vapour resistance) by 13% than the other fabric.

Differences in the thermal resistance of fabrics were mainly due to differences in their optical porosity, air permeability and porosity, predominantly the number of pores and their distribution. This finding was consistent with previous studies (Gibson 1993; Hatch et al. 1990). Presence of air within the fabric structure (high porosity) increases thermal resistance, as air has a lower thermal conductivity than most fibres (Salopek Čubrić et al. 2012); while easy passage of air through the fabric (greater pore size and high air permeability) increases the heat transfer through convection, therefore reducing the thermal resistance of fabrics.

The difference in the water-vapour resistance of fabrics was due to the differences in their thickness and mass per unit area. Thickness was reported by many researchers to be influential on the thermo-physiological comfort of fabrics, where decrease in fabric thickness resulted in lower water-vapour resistance (Bedek et al. 2011), confirming the above findings.

Thermal resistance and water-vapour resistance of the two fabrics were also measured under 25% strain applied in weft direction. The introduction of wooden frame for testing the fabrics in strained formation disrupted the air flow in the chamber and increased both the thermal and water-vapour resistance of fabrics. The effect of strain in the weft direction on the thermal and water-vapour resistance of fabrics was highly significant; it increased the thermal resistance, due to the increased porosity in strained fabrics, while it reduced the water-vapour resistance of fabrics. Fabric thickness and mass per unit area were decreased due to strain in weft direction, leading to lower water-vapour resistance, confirming the reports by Majumdar, Mukhopadhyay & Yadav (2010), where reduced fabric thickness and mass per unit area resulted in higher air permeability and thus improved the water-vapour transmission. The influence of the wooden frame was

subtracted from the recorded thermal and water-vapour resistance of fabrics and an approximation of these values in strained formation without the influence of wooden frame were calculated.

Air within the fabric structure and above the fabrics (boundary air layer) and air velocity are found to be very influential on thermal and water-vapour resistance values of fabrics (Hatch et al. 1990; Huang 2006a) as well as various fabric parameters such as stitch density, mass per unit area, thickness, fabric pore size, air permeability and porosity. Furthermore, it was found in this research that strained fabrics would perform differently in terms of heat and water-vapour transmission compared to relaxed fabrics; according to the approximate values derived in this research, strained fabrics had higher thermal resistance and lower water-vapour resistance in comparison to relaxed fabrics in steady state. In real life, however, steady conditions rarely exist; therefore it is expected that the thermal resistance of strained fabrics would decrease in activity, where higher air velocity is present. Higher air velocity would improve the passage of air within the strained fabric and enhance the heat transfer through convection. Furthermore, increase in temperature and/or humidity may influence the water-vapour resistance of fabrics. Thus further analysis of the thermal and water-vapour resistance of fabrics is required in both relaxed and strained formation in conditions as close as possible to their end-use and under transient conditions.

Overall the moisture management capability of fabrics under investigation was rated as poor; this was due to low surface energy of fibres composing the fabrics, tight construction and high stitch density. These findings are in line with reports of other researchers (Fan 2009; Hatch et al. 1990). The hydrophilic finish was either not applied at all or not applied consistently on the surface of the fabrics investigated; therefore the overall (liquid) moisture management capability of the fabrics was very poor. Furthermore, the moisture management property of fabrics was analysed in relaxed formation where the water was dropped on the fabric; while in reality, the interaction of liquid perspiration in under the influence of constant pressure and contact between the skin and the fabric, which may affect its moisture management property.

In terms of tactile comfort properties, all fabrics had low friction and relatively low surface roughness in a relaxed state. The fabrics were also tested in conditions which mimicked their intended end-use conditions: in strained formation and moist conditions.

Introduction of strain in the weft direction had a statistically significant influence on the friction and roughness of the fabric, where it reduced both friction and surface roughness of the fabric. The reason for this was the reduced number of contact points in the fabric and the relatively homogenous surface geometry when strained, respectively. Introduction of moisture had a significant influence on fabric friction: friction increased, as expected and confirmed from previous studies (Das & Alagirusamy 2011; Kilinc-Balci 2011a). Meanwhile, the presence of moisture decreased the surface roughness of the fabric due to the swelling of yarns and a decrease in irregularities in the surface of the fabric. The influence of moisture on fabric surface roughness, however, was not significant. Barker (2002) reported that surface properties of fabrics correlated with prickliness when dry and Das & Alagirusamy (2011) suggested that sweat-wetted skin caused wet cling; thus, it is

important that fabrics worn next to the skin have low friction and roughness when strained and moist, which are the conditions SCGs are usually worn in.

Since SCGs are strained over the body when worn, and in active conditions, moisture from perspiration or from the environment would be present at skin level. The fabrics must therefore be tested relative to these conditions if possible, as the presence of strain and moisture could potentially influence the comfort properties of the fabrics in comparison to relaxed and dry state, as also interpreted in this research. Furthermore, the performance of the fabrics cannot be directly translated into performance of the garments, due to potential changes in the physical parameters of fabrics when the garment is worn (for instance under strain), the amount of body covered by the garment, the air gap (if existent) between the garment and the body as well as various thermal conditions present in real life other than steady state under which the fabrics are usually tested.

4.4. Lower-body size and configuration - 3D body-scanning

In this section, reliability of $[TC]^2$ 3D body-scanner is investigated. Group of participants are scanned and the circumference and height measurements of different body parts are recorded, processed, analysed and compared between genders and within each size group. Human body proportions are calculated and investigated amongst both genders.

4.4.1. Reliability of $[TC]^2$ 3D body-scanner

Mode and STDEV of the body measurements for participants 1 and 2 were calculated. Range of STDEVs for all scanned measurements was 0.1 to 2.0 cm for participant 1 and 0.1 to 1.5 cm for participant 2, which was smaller than scanner resolution.

Few relatively important measurement points were selected and compared between the two participants, summarized in Table 4.6. Minimum and maximum differences to Mode for measurement points are also provided. Difference to Mode of the selected measurement points had a range of -3.2 to 1.54 cm.

MAD (mean absolute difference) was calculated by averaging absolute differences of scanned measurements to Mode for each participant. On average, there was 0.9 cm MAD for both participants on the few chosen scanned measurements. In some points such as waist, waist height and ankle height the MAD for participant 1 was over twice as much as other points, and for participant 2, this was the case for thigh-max, mid-thigh and crotch height. Measurement points such as elbow, knee and calf had very small MAD; hence, the measurements at these points were relatively more reliable than other measurement points discussed. Bust, hips, ankle, hips height and knee height were average in terms of MAD calculations. Figure 4.38 demonstrates how MAD was different between participants at various measuring points.

Table 4.6 Body measurements from 3D body-scans - participants 1 and 2

Measuring point	Participant 1				Participant 2			
	Mode	STDEV	Minimum difference	Maximum difference	Mode	STDEV	Minimum difference	Maximum difference
	cm				cm			
Bust	86.1	0.7	-1.1	1.9	82.3	0.6	-0.7	2.1
Waist	69.9	1.5	-2.4	4.4	68.9	1.0	-0.6	3
Hips	98.8	0.6	-1.5	0.7	96.3	0.4	-1.4	0.6
Elbow	21.3	0.2	-0.2	0.4	21.2	0.2	-0.5	0.5
Thigh-max	54.0	0.5	-0.1	1.4	55.0	0.5	-2.0	1.0
Mid-thigh	44.9	0.2	-0.4	0.4	45.7	0.6	-1.9	0.4
Knee	34.0	0.3	-0.7	0.6	35.1	0.2	-0.3	0.5
Calf	34.0	0.1	-0.3	0.1	34.2	0.1	-0.4	0.2
Ankle	21.5	0.5	-0.5	1.9	22.3	0.5	-1.2	0.8
Waist height	100.6	1.0	-3.2	1.2	97.9	0.6	-1.2	1.4
Hips height	77.0	0.6	-1.2	1.5	74.3	0.4	-0.8	1.0
Crotch height	76.4	0.5	-1.0	1.3	74.5	0.9	-3.0	1.4
Knee height	45.1	0.5	-1.4	0.7	43.8	0.4	-0.8	1.1
Ankle height	7.8	0.7	-2.8	0.5	6.8	0.5	-0.5	2.2

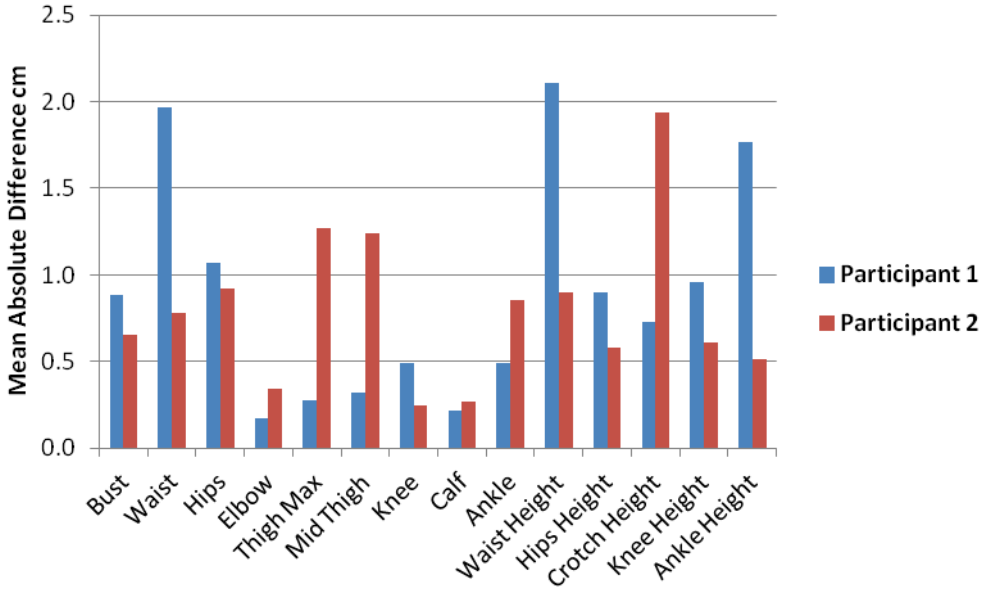

Figure 4.38 Mean absolute difference to Mode for few of the scanned measurements – participants 1 and 2

For instance and as seen in Figure 4.38, measuring points such as bust, hips and elbow recorded similar MAD for participants 1 and 2, while MAD for the participants were very different in waist, thigh-max, mid-thigh, as well as waist height, crotch height and ankle height. These values indicate that the discrepancies in body measurements were not specific to certain measurement points and occurred occasionally for one participant but not the other.

Since $[TC]^2$ 3D body-scanner has an error of ≤ 3mm in circumference ($[TC]^2$ n.d.), the measurements were ranked against 0.3 cm error. Each body scan and each measurement point was assessed and ranked against the mode and the error range, and

the percentage of measurement points for each body scan within the acceptable error was calculated. There was 27% to 59% and 32% to 65% of measurement points for each scan within the acceptable error range for participants 1 and 2, respectively. The body scan with highest percentage of measurement points within the acceptable error was ranked one and so forth.

Measurement points such as upper arm, elbow, wrist, maximum thigh, mid-thigh, knee, calf, ankle, hips height and ankle height were ranked 50% and higher within the acceptable error in all thirty body scans for both participants. This shows that the lower-body measurements, which are the main focus in this research, had relatively high rankings. Between every six consecutive body scans, there was at least one body scan ranked below ten. Thus, it was decided that six 3D body-scans was required for each participant and the 3D body-scan with highest number of measuring points within the error range to be chosen for further analysis.

4.4.2. Lower-body size and shape

Height and weight of female and male participants, reflecting their garment size according to existing sizing chart, is listed (Appendice 32).

Figure 4.39 and Figure 4.40 shows the various body shapes and sizes belong to same sizing category of SCGs. Each participant engaged in some sort of activity such as swimming, running, cycling, playing soccer, dancing, or general fitness. As generally the dominant leg of participants was right leg except for W005, the measurements were extracted from right leg.

Lower-body circumferences at critical measuring points B to G are plotted for participants belonging to same size category (Figure 4.41, Figure 4.42 and Appendice 33) and demonstrate the variations in their body measurements.

Figure 4.39 Postural photos of male participants belonging to size Medium

Figure 4.40 Postural photos of female participants belonging to size Small

Highest difference between minimum and maximum circumferences was determined: 16% at point C amongst male and 45% at point G amongst female participants (Figure 4.41 and Figure 4.42).

It should be noted that the differences in circumferential measurements at points C (usually close to calf), F and G were relatively high in both males and females belonging to same size category, while circumferential measurements close to the joints, such as point B (2 cm above the ankle) and the knee not covered with much muscle tissue, were very similar amongst participants belonging to the same size category; for instance, substantially greater circumference at point G on W006 would lead to much greater pressure generated by same sized SCG compared to other participants in the same group (as evident from Figure 4.42).

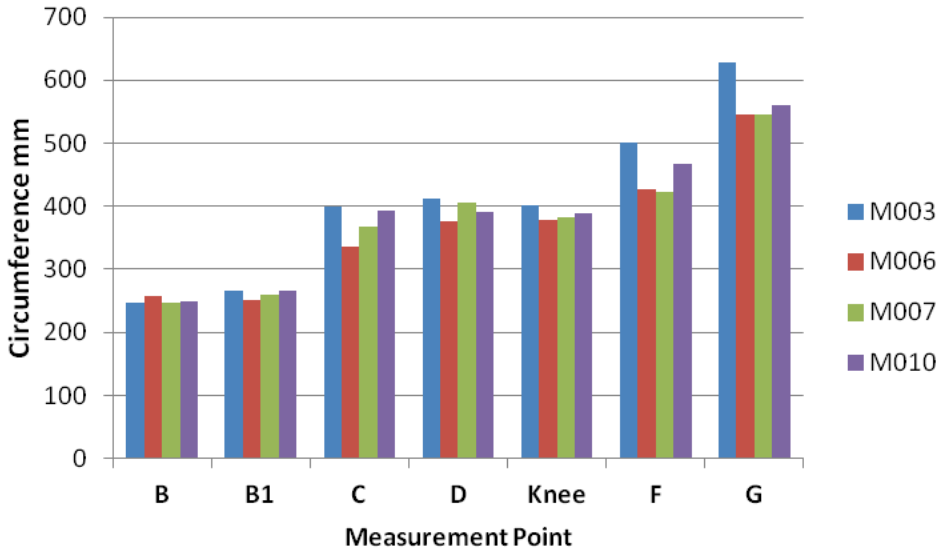

Figure 4.41 Circumferential measurements - male participants in size Medium

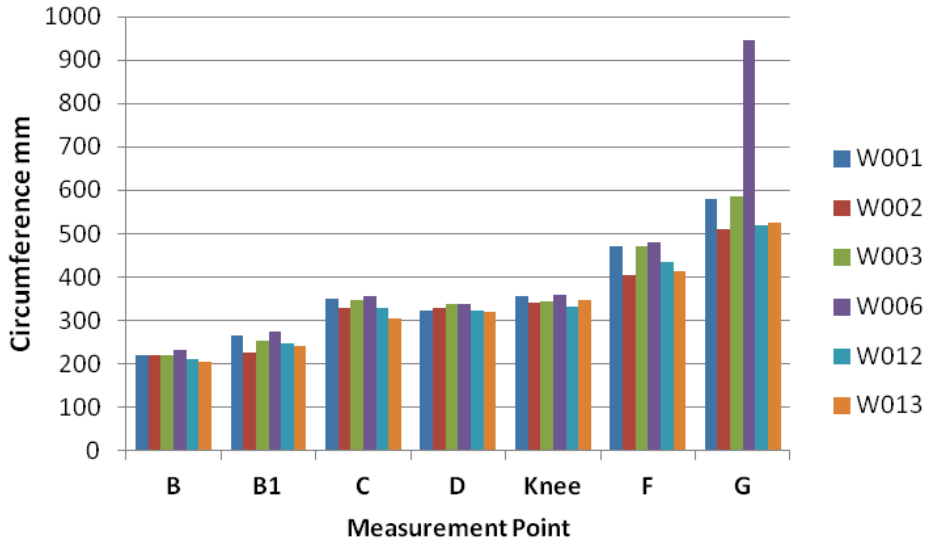

Figure 4.42 Circumferential measurements - female participants in size Small

The position of the critical points such as calf and knee relative to crotch height along the leg was also varied within the individuals in a same size group. The position of critical points mentioned above is demonstrated in Figure 4.43 and Figure 4.44. Thigh-max, however, was identified at the crotch point for all participants, both male and female (100% to crotch height).

Calf was positioned at average of 44% (42% to 49%) to crotch height along the leg and knee was positioned at average of 62% (59% to 65%) amongst male participants (Figure 4.43). As for female participants, calf was positioned at average of 43% (38% to 51%) to crotch height along the leg and knee at average of 58% (48% to 62%).

It could be inferred that calf of both male and female participants was positioned similarly at around 44% to crotch height along the leg and knee was positioned higher than the middle of the leg, above 50% of crotch height, for both genders, while being

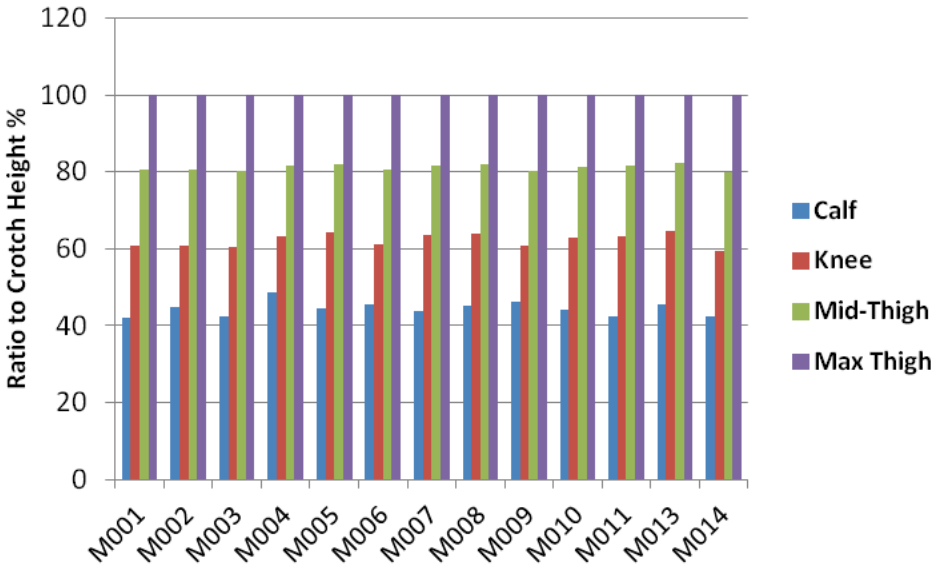

Figure 4.43 Few lower-body point's height ratio to crotch height – male participants

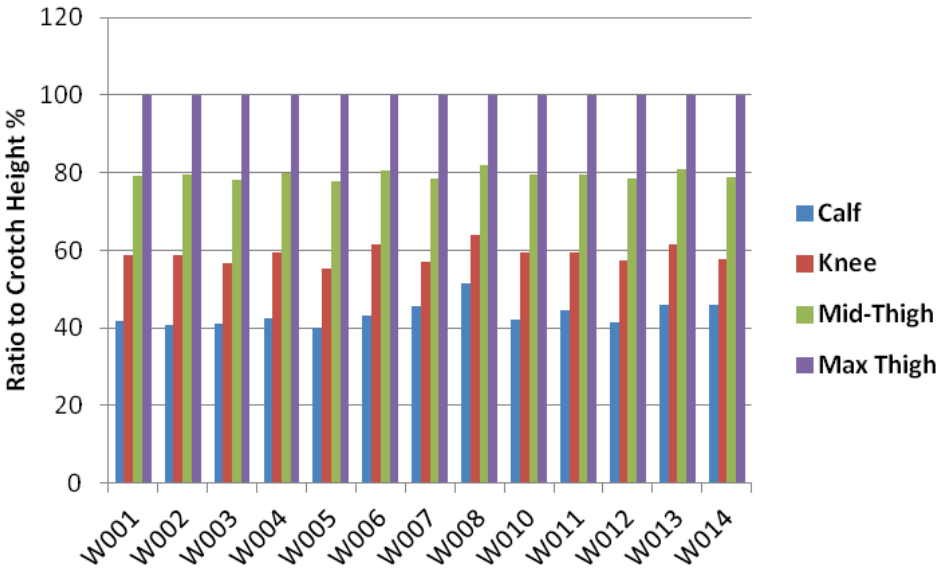

Figure 4.44 Few lower-body point's height ratio to crotch height – female participants

proportionally higher along the leg in male participants in comparison to females; this reveals that female participants had slightly longer thighs than males. Assuming that the garment would extend proportionally along its length and knowing that knee was positioned higher than the middle of the leg, knee would not be positioned in the middle of the garment leg length, but at the lower half.

Mid-thigh was positioned at average 81% (79% to 82%) of crotch height along the leg amongst male participants and for female participants, since they had slightly longer thighs, mid-thigh was positioned a little lower along the leg, at average 79% (74% to 81%) of crotch height. Mid-thigh and thigh-max circumferential measurements of male and female participants are provided in Figure 4.45 and Figure 4.46.

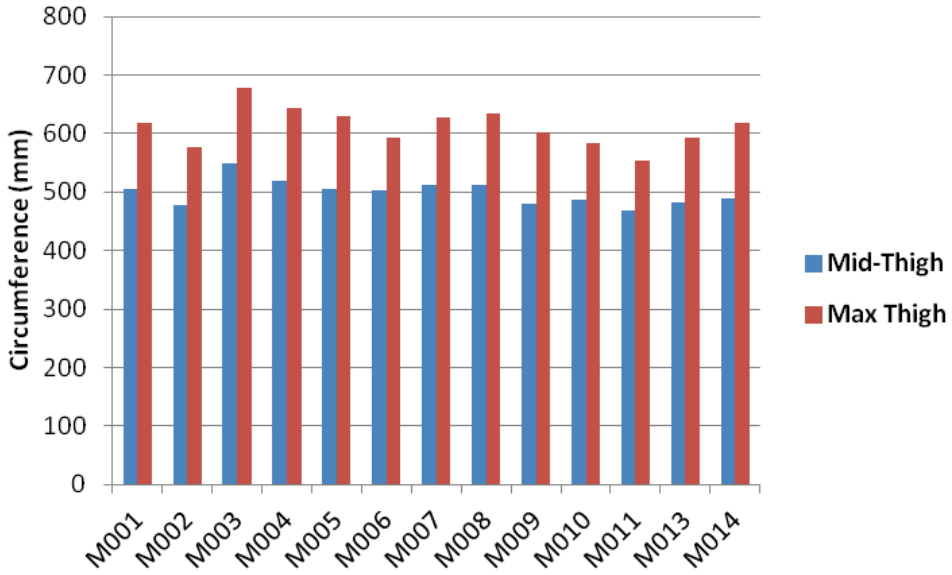

Figure 4.45 Circumferential measurements at mid-thigh and thigh-max – male participants

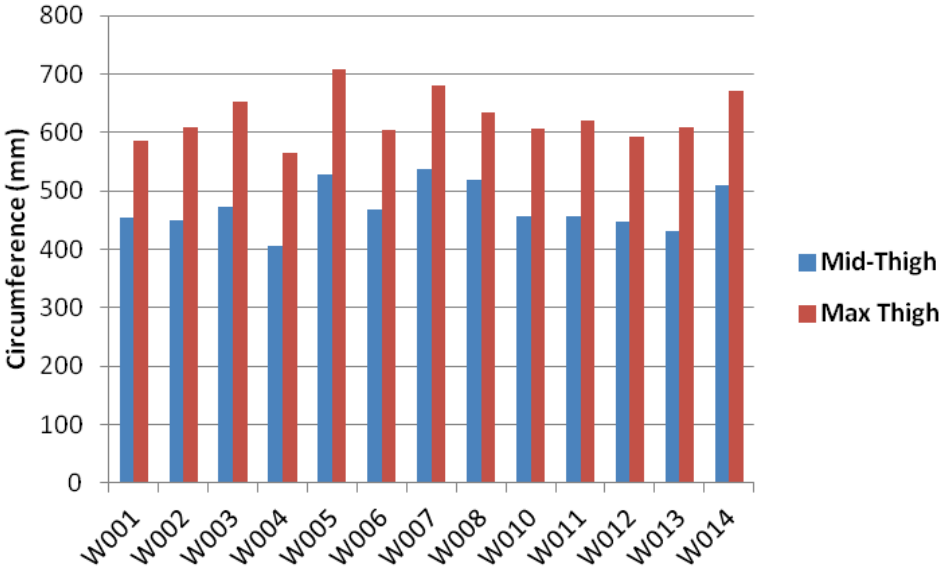

Figure 4.46 Circumferential measurements at mid-thigh and thigh-max – female participants

Mid-thigh circumferential measurement was approximately 81% and 75% of the thigh-max circumferential measurement for male and female participants, respectively. This shows a considerable increase of 19% and 25% in circumferential measurements from mid-thigh towards the crotch for male and female participants, respectively; this increase in circumferential measurement must be taken into account, as it affects the fit and comfort as well as the pressure gradient of the garment.

As stated in section 2.4.3, body proportions are usually assessed as a ratio to body height. Figure 4.47 and Figure 4.48 demonstrate few critical measuring points on lower-body, including calf, knee, mid-thigh, crotch and hip deep height as a proportion to body height of participants.

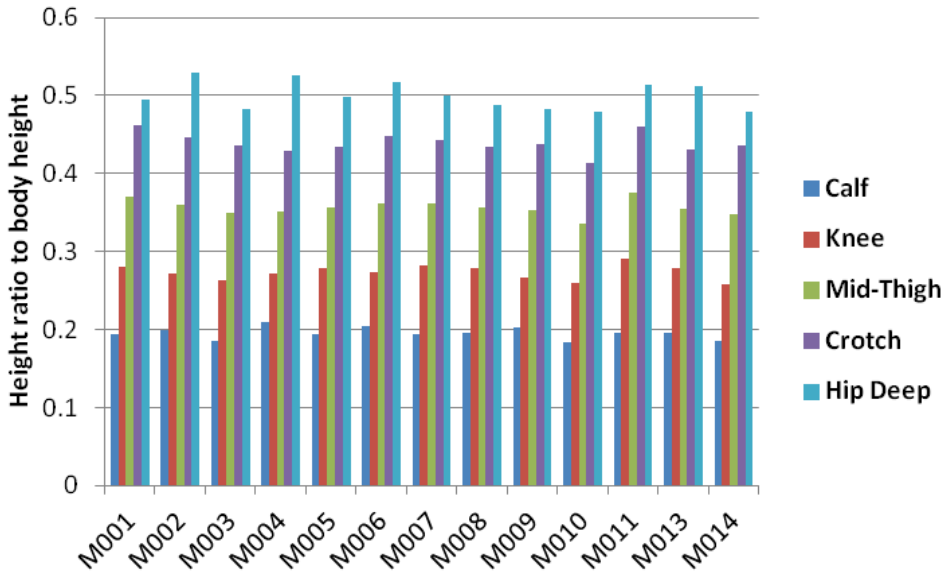

Figure 4.47 Height of few points on lower-body in relation to body height – male participants

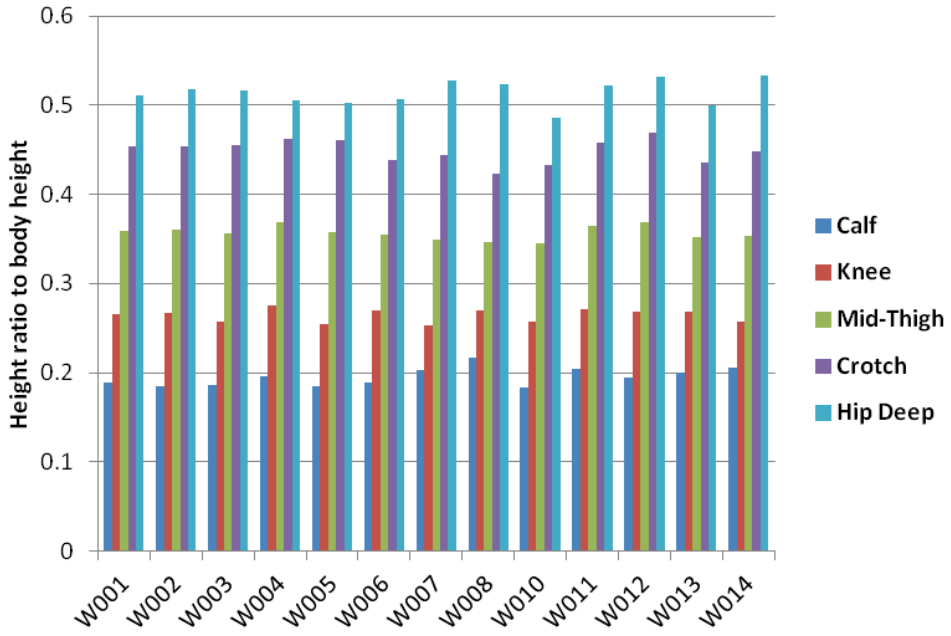

Figure 4.48 Height of few points on lower-body in relation to body height – female participants

As evident from Figure 4.47 and Figure 4.48, the height ratios of measuring points plotted to body height were similar at relative points in each gender. Mean and range of height of each point in relation to body height were analysed further (Appendice 34); low STDEVs for data shows that the height ratio of these points to body height in this population was very similar. Calf and mid-thigh height proportion to body height of male and female participants was the same; knee on female participants was slightly lower along the body height in comparison to male participants; crotch was slightly higher along the body height in females than males. This was in line with the findings from height proportions to crotch height, explained in Figure 4.43 and Figure 4.44, where female participants had longer thighs than male participants. Lastly, male participants had their hip deep slightly lower along the body height in comparison to female participants.

Critical lower-body circumferential measurements along the leg of the Base Model, such as ankle, calf, knee, mid-thigh, max-thigh and abdomen, were analysed in bare and wearing Elite SCT in sizes Small, Medium and Large according to the existing sizing chart of SCGs, as detailed in Figure 4.49.

Circumferential measurements at ankle and knee, where there was low muscle tissue available, were similar in bare and when tights were worn. The circumferential measurements at calf were also very close, especially since the Base Model was an athlete and his calf was muscular. However, at the upper section of the lower-body and the abdomen, the circumferential measurements at mid-thigh, thigh-max and abdomen were at their highest when Base Model was bare. Difference in circumferential measurements of approximately 1 cm (2%) was recorded for mid-thigh and thigh-max, and 5 to 8 cm (5% to 7%) at abdomen; it could be assumed that the SCT had compressed/displaced the tissue at thigh area, where in comparison to calf, more fat was available. Meanwhile, the waist of the tight had cut into the abdomen.

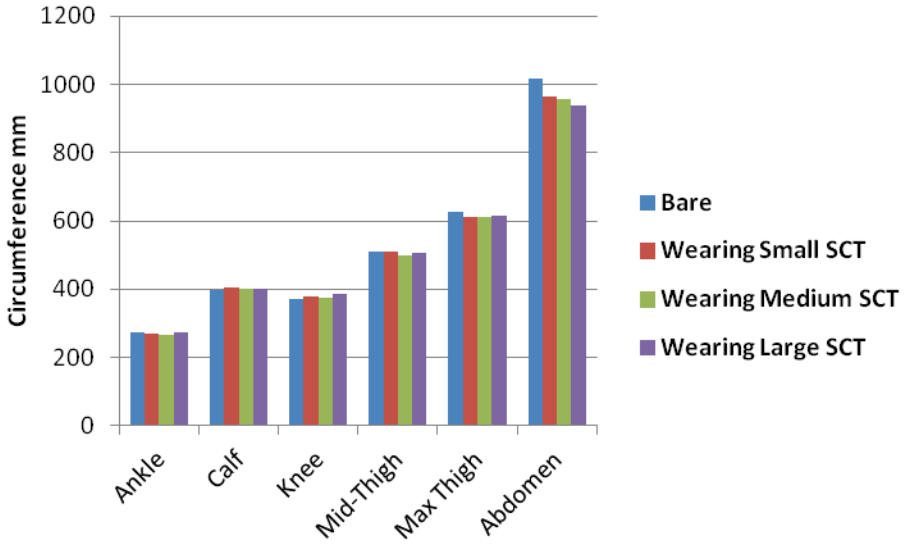

Figure 4.49 Critical lower-body circumferential measurements – Base Model, bare and wearing sizes Small, Medium and Large SCTs

The generation of adequate compression on the tissue at thigh area provides support for the wearer; however, the fit and compression at waist of the garment affects the comfort of the wearer; interestingly, abdomen circumference became smaller with increase in the size of the tight. This could be due to the fact that the wearer had the waist band tighter to hold the tight in place as the garment increased in size. This is an important point in design of the garment to provide comfortable fit for the wearer.

4.4.3. Discussion and conclusions

The reliability of the $[TC]^2$ 3D body-scanner was investigated and it was found that the discrepancies in body measurements were not specific to certain measurement points, but that some discrepancies occurred at certain measuring points for one participant but not the other. It was found that lower-body measurements had relatively high rankings in terms of being within the acceptable error of ≤ 3 mm in circumference ($[TC]^2$ n.d.). It was decided that six scans would be required for each participant to achieve a statistically significant result.

According to Keiser & Garner (2008), circumferential measurements vary more widely than length measurements between humans. A maximum of 16% and 45% differences in circumference measurements at points C and G were recorded amongst thirteen male and amongst thirteen female participants, respectively, belonging to the same size category; while the circumferential measurements close to the joints (point B and knee) were very similar in participants in each genders.

The calf of both male and female participants was positioned similarly at around 44% of crotch height along the leg; female participants had slightly longer thighs than males, as their knee was positioned slightly lower along the leg than males; thigh-max was reported at crotch height for both genders. When the positioning of these points along the leg are compared to reports by Lehto and Buck (2008), the differences in body proportions

between ethnicities and genders are revealed; this is crucial in designing/developing the garment and the sizing system, to take account of differences amongst populations.

SCT in different sizes were worn by one participant and the body measurements were compared to when bare; the circumferential measurements at joints and the calf were similar while circumferential measurements at mid-thigh, thigh-max and abdomen were at their highest (2%, 2% and 6%, respectively) when the participant was bare in comparison to when SCT was worn. SCT had in fact compressed/displaced the tissue at thigh area, where more fat was available in comparison to calf.

In conclusion, the positioning of knee and also the variations in circumference measurements especially at the calf (point C), mid-thigh (point G) and thigh-max are very important in garment design and pressure generation along the leg of the wearer; In order to achieve gradient pressure along the leg, the positioning of calf and knee should be considered, as it could potentially reverse the required gradient pressure. Generally, the pressure induced at the knee should be to an extent not to impede joint movement; thus, the knee position is important and was found to differ between males and females.

The lower-body segment heights could be calculated from the expected height of the wearer, and since the garment sizing mechanism takes the height of the wearer as a parameter, the pattern of the garment could be designed and/or developed so as to address the relative critical lower-body segment measurements. Yet in order to estimate lower-body segment proportions and circumference variations further, anthropometrical investigation with greater sample size is necessary to provide data from the particular population that would wear SCGs.

5. Discussion and conclusions summary

The concept of SCGs came from medical applications. However there are differences in terms of fabric(s), the construction, fit, the required pressure and the application conditions between medical and sport CGs. Without any standards specifying the requirements of SCGs, the methods engaged in evaluation of SCGs were comparable to methods engaged in evaluation of MCGs.

Interaction between the SCG and the underlying limb and the amount of pressure generated over the body is important for the wellbeing of the wearer; high pressure generated on the underlying limb could have adverse effects on health of the wearer, while low pressure could impede the potential positive influence of wearing SCGs.

CGs would only benefit the wearer if the correct pressure profile is achieved over the limb – thus the importance of prediction and investigation on the pressure delivery of such garments, which is rarely investigated or reported by manufacturers and researchers. In this research, preliminary investigation on commercially sourced SCTs placed the tights in the lower range of compression classification for medical compression hosiery (RAL 2008). For the two sizes of SCTs investigated, one size provided gradient pressure over the wooden legs; while for the other size, the gradient pressure was disrupted below the knee.

Troynikov et al. (2010) reported that the induced pressure was dependent on the properties of fabric(s) comprising the garment, the construction and fit of the garment, the limb shape and measurement, as well as the activity undertaken. Researchers tend to eliminate some of the many complex factors such as the limb morphology and underlying tissue composition and compressibility, and would evaluate the performance of CGs in static conditions with few variables. The remaining variables, which are tensile properties of fabric(s) comprising the garments and limb circumference, are used in the prediction and validation of pressure induced by CGs. Meanwhile, there is no consensus on the suitable method of testing for tensile properties of fabrics comprising CGs and validation of theoretical pressure induced by these garments. Some attempts by researchers in the prediction and validation of pressure resulted in satisfying outcomes, where the theoretical pressure was validated with high accuracy, while some reported variations, having used similar methods. Some of the reasons were differences in the evaluation of tensile properties of fabrics comprising CGs, varied interface pressure measurement devices with differences in resolution and sensitivity and pressure measurement sites.

This research attempted to develop a suitable testing method relative to fabrics comprising SCGs. The developed method was found relevant in representing wear conditions of SCGs. It was based on a standard method of testing for elastic fabrics and mimicked the actual donning and wear of SCGs. The results from testing the fabrics for elastic properties to the developed method provided a range of strains expected from SCG when worn, and enabled a prediction of theoretical pressure using Law of Laplace. Using a linear regression model, the measured interface pressure from fabric sleeves over rigid cylinders was interpreted by the theoretical predicted pressure for the fabrics investigated, indicating a high level of model representativeness.

Furthermore and unlike MCGs, SCTs investigated were made of two fabrics with different properties with varied compositions along the leg. The investigation of tensile properties and pressure generation from composed samples comprising SCGs were also attempted. A linear regression model for prediction of measured interface pressure could also be applied to composed samples representing commercial SCGs comprised with different fabrics, providing a statistically significant sample size.

While standard methods are available and common in the evaluation of the physiological comfort properties of fabrics, it was observed that the outcomes would differ significantly when the standard static conditions of testing were modified to represent the application conditions of SCGs.

SCGs have a negative fit over the body; therefore, the fabrics are strained over the limb. The introduction of strain in fabrics had significant influence on their thermo-physiological performance as well as their tactile feeling in comparison to their relaxed state. On the other hand, moisture from perspiration or the environment may be present on the skin in active conditions when SCGs are worn. It was found that presence of moisture on skin influenced the tactile feeling next to the skin, also investigated by other researchers (Das & Alagirusamy 2011; Kilinc-Balci 2011a); yet based on resources gathered, this is the first study evaluating the influence of strain on comfort properties of fabrics. It is also expected that evaluation of same parameters including but not limited to thermo-physiological comfort properties of fabrics in transient conditions would reach

different outcomes; further work, should therefore evaluate the same parameters with the change in temperature and humidity which are expected variations in conditions when SCGs are worn in activity.

As mentioned earlier, the limb geometry and measurements were two of the influential parameters on the induced pressure from CGs. The evaluation of lower-body measurements of a small but good representative sample of the populace, who wore SCGs, represented the variations within same height/weight range (belonging to same size category of SCGs). It was important to evaluate the body measurements of a group of people related to the application under investigation, due to reported variations caused by the age, race, body type, vocational or professional occupation (Croney 1971; Le Pechoux & Ghosh 2002; Lehto & Buck 2008; Yu 2004b).

The variations in lower-body measurements and positioning of important lower-body parts relative to the leg length, especially within one size group, influence the fit, comfort and pressure profile of SCGs. The positioning of calf, knee, mid-thigh and thigh-max along the leg and variations in circumferential measurements influence the gradient pressure induced by CGs, as observed in SCTs assessed. It was also observed that strain in length wise as well as width wise direction of the garment influenced the resultant pressure. Thus the acquisition of body measurements of the particular population who would be the end-users of these garments is crucial in the development of a more accurate sizing mechanism for the garments. This also enables improvements of garment design, to achieve the gradient pressure for majority of users of SCGs within one size category, as well as in different sizes.

The investigations carried out on fabrics/garments must represent the conditions the garments are worn in; for this purpose, fabrics comprising SCGs were investigated for their elastic properties and pressure generation with strains expected and cylinder/limb measurements relative to the application of SCGs and their wearers, respectively. Composed samples with compositions observed in commercially sourced SCTs were evaluated for their tensile properties and pressure generation. The evaluation of physiological comfort properties of fabrics were attempted when the fabrics were strained, representing SCGs when worn as well as when moist in active conditions.

Through this research, the manufacturers and designers of SCGs could have a better understanding on how the chosen material, design and construction as well as the fit of the garments influence the pressure delivery and comfort of the garments. They could understand how variable compositions of different fabrics within one garment would eventually influence the resultant pressure over the limb, and how variations in body measurements within one size category could reverse the potential benefit of wearing these garments. Furthermore, the potential physiological benefits of SCGs, such as wearer's performance enhancement, reduced fatigue and faster recovery, would be of no value if the comfort of the wearer is compromised.

6. Recommendations

The main aim of this research was achieved, which was to predict, measure and validate pressure generated by SCGs on the underlying tissue of human and to evaluate the physiological comfort performance of the garments; however, further investigations should be considered in regards to SCGs and their application.

Prediction and validation of pressure generated by fabrics comprising SCGs on model legs with true geometrical shape and human tissue simulation should be explored. As mentioned earlier, this evaluation was carried out with elimination of human leg complexities by measuring the interface pressure over rigid cylinders, while it is known that the eliminated parameters are influential on pressure generation by SCGs. Furthermore, validation of the theoretical predicted pressure using calibrated interface pressure-measuring device would be useful.

Future work should analyse the tensile properties and pressure generation of samples composed of fabrics with variable tensile properties, due to existence of fabrics with different properties within one SCG.

Theoretical pressure prediction, measurement and validation of pressure generated by SCGs with a combination of strains in both weft and warp directions is recommended.

Last but not least, this study attempted to evaluate the physiological comfort of fabrics comprising SCGs in conditions close to SCG applications; however, the influence of strain applied to the fabric on its air permeability and moisture management properties remains to be identified. Further work is required in order to evaluate the physiological comfort attributes of these fabrics strained and in transient conditions.

7. References

[TC]² n.d., *NX-16 3D Body Scanner Brochure*, <http://www.tc2.com/pdf/nx16.pdf>.

AATCC 2009, *Liquid Moisture Management Propeties of Textile Fabrics AATC TM 195-2009*, AATCC Commitee.

Aldegheri, R & Agostini, S 1993, 'A chart of anthropometric values', *The Journal Of Bone And Joint Surgery*, vol. 75-B, no. 1, pp. 86-8.

Ali, A, Caine, MP & Snow, BG 2007, 'Graduated compression stockings: Physiological and perceptual responses during and after exercise', *Journal of Sports Sciences*, vol. 25, no. 4, pp. 413-9.

Ali, A, Creasy, RH & Edge, JA 2010, 'Physiological effects of wearing graduated compression stockings during running', *European Journal of Applied Physiology*, vol. 109, no. 6, pp. 1017--25.

Allen, RM, Bougourd, J, Staples, RAJ, Orwin, C & Bradshaw, M 2005, 'Scanner Benchmarking for SizeUK', paper presented to EMPA, Switzerland, <http://www.shapeanalysis.com/SizeUK%20Scanner%20Benchmarking.htm>.

Allen, V, Ryan, DW & Murray, A 1993, 'Accuracy of interface pressure measurement systems', *Journal of Biomechanical Engineering*, vol. 15, no. 4, pp. 344-8.

AS 1987, *Methods of test for textiles - Part 2 - Physical tests: Determination of mass per unit area and mass per unit length of fabrics AS 2001.2.13-1987* Standards Australia, Australia.

---- 1989, *Methods of test for textiles - Method 2.15: Physical tests - Determination of thickness of textile fabrics AS 2001.2.15-1989*, Standards Australia, Australia.

---- 1995, *Methods of test for textiles Part 1: Conditioning procedures AS 2001.1—1995*, Standards Australia, Australia.

Ashdown, SP 2011, 'Improving body movement comfort in apparel', in G Song (ed.), *Improving comfort in clothing*, Woodhead Publishing Limited in association with The Textile Institute, Cambridge, vol. 106, pp. 278-302.

ASQUL 1999, *Certificat de qualite-produits. Referentiel technique prescript pour les otheses elastiques de contention des members*, Paris.

Avril, S, Bouten, L, Dubuis, L, Drapier, S & Pouget, JF 2010, 'Mixed Experimental and Numerical Approach for Characterizing the Biomechanical Response of the Human Leg Under Elastic Compression', *Journal of Biomechanical Engineering*, vol. 132, no. 3, p. 031006 (8 pages).

Baranoski, S, Ayello, EA, Mclntosh, A, Galvan, L & Scarborough, P 2008, 'Wound treatment options', in S Baranoski & EA Ayello (eds), *Wound Care Essentials: practice principles*, 2nd edn, Lippincott Williams & Wilkins, Philadelphia pp. 136-71.

Barker, RL 2002, 'From fabric hand to thermal comfort: the evolving role of objective measurements in explaining human comfort response to textiles', *International Journal of Clothing Science and Technology*, vol. 14, no. 3/4, pp. 181-200.

Bartels, VT 2005, 'Physiological comfort of sportswear', in R Shishoo (ed.), *Textiles in Sport*, Woodhead Publishing Limited in association with The Textile Institute, Cambridge, pp. 177-203.

Bartels, VT 2011, 'Improving comfort in sports and leisure wear', in G Song (ed.), *Improving comfort in clothing*, Woodhead Publishing Limited in association with The Textile Institute, Cambridge, vol. 106, pp. 385-411.

Baumgartner, R, Chumlea, W & Roche, A 1989, 'Estimation of body composition from bioelectric impedance of body segments', *The American Journal of Clinical Nutrition*, vol. 50, no. 2, pp. 221-6.

Baussan, E, Bueno, M-A, Rossi, RM & Derler, S 2010, 'Experiments and modelling of skin-knitted fabric friction', *Wear*, vol. 268, no. 9-10, pp. 1103-10.

Bedek, G, Salaün, F, Martinkovska, Z, Devaux, E & Dupont, D 2011, 'Evaluation of thermal and moisture management properties on knitted fabrics and comparison with a physiological model in warm conditions', *Applied Ergonomics*, vol. 42, no. 6, pp. 792-800.

Bernhardt, T & Anderson, GS 2005, 'Influence of Moderate Prophylactic Compression on Sport Performance', *Journal of Strength and Conditioning Research*, vol. 19, no. 2, pp. 292-7.

Bhattacharjee, D & Kothari, VK 2009, 'Heat transfer through woven textiles', *International Journal of Heat and Mass Transfer*, vol. 52, no. 7–8, pp. 2155-60.

Blair, V 1924, 'The influence of mechanical pressure on wound healing', *Illinois Medical Journal*, vol. 46, pp. 249-52.

Bogin, B & Varela-Silva, MI 2010, 'Leg Length, Body Proportion, and Health: A Review with a Note on Beauty', *International Journal of Environmental Research and Public Health*, vol. 7, no. 3, pp. 1047-75.

Bramel, S 2005, 'Key trends in sportswear design', in R Shishoo (ed.), *Textiles in sport*, Woodhead Publishing Limited in association with The Textile Institute, Cambridge, pp. 25-43.

Brooke-Wavell, K, Jones, PRM & West, GM 1994, 'Reliability and repeatability of 3-D body scanner (LASS) measurements compared to anthropometry', *Annals of Human Biology*, vol. 21, no. 6, pp. 571-7.

BS 2006, *Textiles. Knitted fabrics. Determination of number of stitches per unit of length and unit area BS EN 14971:2006*, British Standards.

BSI 1985, *British Standard Specification for Graduated compression hosiery BS 6612:1985*, London, 28 June 1985.

---- 1992, *Methods of test for Elastic Fabrics BS 4952:1992*, British Standards Institution, 31 March 1992.

---- 1993, *Specification for Compression, stiffness and labelling of anti-embolism hosiery BS 7672:1993*, British Standard Institute, London, September 1993.

---- 1999, *Specification for Non-prescriptive graduated support hosiery BS 7563:1999*, British Standard Institute, London, May 1999.

Chan, AP & Fan, J 2002, 'Effect of clothing pressure on the tightness sensation of girdles', *International Journal of Clothing Science and Technology*, vol. 14, no. 2, pp. 100-10.

Clark, M & Krimmel, G 2006, *Lymphoedema and the construction of compression hosiery*, Medical Education Partnership Ltd, London, <http://www.woundsinternational.com/pdf/content_177.pdf>.

Croney, J 1971, *Anthropometrics for designers*, B.T. Batsford Ltd; Van Nostrand Reinhold Company, London; New York.

Daanen, H & Hong, S-A 2008, 'Made-to-measure pattern development based on 3D whole body scans', *International Journal of Clothing Science and Technology*, vol. 20, no. 1, pp. 15-25.

Dai, XQ, Liu, R, Li, Y, Zhang, M & Kwok, YL 2007, 'Numerical Simulation of Skin Pressure Distribution Applied by Graduated Compression Stockings', in X Zeng, Y Li, D Ruan & L Koehl (eds), *Computational Textile*, Springer, Berlin, vol. 55, pp. 301-9.

Dale, JJ, Ruckley, CV, Gibson, B, Brown, D, Lee, AJ & Prescott, RJ 2004, 'Multi-layer Compression: Comparison of Four Different Four-layer Bandage Systems Applied to the Leg', *European Journal of Vascular and Endovascular Surgery*, vol. 27, no. 1, pp. 94-9.

Das, A & Alagirusamy, R 2010, *Science in clothing comfort*, Woodhead Publishing, New Delhi.

Das, A & Alagirusamy, R 2011, 'Improving tactile comfort in fabrics and clothing', in G Song (ed.), *Improving comfort in clothing*, Woodhead Publishing Limited in association with The Textile Institute, Cambridge, vol. 106, pp. 216-44.

Dascombe, B, Scanlan, A, Osbourne, M, Humphries, B & Reaburn, P 2006, *The physiological and performance effects of lower-body compression garments in high-performance cyclists - Report*, CQU, Queensland Academy of Sport and Skins™ Compression Garments.

Davies, V, Thompson, KG & Cooper, S-M 2009, 'The Effects of Compression Garments on Recovery', *Journal of Strength and Conditioning Research*, vol. 23, no. 6, pp. 1786-94.

Deason, VA 1997, 'Anthropometry: the human dimension', *Optics and Lasers in Engineering*, vol. 28, no. 2, pp. 83-8.

Derler, S, Schrade, U & Gerhardt, LC 2007, 'Tribology of human skin and mechanical skin equivalents in contact with textiles', *Wear*, vol. 263, pp. 1112-6.

Dias, T & Delkumburewatte, GB 2008, 'Changing porosity of knitted structures by changing tightness', *Fibers and Polymers*, vol. 9, no. 1, pp. 76-9.

Doan, BK, Kwon, Y-H, Newton, RU, Shim, J, Popper, EM, Rogers, RA, Bolt, LR, Robertson, M & Kraemer, WJ 2003, 'Evaluation of a lower-body compression garment', *Journal of Sports Sciences*, vol. 21, no. 8, pp. 601–10.

Duffield, R, Cannon, J & King, M 2010, 'The effects of compression garments on recovery of muscle performance following high-intensity sprint and plyometric exercise', *Journal of Science and Medicine in Sport*, vol. 13, no. 1, pp. 136-40.

Duyar, I & Pelin, C 2003, 'Body height estimation based on tibia length in different stature groups', *American Journal of Physical Anthropology*, vol. 122, no. 1, pp. 23-7.

EESTI 2001, *Meditsiinilised survesukad ja -sokid*, Brussels.

Fan, J 2009, 'Physiological comfort of fabrics and garments', in J Fan & L Hunter (eds), *Engineering apparel fabrics and garments*, Woodhead Publishing Limited in association with The Textile Institute, Cambridge, vol. 96, pp. 201-50.

Ferguson-Pell, M, Hagisawa, S & Bain, D 2000, 'Evaluation of a sensor for low interface pressure applications', *Medical Engineering & Physics*, vol. 22, no. 9, pp. 657-63.

Field, D & Hutchinson, JO 2008, *Field's Lower Limb Anatomy, Palpation and Surface Markings*, ed. A Redmond, Churchill Livingstone Elsevier, viewed 21 02 2012, via ScienceDirect.

Finnie, A 2000, 'Interface pressure measurements in leg ulcer management', *British Journal of Nursing*, vol. 9, no. 6, pp. S8 - S18.

Flaud, P, Bassez, S & Counord, J-L 2010, 'Comparative In Vitro Study of Three Interface Pressure Sensors Used to Evaluate Medical Compression Hosiery', *Dermatologic Surgery*, vol. 36, no. 12, pp. 1930-40.

Fourt, L & Hollies, NRS 1970, 'Clothing considered as a system interacting with the body', in *Clothing comfort and function*, Marcel Dekker, New York, pp. 31-56.

Gaied, I, Drapier, S & Lun, B 2006, 'Experimental assessment and analytical 2D predictions of the stocking pressures induced on a model leg by Medical Compressive Stockings', *Journal of Biomechanics*, vol. 39, no. 16, pp. 3017-25.

Gavin, TP 2003, 'Clothing and thermoregulation during exercise', *Sports Medicine*, vol. 33, no. 13, pp. 941-7.

Ghosh, P 2004, *Fibre science and technology*, Tata McGraw-Hill, New Delhi.

Ghosh, S, Mukhopadhyay, A, Sikka, M & Nagla, KS 2008, 'Pressure mapping and performance of the compression bandage/garment for venous leg ulcer treatment', *Journal of Tissue Viability*, vol. 17, no. 3, pp. 82-94.

Gibson, PW 1993, 'Factors Influencing Steady-State Heat and Water Vapor Transfer Measurements for Clothing Materials', *Textile Research Journal*, vol. 63, no. 12, pp. 749-64.

Giele, HP, Liddiard, K, Currie, K & Wood, FM 1997, 'Direct measurement of cutaneous pressures generated by pressure garments', *Burns*, vol. 23, no. 2, pp. 137-41.

Goh, SS, Laursen, PB, Dascombe, B & Nosaka, K 2011, 'Effect of lower body compression garments on submaximal and maximal running performance in cold (10°C) and hot (32°C) environments', *European Journal of Applied Physiology*, vol. 111, no. 5, pp. 819-26.

Hafner, J, Lüthi, W, Hänssle, H, Kammerlander, G & Burg, G 2000, 'Instruction of Compression Therapy by Means of Interface Pressure Measurement', *Dermatologic Surgery*, vol. 26, no. 5, pp. 481-8.

Han, H, Nam, Y & Choi, K 2010, 'Comparative analysis of 3D body scan measurements and manual measurements of size Korea adult females', *International Journal of Industrial Ergonomics*, vol. 40, no. 5, pp. 530-40.

Hatch, KL 1993, *Textile Science*, West Publishing Company, St. Paul.

Hatch, KL, Woo, SS, Barker, RL, Radhakrishnaiah, P, Markee, NL & Maibach, HI 1990, 'In Vivo Cutaneous and Perceived Comfort Response to Fabric: Part I: Thermophysiological Comfort Determinations for Three Experimental Knit Fabrics', *Textile Research Journal*, vol. 60, no. 7, pp. 405-12.

Holliday, TW & Ruff, CB 2001, 'Relative variation in human proximal and distal limb segment lengths', *American Journal of Physical Anthropology*, vol. 116, no. 1, pp. 26-33.

Huang, J 2006a, 'Sweating guarded hot plate test method', *Polymer Testing*, vol. 25, no. 5, pp. 709-16.

Huang, J 2006b, 'Thermal parameters for assessing thermal properties of clothing', *Journal of Thermal Biology*, vol. 31, no. 6, pp. 461-6.

Hui, CL & Ng, SF 2001, 'Model to Predict Interfacial Pressures in Multilayer Elastic Fabric Tubes', *Textile Research Journal*, vol. 71, no. 8, pp. 683-7.

ISO 1993, *Textiles - Physiological effects - Measurement of thermal and water-vapour resistance under steady-state conditions (sweating guarded-hotplate test) ISO 11092:1993(E)* ISO Standards.

---- 1995, *Textiles - Determination of the permeability of fabrics to air ISO 9237:1995*, ISO Standards.

---- 2008, *Basic human body measurements for technological design - Part 1: Body measurement definitions and landmarks ISO 7250-1:2008(E)*, ISO Standards.

---- 2010, *3-D scanning methodologies for internationally compatible anthropometric databases ISO 20685:2010*, 27 May 2010.

Istook, CL 2008, 'Three-dimensional body scanning to improve fit', in C Fairhurt (ed.), *Advances in apparel production*, Woodhead Publishing Limited in association with The Textile Institute, Cambridge, pp. 94-116.

Jakeman, JR, Byrne, C & Eston, RG 2010, 'Lower limb compression garment improves recovery from exercise-induced muscle damage in young, active females', *European Journal of Applied Physiology*, vol. 109, no. 6, pp. 1137--44.

Karaguzel, B 2004, 'Characterization And Role Of Porosity In Knitted Fabrics', Thesis (M.S.) - North Carolina State University.

Keiser, SJ & Garner, MB 2008, 'Sizing and Fit', in OT Kontzias (ed.), *Beyond Design: The synergy of apparel product development*, Fairchild Publications, New York, pp. 349-80.

Kemmler, W, von Stengel, S, Köckritz, C, Mayhew, J, Wassermann, A & Zapf, J 2009, 'Effect of Compression Stockings on Running Performance in Men Runners', *Journal of Strength and Conditioning Research*, vol. 23, no. 1, pp. 101--5.

Kilinc-Balci, FS 2011a, 'How consumers perceive comfort in apparel', in G Song (ed.), *Improving comfort in clothing*, Woodhead Publishing Limited in association with The Textile Institute, Cambridge, vol. 106, pp. 97-113.

Kilinc-Balci, FS 2011b, 'Testing, analyzing and predicting the comfort properties of textiles', in G Song (ed.), *Improving comfort in clothing*, Woodhead Publishing Limited in association with The Textile Institute, Cambridge, vol. 106, pp. 138-62.

King, TI & Doessler, JL 2001, 'Physical Properties of Short-Stretch Compression Bandages Used To Treat Lymphodema', *The American Journal of Occupational Therapy*, vol. 55, no. 5, pp. 573-6.

Kissa, E 1996, 'Wetting and Wicking', *Textile Research Journal*, vol. 66, no. 10, pp. 660-8.

Kouchi, M & Mochimaru, M 2011, 'Errors in landmarking and the evaluation of the accuracy of traditional and 3D anthropometry', *Applied Ergonomics*, vol. 42, no. 3, pp. 518-27.

Kraemer, WJ, Flanagan, SD, Comstock, BA, Fragala, MS, Earp, JE, Dunn-Lewis, C, Ho, J-Y, Thomas, GA, Solomon-Hill, G, Penwell, ZR, Powell, MD, Wolf, MR, Volek, JS, Denegar, CR & Maresh, CM 2010, 'Effects of a Whole Body Compression Garment on Markers of Recovery After a Heavy Resistance Workout in Men and Women', *Journal of Strength and Conditioning Research*, vol. 24, no. 3, pp. 804-14.

Lawrence, D & Kakkar, VV 1980, 'Graduated, static external compression of the lower limb: a physiological assessment', *The British Journal of Surgery*, vol. 67, no. 2, pp. 119-21.

Le Pechoux, B & Ghosh, TK 2002, *Apparel Sizing and Fit: A critical appreciation of recent developments in clothing sizes*, vol. 32, no. 1, Textile Progress, The Textile Institute, Manchester.

Lehto, MR & Buck, JR 2008, 'The Human System', in *Introduction to human factors and ergonomics for engineers*, Lawrence Erlbaum, New York, pp. 41-92.

Li, Y 2001, *The science of clothing comfort : a critical appreciation of recent developments*, vol. 31, no. 1/2, Textile progress, The Textile Institute Manchester.

Li, Y & Wong, ASW 2006, 'Physiology of thermal comfort', in Y Li & ASW Wong (eds), *Clothing biosensory engineering*, Woodhead Publishing Limited in association with The Textile Institute, Cambridge, pp. 60-73.

Lin, Y, Lei, Y, Choi, K-F, Luximon, A & Li, Y 2010, 'Contact pressure of tubular fabrics for compression sportswear', in Y Li, Y-P Qiu, X-N Luo & J-S Li (eds), *Textile Bioengineering and Informatics Symposium Proceedings 2010*, Textile Bioengeinnering and Informatics Society Limited Binary Information Press, Shanghai, P. R. China.

Liu, R, Kwok, Y-L, Li, Y, Lao, T-T, Dai, XQ & Zhang, X 2007, 'Numerical simulation of internal stress profiles and three-dimensional deformations of lower extremity beneath medical graduated compression stocking (GCS)', *Fibers and Polymers*, vol. 8, no. 3, pp. 302-8.

Liu, R, Kwok, YL, Li, Y, Lao, TTH & Zhang, X 2007, 'Skin pressure profiles and variations with body postural changes beneath medical elastic compression stockings', *International Journal of Dermatology*, vol. 46, pp. 514-23.

Liu, R, Kwok, YL, Li, Y, Lao, TTH, Zhang, X & Dai, XQ 2005, 'Objective Evaluation of Skin Pressure Distribution of Graduated Elastic Compression Stockings', *Dermatologic Surgery*, vol. 31, no. 6, pp. 615-24.

Liu, R & Little, T 2009, 'The 5Ps Model to Optimize Compression Athletic Wear Comfort in Sports', *Journal of Fiber Bioengineering and Informatics*, vol. 2, no. 1, pp. 41-52.

Lu, J-M & Wang, M-JJ 2010, 'The Evaluation of Scan-Derived Anthropometric Measurements', *Instrumentation and Measurement, IEEE Transactions on*, vol. 59, no. 8, pp. 2048-54.

Macintyre, L 2007, 'Designing pressure garments capable of exerting specific pressures on limbs', *Burns*, vol. 33, no. 5, pp. 579-86.

Macintyre, L 2011, 'New calibration method for I-scan sensors to enable the precise measurement of pressures delivered by 'pressure garments'', *Burns*, vol. 37, no. 7, pp. 1174-81.

Macintyre, L & Baird, M 2005, 'Pressure garments for use in the treatment of hypertrophic scars - an evaluation of current construction techniques in NHS hospitals', *Burns*, vol. 31, no. 1, pp. 11-4.

Macintyre, L, Baird, M & Weedall, P 2004, 'The study of pressure delivery for hypertrophic scar treatment', *International Journal of Clothing Science and Technology*, vol. 16, no. 1/2, pp. 173-83.

MacRae, BA, Cotter, JD & Laing, RM 2011, 'Compression Garments and Exercise: Garment Considerations, Physiology and Performance', *Sports Medicine*, vol. 41, no. 10, pp. 815-43.

Majumdar, A, Mukhopadhyay, S & Yadav, R 2010, 'Thermal properties of knitted fabrics made from cotton and regenerated bamboo cellulosic fibres', *International Journal of Thermal Sciences*, vol. 49, no. 10, pp. 2042-8.

Maklewska, E, Nawrocki, A, Kowalski, K, Andrzejewska, E & Kuzanski, W 2007, 'New measuring device for estimating the pressure under compression garments', *International Journal of Clothing Science and Technology*, vol. 19, no. 3/4, pp. 215-21.

McCann, J 2005, 'Materials requirements for the design of performance sportswear', in R Shishoo (ed.), *Textiles in sport*, Woodhead Publishing Limited in association with The Textile Institute, Cambridge, pp. 44-85.

McCullough, EA 1993, 'Factors affecting the resistance to heat transfer provided by clothing', *Journal of Thermal Biology*, vol. 18, no. 5-6, pp. 405-7.

Mckinnon, L & Istook, C 2001, 'Comparative analysis of the image twin system and the 3T6 Body Scanner', *Journal of Textile and Apparel, Technology and Management*, vol. 1, no. 2, pp. 1-7.

Mckinnon, L & Istook, CL 2002, 'Body Scanning - The effects of subject respiration and foot positioning on the data integrity of scanned measurements', *Journal of Fashion Marketing and Management*, vol. 6, no. 2, pp. 103-21.

Melhuish, JM, Clark, M, Williams, R & Harding, KD 2000, 'The physics of sub-bandage pressure measurement', *Journal of Wound Care*, vol. 9, no. 7, pp. 308-10.

Millet, G, Perrey, S & Foissac, M 2006, 'The Role of Engineering in Fatigue Reduction', in EF Moritz & S Haake (eds), *The Engineering of Sport 6*, Springer, New York, vol. 3, pp. 381-6.

Mohanty, SP, Suresh Babu, S & Sreekumaran Nair, N 2001, 'The use of arm span as a predictor of height: A study of South Indian women', *Journal of Orthopaedic Surgery*, vol. 9, no. 1, pp. 19-23.

Mosti, GB & Mattaliano, V 2007, 'Simultaneous Changes of Leg Circumference and Interface Pressure Under Different Compression Bandages', *European Journal of Vascular and Endovascular Surgery*, vol. 33, no. 4, pp. 476-82.

Ng-Yip, FSF 1993, 'Medical Clothing: A TUTORIAL PAPER ON PRESSURE GARMENTS', *International Journal of Clothing Science and Technology*, vol. 5, no. 1, pp. 17-24.

Ng, SF, Parkinson, JM & Schofield, B 1999, 'The design of pressure garments for the treatment of hypertropic scarring caused by burns', paper presented to Medical textiles: the 2nd International Conference, Bolton Institute, UK, 24th & 25th August 1999.

Ng, SFF & Hui, CLP 1999, 'Effect of hem edges on the interface pressure of pressure garments', *International Journal of Clothing Science and Technology*, vol. 11, no. 5, pp. 251-61.

Nusser, M & Senner, V 2010, 'High - tech - textiles in competition sports', *Procedia Engineering*, vol. 2, no. 2, pp. 2845-50.

Okss, B & Lyashenko, I 1999, 'Methods of Calculation of Local Pressure of Elastomer Products', paper presented to Medical Textiles ’99 International Conference, Bolton, England, August 24-25.

Otieno, RB 2008, 'Improving sizing and fit', in C Fairhurst (ed.), *Advances in apparel production*, Woodhead Publishing in association with the Textile Institute, Cambridge, pp. 73-93.

Özaslan, A, İşcan, MY, Özaslan, İ, Tuğcu, H & Koç, S 2003, 'Estimation of stature from body parts', *Forensic Science International*, vol. 132, no. 1, pp. 40-5.

Partsch, H 2003, *Understanding the pathophysiological effects of compression*, Medical Education Partnership Ltd, London, <http://ewma.org/fileadmin/user_upload/EWMA/pdf/Position_Documents/2003/Spring_2003__English_.pdf>.

Partsch, H 2005, 'The Static Stiffness Index: A Simple Method to Assess the Elastic Property of Compression Material In Vivo', *Dermatologic Surgery*, vol. 31, no. 6, pp. 625–30.

Partsch, H, Clark, M, Bassez, S, Benigni, J-P, Becker, F, Blazek, V, Caprini, J, Cronu-Thénard, A, Hafner, J, Flour, M, Jünger, M, Moffatt, C & Neumann, M 2006, 'Measurement of Lower Leg Compression In Vivo: Recommendations for the Performance of Measurements of Interface Pressure and Stiffness', *Dermatologic Surgery*, vol. 32, pp. 224-33.

Partsch, H & Jünger, M 2006, *Evidence for the use of compression hosiery in lymphoedema*, Medical Education Partnership Ltd, London, <http://www.woundsinternational.com/pdf/content_177.pdf>.

Partsch, H, Partsch, B & Braun, W 2006, 'Interface pressure and stiffness of ready made compression stockings: Comparison of in vivo and in vitro measurements', *Journal of Vascular Surgery*, vol. 44, no. 4, pp. 809-14.

Perrey, S 2008, 'Compression Garments: Evidence for their Physiological Effects', in M Estivalet & P Brisson (eds), *The Engineering of Sport 7*, Springer Paris, pp. 319-28.

Prahsarn, C, Barker, RL & Gupta, BS 2005, 'Moisture Vapor Transport Behavior of Polyester Knit Fabrics', *Textile Research Journal*, vol. 75, no. 4, pp. 346-51.

RAL 2008, *Medical Compression Hosiery - Quality Assurance RAL-GZ 387/1*, RAL Deutsches Institut für Gütesicherung und Kennzeichnung e.V., Sankt Augustin, January 2008.

Rengasamy, RS 2011, 'Improving moisture management in apparel', in G Song (ed.), *Improving comfort in clothing*, Woodhead Publishing Limited in association with The Textile Institute, Cambridge, vol. 106, pp. 182-215.

Salopek Čubrić, I, Skenderi, Z, Mihelić-Bogdanić, A & Andrassy, M 2012, 'Experimental study of thermal resistance of knitted fabrics', *Experimental Thermal and Fluid Science*, vol. 38, pp. 223-8.

Sánchez-García, S, García-Peña, C, Duque-López, MX, Juárez-Cedillo, T, Cortés-Núñez, AR & Reyes-Beaman, S 2007, 'Anthropometric measures and nutritional status in a healthy elderly population', *BMC Public Health*, vol. 7, no. 2.

Saville, BP 1999, 'Strength and elongation tests', in *Physical testing of textiles*, Woodhead Publishing Limited in association with The Textile Institute, Cambridge, pp. 115-67.

Sawada, Y 1993, 'Pressure developed under pressure garment', *British Journal of Plastic Surgery*, vol. 46, no. 6, pp. 538-41.

Sear, JA, Hoare, TK, Scanlan, AT, Abt, GA & Dascombe, BJ 2010, 'The effects of whole-body compression garments on prolonged high-intensity intermittent exercise', *Journal of Strength and Conditioning Research*, vol. 24, no. 7, pp. 1901-10.

Serway, RA & Jewett, JW 2010, 'Fluid Mechanics', in *Physics for scientists and engineers with modern physics*, 8th edn, Brooks/Cole Cengage Learning, 2009, Belmont.

Sieggreen, MY, Kline, RA & Geyer, MJ 2008, 'Venous Leg ulcers, lymphedema, and compression therapy', in S Baranoski & EA Ayello (eds), *Wound Care Essentials: practice principles*, 2nd edn, Lippincott Williams & Wilkins, Philadelphia, pp. 287-316.

Simmons, KP & Istook, CL 2003, 'Body measurement techniques: Comparing 3D body-scanning and anthropometric methods for apparel applications', *Journal of Fashion Marketing and Management*, vol. 7, no. 3, pp. 306-32.

Skinkle, JH 1940, 'Fabric Testing (Continued)', in *Textile Testing: Physical, Chemical and Microscopical*, Chemical Publishing Co., New York, pp. 71-86.

Slater, K 1977, *Comfort Properties of Textiles*, vol. 9, Textile Institute, Manchester.

Slater, K 1986, 'DISCUSSION PAPER THE ASSESSMENT OF COMFORT', *Journal of Textile Institute*, vol. 77, no. 3, pp. 157-71.

Stolk, R, Wegen van der-Franken, CPM & Neumann, HAM 2004, 'A Method for Measuring the Dynamic Behavior of Medical Compression Hosiery during Walking', *Dermatologic Surgery*, vol. 30, pp. 729–36.

Strecker, W, Keppler, P, Gebhard, F & Kinzl, L 1997, 'Length and Torsion of the Lower Limb', *The Journal Of Bone And Joint Surgery*, vol. 79-B, no. 6, pp. 1019-23.

Thomas, S 2002, 'The use of the Laplace equation in the calculation of sub-bandage pressure', *World Wide Wounds*, viewed 13 June 2010, <http://www.worldwidewounds.com/2003/june/Thomas/Laplace-Bandages.html>.

Thomas, S & Fram, P 2003, 'An evaluation of a new type of compression bandaging system ', *World Wide Wounds*, viewed 13 June 2010,

<http://www.worldwidewounds.com/2003/september/Thomas/New-Compression-Bandage.html >.

Treleaven, P, Furnham, A & Swami, V 2006, 'The science of body metrics', *The Psychologist*, vol. 19, no. 7, pp. 416-9.

Treleaven, P & Wells, JCK 2007, '3D body scanning and healthcare applications', *Computer*, vol. 40, no. 7, pp. 28-34.

Troynikov, O, Ashayeri, E, Burton, M, Subic, A, Alam, F & Marteau, S 2010, 'Factors influencing the effectiveness of compression garments used in sports', *Procedia Engineering*, vol. 2, no. 2, pp. 2823-9.

Van den Kerckhove, E, Fieuws, S, Massagé, P, Hierner, R, Boeckx, W, Deleuze, J-P, Laperre, J & Anthonissen, M 2007, 'Reproducibility of repeated measurements with the Kikuhime pressure sensor under pressure garments in burn scar treatment', *Burns*, vol. 33, no. 5, pp. 572-8.

van der Wegen-Franken, K, Roest, W, Tank, B & Neumann, M 2006, 'Calculating the Pressure and the Stiffness in Three Different Categories of Class II Medical Elastic Compression Stockings', *Dermatologic Surgery*, vol. 32, no. 2, pp. 216-23.

van Geest, AJ, Franken, CPM & Neumann, HAM 2003, 'Medical Elastic Compression Stockings in the Treatment of Venous Insufficiency', in P Elsner, K Hatch & W Wigger-Alberti (eds), *Textiles and the Skin*, Karger, Basel, vol. 31, pp. 98-107.

Veraart, JCJM, Pronk, G & Neumann, HAM 1997, 'Pressure Differences of Elastic Compression Stockings at the Ankle Region', *Dermatologic Surgery*, vol. 23, pp. 935-9.

Voyce, J, Dafniotis, P & Towlson, S 2005, 'Elastic textiles', in R Shishoo (ed.), *Textiles in sport*, Woodhead Publishing Limited in association with The Textile Institute, Cambridge, pp. 204-30.

Wang, EM-Y & Chao, W-C 2010, 'In searching for constant body ratio benchmarks', *International Journal of Industrial Ergonomics*, vol. 40, no. 1, pp. 59-67.

Watkins, P 2011, 'Garment pattern design and comfort', in G Song (ed.), *Improving comfort in clothing*, Woodhead Publishing Limited in association with The Textile Institute, Cambridge, vol. 106, pp. 245-77.

Wertheim, D, Melhuish, J, Williams, R & Harding, K 1999, 'Measurement of forces associated with compression therapy', *Medical and Biological Engineering and Computing*, vol. 37, no. 1, pp. 31-4.

Wienert, V 2003, 'Compression Treatment after Burns', in P Elsner, K Hatch & W Wigger-Alberti (eds), *Textiles and the Skin*, Karger, Basel, vol. 31, pp. 108-13.

Wildin, CJ, Hui, ACW, Esler, CNA & Gregg, PJ 1998, 'In vivo pressure profiles of thigh-length graduated compression stockings', *British Journal of Surgery*, vol. 85, pp. 1228-31.

Williams, F, Knapp, D & Wallen, M 1998, 'Comparison of the characteristics and features of pressure garments used in the management of burn scars', *Burns*, vol. 24, no. 4, pp. 329-35.

Yildiz, N 2007, 'A novel technique to determine pressure in pressure garments for hypertrophic burn scars and comfort properties', *Burns*, vol. 33 pp. 59-64

Yu, W 2004a, '3D body scanning', in J Fan, W Yu & L Hunter (eds), *Clothing appearance and fit: science and technology*, Woodhead Publishing, Cambridge, pp. 135-68.

---- 2004b, 'Human anthropometrics and sizing systems', in J Fan, W Yu & L Hunter (eds), *Clothing appearance and fit: science and technology*, Woodhead Publishing, Cambridge, pp. 169-95.

8. Appendices

Appendice 1 Fabric sleeve circumferential measurement relative to weft strain for each cylinder

Cylinder diameter	Cylinder circumference	Weft strain	Fabric sleeve circumference
mm	mm	%	mm
90	282.6	25	226
		50	188
		75	162
130	408.2	25	327
		50	272
		75	233
160	502.4	25	402
		50	335
		75	287

Appendice 2 Salzmann wooden leg circumferential measurements at measuring points B to D

Salzmann wooden leg size	Circumferential measurements at each measuring point					
	B	B1	C	D	F	G
	mm					
9	240	300	375	355	485	540
12	270	340	420	400	530	600
14	290	365	450	430	560	640

Appendice 3 Fabric sleeve dimensions for tactile comfort measurements

Perspex plate circumference	mm	294					
Weft strain	%	13	26	41	56	69	82
Fabric sleeve circumference	mm	260	233	209	188	174	162

Appendice 4 SCT measurements for men in sizes Medium and Large

	Measurement site		SCT size	
			Medium	Large
Length	Height from Hem to Crotch	mm	635	635
	Height from Hem to Waist		835	855
	Inseam		640	640
	Outseam		850	870
Circumference	Leg Opening	mm	170	180
	Measuring point B		184	190
	Measuring point B1		218	226
	Measuring point C		256	266
	Measuring point D		300	322
	Measuring point F		380	404
	Measuring point G		458	470

Appendice 5 Measured pressure by SCTs on Salzmann wooden legs - sizes Medium and Large on side and back

SCT size	Salzmann wooden leg size	Pressure measurement position	Pressure (mmHg)					
			B	B1	C	D	F	G
Medium	9	Back	17.8	13.4	14.7	8.8	7.4	3.4
		Side	15.3	14.3	14.2	8.5	5.8	2.7
	12	Back	19.5	20.1	18.7	10.3	7.6	4.7
		Side	16.6	21.2	20.1	10.3	7.5	4.1
Large	12	Back	16.7	16.1	15.3	8.2	6.6	3.9
		Side	15	16.5	16.2	8.8	7.2	3.2
	14	Back	17.9	17.6	16	9.5	7.1	4
		Side	16.2	18	17.2	9.2	7.3	3.9

Appendice 6 Fabrics A to D tested for tensile properties to standard method in strip formation - descriptive statistics

Fabric label	Direction	STDEV			Coefficient of variation		
		5 specimens	3 specimens	2 specimens	5 specimens	3 specimens	2 specimens
A	Warp	1.870	2.163	0.848	0.010	0.011	0.004
	Weft	1.070	0.625	0.465	0.006	0.003	0.003
B	Warp	1.338	1.825	1.073	0.008	0.011	0.006
	Weft	1.109	1.473	0.943	0.009	0.012	0.008
C	Warp	1.564	0.763	0.907	0.014	0.007	0.008
	Weft	3.464	3.045	1.626	0.027	0.024	0.013
D	Warp	0.517	0.179	0.124	0.004	0.001	0.001
	Weft	3.344	2.672	0.908	0.029	0.022	0.008

Appendice 7 Stress at 100% strain – composition of fabrics A and C in weft direction and strip formation

Composition no.	Sample composition	Stress N	Composition no.	Sample composition	Stress N
0	0%A - 100%C	2.04	11	55%A - 45%C	1.66
1	5%A - 95%C	1.80	12	60%A - 40%C	1.67
2	10%A - 90%C	1.81	13	65%A - 35%C	1.60
3	15%A - 85%C	1.80	14	70%A - 30%C	1.56
4	20%A - 80%C	1.77	15	75%A - 25%C	1.52
5	25%A - 75%C	1.79	16	80%A - 20%C	1.53
6	30%A - 70%C	1.74	17	85%A - 15%C	1.49
7	35%A - 65%C	1.74	18	90%A - 10%C	1.45
8	40%A - 60%C	1.70	19	95%A - 5%C	1.48
9	45%A - 55%C	1.70	20	100%A - 0%C	1.52
10	50%A - 50%C	1.71			

Appendice 8 Stress at various strains for composition of fabrics A and C in weft direction and strip formation - descriptive statistics

Strain in weft direction	Stress N			
	Range	Minimum	Maximum	Mean
100%	0.36	1.45	1.81	1.66
90%	0.25	1.23	1.47	1.37
80%	0.16	1.03	1.20	1.13
70%	0.09	0.87	0.97	0.93
60%	0.05	0.72	0.78	0.75
50%	0.02	0.59	0.61	0.60

Appendice 9 Stress at 100% strain – composition of fabrics A and C in warp direction and strip formation

Composition no.	Sample composition	Stress N
P1	0%A - 100%C	2.69
P2	50%A - 50%C	4.19
P3	100%A - 0%C	1.29

Appendice 10 Theoretical pressure calculation – fabric D in strip formation

Cylinder diameter	Cylinder circumference	Strain	Stress	Pressure
mm	mm	%	N	mmHg
90	282.6	25	0.33	5.4
		50	0.80	13.3
		75	1.41	23.5
130	408.2	25	0.33	3.7
		50	0.80	9.2
		75	1.41	16.3
160	502.4	25	0.33	3.0
		50	0.80	7.5
		75	1.41	13.2

Appendice 11 Theoretical pressure calculation – fabric C in strip formation

Cylinder diameter	Cylinder circumference	Strain	Stress	Pressure
mm	mm	%	N	mmHg
90	282.6	25	0.25	4.2
		50	0.55	9.1
		75	0.89	14.8
130	408.2	25	0.25	2.9
		50	0.55	6.3
		75	0.89	10.2
160	502.4	25	0.25	2.4
		50	0.55	5.1
		75	0.89	8.3

Appendice 12 Theoretical pressure calculation from composition of fabrics C and D at 50% and 75% strain on cylinder 90 – strip formation

Composition no.	Fabric C	Fabric D	Strain	Stress	Pressure
	%	%	%	N	mmHg
1	10	90	50	0.85	14.1
			75	1.58	26.3
2	20	80	50	0.75	12.5
			75	1.36	22.6
3	30	70	50	0.75	12.4
			75	1.36	22.6
4	40	60	50	0.68	11.3
			75	1.22	20.3
5	50	50	50	0.66	10.9
			75	1.16	19.4
6	60	40	50	0.61	10.2
			75	1.10	18.3
7	70	30	50	0.60	10.0
			75	1.02	17.0
8	80	20	50	0.58	9.6
			75	0.99	16.5
9	90	10	50	0.57	9.5
			75	0.95	15.9

Appendice 13 Theoretical calculated pressure from 'Base' to 'Base+3'

	Weight	Force	Calculated pressure	
	Kg	$kg*m/s^2$	Pa	mmHg
Base	0.860	8.424	107307.2	806.8
Base+1	1.542	15.107	192447.3	1447.0
Base+2	2.227	21.823	278000.7	2090.2
Base+3	2.913	28.549	363684.2	2734.5

Appendice 14 Measured pressure from 'Base' to 'Base+3' – descriptive statistics

Pressure mmHg		Base	Base+1	Base+2	Base+3
Mean		20.2	34.9	51.2	62.2
95% Confidence Interval for Mean	Lower bound	19.0	32.8	49.4	60.7
STDEV		5.54	9.63	8.45	6.70
Minimum		10.8	18.9	38.2	53.0
Maximum		29.1	49.3	66.2	75.2

Appendice 15 Measured pressure (mmHg) by fabric D on cylinder 90 - descriptive statistics

Strain		Descriptive statistics					
		Range	Minimum	Maximum	Mean	STDEV	Variance
25%	B	1.1	8.5	9.6	9.2	0.28	0.08
	B1	1.1	8.2	9.3	8.6	0.36	0.13
	C	1.3	7.5	8.8	8.1	0.45	0.21
	D	1.6	5.7	7.3	6.3	0.44	0.19
50%	B	1.2	15.5	16.7	16.2	0.39	0.15
	B1	1.1	15.0	16.1	15.6	0.31	0.10
	C	1.0	13.7	14.7	14.3	0.30	0.09
	D	1.4	11.7	13.1	12.4	0.51	0.26
75%	B	1.6	22.5	24.1	23.2	0.50	0.25
	B1	1.2	22.9	24.1	23.3	0.39	0.15
	C	2.4	19.7	22.1	21.3	0.73	0.54
	D	3.5	16.8	20.3	18.3	1.25	1.56

Appendice 16 Measured pressure (mmHg) by fabric D on cylinder 130 - descriptive statistics

Strain		Descriptive statistics					
		Range	Minimum	Maximum	Mean	STDEV	Variance
25%	B	1.4	6.2	7.6	6.8	0.50	0.25
	B1	1.5	6.1	7.6	6.8	0.54	0.29
	C	1.7	5.4	7.1	6.4	0.51	0.26
	D	1.7	4.5	6.2	5.3	0.66	0.44
50%	B	1.3	9.9	11.2	10.5	0.38	0.15
	B1	0.8	10.5	11.3	11.0	0.26	0.07
	C	0.7	9.7	10.4	10.0	0.19	0.04
	D	1.8	8.2	10.0	9.0	0.64	0.41
75%	B	2.4	16.6	19.0	17.8	0.85	0.72
	B1	3.2	16.7	19.9	18.3	1.03	1.06
	C	2.0	14.3	16.3	15.3	0.59	0.35
	D	1.5	12.1	13.6	13.1	0.35	0.12

Appendice 17 Measured pressure (mmHg) by fabric D on cylinder 160 - descriptive statistics

Strain		Descriptive statistics					
		Range	Minimum	Maximum	Mean	STDEV	Variance
25%	B	1.1	5.4	6.5	5.8	0.19	0.04
	B1	1.1	5.4	6.5	5.6	0.20	0.04
	C	0.7	4.7	5.4	5.1	0.16	0.03
	D	0.5	4.2	4.7	4.4	0.14	0.02
50%	B	1.1	9.1	10.2	9.5	0.32	0.10
	B1	0.7	8.8	9.5	9.0	0.21	0.04
	C	1.0	8.3	9.3	8.6	0.21	0.05
	D	1.4	6.9	8.3	7.5	0.45	0.20
75%	B	0.9	14.5	15.4	14.8	0.20	0.04
	B1	1.0	13.8	14.8	14.3	0.29	0.08
	C	2.1	11.4	13.5	12.5	0.70	0.49
	D	1.4	10.1	11.5	10.7	0.45	0.20

Appendice 18 Theoretical and measured pressure by fabric D – variable cylinders and strains

Weft strain		Cylinder 90		Cylinder 130		Cylinder 160	
		Theoretical pressure	Measured pressure	Theoretical pressure	Measured pressure	Theoretical pressure	Measured pressure
%		mmHg					
25	B	5.4	9.2	3.7	6.8	3.0	5.8
	B1		8.6		6.8		5.6
	C		8.1		6.4		5.1
	D		6.3		5.3		4.4
50	B	13.3	16.2	9.2	10.5	7.5	9.5
	B1		15.6		11.0		9.0
	C		14.3		10.0		8.6
	D		12.4		9.0		7.5
75	B	23.5	23.2	16.3	17.8	13.2	14.8
	B1		23.3		18.3		14.3
	C		21.3		15.3		12.5
	D		18.3		13.1		10.7

Appendice 19 Separate linear regression model – theoretical and measured pressure by fabric D at measuring points B to D

Predictor (constant)	Dependant	R Square	Model	Un-standardised Coefficients		Standardised Coefficients
				B	Std. Error	Beta
Theoretical pressure	B	0.979	(Constant)	3.590	0.094	0.989
			Theoretical pressure	0.855	0.008	
	B1	0.982	(Constant)	3.281	0.088	0.991
			Theoretical pressure	0.872	0.007	
	C	0.979	(Constant)	3.248	0.085	0.989
			Theoretical pressure	0.760	0.007	
	D	0.970	(Constant)	2.606	0.088	0.985
			Theoretical pressure	0.666	0.007	

Appendice 20 Linear regression model split by weft strain – theoretical and measured pressure by fabric D at measuring point B1

Split by weft strain	R Square	Model	Un-standardised Coefficients		Standardised Coefficients
			B	Std. Error	Beta
25% strain	0.898	(Constant)	2.048	0.184	0.948
		Theoretical pressure	1.223	0.44	
50% strain	0.991	(Constant)	0.550	0.117	0.996
		Theoretical pressure	1.129	0.011	
75% strain	0.945	(Constant)	3.636	0.399	0.972
		Theoretical pressure	0.850	0.022	

Appendice 21 Measured pressure (mmHg) by fabric C on cylinder 90 - descriptive statistics

Strain		Descriptive statistics					
		Range	Minimum	Maximum	Mean	STDEV	Variance
25%	B	1.6	9.0	10.6	9.7	0.42	0.18
	B1	1.5	9.1	10.6	9.8	0.40	0.16
	C	1.4	7.7	9.1	8.6	0.39	0.15
	D	2.7	5.8	8.5	7.2	0.91	0.83
50%	B	4.1	12.7	16.8	14.6	1.38	1.91
	B1	3.1	13.5	16.6	14.5	1.23	1.52
	C	1.3	12.4	13.7	12.9	0.47	0.22
	D	3.3	9.9	13.2	11.0	1.35	1.82
75%	B	4.5	18.9	23.4	20.5	1.38	1.90
	B1	6.5	19.3	25.8	21.0	2.06	4.23
	C	5.1	17.0	22.1	18.3	1.72	2.95
	D	9.0	13.7	22.7	17.5	3.50	12.26

Appendice 22 Measured pressure (mmHg) by fabric C on cylinder 130 - descriptive statistics

Strain		Descriptive statistics					
		Range	Minimum	Maximum	Mean	STDEV	Variance
25%	B	1.1	6.5	7.6	7.0	0.33	0.11
	B1	1.4	5.9	7.3	6.6	0.41	0.17
	C	0.6	5.4	6.0	5.7	0.22	0.05
	D	0.7	4.0	4.7	4.4	0.21	0.04
50%	B	1.4	9.2	10.6	10.1	0.49	0.24
	B1	1.4	8.8	10.2	9.6	0.42	0.17
	C	1.0	8.1	9.1	8.6	0.29	0.09
	D	0.8	6.7	7.5	7.0	0.30	0.09
75%	B	1.7	13.0	14.7	13.6	0.53	0.29
	B1	1.4	12.3	13.7	13.0	0.43	0.18
	C	0.8	11.3	12.1	11.7	0.31	0.10
	D	1.5	8.8	10.3	9.6	0.63	0.40

Appendice 23 Measured pressure (mmHg) by fabric C on cylinder 160 - descriptive statistics

Strain		Descriptive statistics					
		Range	Minimum	Maximum	Mean	STDEV	Variance
25%	B	1.3	5.7	7.0	6.4	0.35	0.12
	B1	1.1	5.5	6.6	6.0	0.34	0.12
	C	1.1	4.8	5.9	5.3	0.33	0.11
	D	1.4	4.0	5.4	4.6	0.46	0.22
50%	B	1.6	8.3	9.9	9.2	0.55	0.31
	B1	1.6	8.2	9.8	8.9	0.59	0.35
	C	1.7	7.2	8.9	8.0	0.54	0.29
	D	1.4	6.0	7.4	6.6	0.44	0.19
75%	B	2.4	10.6	13.0	12.0	0.78	0.60
	B1	2.4	10.3	12.7	11.6	0.76	0.57
	C	2.1	8.9	11.0	10.1	0.77	0.59
	D	2.5	7.4	9.9	8.9	0.75	0.56

Appendice 24 Linear regression model – theoretical and measured pressure by fabric C at measuring point B1

Predictor (constant)	Dependant	R Square	Model	Un-standardised Coefficients		Standardised Coefficients
				B	Std. Error	Beta
Theoretical pressure	B1	0.908	(Constant)	3.376	0.246	0.953
			Theoretical pressure	1.124	0.031	

Appendice 25 Measured pressure (mmHg) by fabric sleeves composed of fabrics C and D at measuring point B1 on cylinder 90 - descriptive statistics

Composition no.	Strain	Range	Minimum	Maximum	Mean	STDEV	Variance
1	50%	1.00	16.2	17.2	16.6	0.47	0.222
2		0.25	17.0	17.2	17.0	0.10	0.010
3		0.20	14.0	14.2	14.0	0.08	0.007
4		0.45	15.3	15.8	15.5	0.18	0.033
5		0.35	12.3	12.7	12.5	0.12	0.014
6		0.20	14.3	14.5	14.3	0.07	0.005
7		0.35	13.7	14.1	13.9	0.17	0.028
8		0.40	12.8	13.2	13.0	0.14	0.018
9		0.95	12.7	13.7	13.2	0.44	0.191
1	75%	0.40	22.0	22.4	22.1	0.14	0.020
2		0.25	21.4	21.7	21.5	0.09	0.009
3		0.65	21.4	22.1	21.7	0.31	0.098
4		0.15	19.9	20.1	20.0	0.05	0.002
5		0.65	20.9	21.5	21.2	0.29	0.085
6		1.50	20.0	21.5	20.7	0.80	0.632
7		0.55	17.3	17.9	17.6	0.22	0.047
8		0.25	18.6	18.9	18.7	0.09	0.008
9		1.25	15.5	16.8	16.1	0.61	0.368

Appendice 26 Theoretical and measured pressure by samples composed of fabrics C and D on cylinder 90

Composition no.	Fabric C	Fabric D	Weft strain	Theoretical pressure	Measured pressure
	%	%	%	mmHg	
1	10	90	50%	14.1	16.6
2	20	80		12.5	17.0
3	30	70		12.4	14.0
4	40	60		11.3	15.5
5	50	50		10.7	12.5
6	60	40		10.2	14.3
7	70	30		10.0	13.9
8	80	20		9.6	13.0
9	90	10		9.5	13.2
1	10	90	75%	26.3	22.1
2	20	80		22.6	21.5
3	30	70		22.6	21.7
4	40	60		20.3	20.0
5	50	50		19.4	21.2
6	60	40		18.3	20.7
7	70	30		17.0	17.6
8	80	20		16.5	18.7
9	90	10		15.9	16.1

Appendice 27 Linear regression model – theoretical and measured pressure by samples composed of fabrics C and D at measuring point B1

Predictor (constant)	Dependant	R Square	Model	Un-standardised Coefficients		Standardised Coefficients
				B	Std. Error	Beta
Theoretical pressure	B1	0.884	(Constant)	7.721	0.350	0.940
			Theoretical pressure	0.611	0.021	

Appendice 28 Linear regression model split by weft strain – theoretical and measured pressure by samples composed of fabrics C and D at measuring point B1

Split by weft strain	R Square	Model	Un-standardised Coefficients		Standardised Coefficients
			B	Std. Error	Beta
50% strain	0.579	Constant	5.601	1.055	0.761
		Theoretical pressure	0.794	0.094	
75% strain	0.675	(Constant)	9.982	0.972	0.822
		Theoretical pressure	0.502	0.048	

Appendice 29 Paired t-test results split by weft strain - measured pressure by fabric C with combination of strains in both weft and warp direction on variable cylinders

Cylinder diameter	Weft strain	Warp strain	Sig. (2-tailed)	Cylinder diameter	Weft strain	Warp strain	Sig. (2-tailed)
mm	%	%		mm	%	%	
90	25	10	0.226	90	25	30	0.023
	50		0.499		50		0.010
	75		0.013		75		0.095
130	25		0.754	130	25		0.004
	50		0.009		50		0.002
	75		0.948		75		0.002
160	25		0.199	160	25		0.019
	50		0.822		50		0.006
	75		0.006		75		0.003

Appendice 30 Physical and structural properties of fabric D in variable strains in weft direction

Weft strain	Mean mass / unit area	Mean no. courses / cm	Mean no. wales / cm	Mean stitch density /cm^2	Mean thickness	Porosity	Mean optical porosity
%	kg/m^2				mm	%	%
0	0.240	38	21	798	0.445	53.9	3.32
13	0.226	38	16	608	0.445	56.6	6.31
26	0.207	38	14	532	0.445	60.2	6.53
41	0.176	38	13	494	0.395	61.9	7.18
56	0.172	38	12	456	0.395	62.8	7.49
69	0.154	38	11	418	0.345	61.8	9.07
82	0.143	38	10	380	0.345	64.6	10.27

Appendice 31 Wet pick-up - fabric D

Weft strain	%	0	13	26	41	56	69	82
Dry weight	g	9.33	14.35	17.28	10.95	13.36	9.30	10.80
Wet weight	g	12.88	19.12	23.18	14.65	17.97	12.29	14.58
Wet pick-up	%	38	33	34	34	35	32	35

Appendice 32 Basic information on scanned participants

Participant code - female	Garment size	Height	Weight	Participant code - male	Garment size	Height	Weight
		cm	kg			cm	kg
W001	S	155.0	52.3	M001	S	180.0	70.5
W002	S	171.5	58.8	M002	S	170.0	66.6
W003	S	160.5	56.8	M003	M	176.0	88.4
W004	XS	158.0	49.8	M004	L	181.5	101.1
W005	M	167.0	67.6	M005	MT	187.0	86.4
W006	S	156.0	56.0	M006	M	180.0	76.5
W007	M	149.0	61.8	M007	M	184.5	84.0
W008	L	170.0	80.9	M008	LT	189.0	89.3
W010	XS	160.0	51.8	M009	MT	191.0	84.0
W011	M	173.0	65.4	M010	M	178.3	83.4
W012	S	160.0	51.0	M011	S	181.5	69.9
W013	S	170.0	55.5	M013	S	179.0	74.5
W014	M	157.0	61.8	M014	S	180.0	75.1

Appendice 33 Few body measurements of participants belonging to same size category – male and female

Participant code	Garment size	Height	Weight	Circumference					
				B	B1	C	D	F	G
		cm	kg	mm					
M006	M	180.0	76.5	257.5	250.2	335.2	375.9	427.9	545.4
M007		184.5	84.0	248.1	260.1	368.7	404.8	422.1	545.2
M003		176.0	88.4	247.2	266.8	400.0	411.6	501.9	627.4
M010		178.3	83.4	248.6	265.3	393.5	391.8	468.0	560.0
W001	S	155.0	52.3	218.4	266.2	351.2	323.9	470.3	579.3
W002		171.5	58.8	220.9	227.3	329.4	328.0	403.4	510.3
W003		160.5	56.8	219.1	253.5	345.8	337.5	470.1	585.2
W012		160.0	51.0	209.3	245.6	329.8	322.5	436.1	519.1
W013		170.0	55.5	204.4	239.7	305.4	320.4	413.5	526.2
W006		156.0	56.0	231.6	273.3	355.0	337.4	479.6	945.5

Appendice 34 Height of few points on lower-body in relation to body height - descriptive statistics

		Calf	Knee	Mid-thigh	Crotch	Hip deep
Male participants	Mean	0.18	0.26	0.34	0.41	0.48
	Minimum	0.21	0.29	0.37	0.46	0.53
	Maximum	0.20	0.27	0.36	0.44	0.50
	STDEV	0.008	0.009	0.010	0.013	0.018
Female participants	Mean	0.18	0.25	0.34	0.42	0.49
	Minimum	0.22	0.27	0.37	0.47	0.53
	Maximum	0.20	0.26	0.36	0.45	0.51
	STDEV	0.01	0.007	0.008	0.013	0.014